Superparamagnetic nanoparticles for synthesis and purification of polymers prepared via Controlled/"Living" Radical Polymerization (CLRP)

By:
Fozi Saoud

Dissertation presented in fulfilment of the requirements for the degree of PhD in Polymer Science at the University of Stellenbosch

Promotor: Prof, R. D. Sanderson
Co-promotor: Dr, M. P. Tonge
Co-promotor: Dr, W. G. Weber
Department of Chemistry and Polymer Science

March 2010

Declaration

By submitting this dissertation electronically, I declare that the entirety of the work contained therein is my own, original work, that I am the owner of the copyright thereof (unless to the extent explicitly otherwise stated) and that I have not previously in its entirety or in part submitted it for obtaining any qualification.

March 2010

Abstract

Living chains prepared by RAFT polymerization and NMP reactions using Z-carboxylate and Z-phosphate RAFT agents, and X-phosphate NMP initiators, were efficiently attached to the surface of magnetic nanoparticles (MNPs) and used for the separation of dead chains formed in these polymerization reactions prior to the attachment of the RAFT agents and NMP initiators to the surface of MNPs. All the living chains that attach selectively to the surface of MNPs contained RAFT or NMP functionalities, had a low polydispersity index (PDI), and could be reactivated to form new polymer extensions or block copolymers with no detectable deviation from 100% efficiency. RAFT chains prepared by RAFT polymerization using the Z-carboxylate RAFT agent and an excess of free radical initiator were also attached to the surface of MNPs and separated in the presence of an external magnetic field. Separated RAFT-functional chains contained no dead chains formed by combination or disproportionation reactions, but a substantial amount of cross-terminated by-product with a low UV absorbance at 320 nm.

The cross-termination of the intermediate radical formed in the RAFT polymerization reactions was also investigated in the monomer-excluded free radical reaction model of polystyryl benzyl-(4-carboxyl dithiobenzoate) and polystyryl ethyl-2-bromoisobutyrate. The Z-carboxylate 3- and 4-arm star polymers (formed by cross-termination reactions) were then efficiently attached to the surface of MNPs and separated from the remainder of the polymer solution. They were separated from MNPs and characterized by ^{1}H and ^{13}C-NMR spectroscopy, and MALDI-ToF-MS.

Living chains prepared by a RAFT miniemulsion polymerization reaction using Z-carboxylate RAFT agent were attached to the surface of MNPs and used for the separation of all dead chains and uncontrolled high molecular weight polymer of secondary particle formations occur during a miniemulsion polymerization reaction prior to the attachment. Separated dead chains had high PDI values and contained a significant fraction of uncontrolled high molecular weight polymer that lacked RAFT functionality.

Initiator-derived chains formed in RAFT polymerization reactions of styrene (St) and methyl methacrylate (MMA) using phosphate free radical (PFR) initiator were selectively attached to the surface of MNPs and separated from R-group-derived polymer chains in the presence of an external magnetic field. All separated initiator-derived chains

contained large fractions of dead chains with weak UV absorbance, and which lacked RAFT functionality, and small fractions of RAFT polymer chains. The separated initiator-derived chains had higher PDI values than the as-prepared polymer in the polymerization of St, but lower PDI values than the as-prepared polymer in the polymerization of MMA.

RAFT agents attached to the surface of MNPs by the Z group were used as mediating agents for the synthesis of polymers grafted to the surface of MNPs. The polymers grafted to the surface of MNPs were separated from the solution of the free polymer by applying an external magnetic field. The amounts of the polymers grafted to the surface of MNPs greatly increased as the number of RAFT agents attached to the surface of MNPs decreased. When ethyl acetate was used as solvent, it reached 65% by weight and 50% by number of chains. Separated polymers grafted to the surface of MNPs had high PDI values and contained RAFT functionality.

Investigations into the kinetics of the RAFT-mediated polymerization reaction on the surface of MNPs revealed that the polymerization reaction mediated using a RAFT agent attached by its Z group to the surface of MNPs had a faster polymerization rate than that mediated using a free Z group RAFT agent. The molecular weight of the grafted polymer increased linearly with conversion, and the reaction rate was pseudo-first-order.

Opsomming

Lewende polimeerkettings, berei deur middel van RAFT-beheerde polimerisasie en NMP reaksies waarin Z-karboksilaat en Z-fosfaat RAFT-verbindings en 'n X-fosfaat NMP afsetter gebruik is, is geheg aan die oppervlaktes van magnetisenanopartikels (MNPs), en gebruik vir die skeiding van dooie kettings wat tydens die RAFT en NMP reaksies gevorm is**.** Alle lewende kettings wat aan die oppervlakte van die MNPs geheg is, is geskei van die oorblywende polimeeroplossing deur die aanwending van ‘n eksterne magnetise veld. Alle kettings wat selektief aan die oppervlaktes van die MNPs gekoppel is met RAFT of NMP funksionaliteit, het ‘n laë poliverspreidingswaarde (PDI) gehad en kon heraktiveer word om ‘n nuwe polimeerverlengings of blokkopolimere te vorm met geen merkbare afwyking van 100% doeltreffendheid nie. RAFT-kettings wat gedurende RAFT-polimerisasie met 'n Z-karboksilaat RAFT-agent en oormaat vrye-radikaalafsetter berei is, is ook geheg aan die oppervlaktes van MNPs en geskei in die teenwoordigheid van 'n eksterne magnetiese veld. Die geskeide RAFT-funksionele kettings het geen dooie kettings bevat nie (gevorm deur kombinasie reaksies), maar 'n aansienlike hoeveelheid ongekontroleerde hoë molekulêremassa polimeer (met lae UV absorpsie by 320 nm).

Die kruis-beëindiging van die intermediêre radikaal wat gevorm is tydens die RAFT-proses is ondersoek in die monomeer-uitsluitende vrye-radikaalreaksiemodel van polistirielbensiel-4-karboksielditiobensoaat en polistirieletiel-2-bromoisobutiraat. Die Z-karboksilaat 3- en 4-arm sterpolimere (gevorm a.g.v. kruis-terminasiereaksies) is effektief geheg aan die oppervlaktes van MNPs en geskei van die res van die polimeeroplossing, en daarna gekarakteriseer met behulp van ^{1}H en ^{13}C KMR, en MALDI-ToF-MS.

Lewende kettings, berei m.b.v. RAFT miniemulsiepolimerisasies met 'n Z-karboksilaat RAFT-agent, is geheg aan die oppervlaktes van MNPs en gebruik vir die skeiding van alle dooie kettings en sekondêre partikels wat tydens die reaksie voor die aanhegting gevorm het. Die geskeide dooie kettings wat agtergebly het, het 'n wye PDI getoon en het 'n aansienlike hoeveelheid ongekontroleerde hoë molekulêremassa polimeer, met geen RAFT-funksionaliteit nie, bevat.

Afsetterafkomstigekettings wat gevorm is tydens die RAFT polimerisasiereaksies van stireen (St) en metielmetakrilaat (MMA) met 'n fosfaat-vrye vrye-radikaalafsetter is selektief geheg aan die oppervlaktes van MNPs en geskei van R-groep-afkomstige polimeerkettings in die teenwoordigheid van 'n eksterne magnetise veld. Alle geskeide afsetter-afkomstige kettings het 'n groot hoeveelheid dooie kettings gehad (met swak UV absorpsie) en met geen RAFT-

funksionalilteit nie, en klein fraksies van RAFT-polimeerkettings. Die geskeide afsetter-afkomstige kettings het hoër PDI waardes gehad as die ('as-prepared') polimeer in die polimerisasie van St, maar laer PDI waardes as die ('as-prepared') polimeer in die polimerisasie van MMA.

RAFT-verbindings wat aan die oppervlaktes van die MNPs geheg is deur middel van die Z-groep is as bemiddellingsagente (Eng: mediating agents) gebruik vir die sintese van polimere wat geënt is aan die oppervlakte aan MNPs. Die polimere wat aan die oppervlakte van die MNPs geënt is is geskei van die res van die polimeeroplossing deur die aanwending van ‘n eksterne magnetise veld. Die hoeveelhede van die polimere wat aan die oppervlaktes van die MNPs geënt is het sterk toegeneem namate die aantal RAFT-agente wat aan die oppervlaktes van MNPs geheg is afgeneem het. Wanneer etielasetaat as oplosmiddel gebruik is, was die waardes 55% m.b.t. gewig en 45% m.b.t. die aantal kettings. Die geskeide polimere wat aan die oppervlaktes van MNPs geënt is het hoë PDI getoon en het RAFT-funksionaliteit bevat.

Die kinetika van die RAFT-beheerde polimerisasiereaksies van St, wat gebruik maak van ‘n RAFT-agent wat aan die oppervlakte van die MNPs geheg is deur middel van die Z-groep, is ook ondersoek. Die tempo van polimerisasie was vinniger in die geval waarin die RAFT-agent geheg is deur sy Z-groep aan die oppervlakte van die MNPs as die reaksie met 'n RAFT agent met 'n vrye Z-groep. Die molekulêremassas van die entpolimere het liniêr toegeneem met omsetting, en die reaksie was pseudo-eerste-orde.

Dedication

This dissertation is dedicated to the following people:

To my parents who provided their financial and inspiration support during my graduate studies.

To my wife and children who shared with me equally all the emotional and financial support involved.

To my sisters, brothers, relatives and friends.

Acknowledgments

I owe many thanks to Allah for giving me the strength to complete my study. I also would like to thank the Macromolecular Institute in Libya and UNESCO Centre for Macromolecules for the financial support. The following people must also be acknowledged:

- My promoter, professor Sanderson for the opportunity to study at the Institute of Chemistry and Polymer Science. Thank you for all your support
- My supervisor doctor M. Tonge for your time and valuable advice in reviewing my work.
- My supervisor doctor W. Weber for your support and advice.
- Doctor Margie Hurndall for your advice and help
- Professor Bert Klumperman for MALDI-ToF analysis, doctor Alpheus Mautjana, and Gareth Bayley for GPC analysis
- All the NMR lab analysts for the NMR analysis

Table of contents

Chapter 3: Synthesis of RAFT agents, and NMP and free radical initiators

Chapter 4: Synthesis, stabilization and functionalization of MNPs

Chapter 5: Use of MNPs for purification of polymers prepared via the RAFT process

Chapter 6*: Use of MNPs for purification of polymers prepared via the NMP process*

Chapter 7: Use of MNPs for separation of by-products formed in a RAFT/ATRP model reaction

Chapter 8: Synthesis and separation of polymers grafted onto the surface of MNPs

List of abbreviations

ATRP	Atom Transfer Radical Polymerization
AIBN	2,2′-Azobis(isobutyronitrile)
Aerosol AOT	Sodium dioctyl sulfosuccinate
Blank RAFT agent	2-cyanoprop-2-yl dithiobenzoate RAFT agent
CMRP	Cobalt- Mediated polymerization
CLRP	Controlled/ "Living" Radical Polymerization
DEPN	N-tert-butyl-N-(1-diethylphosphono-2,2-dimethylpropyl) nitroxide
DRI	Differential Refractive Index detector
DCM	Dichloromethane
DMSO	Dimethyl sulfoxide
EBiB	Ethyl-2-bromoisobutyrate
ESR	Electron Spin Resonance
FRP	Free radical polymerization
FT-IR	Fourier Transform-Infrared spectroscopy
$Fe(acac)_3$	Iron acetylacetonate
GPC	Gel Permeation Chromatography
ITP	Iodine Transfer Polymerization
MALD-ToF-MS	Matrix Assisted Laser Desorption Ionization Time-of-Flight Mass Spectroscopy
MADIX	Xanthate Mediated-Polymerization
MMA	Methyl methacrylate
M	Molecular weight
MWD	Molecular Weight Distribution
MNPs	Superparamagnetic or magnetic nanoparticles
NMP	Nitroxide-Mediated Polymerization
NaOl	Sodium oleate
NMR	Nuclear Magnetic Resonance

NBS	N-bromosuccinimide
PSt	Polystyrene
PSt-carboxylate	Polystyryl benzyl-(4-carboxydithiobenzoate)
PSt-Br	Polystyryl ethyl-2-bromoisobutyrate
PMA	Polymethyl acrylate
PMMA	Poly methyl methacrylate
PRE	Persistent radical effect
PDI	Polydispersity index
PRI	Phosphate free radical initiator
RAFT	Reversible Addition-Fragmentation Chain Transfer
SET-DTLRP	Single Electron Transfer Degenerative Chain Transfer-Mediated Living Radical Polymerization
SEC	Size Exclusion Chromatography
SBRP	Organostibine Mediated-Polymerization
St	Styrene
TERP	Organotellurium-Mediated Polymerization
TEMPO	2,2,6,6-tetramethyl-1-piperidine hydroxyl
THF	Tetrahydrofuran
TEM	Transmission Electron Microscopy
UV/Vis	Ultraviolet/Visible
VSM	Vibration Sample Magnetometer
VAc	Vinyl acetate
Z-carboxylate-MNPs	Z-carboxylate RAFT agent attached to the surface of MNPs
Z-carboxylate RAFT agent	Benzyl-(4-carboxyldithiobenzoate) RAFT agent
Z-phosphate RAFT agent RAFT agent	S-benzyl-S′-(11-phosphonoxy-undecyl)trithiocarbonate

Z-phosphate-MNPs	Z-phosphate RAFT agent attached to the surface of MNPs

List of symbols

C_{tr}	Chain transfer constant
C_{M}	Chain transfer constant to monomer
C_{S}	Transfer constant to solvent
f	Efficiency of initiator
[I]	Initiator concentration
k_{d}	Constant rate coefficient for the decomposition of an initiator
k_{p}	Propagation rate coefficient
$k_{\mathrm{t,c}}$	Average termination rate coefficient by combination
$k_{\mathrm{t,d}}$	Average termination rate coefficient by disproportionation
k_{a}	Rate coefficient of activation
k_{d}	Rate coefficient of deactivation
k_{t}	Rate coefficient of termination
k_{add}	Addition rate coefficient
$k_{\text{-add}}$	Addition rate coefficient
L^{-}	Adsorbing ligand
[M]	Monomer concentration
$[\mathrm{M}]_0$	Initial monomer concentration
M_{n}	Predicted number average molecular weight
M_{monomer}	Monomer's molecular weight
M_{RAFT}	RAFT agent's molecular weight
$\mathrm{P}_n^{\bullet}$ and $\mathrm{P}_m^{\bullet}$	Polymeric radicals
[P•]	Concentration of the propagating radical
R_{i}	Rate of initiation
R_{p}	Rate of radical propagation
$R_{\mathrm{t,c}}$	Termination rate by combination

$R_{t,d}$	Termination rate by disproportionation
R_t	Overall termination rate
$[RAFT]_0$	Initial concentration of a RAFT agent
R	Initiating or leaving group of a NMP initiator or a RAFT agent
[S]	Solvent concentration
t	Reaction time
$\bar{X}_n$	Average degree of polymerization
X	Monomer conversion
$X^{\bullet}$	Mediating radical
Z	Activating or stabilizing group of the RAFT agent
β	Fraction of disproportionation

List of schemes

List of tables

List of figures

Chapter 1: Introduction and objectives

1.1 Background

1.1.1 Free radical polymerization

Free radical polymerization is an important and widely used method for the preparation and production of polymeric materials. It is used for the production of more than 50% of polymers worldwide.[1] This is due to the following advantages: it is very versatile with respect to compatibility with different functional monomers; it is tolerant to impurities and the presence of water, and it can be applied over a wide temperature range (–80 to 250 °C).[2]

The term radical in this context refers to an atom that has at least one unpaired electron; it is deliberately produced in polymerization reactions, by, for example thermal homolytic cleavage of unsaturated small molecules called initiators. The radicals thus produced then react with vinyl monomers, that is, monomers containing carbon–carbon double bonds, resulting in the formation of new radicals that react with many monomer units in the same way, until two growing chain radicals meet, react with each other via a termination reaction, or a growing chain radical undergoes another chain stopping event, such as transfer to monomer, or solvent, to afford a polymer.

Free radical polymerization does have some limitations, however: the poor control over the molecular structure, end-functionality, polydispersity index (PDI) and molecular weight (M) of the produced polymers.[3] The development of Controlled/"Living" Radical Polymerization (CLRP) techniques, by which the polymerization process can be controlled with respect to the M, molecular weight distribution (MWD), and molecular architecture of the polymer product, and to satisfy industrial demands to overcome the limitations of free radical polymerization, is significant.

1.1.2 Controlled/"Living" Radical Polymerization

Reversible Addition-Fragmentation Chain Transfer (RAFT),[4,5] Nitroxide-Mediated Polymerization (NMP)[6,7] and Atom Transfer Radical Polymerization[8,9] are among the most well developed CLRP techniques for the production of well-defined block, star and comb polymers with controlled *M* and PDIs.[4,10-12]

All CLRP techniques are based on conventional radical reactions in which chain termination and other chain transfer reactions also occur. These termination reactions produce "dead chains" – dead because they are not reactivated when a similar or second monomer is added to the RAFT, NMP or ATRP polymers during the synthesis of block copolymers, – thus their chain growth has ended. Classical separation methods such as column chromatography, precipitation, filtration and distillation are often not efficient methods for the separation of dead chains from living chains. This possibly because dead chains are chemically and physically similar to living chains, thus, making separation difficult.

1.1.3 The RAFT process

The RAFT process is the most recently developed technique in this fast growing field of CLRP. It is also one of the most versatile process, compared to the other CLRP processes with respect to suitable monomers and reaction conditions.[13] Numerous polymeric materials produced by the RAFT-mediated polymerization process have been reported in the literature.[5,14]

The two most known equilibrium processes occurring in the RAFT-mediated polymerization reactions are the pre-equilibrium in which the initial RAFT agent is consumed (in some cases complete consumption of the initial RAFT agent [initialization process] might not occur before the reaction has ceased, and in such cases a true long-chain equilibrium might not be reached), and the main equilibrium in which polymeric radicals react with dormant RAFT agents. These two equilibrium reactions are illustrated in Scheme 1.1.[15] Although these equilibrium processes might hold for many RAFT agents, they are however not strictly true when the activating (Z group) of the RAFT

agent (see Scheme 1.1) is a phenyl group.[16,17] The elucidation of the exact mechanism of the RAFT process is still therefore an ongoing issue. On the one hand this is because of the other factors such as inhibition and retardation that are not simply described by considering these equilibrium processes; the interpretation of inhibition/retardation of RAFT-mediated polymerization reactions is an ongoing debate. This is discussed in more detail in Chapter 2.[16,18,19]

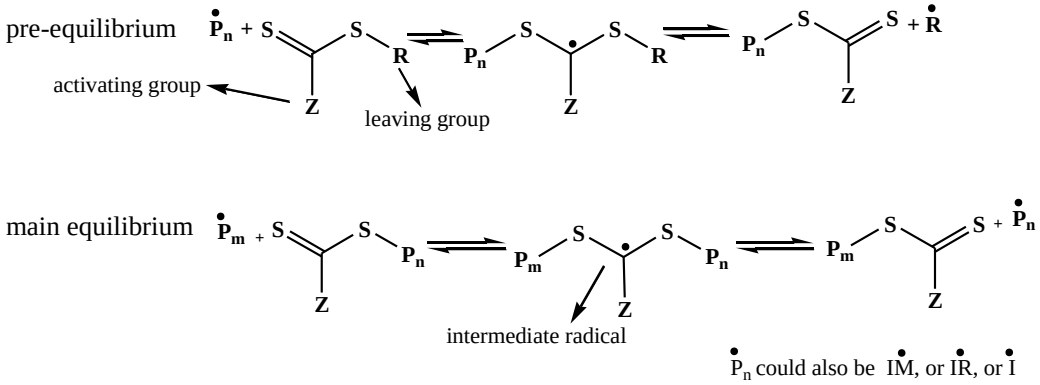

Scheme 1.1: Pre-equilibrium and main equilibrium reactions in the RAFT-mediated polymerization process.[15]

On the other hand this is due to different mechanistic behaviour of the RAFT process for different pairs of RAFT agent/monomer, i.e. different from the depicted general equilibrium reactions in Scheme 1.1.[20] For the most common monomers being used are styrene (St) and acrylate monomers (e.g. methyl methacrylate (MMA)), with RAFT-mediated polymerization of St being at a retarded rate,[16,21-30] while that of MMA exhibited an inhibition/retardation period when the polymerization was mediated by cumyl dithiobenzoate RAFT agent.[31-34] Further research into the mechanism of the RAFT process is clearly required.

Most of the RAFT-mediated polymerization reactions proceed via dithioester mediating agents of the generic structure (Z–C(=S)S–R), which comprises two characteristic moieties. The R group, also refers to as leaving group of the RAFT agent (illustrated in Scheme 1.1), is, the group that forms a radical when it is displaced by another radical that

reacts with the RAFT agent in the pre-equilibrium reaction (see Scheme 1.1). The Z group (illustrated in Scheme 1.1) is the living or stabilizing or activating group, i.e., the mediating-dithio moiety of a RAFT agent.

1.1.4 NMP agents

The most successful NMP agents are the nitroxides, and their associated derivatives, the alkoxyamines.[7] A unimolecular NMP initiator (R–X) comprises X and R groups. The X group is also called the mediating group. It is the group that forms a nitroxide mediating radical ($X^{\bullet}$) from thermal decomposition of the unimolecular NMP initiator (see Scheme 1.2). The mediating radical is a stable radical that does not undergo significant coupling by another mediating radical, but it reacts with a propagating radical ($P^{\bullet}$) to afford (P–X) dormant NMP chains. The R group is the initiating group, i.e., the group that forms an initiating radical ($R^{\bullet}$) from the thermal decomposition of the unimolecular NMP initiator. The initiating radical can react with monomer to produce a propagating radical ($P^{\bullet}$). The propagating radical reacts with the mediating radical to afford a dormant NMP chain, or it reacts otherwise with another propagating radical via a termination reaction to produce a dead chain, or transfers to monomer, or solvent. These expected reactions are illustrated in Scheme 1.2.

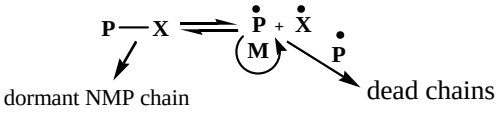

Scheme 1.2: Association and disassociation of an unimolecular NMP initiator.

1.1.5 Separation of living chains from dead chains formed in the CLRP processes

The immobilization of various RAFT agents and NMP agents/initiators onto solid supports has been reported in the literature.[35-41] Such immobilization is a convenient way for separating living chains from dead chains formed during RAFT-mediated polymerization and NMP reactions. In most of the studies reported, the RAFT agents and NMP initiators were however attached to solid supports by their R groups. These attached

RAFT and NMP agents were mainly developed for the formation of densely grafted polymer brushes, and the focus was not on the separation of the living chains from the dead chains. The separation of polymers grafted onto solid substrates by their R groups does however not necessarily result in the separation of all dead chains from living chains. This is because dead chains that possess at least one of the R groups of the RAFT agent, or the NMP initiator, will also be attached to the solid substrate, and thus they will also be separated with the living chains.

There are some reports on the separation of living chains from dead chains formed in polymerization reactions mediated by RAFT agents attached to silica particle surfaces by their Z groups.[42-45] Most of these reports indicate that it is difficult to separate living chains from dead chains.[46] Furthermore the separated living chains exhibited bimodal MWDs, with high PDI,[43]or required the addition of free RAFT agent to the solution phase in order to improve the MWD and PDI of the generated living chains.[42,44,45]

1.1.6 Superparamagnetic nanoparticles

Superparamagnetic nanoparticles (MNPs) of the formula Fe_3O_4 (magnetite) and γ-Fe_2O_3 (maghemite) are used for the immobilization of proteins and enzymes, for biomedical applications.[47-49] The term superparamagnetic nanoparticles means that these nanoparticles are strongly attracted to an applied external magnetic field, but retain no residual magnetization after the magnetic field is removed.[47] MNPs have been widely used in the separation of biochemical materials due to their strong magnetization properties based on their small size (< 15 nm in all three dimensions),[50] and recently for the removal of the catalyst used in ATRP.[51] The best of the author's knowledge, they have not yet been used for the separation of living polymers.

In colloidal dispersions of MNPs each particle contains a single magnetic domain and has no net magnetism in the absence of an external magnetic field, but the MNPs will be attracted to an external magnetic field. This allows for the convenient and easy separation of all MNPs from the remainder of a mixture, and with much higher purity than can be

achieved with sedimentation or ultracentrifugation. Polymer containing a group capable of a strong attachment force to the surface of MNPs can be thus separated.

The main focus of this study is on using MNPs for the separation of all dead chains form living chains formed in RAFT-mediated polymerization and NMP reactions.

1.2 Objectives

The main objectives of this study were the following:

(1) To determine a suitable extraction (separation) process using MNPs for purification of products of RAFT and NMP polymerization reactions (separation of living chains from dead chains formed in RAFT-mediated and NMP reactions)

(2) To investigate the use of the extraction process using MNPs to selectively separate functional living chains from a mixture of RAFT chains formed during RAFT-mediated polymerization reactions and non-functional polymer chains (e.g. polymer standards)

(3) To investigate the possible use of the extraction process using MNPs to determine secondary particle formation in RAFT-mediated miniemulsion polymerization reactions

(4) To investigate the possible use of the extraction process using MNPs to separate side products (by-products) formed in RAFT-mediated polymerization reactions when a high concentration of free radical initiator is used

(5) To investigate the extraction process using MNPs for separation of initiator derived chains formed in RAFT/St and RAFT/acrylates polymerization reactions as effort to learn more about mechanistic behaviour of these reactions.

(6) To investigate the use of MNPs to separate by-products formed in a polymeric RAFT/and an ATRP free radical model polymerization reaction in the absence of

monomer (model meaning that this polymerization reaction mimics the RAFT process)

(7) To investigate the effect of the presence of MNPs on RAFT-mediated polymerization reactions

(8) To investigate the RAFT-mediated polymerization reactions using RAFT agents attached by their Z groups to the surface of MNPs for the synthesis of grafted polymers to the surface of MNPs. Thus, to investigate the possible separation of the grafted polymer to the surface of MNPs form a solution containing a free polymer by applying an external magnetic field

(9) To investigate the kinetics of a RAFT-mediated polymerization reaction on the surface of MNPs using RAFT agent attached by its Z group to the surface of MNPs and that of a RAFT-mediated polymerization reaction using free Z group RAFT agent in the absence of MNPs for comparison.

1.3 Methodology

A. Various RAFT agents, NMP and free radical initiators that contain carboxylate or phosphate groups that have strong attachment forces to the surface of MNPs. The groups with strong attachment forces to the MNPs are incorporated into the Z groups, X groups of the RAFT agents and NMP initiators, respectively.

B. MNPs and modification of the surface of the MNPs to minimize the particles aggregation by stabilization with surfactants such as oleic and decanoic acids.

C. Various polystyrene (PSt) polymers mediated by Z-carboxylate RAFT-mediated (solution and bulk) polymerization of styrene.

D. PSt polymer to be prepared by Z group (carboxylate) (Z-carboxylate) RAFT-mediated miniemulsion polymerization of styrene.

E. PSt polymer to be prepared by Z-carboxylate RAFT-mediated polymerization of St using high concentration of free radical initiator.

F. Various blank RAFT agents that contain no attachment force to the surface of the MNPs.

G. PSt and poly methyl methacrylate (PMMA) polymers synthesized by RAFT-mediated polymerization of St using blank RAFT agents and that of MMA, in the presence of a free radical initiator that contains a phosphate group with a strong attachment force to the surface of the MNPs.

H. PSt polymers prepared by ATRP of St using non-functional ATRP initiator and that prepared by RAFT-mediated polymerization of St using Z-carboxylate RAFT agent. These polymers to be used in a free radical reaction model in the absence of monomer.

I. All synthesized polymers were used in the extraction process for separation of polymer chains that contain strong attachment forces to the surface of MNPs in the presence of an external magnetic field.

J. PSt polymer synthesized by RAFT-mediated polymerization of St using blank RAFT agent in the presence of MNPs.

K. Z-carboxylate and Z-phosphate RAFT agents attached onto the MNP surfaces.

L. PSt polymers grafted onto the MNPs surface synthesized by RAFT-mediated polymerization of St using Z-carboxylate RAFT agents attached onto the surface of MNPs.

The following analytical techniques were to be used in this study, for the specific purposes indicated.

- Nuclear Magnetic Resonance (NMR) spectroscopy for characterization of the RAFT agents, NMP and free radical initiators, and polymers.

- Fourier Transform-Infrared (FT-IR) spectroscopy was used to confirm the attachment of RAFT agents onto the surface of MNPs.

- Transmission Electron Microscopy (TEM) was used to determine particle size, size distribution and morphology of MNPs, and polystyrene polymer latexes.

- Ultraviolet/Visible (UV/visible) spectroscopy was used to determine the absorbance wavelengths at which the RAFT agents, NMP initiators, and free radical initiators absorb strongly. It was also used to determine the quantities of the RAFT agents attached onto the surface of MNPs.

- Size Exclusion Chromatography (SEC) was used to determine the molecular weights, molecular weight distributions, and UV absorbances of the polymers synthesized in this study.

- Matrix Assisted Laser Desorption Ionization Time-of-Flight Mass Spectroscopy (MALDI-ToF-MS) was used to determine polymer end-groups and general structures.

1.4 Layout of dissertation

The dissertation comprises of nine chapters. The body of the text is complied in the format of publications.

Chapter 1: *Introduction and objectives*

A brief introduction to free radical polymerization (FRP), CLRP, and separation of by-products formed in RAFT and NMP processes are given. The objectives, methodology, and layout of the present project are presented

Chapter 2: *Theoretical and historical background*

This chapter presents a detailed review on MNPs (e.g. the importance of MNPs in modern technology, their available synthesis methods, their stabilization and handling, and surface modifications of MNPs). It includes a review of the methods available for the

synthesis of polymers grafted onto solid substrates. Second it gives a background of FRP and development of CLRP, and includes a summary of some relevant results achieved by other groups in the field.

Chapter 3: *Synthesis of RAFT agents, NMP and free radical initiators*

This chapter focuses on the experimental conditions used for the preparation of the various RAFT agents, NMP and free radical initiators that were used in this study. The analytical techniques used to characterize these agents and initiators are also discussed in this chapter.

Chapter 4: *Synthesis, stabilization and surface modification of MNPs*

This chapter gives detailed information of experimental and reaction conditions used for the synthesis and stabilization of MNPs. Methods of attachment of Z groups (carboxylate and phosphate) RAFT agents onto the surface of MNPs with regard to reaction conditions are also discussed in this chapter. This chapter also includes detailed descriptions of the characterization techniques.

Chapter 5: *Magnetic separation of products of RAFT-mediated polymerization reactions*

Results of the following areas of investigation are described and discussed in this chapter.

a. The general extraction process using MNPs for the separation of living chains from dead chains formed in RAFT-mediated polymerization reactions in the preparation of pure polymers is discussed.

b. The effect of non-functional polymers on the extraction process.

c. Use of the extraction process to determine the existence of a secondary particle formation that occurs in RAFT-mediated miniemulsion polymerization reaction.

d. Improvement of the extraction process for the separation of living chains from dead chains formed during RAFT-mediated polymerization by investigating different

affinities of attachment force to the surface of MNPs (e.g. phosphate vs. carboxylate groups).

e. Separation of living chains from dead chains formed in RAFT-mediated polymerization reactions using high concentrations of free radical initiators. These accentuated the separation of by products and living chains from dead chains formed in the RAFT-mediated polymerization reactions.

f. Separation of initiator derived chains formed in RAFT-mediated polymerization reactions of St and that of MMA.

Chapter 6: *Magnetic separation of by-products formed in RAFT/ATRP polymerization reactions*

The free radical reaction of PSt RAFT polymer (prepared by RAFT-mediated polymerization of St using Z-carboxylate RAFT agent) and PSt ATRP polymer (prepared by ATRP of St using non-functional ATRP initiator) in the absence of monomer is described. Results of magnetic separation of by-products formed in this reaction are investigated and discussed.

Chapter 7: *Magnetic separation of products of NMP polymerization reactions*

Polymerization reactions of St mediated by X-phosphate NMP initiator are described. Results of magnetic separation of living chains from dead chains formed during these polymerization reactions are investigated and discussed. Various separation methods used to separate the living chains from dead chains formed in these polymerization reactions, using MNPs, are investigated.

Chapter 8: *RAFT-mediated polymerization of styrene onto the surface of MNPs*

The following areas of investigation are described and discussed.

a) RAFT-mediated polymerization of St using blank RAFT agent in the presence of MNPs.

b) Various RAFT-mediated polymerization reactions of St using Z-carboxylate RAFT agent attached onto the surface of MNPs at different concentrations of RAFT agents/ magnetite nanoparticles.

c) Kinetics of the RAFT-mediated polymerization reaction of St onto the surface of MNPs using the Z-carboxylate RAFT agents attached onto the surface of MNPs, and that of the RAFT mediated polymerization reaction of St using Z-carboxylate free RAFT agents, for comparison.

Chapter 9: *Conclusions and recommendations*

This chapter summarizes conclusions of this study, which correlate to the initial objectives. Several recommendations are also made: on the possible future use of the extraction process to afford a large scale; of pure RA**F**T and NMP polymers, and purer block copolymers, and use of the extraction process to optimize reaction conditions to avoid or minimize by products formed during RAFT-mediated polymerization reactions.

1.5 References

1. Matyjaszewski, K., *Advances in Controlled/"Living" Radical Polymerization*; ACS Symposium Serires 854; American Chemical Society: Washington, DC, **2003**; p 2.
2. Sandler, S. R.; Karo, W., *Academic Press*, INC: London, **1974**; Vol. I, p3.
3. Wang, J.-S.; Matyjaszewski, K. *J. Am. Chem. Soc*. **1995**, 117, 5614-5615.
4. Chiefari, J.; Chong, Y. K.; Ercole, F.; Krstina, J.; Jeffery, J.; Le, T. T. P.; Mayadunne, R. T. A.; Meijs, G. F.; Moad, C. L.; Moad, G.; Rizzardo, E.; Thang, S. H. *Macromolecules* **1998**, 31, 5559-5562.
5. Moad, G.; Rizzardo, E.; Thang, S. H. *Aust. J. Chem*. **2005**, 58, 379-410.
6. Solomon, D. H.; Rizzardo, E.; Cacioli, P. EP0135280, **1985**.
7. Hawker, C. J.; Bosman, A. W.; Harth, E. *Chem. Rev*. **2001**, 101, 3661-3688.
8. Wang, J.-S.; Matyjaszewski, K. *J. Am. Chem. Soc*. **1995**, 117, 5614-5615.
9. Matyjaszewski, K.; Xia, J. *Chem. Rev*. **2001**, 101, 2921-2990.
10. Chong, B. Y. K.; Le, T. T. P.; Moad, G.; Rizzardo, E.; Thang, S. H. *Macromolecules* **1999**, 32, 2071-2074.
11. Mayadunne, R. T. A.; Rizzardo, E.; Chiefari, J.; Krstina, J.; Moad, G.; Postma, A.; Thang, S. H. *Macromolecules* **2000**, 33, 243-245.
12. Mayadunne, R. T. A.; Rizzardo, E.; Chiefari, J.; Moad, G.; Thang, S. H. *Macromolecules* **1999**, 32, 6977-6980.
13. Krstina, J.; Moad, G.; Rizzardo, E.; Winzor, C. L.; Berge, C. T.; Fryd, M. *Macromolecules* **1995**, 28, 5381-5388.
14. Perrier, S.; Takolpuckdee, P. *J. Polym. Sci., Part A: Polym. Chem*. **2005**, 43, 5347-5393.
15. Vana, P.; Nguyen, D. H. *Polym. Adv. Technol*. **2006**, 17, 625-633.
16. Moad, G.; Chiefari, J.; Chong, Y. K.; Krstina, J.; Mayadunne, R. T. A.; Postma, A.; Rizzardo, E.; Thang, S. H. *Polym. Int*. **2000**, 49, 993-1001.
17. Ganachaud, F.; Monteiro, M. J.; Gilbert, R. G.; Dourges, M.-A.; Thang, S.; Rizzardo, E., *Macromolecules* **2000**, 33, 6738-6745.
18. Calitz, F. M.; McLeary, J. B.; McKenzie, J. M.; Tonge, M. P.; Klumperman, B.;

Sanderson, R. D. *Macromolecules* **2003**, 36, 9687-9690.

19. Calitz, F. M.; Tonge, M. P.; Sanderson, R. D. *Macromolecules* **2003**, 36, 5-8.
20. Han, X.; Fan, J.; He, J.; Xu, J.; Fan, D.; Yang, Y. *Macromolecules* **2007**, 40, 5618-5624.
21. Kwak, Y.; Goto, A.; Tsujii, Y.; Murata, Y.; Komatsu, K.; Fukuda, T. *Macromolecules* **2002**, 35, 3026-3029.
22. Barner-Kowollik, C.; Vana, P.; Quinn, J. F.; Davis, T. P. *J. Polym. Sci., Part A: Polym. Chem.* **2002**, 40, 1058-1063.
23. Kwak, Y.; Goto, A.; Fukuda, T. Macromolecules **2004**, 37, 1219-1225.
24. Barner-Kowollik, C.; Quinn, J. F.; Morsley, D. R.; Davis, T. P. J. J. *Polym. Sci., Part A: Polym. Chem*. **2001**, 39, 1353-2365.
25. Brouwer, H. D.; Schellekens, M. A. J.; Klumperman, B.; Monteiro, M. J.; German, A. L. *J. Polym. Sci., Part A: Polym. Chem*. **2000**, 38, 3596-3603.
26. Monteiro, M. J.; de Brouwer, H. *Macromolecules* **2001**, 34, 349-352.
27. Venkatesh, R.; Staal, B. B. P.; Klumperman, B.; Monteiro, M. J. *Macromolecules* **2004**, 37, 7906-7917.
28. Kwak, Y.; Goto, A.; Komatsu, K.; Sugiura, Y.; Fukuda, T. *Macromolecules* **2004**, 37, 4434-4440.
29. Goto, A.; Sato, K.; Tsujii, Y.; Fukuda, T.; Moad, G.; Rizzardo, E.; Thang, S. H. *Macromolecules* **2001**, 34, 402-408.
30. Kubo, K.; Goto, A.; Sato, K.; Kwak, Y.; Fukuda, T. *Polymer* **2005**, 46, 9762-9786.
31. Benaglia, M.; Rizzardo, E.; Alberti, A.; Guerra, M. *Macromolecules* **2005**, 38, 3129-3140.
32. Chong, Y. K.; Krstina, J.; Le, T. P. T.; Moad, G.; Postma, A.; Rizzardo, E.; Thang, S. H. *Macromolecules* **2003**, 36, 2256-2272.
33. Chiefari, J.; Mayadunne, R. T. A.; Moad, C. L.; Moad, G.; Postma, A.; Rizzardo, E.; Postma, A.; Skidmore, M. A.; Thang, S. H. *Macromolecules* **2003**, 36, 2273-2283.
34. Moad, G.; Chiefari, J.; Mayadunne, R. T. A.; Moad, C. L.; Postma, A.; Rizzardo, E.; Thang, S. H. *Macromol. Symp*. **2002**, 182, 65-80.

35. Li, C.; Benicewicz, B. *Polym. Prepr*. **2005**, 46(2), 247-275.
36. Li, C.; Benicewicz, B. *Macromolecules* **2005**, 38, 5929-5936.
37. Baum, M.; Brittain, W. J. *Macromolecules* **2002**, 35, 610-615.
38. Takolpuckdee, P.; Mars, C. A.; Perrier, S. *Org. Lett*. **2005**, 7, 3449-3452.
39. Peng, Q.; Lai, D. M. Y.; Kang, E. T.; Neoh, K. G. *Macromolecules* **2006**, 39, 5577-5582.
40. Husseman, M.; Malmstrom, E. E.; McNamara, M.; Mate, M.; Mecerreyes, D.; Benoit, D. G.; Hedrick, J. L.; Mansky, P.; Huang, E.; Russell, T. P.; Hawker, C. J. *Macromolecules* **1999**, 32, 1424-1431.
41. Bian, K. J.; Cunningham, M. F. *J. Polym. Sci., Part A: Polym. Chem*. **2005**, 43, 2145-2154.
42. Perrier, S.; Takolpuckdee, P.; Mars, C. A. *Macromolecules* **2005**, 38, 6770-6774.
43. Nguyen, D. H.; Vana, P. *Polym. Adv. Technol*. **2006**, 17, 625-633.
44. Zhao, Y.; Perrier, S. *Macromolecules* **2006**, 39, 8603-8608.
45. Nguyen, D. H.; Wood, M. R.; Zhao, Y.; Perrier, S. V., P *Macromolecules* **2008**, 41, 7071-7078.
46. Li, C.; Han, J.; Ryu, C. Y.; Benicewicz, B. *Macromolecules* **2006**, 39, 3175-3183.
47. Yang, H.-H.; Zhang, S.-Q.; Chen, X.-Q.; Zhaung, Z.-X.; Xu, J.-G.; Wang, X.-R. *Anal. Chem*. **2004**, 76, 1316-1321.
48. Tanaka, T.; Matsunaga, T. *Anal. Chem*. **2000**, 72, 3518-3522.
49. Matsunaga, T.; Kwasaki, M.; Yu, X.; Tsiujimura, N.; Nakamura, N. *Anal. Chem*. **1996**, 68, 3551-3554.
50. Dresco, P. A.; Zaitsev, V. S.; Gambino, R. J.; Chu, B. *Langmuir* **1999**, 15, 1945-1951.
51. Ding, S.; Xing, Y.; Radosz, M.; Shen, Y. *Macromolecules* **2006**, 39, 5921-5928.

Chapter 2:
Historical and theoretical background

2.1 Magnetite nanoparticles

2.1.1. Introduction

Nanoparticles have attracted increasing attention over the past decade due to their unique size, physical, chemical, optical, mechanical and magnetic properties.[1,2] They are typically particles of 100 nm or less in all three dimensions, and are of the most commonly used particles in modern science.[3] This is because of their greater magnetic susceptibility, high saturation magnetization, ease of modification and manipulation, and strong magnetic behaviour.[4]

A magnetic nanoparticle (MNP) of formula Fe_3O_4 is a black material with strong magnetic behaviour, and it has a crystal-containing spinal structure. It contains both iron(II) (Fe^{2+}) and iron(III) (Fe^{3+}).[5,6] The magnetic behaviour of the MNPs is largely affected by the morphology, size and physical characteristic of the individual particles, and interface-to-face interactions.[3,7] It can be described by measuring the change of magnetic moment over the strength of an external magnetic field, using a vibrating sample magnetometer (VSM).[8] MNPs with sizes ranging from 1 – 20 nm are of a great interest in many applications due to their unique strong magnetic properties.[9]

Fe_3O_4-based MNPs behave as superparamagnetic nanoparticles. In the absence of an external magnetic field each MNP's net magnetization points in different directions, or approximately zero (in most cases we would expect only a single magnetic domain per MNP), thus the overall bulk magnetic moment is zero.[9,10] When an external magnetic field is applied, magnetism can be induced to these MNPs. This occurs because of the magnetic interaction between these MNPs and the applied field aligns the magnetization of the MNPs along the field.[2,9]

MNPs have been widely used in the immobilization and separation of proteins or enzymes, drug delivery and purification of DNA.[11-15] They have also been used for the removal of catalyst, and toxic elements from industrial wastes.[16,17] Nanomagnetic films are widely used in electrical and electronic devices, sensors, high density digital storage

devices, and electromagnetic shielding.[18] Magnetite films have also been widely studied and applied in tumorhyperthermia and as magnetic field guide carriers for localizing radioactive therapies and drugs.[10,19]

2.1.2 Synthesis of magnetic nanoparticles

There are three general methods of synthesis of crystalline nanoparticles, and MNPs: chemical routes from solution, physical vapour deposition and mechanical attrition.[3] In the physical vapour deposition method the nanoparticles are formed by the assembly of the particles from small individual atoms, while the mechanical attrition method is based on the fracturing of large-grained materials to form small particles.[3] MNPs are most commonly prepared by chemical routes, using divalent and trivalent iron salts in reactions with hydroxide bases (pH 9 – 10).[10]

In this study it is the chemical route that will be used for synthesis of the MNPs. The method has advantages over the physical and mechanical attrition methods. It allows control of the size, size distributions, and morphology of the prepared MNPs.[20] Agglomeration of the MNPs during the synthesis can be controlled by controlling parameters that determine nucleation and growth. Most important is the ease with which the MNP surfaces can be modified during and after synthesis, which can provide for additional functionality to the MNP surfaces.

Practically, the chemical synthesis of the MNPs can also be divided into different methods. These methods, are, in principle all based on chemical reactions between reactants. The MNP sizes, size distribution, and structural defects, are dependent on the preparation method. The most widely used methods are now briefly discussed (Sections 2.1.2.1 – 2.1.2.5).

2.1.2.1 Co-precipitation from solution

The co-precipitation method is one of the most commonly used methods for the synthesis of the MNPs. It offers rigorous control of size and shape of particles, and affords a large quantity of MNPs in high yield.[21] The method involves dissolving a metal precursor of

Fe^{2+} and Fe^{3+} with ammonium hydroxide in water (pH 9 – 10) to form a black dispersion of Fe_3O_4.[1] The chemical reaction that leads to Fe_3O_4 precipitation under non-oxidizing conditions is shown in Scheme 2.1.[11]

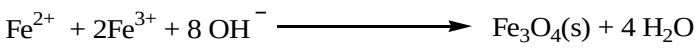

Scheme 2.1: Preparation of MNPs of formula Fe_3O_4 by the co-precipitation method.

The thermodynamic modeling of this reaction revealed that complete precipitation of Fe_3O_4 is expected in the pH range 9 – 10 when a molar ratios of Fe^{2+}/ Fe^{3+} = 1:2 is used, under non-oxidizing conditions.[22]

Under oxidizing conditions Fe_3O_4 oxidizes to form hematite (Fe_2O_3), as described in the following reactions.

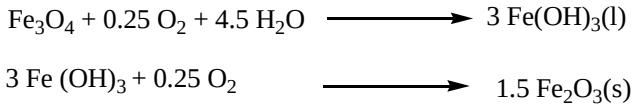

Scheme 2.2: Reactions of Fe_3O_4 under oxidizing conditions to form hematite (Fe_2O_3).

The choice of the precipitating agent plays an important role in the determination of the overall particle size and purity of the product. The precipitating agents that have been used in the past include citric and oxalic acid.[23-25] The chelating effect in those cases, facilitates a complete precipitation of Fe_3O_4. The precipitating agent can then be evaporated through subsequent heating cycles, and the metal hydroxides (Fe_2O_3) can easily be precipitated in alkaline media, resulting in products with less agglomeration.[3]

2.1.2.2 Microemulsion method

The microemulsion method is based on the oxidation of the metal precursors (Fe^{2+} and Fe^{3+}) in the presence of surfactants in small aggregates (e.g. micelles). A surfactant such as sodium dioctyl sulfosuccinate (aerosol AOT) is commonly used in this method.[26] The advantage of this method is that it offers good control over the size of the prepared

MNPs.[21] The main drawback of this method is however that it is limited by the low maximum achievable yield of the prepared MNPs, compared to the co-precipitation and thermal decomposition methods.

2.1.2.3 Polyol method

In this method the polyol (e.g. polyethylene glycol) acts as the solvent for the metal precursors, and the reducing agent.[21,27,28] Stirring a mixture of a polyol and metal precursors, followed by heating the mixture to the boiling point of the polyol, affords fine metallic particles of Fe_2O_3. Improved control over the particle size can be obtained by seeding the medium with foreign particles.[21]

2.1.2.4 Thermal decomposition method (an organic phase process)

The organic phase process is based on the reaction of iron(III) acetylacetonate, $Fe(acac)_3$, in phenyl ether, with a long-chain alcohol at high temperature (260 °C).[20] Monodisperse MNPs can be produced using this method.

2.1.2.5 Other methods

The above four methods are the most widely used for the synthesis of MNPs, however, there are other synthetic methods described in the literature, including: borohydride reduction, hydrothermal, electrochemical/electrodeposition and sol – gel methods, and flammable spry methods which has recently been developed to an industrial scale.[3,20,29,30]

2.1.3 Stabilization (coating, or surface modification) of the MNPs

Stabilization (coating, or surface modification of MNPs) is often necessary to prevent the formation of a large cluster of MNP aggregates. Large clusters of aggregates occur during or after the synthesis of the MNPs because of the van der Waals forces between the MNPs and the tendency of these particles to minimize the total surface energy.[31,32] MNP aggregation makes these MNPs unsuitable for use in applications in industry and fields where dispersed particles are required.[6] Stabilization and surface modification of the particles with small organic molecules, or polymers, not only prevents uncontrollable

growth of magnetite particles and protects them from the aggregation, but also allows them to be dispersed in various organic solvents.[10]

One of the practical methods used to stabilize the MNPs is the electrostatic stabilization method. This method, as illustrated in Figure 2.1, is based on the creation of an electrical double layer of charges around the particles, which results in repulsive forces between the MNPs (e.g. ionic surfactant). The repulsive force is dependent on the ionic strength, pH and the concentration of the medium.[22]

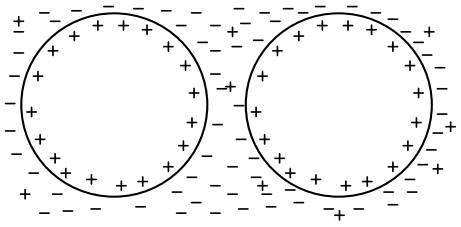

Figure 2.1: Electrostatic stabilization of MNPs.

The MNPs can also be coated by suitable surfactants such as sodium oleate (NaOl).[31] Surfactants are used during and after the synthesis of the particles to reduce particle surface tension by increasing the steric repulsive forces.[3] The surfactant's chemical nature and properties are also important for offering good dispersion conditions.[10] Another form of stabilization is achieved by coating (grafting) a polymer shell onto the MNPs (Figure 2.2). These polymeric chains provide steric stabilization that will prevent particle aggregation.[22]

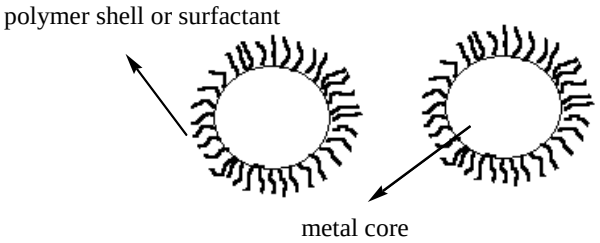

Figure 2.2: MNPs coated with a surfactant or a polymeric shell.

2.1.4 Surface functional groups of the MNPs

The exposed Fe atoms at the surface of the MNPs (Fe_3O_4) in an aqueous medium coordinate with hydroxyl ions or water molecules, which share their lone electron pairs with the Fe. The adsorption of water molecules causes them to dissociate, leading to a surface covered by hydroxyl groups coordinated to the Fe atoms. Hydroxylation of iron oxide is usually a fast reaction. It is followed by the adsorption of water molecules that are hydrogen bonded to the surface hydroxyl groups. These functional groups possess two pairs of electrons and a dissociable hydrogen atom that enables them to react with bases and acids. Depending on the crystal structure of the MNPs the hydroxyl group can be coordinated to one, two or three Fe atoms. A geminal group in which two hydroxyl (OH) groups are coordinated to one Fe atom might also occur. These types of coordinations are shown in Figure 2.3.[33]

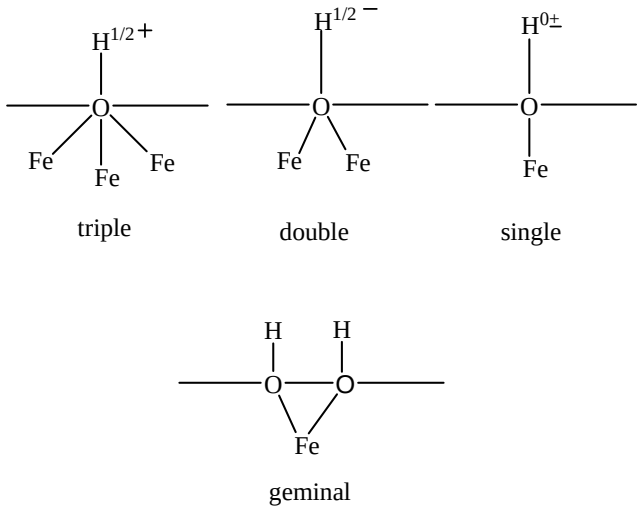

Figure 2.3: Single, double, triple and geminal coordinations of surface hydroxyl groups on iron oxides.

2.1.5 Anion adsorption

Anions are ligands with one or two atoms bearing lone electron pairs, and are negatively charged. Ligands might either be specifically or non-specifically adsorbing.

In the specifically adsorbing case, the hydroxyl group on the MNP is replaced by an adsorbing ligand (L^-), as shown in Scheme 2.3. It involves direct coordination of the adsorbing species to the MNP surface, and no solvent molecule is involved between the adsorbing species and the metal surface. Anions that adsorb specifically onto MNPs include phosphate, selenite, chloride, fluoride, citrate and oxalate.[34]

$$FeOH + L^- \longleftrightarrow FeL + OH^-$$

$$Fe(OH)_2 + L^- \longleftrightarrow Fe_2L + 2\,OH^-$$

Scheme 2.3: Specific ligand (L) exchanges on Fe MNPs.

Non-specifically adsorption is dominated by electrostatic adsorption and at least one water molecule interposes between the anion and the metal surface. Examples of non-specific adsorbing ions are nitrate and perchlorate ions (these were not used in this study).

Anion adsorption is dependent on the pH of the solution and the concentration of the adsorbent.[34] At any pH, anion adsorption increases as the concentration of the adsorbing ions increase and reaches a maximum level at lower pH, but decreases as the pH of the solution increases, except, however, in the case of silicate adsorption.[34]

2.1.6 Modes of coordination

The adsorption of ligands to an oxide surface can either yield mononuclear monodentate, mononuclear bidentate or binuclear complexes, as shown in Figure 2.4.

Monodentate complexes are formed by the adsorption of monocarboxylic acids either from the vapour phase or an organic solvent.[34] Phosphate, sulphate and selenite ions form binuclear complexes with the surface of iron oxides.[35]

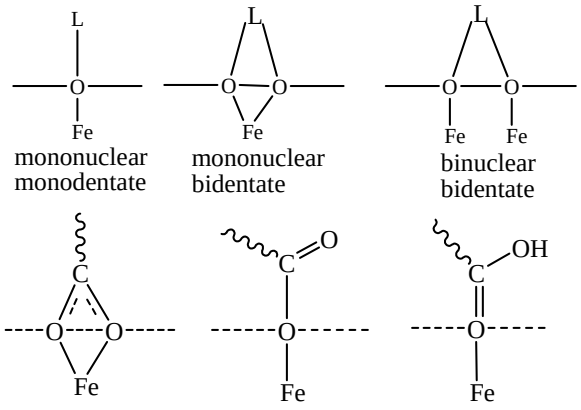

Figure 2.4: Ligand coordination to the iron oxide surface and modes of coordination through acid (COOH) groups.

2.2 Organic/inorganic nanomaterials

2.2.1 Introduction

There is considerable interest in the synthesis of organic/inorganic nanomaterials that can be manipulated by external stimuli such as thermal, electrical or magnetic field stimuli. These materials are nanostructured materials that combine the characteristics of inorganic and organic materials within the same composite. Magnetic-polymeric materials are interesting materials due to the combination of the inorganic magnetism and the polymeric properties, and have been widely studied.[36]

There are three basic approaches to the synthesis of a polymer grafted onto a solid support: the "grafting-onto", "grafting-from", and "grafting-through" approaches.[37] In the "grafting-onto" approach end-functionalized polymers react with appropriate surface-modified particles (e.g., MNP surface modified by oleic acid). In this case the end-functionalized polymer can be grafted onto the surface of the particle via ligand exchange (surface transformation) of oleic acid.[38] The main advantage of this method is that it is easy to perform. The drawback of the method is that the total number of polymer chains that can be grafted per unit surface area is limited due to steric hindrance imposed by the already grafted chains, making it difficult for other chains to penetrate and reach the surface of the particle.[37]

In the "grafting-from" approach, the polymer chains grow directly from the surface of particles using an initiator attached to the surface of particles The initiator can either be a free radical, ionic, a ring-opening event or controlled radical species, all of which have been widely used for the synthesis of polymer grafted onto solid surfaces by means of this approach.[39-44]

In the "grafting through" approach, the polymer chain grafted onto the surface of particles using copolymerization of a macromonomer or polymer with end functional polymerizable group attached to the surface of particles, with another monomer.

Recently, significant attention has been given to the use of the Reversible Addition-Fragmentation Chain Transfer (RAFT) process for the synthesis of well-defined polymers grafted onto silica, silicate, gold, silicon (100TM), and Merrifield resin.[37,45-50] Recently, polymers grafted onto magnetite nanoparticles using a free RAFT agent in solution and peroxide generated radicals on MNPs surfaces have been reported.[51]

2.3 Free radical polymerization

2.3.1 Introduction

Free radical polymerization (FRP) is one of the most versatile synthetic techniques for the synthesis of polymers that can be carried out under reasonably undemanding conditions.[52] The main advantage of FRP over the ionic and coordination polymerization techniques is its tolerance of traces of impurities (oxygen, solvents and water). As a result, it is now one of the most widely used polymerization techniques for the production of high molecular weight polymers. FRP has limitations in terms of control over the molecular weight and molecular structure of the produced polymer.

Vinyl monomers are the most common monomers used in FRP. The R and X substitutions on the vinyl group (Figure 2.5) are the main factors that affect the reactivity of the monomer. They also determine the applicability of this monomer in FRP. The R group should stabilize the radical that forms in FRP, and therefore that monomer will be more reactive than in the case where the R group destabilizes the radical (e.g., compare

styrene (St) with vinyl chloride, respectively). The substitution groups (R and X) on the vinyl monomer also have an impact on the propagation rate coefficient of the monomer in FRP. Different propagation rate coefficients of different monomers have been reported in the literature.[53]

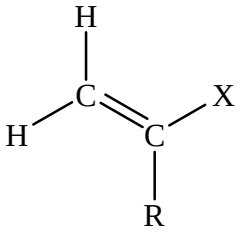

Figure 2.5: Substitutions on a vinyl monomer.

FRP is performed in solution, emulsion and bulk polymerizations. This makes it highly applicable in the industry for the synthesis of different polymers. Polystyrene (PSt), polymethyl methacrylate (PMMA), and polymethyl acrylate (PMA) are the most common polymers produced using this technique. Much effort therefore has been made to obtain a basic understanding of kinetic steps of FRP.

2.3.2 Kinetics of free radical polymerization

The main three reactions in free radical polymerization are initiation, propagation and termination.

1. **Initiation:**

Generation of radicals is the first step in FRP. The radicals can be generated thermally, photochemically, by radiation or by a redox process.[54,55] Thermal initiation using azo compounds, such as 2,2′-azo-bis(isobutyronitrile) (AIBN), are discussed here. In thermal initiation, the radicals are generated by homolytic thermal cleavage of the covalent bond. Among the most common initiators used in this case are the azo and peroxide initiators, which have been well reviewed in the literature.[54,56] Typical examples of the thermal hemolytic cleavage of benzoyl peroxide and AIBN are described in Scheme 2.4.

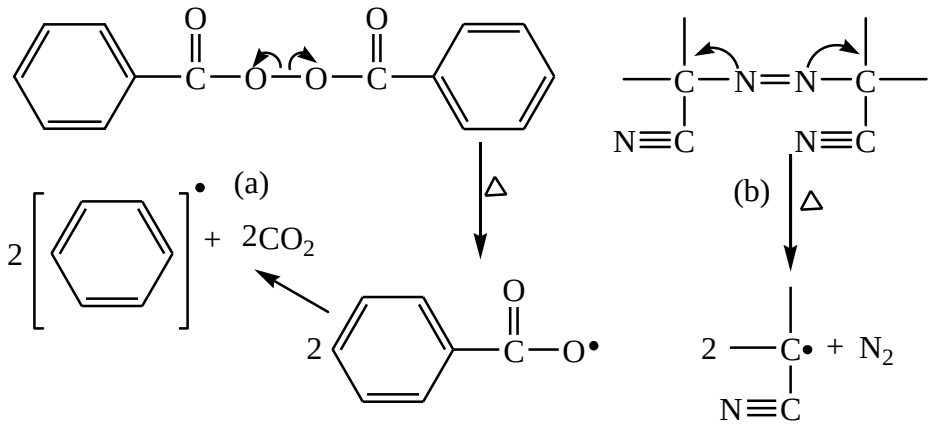

Scheme 2.4: Homolytic thermal cleavage of (a) benzoyl peroxide and (b) 2,2′-azo-bis(isobutyronitrile).

The initiation step in FRP can be generally described as:

$$I \xrightarrow{k_d} 2\ I^{\bullet}$$

Accordingly, the decomposition rate of the initiator (loss event) can generally be defined as follows:

$$-\frac{d[I]}{dt} = k_d\,[I] \qquad (2.1)$$

where k_d is the constant rate coefficient for the decomposition of initiator I.

It should be noted however that the generation efficiency of the primary radicals is not always 100%, and it is dependent on the type of the initiator and the temperature of the reaction. Therefore, the fraction of the radicals generated during the polymerization (efficiency of the initiator *f)* is also an important factor to be considered. The general rate of the initiation can be then described as follows:

$$R_i = \frac{d[I^{\bullet}]}{dt} = 2f\,k_d\,[I] \qquad (2.2)$$

where R_i is the rate of the initiation (i.e. the rate of production of radicals), f is the efficiency of the initiator for generating primary initiating radicals, and [I] is the initiator concentration.

The rate of initiation is multiplied by factor of 2 because usually two radicals are generated from one initiator molecule. It should also be noted that the primary generated radicals might not only react with the monomer, but might rather react with solvent, which may also undergo fragmentation and rearrangement to produce new radical species (secondary radicals).[54,56] However, to simplify the polymerization mechanism, it will be assumed here that the primary radicals only react with the monomer, and which will lead to the second step of the polymerization (propagation).

2. Propagation:

The sequence addition of the primary generated radicals to the monomer comprises the propagation step. The propagation step is described as follows:

$$P_n^{\bullet} + M \xrightarrow{k_p} P_{n+1}^{\bullet}$$

The propagation rate (that excludes any other competition fates for the propagating radicals, which can be significant, and it makes this approximation of the propagation rate poor) is described as:

$$R_p = k_p [P^{\bullet}][M] \qquad (2.3)$$

where R_p is the rate of radical propagation, k_p is the propagation rate coefficient, $[P^{\bullet}]$ is the concentration of propagating radicals, and [M] is the monomer concentration

The rate of the monomer addition to the propagating radical is largely affected by the monomer structure.[57] The propagation rate of many monomers, specified according to α-substituents ranging from hydrogen to methyl and others, has also been reported in the literature: the propagation rate decreases as the substituents change from hydrogen to methyl, and to even more bulky groups.[58]

The k_p is largely dependent on the nature of the monomer and reactivity of the propagating radical. Entropic and electronic factors both influence the absolute value of the propagation rate coefficient. Furthermore, the reactivity of the monomer and that of the propagating radical are opposite to each other. For instance, ethene is an unreactive monomer while an ethene macroradical is extremely reactive, and; on the contrary, St

monomer is a very reactive monomer, but the reactivity of a St macroradical is highly stabilized by the adjacent phenyl group.[59] The propagation rate coefficients in free radical polymerization are also assumed to be dependent on the chain lengths. This is supported by experimental evidence, even for chain lengths longer than 20 monomer units.[60] It is also reported that the propagation rate coefficient for a monomeric radical in the first steps in FRP of methyl methacrylate (MMA) is approximately 16 times greater than the propagation rate coefficient for a radical of a longer chain length, showeing that the propagation rate coefficient of this system is truly chain length dependent.[61,62]

The influence of the solvent on the propagation rate coefficient has been widely studied and it was found that there is no significant influence of the solvent on the propagation rate coefficient.[62] The solvent influence on the propagation rate has only been observed for some specific monomers, including water-soluble monomers such as acrylic acid and ethyl-α-hydroxy methacrylate (which are different from the monomers used in this study).[62]

The growing radicals will not last forever and there will be a point at which the radical activity is stopped by a termination process. Chain growth/radical activity can be stopped by quenching the reaction mixture. Eventaully this will stop chain growth by chain transfer reactions, coupling of the radical with another growing radical, or via a disproportionation termination reaction.

3. Termination:

The termination step might be considered as the most complex step in FRP. This is because of the heterogeneity of the termination reactions that might occur during the polymerization process. The reactions that can lead to chain termination are now discussed.

a. Termination by self reaction of the radicals (combination or disproportionation)

The radical–radical termination of the propagating radicals by combination and disproportionation are illustrated in Scheme 2.5.

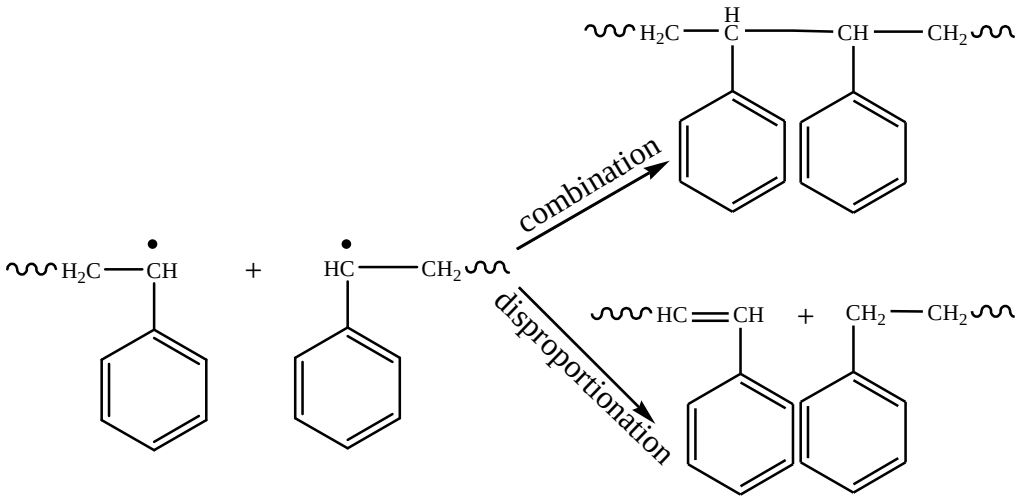

Scheme 2.5: Self-termination of two polymeric styryl radicals.

In termination caused by combination (also required for the disproportionation), two polymeric radicals must approach each other. This is why termination is now generally accepted to be a diffusion controlled process, even at low monomer conversion.[63] The termination reaction, by combination of two growing radicals, will result in a molecular weight equivalent to the sum of the molecular weights of the two growing radicals. The rate expression for self-termination via combination is described by:

$$R_{t,c} = \langle k_{tc} \rangle [P^{\bullet}]^2 \qquad (2.4)$$

where $R_{t,c}$ is the termination rate by combination, the factor 2 is included since two radicals are lost in one reaction, and $\langle k_{tc} \rangle$ is the average termination rate coefficient for termination by combination.

On the other hand, termination by disproportionation occurs by the abstraction of a hydrogen atom from one of the growing radical ends, yielding two stabilized polymer chains. This is illustrated in the lower branch of Scheme 2.5. The expression of termination by disproportionation is:

$$R_{t,d} = 2 \langle k_{td} \rangle [P^{\bullet}]^2 \quad (2.5)$$

where $R_{t,d}$ is the termination rate by disproportionation, the factor 2 is included since two radicals are lost, and two dead chains are produced in one reaction, and $\langle k_{td} \rangle$ is the rate coefficient of termination by disproportionation.

Accordingly, the overall termination rate expression, taking into account both coupling and disproportionation, can be described as follows:

$$R_t = 2\langle k_t \rangle [P^{\bullet}]^2 \quad (2.6)$$

where $2k_t = \beta k_{td} + (1- \beta) k_{tc}$

where β is the fraction of disproportionation

The termination modes might be largely affected by the monomer structure and, to a lesser extent, the reaction conditions and temperature. Most of styrene polymerization studies have shown that termination in polystyrene prepared via FRP is predominately by combination of two growing radicals.[64-69] However, recent studies also show that termination by disproportionation might also take place in FRP of styrene.[70] On the other hand, the nature of termination of PMMA prepared via FRP is predominantly by disproportionation.[71] This might be attributed to the steric effects occurring when two growing radicals approach each other. A slight effect of the temperature on the disproportionation reaction for MMA polymerization is reported in the literture.[72]

In order to derive an overall (classical) rate expression of FRP a constant radical concentration should be assumed. This, in other words, is called steady state polymerization, which is characterized by a constant propagating radical concentration and resulting rate of polymerization (i.e $d[P^{\bullet}]/ dt = 0$). In this case the rates of initiation and termination are equal (Equation 2.2 is equal to Equation 2.6) and the propagation rate can be described as follows:

$$R_p = k_p \left(\frac{f k_d [I]}{\langle k_t \rangle} \right)^{0.5} [M] \qquad (2.7)$$

By assuming steady state polymerization, the monomer concentration can be described as follows:

$$[M] = [M]_0 \, e^{-k_p \left(\frac{f k_d [I]}{\langle k_t \rangle} \right)^{0.5} t} \qquad (2.8)$$

where $[M]_0$ is the initial monomer concentration and t is the reaction time.

b. Chain transfer reactions

The reaction of the propagating radicals with a non-radical species (e.g. monomer, and solvent) to produce a dead polymer chain and a new radical that is capable of initiating new polymer chains is called a transfer reaction. In this case radicals are not truly killed but chain growth of the original chain has effectively ceased. An example of the chain transfer reaction of a propagating radical and a non-radical substrate (X-Y) is described in Scheme 2.6. The transfer agent (X-Y) might be a deliberate additive (e.g. thiol) or it may be a solvent, monomer, polymer or initiator. Deliberate additives are usually added and used to control the molecular weight of the polymer (especially in a system with extensive branching, which can be used to reduce the number of branches per chain, which will reduce cross-linking/gelation, which can be a major problem), or the polymer end groups, or to control the polymerization rate and exotherm (formed due to the gel effect).[73]

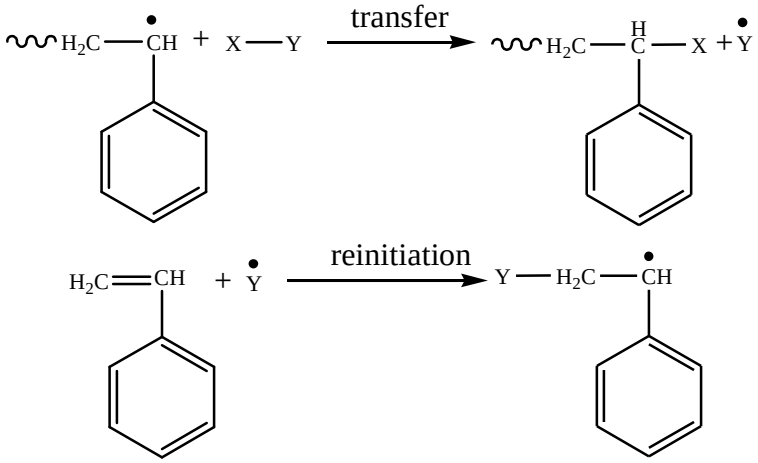

Scheme 2.6: Example of chain transfer reactions for styrene.

The general definition of the chain transfer constant (C_{tr}) is described in equation (2.9).

$$C_{tr} = \frac{k_{tr}}{k_p} \tag{2.9}$$

The effect of the chain transfer constant in a radical polymerization is largely dependent on the reaction conditions (temperature, solvent, monomer, and radical concentration). Because chain transfer reactions will terminate the growing radical and generate a new radical species ($Y^{\bullet}$), the reaction might therefore not affect the polymerization rate. However, the transfer reaction will influence the chain length of the propagating species, which will enhance the termination rate. In radical polymerizations affected by the chain transfer reactions the average degree of the polymerization ($\bar{X}_n$) can therefore be described as follows:

$$\frac{1}{\bar{X}_n} = \frac{(1 + \beta)\langle k_t \rangle [P^{\bullet}]}{k_p[M]} + C_M + C_s\frac{[S]}{[M]} \tag{2.10}$$

where β is the fraction of termination due to disproportionation, $\langle k_t \rangle$ is the average termination rate coefficient, C_M is the chain transfer constant to monomer, C_s is the transfer constant to solvent, and [S] is the solvent concentration.

2.4 Controlled/ "Living" Radical Polymerization

Although FRP may be considered as one of the most applicable polymerization techniques, contributing to about 50% of the world produced polymers,[74] it does have limitations, particularly in terms of control the molecular weight, molecular weight distribution, and polymer architectures, mainly due to the high reactivity of the propagating radicals and their high probability of undergoing bimolecular termination. It is also not easy to obtain end group functionalized polymers via FRP. Therefore, it was necessary to develop new techniques to cover industrial demands.

One of the early techniques that was developed in this area to provide control over the molecular weight and polydispersity of polymers was ionic polymerizations (cationic or anionic polymerizations).[75] This technique is however not as tolerant as FRP to

impurities, and the polymerization and copolymerization of different functional vinyl monomers, due to the incompatibility of the chain end cation or anion with different functional monomers.[76] This limitation motivated scientists to develop newer and more reliable synthetic polymerization techniques, such as Controlled/"Living" Radical Polymerization (CLRP).

The first step in the development of CLRP polymerization dates back to the early 1980s when it was found that the use of iniferter systems exhibited a degree of livingness.[77,78] Extensive research then led to the development of more successful and convenient living polymerization techniques such as Nitroxide-Mediated Polymerization (NMP), Atom Transfer Radical Polymerization (ATRP), and RAFT that made possible the production of polymers with narrow polydispersity index (PDI), tailored molecular weight, and defined molecular architectures.[74,79-92] Xanthate-Mediated Polymerisation (called MADIX) is also a living polymerization technique that yields macromolecular design via interchange.[93] Other living polymerization techniques such as Iodine Transfer Polymerization (ITP), Single Electron Transfer Degenerative Chain Transfer Mediated-Living Radical Polymerization (SET-DTLRP), Organotellurium-Mediated Polymerization (TERP), Organostibine Mediated-Polymerization (SBRP), Cobalt-Mediated polymerization (CMRP), Reversible Chain Transfer Catalyzed Polymerization, and Quinone Transfer Radical Polymerization have also been developed over the past few years.[94,95]

CLRP proceeds in such a manner that bimolecular termination is suppressed (but not stopped) by maintaining the majority of the growing chains in dormant form (see Scheme 2.7). This is in contrast to conventional FRP, where termination is the kinetic event that most shapes the MWD of the prepared polymer. All of the CLRP techniques developed to date basically operate by reversible activation and deactivation of the propagating radicals.

Scheme 2.7: Representation of a living system obtained via a transfer species.

The most well developed techniques in the field of LCRP are now discussed.

2.4.1 Atom Transfer Radical Polymerization

One of the recently developed living techniques in CLRP is ATRP. The technique was first reported in the literature in 1995.[86,96] The accepted mechanism of the technique is described in Scheme 2.8.[97]

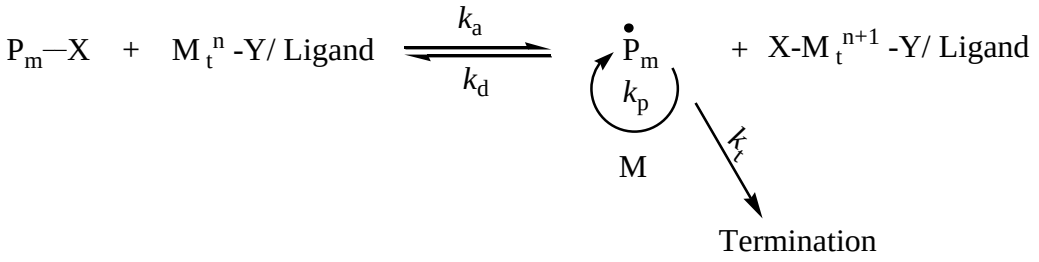

Scheme 2.8: Mechanism of the ATRP process.[93]

where k_a is the rate coefficient of activation, k_d is the rate coefficient of deactivation, k_p is the rate coefficient of propagation, and k_t is the rate coefficient of termination.

The process is based on the activation of the growing radical and deactivation of the dormant species in a reversible way. The radicals are usually generated by a reversible redox process that is catalyzed by the activator (X-M_t^n-Y/Ligand), which will abstract the halogen atom X from the dormant chain P_m-X to form a new ligand (X-M_t^{n+1}-Y/ Ligand) (see Scheme 2.8). The radicals then react reversibly with the oxidized metal complex (X-M_t^{n+1}-Y/ Ligand) to reform the dormant species. The polymer chain grows in a similar manner as in conventional radical polymerization through the addition of monomer (M) to the growing radicals. Termination in ATRP is attributed mainly to combination and disproportionation, and typically 5% or less of the polymer chains are terminated.[97] This is partially because the process generates oxidized metal complexes (deactivator), which

reduce the concentration of the growing radicals, and thus minimize the termination reactions. [98] The advantages of the process are its compatibility with various monomers and tolerance to traces of impurities. However, a drawback of the process is the difficulty of removing the metal catalyst from the produced polymer.

2.4.2 Nitroxide-Mediated Polymerization

The discovery of the NMP process was a key point for the development of CLRP. The process is widely reviewed in the literature.[85,99-101] The mechanism of this process is depicted in Scheme 2.9.[101] It is based on the persistent radical effect (PRE)[102-107] in which activation – deactivation of the growing radical ($P_n^{\bullet}$) with mediating radical species ($X^{\bullet}$) results in reduction of the overall propagating radical concentration and accordingly, a low amount of bimolecular termination.

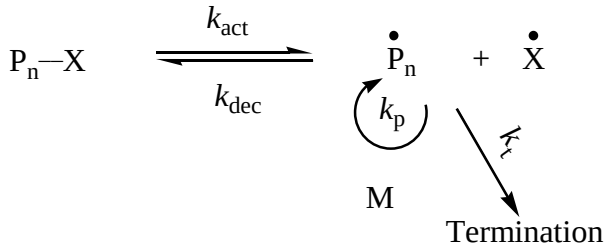

Scheme 2.9: Mechanism of the NMP process.[101]

The choice of $X^{\bullet}$ and its compatibility with different functional monomers plays a big role in obtaining well controlled polymers. A range of persistent or mediating radicals such as triphenyls,[108] (arylazo)oxy,[109] verdazyl,[110] triazonyl[111] and nitroxides[112] have been used in many systems. The most studied and apparently successful compounds to date are the nitroxides and their associated derivatives, such as 2,2,6,6-tetramethyl-1-piperidine hydroxyl free radical (TEMPO) and N-tert-butyl-N-(1-diethylphosphono-2,2-dimethylpropyl) nitroxide (DEPN) (Figure 2.6).[85,113]

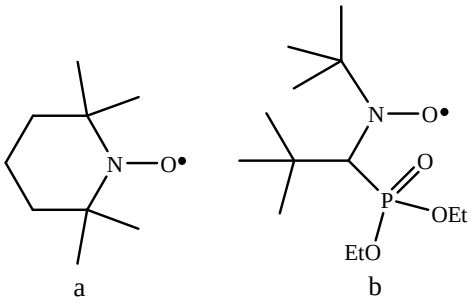

Figure 2.6: Structures of nitroxide derivatives (a) 2,2,6,6-tetramethyl-1-piperidine hydroxyl free radical (TEMPO), and (b) N-tert-butyl-N-(1-diethylphosphono-2,2-dimethylpropyl) nitroxide (DEPN).[114]

The first reported use of the nitroxides as radical mediators appeared in the early 1980s.[115] It was demonstrated that a nitroxide such as TEMPO (species (c) in Scheme 2.10) reacts at a controlled rate with free radical species (b) (generated from the radical addition of the initiator fragment (a) to a vinyl monomer) (see Scheme 2.10). The resulting radicals were stable under reaction conditions (40 – 60 °C), but produced low molecular weight polymers and oligomers at elevated reaction temperatures (80 – 100 °C).

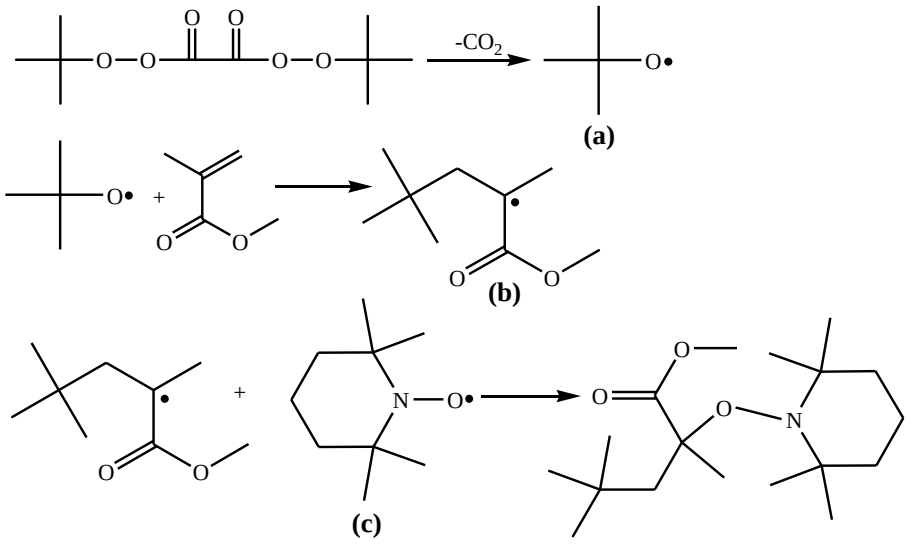

Scheme 2.10: Free radical TEMPO traps in normal free radical reactions at low temperatures (40 – 60 °C).[85]

2.4.2.1 Bimolecular nitroxide initiators

The second contribution in using nitroxides as radical mediators is a bimolecular process. The process is based on the reaction of benzoyl peroxide (Scheme 2.11a), free radical TEMPO and styrene monomer at 130 °C. High molecular weight PSt polymer with a low PDI was produced using this process.[116]

While the reaction of the free radical TEMPO with St monomer at 130 °C, as discussed above, displays the basic fundamentals of CLRP (as indicated by the high molecular weight with low PDI value of the produced PSt polymer), it should however be emphasized that this reaction is not a true living system; as termination events also occur.[113,117-119]

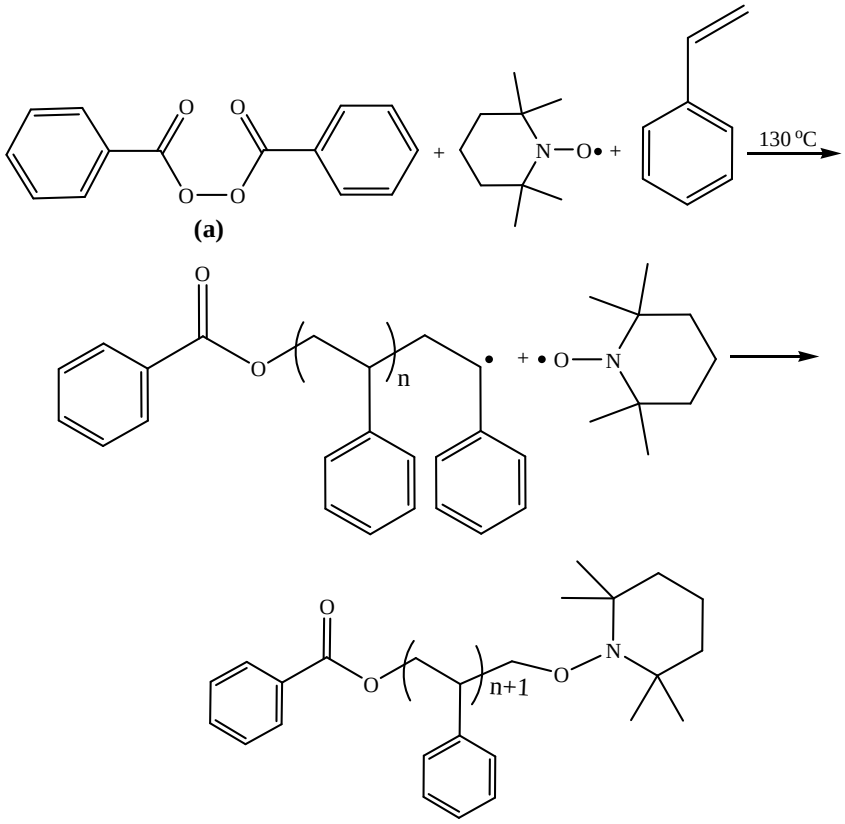

Scheme 2.11: Bimolecular process using free radical TEMPO, benzoyl peroxide initiator, and St monomer at 130 °C.[85]

2.4.2.2 Unimolecular nitroxide initiators

The success that was attained with the bimolecular process prompted scientists to develop well defined single unimolecular nitroxide initiators that would permit control over the molecular weight and MWD.[120,121] The unimolecular process is based on the homolytic thermal decomposition of an alkoxyamine based initiator (Scheme 2.12a) at elevated temperature to afford a stable TEMPO free radical and initiating radical (b). The initiating radical reacts with monomer to yield a polymeric radical (c) that can reversibly react with the free radical TEMPO to afford a dormant polymeric chain (d).

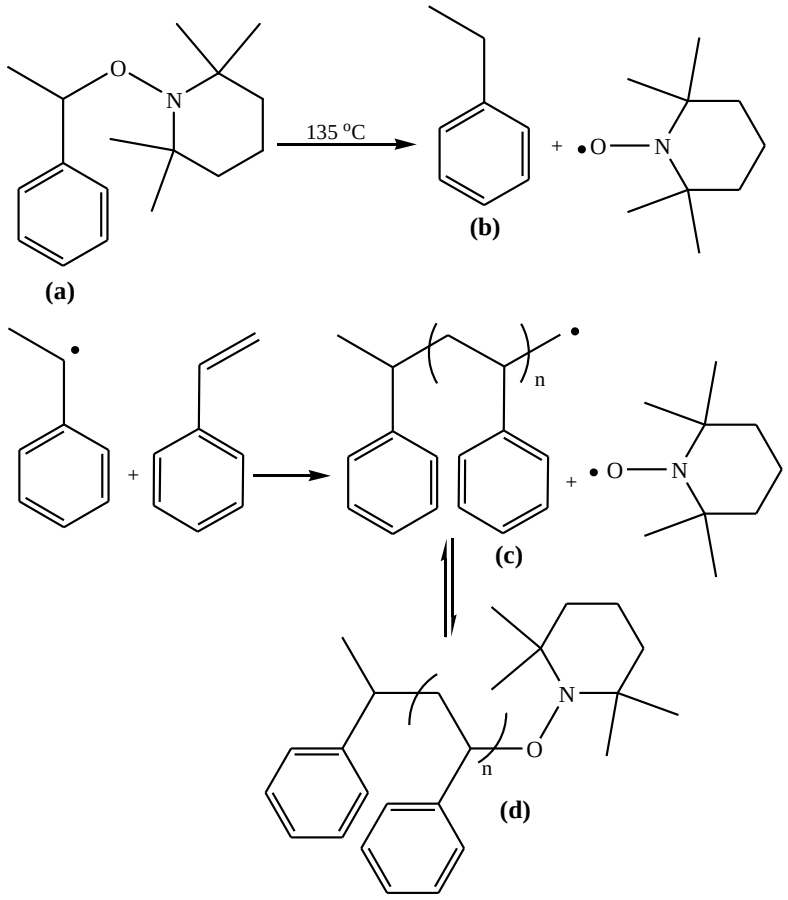

Scheme 2.12: Styrene polymerization mediated by thermolytically unstable unimolecular single alkoxyamine molecule (a) at 135 °C. [85]

2.4.2.3 New generations of nitroxides

Although TEMPO was successfully used to prepare PSt polymers, there were still problems associated with using it as a radical mediator. The high temperature and long reaction times required, and poor compatibility with a number of functional monomers, are the main problems that present when using free radical TEMPO. This has led to the development of a new generation of nitroxides that permit the synthesis of a number of polymers with controlled molecular weight and MWD. The first attempt at the developing the nitroxide mediation was based on changing the free radical TEMPO structure to yield oxo-TEMPO (Figure 2.7a).[122] While this was successful for the polymerization of acrylates, the PDI and living nature of the resultant polymers were poor.[122] The free radical TEMPO substituted with phosphoric acid in the 4-position (Figure 2.7b), which was believed to enhance the mediating ability via hydrogen bonding, was also used as radical mediator for the polymerization of St.[123] This was followed by a number of TEMPO structure modifications, such as the use of di-tert-butyl nitroxides, and the use of additives (e.g acetic acid anhydride and camphorsulfonic acid), to enhance the polymerization rate.[124-126]

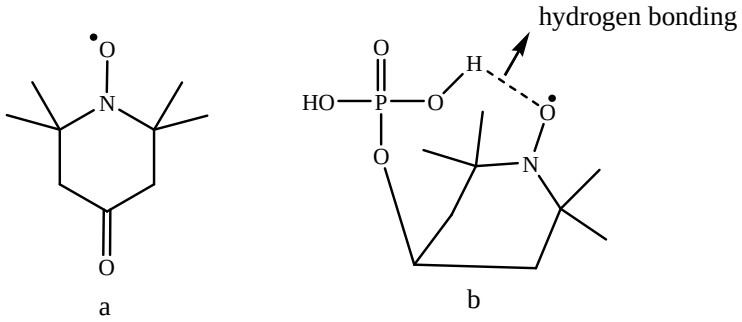

Figure 2.7: TEMPO-like structures: (a) oxo-TEMPO[122] and (b) free radical TEMPO substituted with phosphoric acid in the 4-position.[123]

A significant development and enhancement in nitroxide mediators that made the NMP competitive with other CLRP techniques was the use of alicyclic nitroxides bearing a hydrogen atom at the α-carbon, in contrast to the two quaternary carbons present in the free radical TEMPO. Phosphonate derivatives and arenes (Figure 2.8a and b,

respectively) are the best examples of such nitroxide developments.[127,128] The use of such nitroxide derivatives as radical mediators in NMP permitted the synthesis of acrylates, 1,3-dienes, acrylonitrile and acrylamide polymers in a controlled fashion with polydispersites as low as 1.05.[129]

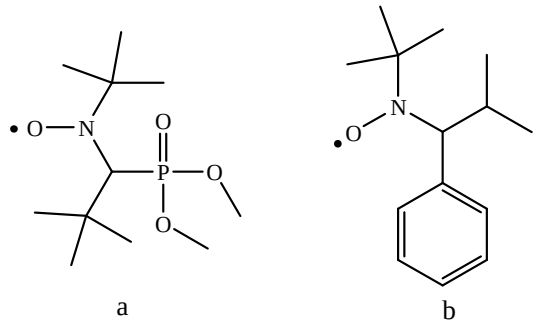

Figure 2.8: Alicyclic nitroxide derivatives (a) phosphonate derivative[127] and (b) arenes.[128]

2.4.3 Reversible Addition-Fragmentation chain Transfer

2.4.3.1 Introduction

The concept of a mechanism involving addition-fragmentation was first observed during a study of the chemistry of a method based on a macromonomer of a general structure (1) (Scheme 2.13), which functioned as chain transfer agents by an addition-fragmentation mechanism.[130]

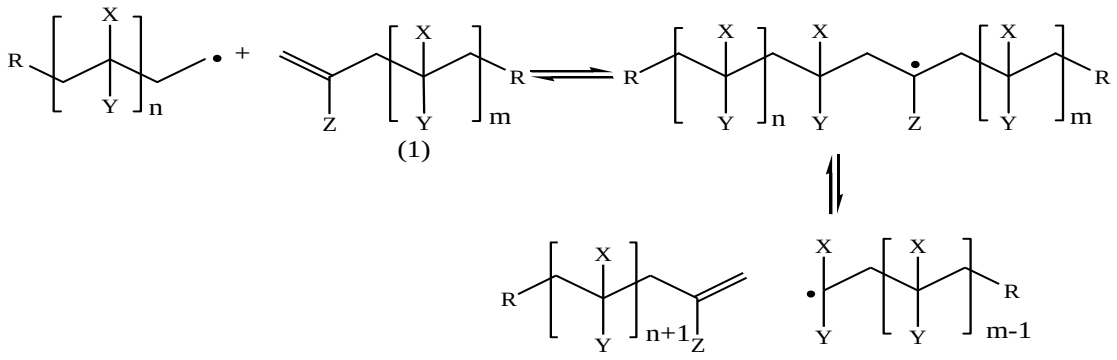

Scheme 2.13: Addition-fragmentation mechanism of a macromonomer functioning as a transfer agent.[120]

To demonstrate the living nature of these macromonomers, narrow PDI block copolymers based on methacrylates were prepared using this method.[130,131] Subsequently, the use of simple organic compounds carrying thiocarbonylthio moieties (S=C–S) was found to be more effective and versatile for inducing the living character by the addition-fragmentation mechanisism.[81,132,133] Accordingly, the terms RAFT process and RAFT agents were coined.[81] The generic structure of the RAFT agent consists of a Z group (stabilizing/activating group) and an R group (leaving group) (Figure 2.9).[134,135]

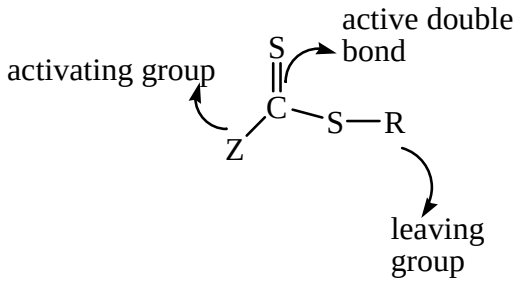

Figure 2.9: Structure of a RAFT agent.

Depending on the nature of the Z group, the RAFT agents can be divided into the following types:

Dithioester RAFT agents (Z = aryl or alkyl)[79,136-140]

Trithiocarbonate RAFT agents (Z = substituted sulphur)[80,141-143]

Dithiocarbamate RAFT agents (Z = substituted nitrogen)[84,144]

Flourodithioformate RAFT agents (Z = substituted fluorine)[145]

Dithiocarbonate (xanthates) RAFT agents (Z = substituted oxygen)[135,144,146]

Phosphoryl dithioformate RAFT agents (Z = substituted phosphoryl or thiophosphoryl dithioformates)[147]

The RAFT process is versatile, and compatible with different monomers and hence it has become one of the most versatile methods in LCRP for the synthesis of different and advanced polymer materials.[81,84,133,148]

2.4.3.2 RAFT mechanism

The mechanism of the RAFT process involves a series of addition-fragmentation reactions.[81] The most accepted mechanism of the RAFT process is described in Scheme 2.14.[81] This mechanism has been widely investigated using Electron Spin Resonance (ESR), NMR, UV/Vis spectroscopy and Matrix Assisted Laser Desorption Ionization Time-of-Flight Mass Spectrometry (MALDI-ToF-MS).[83,149-155]

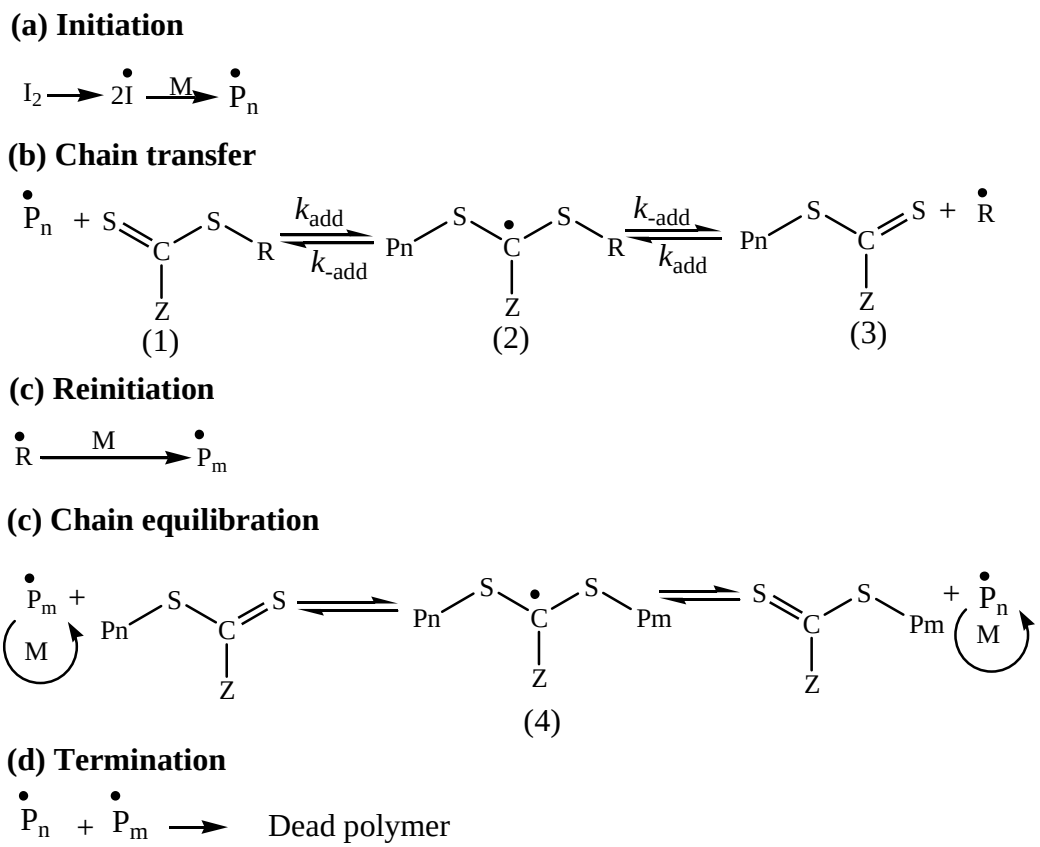

Scheme 2.14: The mechanism of the RAFT process.[81]

As in conventional FRP, the decomposition of the initiator leads to the formation of radicals that will add monomer units to form a polymeric radical ($P_n^{\bullet}$) with a degree of polymerization *n*. Addition of this polymeric radical to the RAFT agent **1** (Scheme 2.14) leads to the formation of an intermediate radical **2,** which can reversibly fragment to form polymeric RAFT agent **3** and a new radical ($R^{\bullet}$). The chain equilibration via the

intermediate radical **4** of the two polymeric radicals ($P_n^{\bullet}$ and $P_m^{\bullet}$) is the main step in the RAFT process.[46] When the polymerization is completed, the majority of the polymeric chains should contain the RAFT agent moieties. This feature has been confirmed by NMR and UV/Vis spectroscopy and MALD-ToF-MS.[81,151]

In the RAFT process, the molecular weight of the produced polymer is controlled by the stoichiometry of the reaction.[133,143] The predicted molecular weight can be reasonably estimated by the following equation:

$$M_{\mathrm{n}} = \frac{X \times [\mathrm{M}]_0 \times M_{\mathrm{monomer}}}{[\mathrm{RAFT}]_0 + 2f[\mathrm{I}]_0(1 - \mathrm{e}^{-k_{\mathrm{d}}t})}) + M_{\mathrm{RAFT}} \qquad (2.11)$$

where M_{n} is the predicted molecular weight, X is the conversion, $[\mathrm{M}]_0$ is the initial monomer concentration, $[\mathrm{RAFT}]_0$ is the initial concentration of the RAFT agent, M_{monomer} is the monomer's molecular weight, and M_{RAFT} is the RAFT agent's molecular weight.

2.4.3.3 The effectiveness of the Z and R groups of the RAFT agent

The effectiveness of the RAFT agent is strongly dependent on the nature of the Z (activating or mediating or living) and R (initiating or leaving) groups, the monomer, and the polymerization conditions.[133,143,156-161]

The Z group of the RAFT agent activates the dithiocarbonyl group toward free radical addition.[81] Therefore, since it is not a true transfer process, the effective transfer coefficient of the RAFT agent is affected by the choice of the Z group. The dependence of the transfer constant on the substituted Z, for St polymerization and other qualitative polymerizations, is summarized in Figure 2.10.[162,163] The arrows indicate the suitable Z groups for different monomers.

The choice and nature of the R group depends on the monomer being polymerized.[79] The R group should be a good leaving group with respect to the propagating radicals and

capable of reinitiating the polymerization. Poor leaving groups might lead to rate retardation and/or inhibition in the polymerization process.[162] The effect of the R group on the effectiveness of the RAFT agent for the polymerization of St, MMA and MA is summarized in Figure 2.11.[37,46,79,164-166] The arrows here also indicate suitable R groups for different monomers.

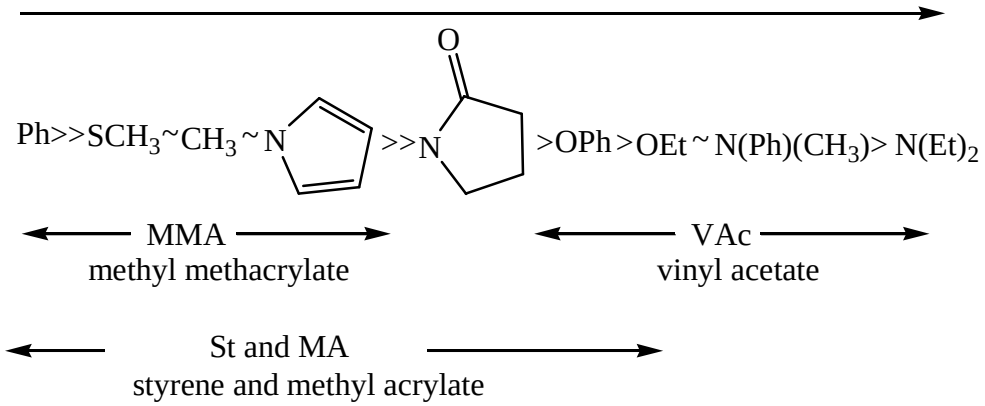

Figure 2.10: The dependence of the transfer constant on the substituent Z group for the polymerization of St, MA, MMA, and VAc monomers (top arrow indicates the decrease of the transfer constant of the RAFT agent (C_{tr}) with respect to the different Z groups).[84]

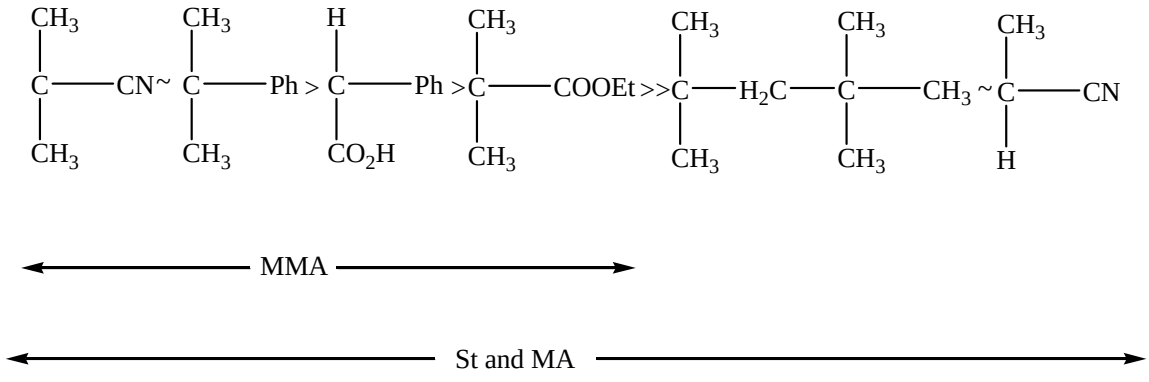

Fig. 2.11: The dependence of the RAFT agent on the substituent R group for the polymerization of St, MA, and MMA monomers.[84]

The initial design of the RAFT agent is crucial for the effectiveness of the synthesis of well defined polymers such as star, comb, and grafted polymers by means of the RAFT process polymerization. [47,167-169]

2.4.3.4 Retardation and side reactions in the RAFT process

One of the major effects related to the use of the RAFT process in free radical polymerization is rate retardation, which has been observed in some systems, particularly those mediated with RAFT agents that have phenyl activating Z groups.[79,164,170-172] Retardation in the polymerization of styrene and methacrylates mediated by a high concentration of the dithiobenzoate RAFT agent is also reported in the literature.[158,164,173-176] However, in polymerization reactions mediated by low concentrations of the RAFT agent, the polymerization rates usually differ from polymerization reactions mediated without RAFT agents.[164] Various reasons have been proposed for the retardation in the RAFT process. One research group postulated that slow fragmentation of the adducts **2** and **4** (Scheme 2.14) causes the retardation, as reported in the literature.[164,173,175,177,178] They attributed this slow fragmentation to the stabilization effect of the phenyl group (Z group) on the intermediate radical, which could increase the lifetime of the intermediate radical. The simulated lifetime of the intermediate radical in the styrene polymerization mediated by cumyl dithiobenzoate was found to be 15 s compared to 1.9 s in the case of phenyldithioacetate.[173] This difference might be attributed to the stabilization effect that the Z group of the RAFT agent has on the lifetime of the intermediate radical, which could lead to retardation due to the slow fragmentation. However, another research group has attributed the retardation to the irreversible cross-termination of the intermediate radical (Scheme 2.15b). This has been experimentally observed in polymerization mediated by RAFT agents with phenyl activating Z groups. [155,174,176] The retardation and side reactions in the RAFT process will be discussed in more detail in Chapters 5 and 6.

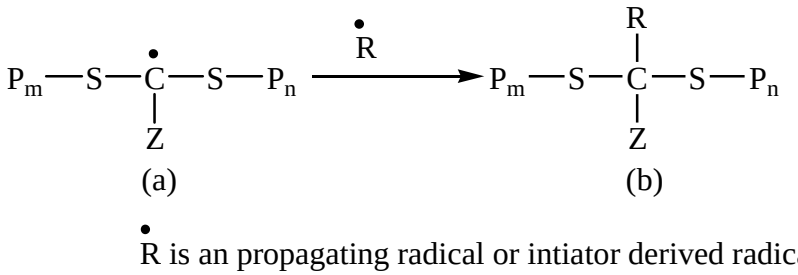

Scheme 2.15: Reaction of the intermediate radical in the RAFT process.

Other side reactions by transfer reactions to monomer, solvent, and termination by combination might also occur in the RAFT process as in conventional FRP. These transfer reactions might be negligible under some RAFT reaction conditions; however they might become significant under other reaction conditions. These possibilities will be discussed in more detail in Chapter 5.

2.5 References

1. Asmatulu, R.; Zalich, M. A.; Claus, R. O.; Riffle, J. S. *J. Magn. Magn. Mater.* **2005,** 292, 108-119.
2. Yang, H.-H.; Zhang, S.-Q.; Chen, X.-L.; Zhuang, Z.-X.; Xu, J.-Q.; Wang, X.-R. *Anal. Chem.* **2004,** 76, 1316-1321.
3. Nalwa, H. S., *Encyclopedia of Nanoscience and Nanotechnology* American Scientific Publishers: California, **2004**; Vol. 1, p 815-848.
4. Stark, D. D.; Weissleder, R. *Radiology* **1988,** 168, 297-301.
5. Cornell, R. M.; Schwertmann, U., *The Iron Oxides*. Weinheim: VCH, **1996**; p 4.
6. LaConte, L.; Nitin, N.; Bao, G. *Nanotoday* **2005,** 8, 32-38.
7. Pouliquen, D.; Perroud, H.; Calza, F.; Jallet, P.; Le Jeune, J. *J. Magn. Reson. Med.* **1992,** 24, 75-84.
8. Foner, S. *Rev. Sci. Instrum.* **1959,** 30, 548-555.
9. Sun, S. *Adv. Mater.* **2006,** 18, 393-403.
10. Harris, L. A.; Goff, J. D.; Carmichael, A. Y.; Riffle, J. S.; Harburn, J. J.; St-Pierre, T. G.; Saunders, M. *Chem. Mater.* **2003,** 15, 1367-1377.
11. Yamaura, M.; Camilo, R. L.; Sampaio, L. C.; Macêdo, M. A.; Nakamura, M.; Toma, H. E. *J. Magn. Magn. Mater.* **2004,** 279, 210-217.
12. Elaïssari, A.; Bourrel, V. *J. Magn. Magn. Mater.* **2001,** 225, 151-155.
13. Sousa, M. H.; Rubim, J. C.; Sobrinho, P. G.; Tourinho, F. A. *J. Magn. Magn. Mater.* **2001,** 225, 67-72.
14. Lacava, L. M.; Lacava, Z. G. M.; Azevedo, R. B.; Chaves, S. B.; Garcia, V. A. P.; Silva, O.; Pelegrini, F.; Buske, N.; Gansau, C.; Da Silva, M. F.; Morais, P. C. *J. Magn. Magn. Mater.* **2002,** 252, 367-369.
15. Jordan, A.; Scholz, R.; Wust, P.; Fähling, H.; Felix, R. *J. Magn. Magn. Mater.* **1999,** 201, 413-419.
16. Nuñez, L.; Kaminski, M. D. *J. Magn. Magn. Mater.* **1999,** 194, 102-107.
17. Ambashta, R. D.; Wattal, P. K.; Singh, S.; Bahadur, D. *J. Magn. Magn. Mater.* **2003,** 267, 335-340.
18. Leslie-Pelecky, D. L.; Rieke, R. D. *Chem. Mater.* **1996,** 8, 1770-1783.

19. Jordan, A.; Scholz, R.; Wust, P.; Schirra, H.; Schiestel, T.; Schmidt, H.; Felix, R. *J. Magn. Magn. Mater.* **1999,** 194, 185-196.
20. Sun, S.; Zeng, H. *J. Am. Chem. Soc.* **2002,** 124, 8204-8205.
21. Tartaj, P.; Morales, M. D. P.; Veintemillas-Verdaguer, S.; Gonzalez-Carreno, T.; Serna, C. J. *J. Phys. D: Appl. Phys.* **2003,** 36, R182-R197.
22. Kim, D. K.; Mikhaylova, M.; Zhang, Y.; Muhamed, M. *Chem. Mater.* **2003,** 15, 1617-1627.
23. Sankaranarayanan, V. K.; Khan, D. C. *J. Magn. Magn. Mater.* **1996,** 153, 337-346.
24. Choy, J. H.; Han, Y.-S.; Song, S.-W. *Mater. Lett.* **1994,** 19, 257-262.
25. Figueroa, C. A.; Sileo, E. E.; Morando, P. J.; Blesa, M. A. *J. Colloid. Inter. Sci.* **2000,** 225, 403-410.
26. Zulauf, M.; Eicke, H. F. *J. Phys. Chem.* **1979,** 83, 480-486.
27. Bianco, A.; Gusmano, G.; Montanari, R.; Montesperelli, G.; Traversa, E. *Mater. Lett.* **1994,** 19, 263-268.
28. Viau, G.; Fiévet-Vincent, F.; Fiévet, F. *J. Magn. Magn. Mater.* **1995,** 140-144, 377-378.
29. Wang, X.; Zhuang, J.; Peng, Q.; Li, Y. *Nature* **2005,** 437, 121-124.
30. Zhao, N.; Gao, M. Y. *Adv. Mater.* **2009,** 21, 184-187.
31. Kim, D. K.; Zhang, Y.; Voit, W.; Rao, K. V.; Muhamed, M. *J. Magn. Magn. Mater.* **2001,** 225, 30-36.
32. Rosensweig, R. E., *Ferrohydrodynamics* Cambridge University Press: Cambridge, **1985**; p 344.
33. Cornell, R. M.; Schwertmann, U., *The Iron Oxides*. Weinheim: VCH, **1996**; p 207-212.
34. Cornell, R. M.; Schwertmann, U., *The Iron Oxides*. Weinheim: VCH, **1996**; p 240-246.
35. Parfitt, R. L.; Atkinson, R. J. *Nature* **1976,** 264, 740-742.
36. Novakova, A. A.; Lanschinskaya, V. Y.; Volkov, A. V.; Gendler, T. S.; Kiseleva, T. Y.; Moskvina, M. A.; Zezin, S. B. *J. Magn. Magn. Mater.* **2003,** 258-259, 354-357.

37. Li, C.; Benicewicz, B. C. *Macromolecules* **2005,** 38, 5929-5936.
38. Gravano, S. M.; Dumas, R.; Liu, K.; Patten, T. E. *J. Polym Sci., Part A: Polym. Chem.* **2005,** 43, 3675-3688.
39. Werne, T. V.; Patten, T. E. *J. Am. Chem. Soc.* **2001,** 123, 7497-7505.
40. Ohno, K.; Koh, K.-M.; Tsujii, Y.; Fukuda, T. *Macromolecules* **2002,** 35, 8989-8993.
41. Pyun, J.; Jia, S.; Kowalewski, T.; Patterson, G. D.; Matyjaszeswski, K. *Macromolecules* **2003,** 36, 5094-5104.
42. Carrot, G.; Diamanti, S.; Manuszak, M.; Charleux, B.; Vairon, J.-P. *J. Polym. Sci., Part A: Polym. Chem.* **2001,** 39, 4294-4301.
43. Husseman, M.; Malmstrom, E. E.; McNamara, M.; Mate, M.; Mecerreyes, D.; Benoit, D. G.; Hedrick, J. L.; Mansky, P.; Huang, E.; Russell, T. P.; Hawker, C. J. *Macromolecules* **1999,** 32, 1424-1429.
44. Carrot, G.; Rutot-Houze, D.; Pottier, A.; Degge, P.; Hilborn, J.; Dubois, P. *Macromolecules* **2002,** 35, 8400-8404.
45. Li, C., Z; Benicewicz, B., C. *Polym. Prepr.* **2005,** 46, 274-275.
46. Li, C.; Han, J.; Ryu, C. Y.; Benicewicz, B. C. *Macromolecules* **2006,** 39, 3175-3183.
47. Peng, Q.; Lai, D. M. Y.; Kang, E. T.; Neoh, K. G. *Macromolecules* **2006,** 39, 5577-5582.
48. Takolpuckdee, P.; Mars, C. A.; Perrier, S. *Org. Lett.* **2005,** 7, 3449-3452.
49. Raula, J.; Shan, J.; Nuopponen, M.; Niskanen, A.; Jiang, H.; Kauppinen, E. I.; Tenhu, H. *Langmuir* **2003,** 19, 3499-3504.
50. Baum, M.; Brittain, W. J. *Macromolecules* **2002,** 35, 610-615.
51. Wang, W.-C.; Neoh, K.-G.; Kang, E.-T. *Macromol. Rapid Comm.* **2006,** 27, 1665-1669.
52. Moad, G.; Solomon, D. H., *The Chemistry of Radical Polymerization* Elsevier: Amsterdam, **2006**; p 1.
53. Beuermann, S.; Buback, M. *Progr. Polym. Sci.* **2002,** 27, 191-254.
54. Matyjaszewski, K.; Davis, T. P., *Handbook of Radical Polymerization*. John Wiely & Sons: Hoboken, NY, **2002**; p 118-119.

55. Bai, B.-K.; You, Y.-Z.; Pan, C.-Y. *Macromol. Rapid Comm.* **2001,** 22, 315-319.
56. Moad, G.; Solomon, D. H., *The Chemistry of Radical Polymerization*. Elsevier: Amsterdam, **2006**; p 50-51.
57. Matyjaszewski, K.; Davis, T. P., *Handbook of Radical Polymerization*. John Wiley & Sons: Hoboken, NY, **2002**; p 132-140.
58. Moad, G.; Solomon, D. H., *The Chemistry of Radical Polymerization* Elsevier: Amsterdam, **2006**; p 218-221.
59. Matyjaszeswski, K.; Davis, T. P., *Handbook of Radical Polymerization*. John Wiley & Sons: Hoboken, NY, **2002**; p 197.
60. O'Driscoll, K. F.; Mahabadi, H. K. *J. Polym. Sci., Polym. Chem. Ed.* **1976,** 14, 869-875.
61. Olaj, O. F.; Vana, P.; Zoader, M. *Macromolecules* **2002,** 35, 1208-1214.
62. Matyjaszewski, K.; Davis, T. P., *Handbook of Radical Polymerization*. John Wiley & Sons: Hoboken, NY, **2002**; p 197.
63. Buback, M.; Egorov, M.; Gilbert, R. G.; Kaminsky, V.; Olaj, O. F.; Russell, G. T.; Vana, P.; Zifferer, G. *Macromol. Chem. Phys.* **2002,** 203, 2570-2582.
64. Dawkins, J. V.; Yeadon, G. *Polymer* **1979,** 20, 981-989.
65. Mayo, F. R.; Gregg, R. A.; Matheson, M. S. *J. Am. Chem. Soc.* **1951,** 73, 1691-1700.
66. Johnson, D. H.; Tobolsky, A. V. *J. Am. Chem. Soc.* **1952,** 74, 938-943.
67. Moad, G.; Solomon, D. H.; Johns, S. R.; Willing, R. I. *Macromolecules* **1984,** 17, 1094-1099.
68. Moad, G.; Solomon, D. H.; Johns, S. R.; Willing, R. I. *Macromolecules* **1982,** 15, 1188-1191.
69. Arnett, L. M.; Peterson, J. H. *J. Am. Chem. Soc.* **1952,** 74, 2031-2033.
70. Moad, G.; Solomon, D. H., *The Chemistry of Radical Polymerization*. Elsevier: Amsterdam, **2006**; p 260.
71. Moad, G.; Solmon, D. H., *The Chemistry of Radical Polmerization*. Elsevier: Amsterdam, **2006**; p 261.
72. Zammit, M. D.; Davis, T. P.; Haddleton, D. M.; Suddaby, K. G. *Macromolecules* **1997,** 30, 1915-1920.

73. Flory, P. J. *J. Am. Chem. Soc.* **1937,** 59, 241-253.
74. Matyjaszewski, K., *In Advances in Controlled/Living Radical Polymerization*. American Chemical Society: Washington, DC, **2003**; p 2.
75. Szwarc, M.; Levy, M.; Milkovich, R. *J. Am. Chem. Soc.* **1956,** 78, 2656-2657.
76. Matyjaszewski, K.; Davis, T. P., *Handbook of Radical Polymerization*. John Wiley & Sons: Hoboken, NY, **2002**; p 464.
77. Otsu, T.; Yoshida, M. *Makromol. Chem., Rapid Commun.* **1982,** 3, 127-132.
78. Otsu, T. J. *J. Polym Sci., Part A: Polym. Chem.* **2000,** 38, 2121-2136.
79. Chong, Y. K.; Krstina, J.; Le, T. P. T.; Moad, G.; Postma, A.; Rizzardo, E.; Thang, S. H. *Macromolecules* **2003,** 36, 2256-2272.
80. Stenzel, M. H.; Davis, T. P.; Fane, A. G. *J. Mater. Chem.* **2003,** 13, 2090-2097.
81. Chiefari, J.; Chong, Y. K.; Ercole, F.; Krstina, J.; Jeffery, J.; Le, T. P. T.; Mayadunne, R. T. A.; Meijs, G. F.; Moad, C. L.; Moad, G.; Rizzardo, E.; Thang, S. H. *Macromolecules* **1998,** 31, 5559-5562.
82. Mayadunne, R. T. A.; Rizzardo, E.; Chiefari, J.; Chong, Y. K.; Moad, G.; Thang, S. H. *Macromolecules* **1999,** 32, 6977-6980.
83. Hawthorne, D. G.; Moad, G.; Rizzardo, E.; Thang, S. H. *Macromolecules* **1999,** 32, 5457-5459.
84. Moad, G.; Rizzardo, E.; Thang, S. H. *Aust. J. Chem.* **2005,** 58, 379-410.
85. Hawker, C. J.; Bosman, A. W.; Harth, E. *Chem. Rev.* **2001,** 101, 3661-3688.
86. Wang, J.-S.; Matyjaszewski, K. *J. Am. Chem. Soc.* **1995,** 117, 5614-5615.
87. Wang, J.-S.; Matyjaszewski, K. *Macromolecules* **1995,** 28, 7901-7910.
88. Barner-Kowollik, C.; Buback, M.; Charleux, B.; Coote, M. L.; Drache, M.; Fukuda, T.; Goto, A.; Klumperman, B.; Lowe, A. B.; McLeary, J. B.; Moad, G.; Monteiro, M. J.; Sanderson, R. D.; Tonge, M. P.; Vana, P. *J. Polym. Sci., Part A: Polym. Chem.* **2006,** 44, 5809-5831.
89. Kamigaito, M.; Ando, T.; Sawamoto, M. *Chem. Rev.* **2001,** 101, 3689-3746.
90. Matyjaszewski, K.; Xia, J. *Chem. Rev.* **2001,** 101, 2921-2990.
91. Pradel, J. L.; Boutevin, B.; Ameduri, B. *J. Polym. Sci., Part A: Polym. Chem.* **2000,** 38, 3293-3302.
92. Miura, Y.; Nakamura, N.; Taninguchi, I. *Macromolecules* **2001,** 34, 447-455.

93. Nguyen, T. L. U.; Eagles, K.; Davis, T. P.; Barner-Kowollik, C.; Stenzel, M. H. *J. Polym. Sci., Part A: Polym. Chem.* **2006,** 44, 4372-4383.
94. Goto, A.; Hirai, N.; Tsujii, Y.; Fukuda, T. *Macromol. symp.* **2008,** 261, 18-22.
95. Debuigne, A.; Caille, J.-R.; Jérôme, R. *Macromolecules* **2005,** 38, 6310-6315.
96. Kato, M.; Kamigaito, M.; Sawamoto, M.; Higashimura, T. *Macromolecules* **1995,** 28, 1721-1723.
97. Matyjaszewski, K.; Davis, T. P., *Handbook of Radical Polymerization*
John Wiely & Sons
Hoboken, NY, **2002**; p 524-525.
98. Fischer, H. *J. Polym. Sci., Part A: Polym. Chem.* **1999,** 37, 1885-1901.
99. Goto, A.; Fukuda, T. *Prog. Polym. Sci.* **2004,** 29, 329-385.
100. Solomon, D. H. *J. Polym. Sci., Part A: Polym. Chem.* **2005,** 43, 5748-5764.
101. Zetterlund, P. B.; Kagawa, Y.; Okubo, M. *Chem. Rev.* **2008,** 108, 3747-3794.
102. Fischer, H. *Macromolecules* **1997,** 30, 5666-5672.
103. Fischer, H. *J. Polym Sci. Part A: Polym. Chem.* **1999,** 37, 1885-1901.
104. Fischer, H. *Chem. Rev.* **2001,** 101, 3581-3610.
105. Fischer, H.; Souaille, M. *Macromol. Symp.* **2001,** 174, 231-240.
106. Souaille, M.; Fischer, H. *Macromolecules* **2000,** 33, 7378-7394.
107. Tang, W.; Fukuda, T.; Matyjaszewski, K. *Macromolecules* **2006,** 39, 4332-4337.
108. Leon-Saenz, E. D.; Morales, G.; Guerrero-santos, R.; Gnanou, Y. *Macromol. Chem. Phys.* **2000,** 201, 74-83.
109. Druliner, J. D. *Macromolecules* **1991,** 24, 6079-6082.
110. Yamada, B.; Nobukane, Y.; Miura, Y. *Polym. Bull.* **1998,** 41, 539-544.
111. Steenbock, M.; Klapper, M.; Mullen, K. *Macromol. Chem. Phys.* **1998,** 199, 763-769.
112. Puts, R. D.; Sogah, D. Y. *Macromolecules* **1996,** 29, 3323-3325.
113. Moad, G.; Rizzardo, E. *Macromolecules* **1995,** 28, 8722-8728.
114. Goto, A.; Fukuda, T. *Macromol. Chem. Phys.* **2000,** 201, 2138–2142.
115. Moad, G.; Rizzardo, E.; Solomon, D. H. *Macromolecules* **1982,** 15, 909-914.
116. Georges, M. K.; Veregin, R. P. N.; Kazmaier, P. M.; Hamer, G. K. *Macromolecules* **1993,** 26, 2987-2988.

117. Odell, P. G.; Veregin, R. P. N.; Michalak, L. M.; Georges, M. K. *Macromolecules* **1997,** 30, 2232-2237.

118. Fukuda, T.; Terauchi, T.; Goto, A.; Ohno, K.; Tsujii, Y.; Yamada, B. *Macromolecules* **1996,** 29, 6393-6398.

119. Li, I. Q.; Howell, B. A.; Koster, R. A.; Priddy, D. B. *Macromolecules* **1996,** 29, 8554-8555.

120. Hawker, C. J. *J. Am. Chem. Soc.* **1994,** 116, 11185-11186.

121. Hawker, C. J.; Barclay, G. G.; Orellana, A.; Dao, J.; Devonport, W. *Macromolecules* **1996,** 29, 5245-5254.

122. Keoshkerian, B.; Georges, M. K.; Quinlan, M.; Veregin, R.; Goodbrand, R. *Macromolecules* **1998,** 31, 7559-7561.

123. Matyjaszewski, K.; Gaynor, S.; Greszta, D.; Mardare, D.; Shigemoto, T. *Macromol. Symp.* **1995,** 95, 217-225.

124. Chong, Y. K.; Ercole, F.; Moad, G.; Rizzardo, E.; Thang, S. H. *Macromolecules* **1999,** 32, 6895-6903.

125. Georges, M. K.; Veregin, R. P. N.; Kazmaier, P. M.; Hamer, G. K.; Saban, M. *Macromolecules* **1994,** 27, 7228-7229.

126. Malmstrom, E. E.; Hawker, C. J.; Miller, R. D. *Tetrahedron* **1997,** 53, 15225-15236.

127. Benoit, D.; Grimaldi, S.; Robin, S.; Finet, J. P.; Tordo, P.; Gnanou, Y. *J. Am. Chem. Soc.* **2000,** 122, 5929-5939.

128. Benoit, D.; Chaplinski, V.; Braslau, R.; Hawker, C. J. *J. Am. Chem. Soc.* **1999,** 121, 3904-3920.

129. Benoit, D.; Harth, E.; Fox, P.; Waymouth, R. M.; Hawker, C. J. *Macromolecules* **2000,** 33, 363-370.

130. Kristina, J.; Moad, G.; Rizzardo, E.; Winzor, C. L.; Berge, C. T.; Fryd, M. *Macromolecules* **1995,** 28, 5381-5385.

131. Moad, G.; Moad, C. L.; Krstina, J.; Rizzardo, E.; Berge, C. T.; Darling, T. R. WO 96/15157, **1996**.

132. Le, T. P. T.; Moad, G.; Rizzardo, E.; Thang, S. H. WO 9801478/A1, **1998**.

133. Chong, Y. K.; Le, T. P. T.; Moad, G.; Rizzardo, E.; Thang, S. H. *Macromolecules* **1999,** 32, 2071-2074.

134. Smulders, W.; Gilbert, R. G.; Monteiro, M. J. *Macromolecules* **2003,** 36, 4309-4318.

135. Bouhadir, G.; Legrand, N.; Quiclet-Sire, B.; Zard, S. Z. *Tetrahedron Lett.* **1999,** 40, 277-280.

136. Tonge, M. P.; McLeary, J. B.; Vosloo, J. J.; Sanderson, R. D. *Macromol. Symp.* **2003,** 193, 289-304.

137. Barner, L.; Quinn, J. F.; Barner-Kowollik, C.; Vana, P.; Davis, T. P. *Eur. Polym. J.* **2003,** 39, 449-459.

138. Perrier, S.; Davis, T. P.; Carmichael, A. J.; Haddleton, D. M. *Eur. Polym. J.* **2003,** 39, 417-422.

139. Severac, R.; Lacroix-Desmazes, P.; Boutevin, B. *Polym. Int.* **2002,** 51, 1117-1122.

140. Prescott, S. W.; Ballard, M. J.; Rizzardo, E.; Gilbert, R. G. *Macromolecules* **2002,** 35, 5417-5425.

141. Degani, I.; Fochi, R.; Gatti, A.; Regondi, V. *Synthesis* **1986,** 11, 894-899.

142. Stenzel, M. H.; Davis, T. P. *J. Polym. Sci., Part A: Polym. Chem.* **2002,** 40, 4498-4512.

143. Mayadunne, R. T. A.; Rizzardo, E.; Chiefari, J.; Krstina, J.; Moad, G.; Postma, A.; Thang, S. H. *Macromolecules* **2000,** 33, 243-245.

144. Thang, S. H.; Chong, Y. K. B.; Mayadunne, R. T. A.; Moad, G.; Rizzardo, E. *Tetrahedron Lett.* **1999,** 40, 2435-2438.

145. Coote, M. L.; Izgorodina, E. I.; Cavigliasso, G. E.; Roth, M.; Busch, M.; Barner-Kowollik, C. *Macromolecules* **2006,** 39, 4585-4591.

146. Quiclet-Sire, B.; Wilczewska, A.; Zard, S. Z.; . *Tetrahedron Lett* **2000,** 41, 5673-5677.

147. Laus, M.; Papa, R.; Sparnacci, K.; Alberti, A.; Benaglia, M.; Macciantelli, D. *Macromolecules* **2001,** 34, 7269-7275.

148. Perrier, S.; Takolpuckdee, P. *J. Polym. Sci., Part A: Polym. Chem.* **2005,** 43, 5347-5393.

149. Calitz, F. M.; Tonge, M. P.; Sanderson, R. D. *Macromolecules* **2003,** 36, 5-8.

150. Tonge, M. P.; Calitz, F. M.; Sanderson, R. D. *Macromol. Chem. Phys.* **2006,** 207, 1852-1860.

151. Zhou, G.; Haruna, I. I. *Anal. Chem.* **2007,** 79, 2722-2727.

152. Schilli, C.; Lanzendorfer, M. G.; Muller, A. H. E. *Macromolecules* **2002,** 35, 6819-6827.

153. Favier, A.; Ladaviere, C.; Charreyre, M.-T.; Pichot, C. *Macromolecules* **2004,** 37, 2026-2034.

154. Alberti, A.; Benaglia, M.; Laus, M.; Macciantelli, D.; Sparnacci, K. *Macromolecules* **2003,** 36, 736-740.

155. Calitz, F. M.; McLeary, J. B.; McKenzie, J. M.; Tonge, M. P.; Klumperman, B.; Sanderson, R. D. *Macromolecules* **2003,** 36, 9687-9690.

156. Barner-Kowollik, C.; Quinn, J. F.; Nguyen, U. T. L.; Heuts, J. P. A.; Davis, T. P. *Macromolecules* **2001,** 34, 8872-8878.

157. Ladaviere, C.; Dorr, N.; Claverie, J. P. *Macromolecules* **2001,** 34, 5370-5372.

158. Goto, A.; Sato, K.; Tsujii, Y.; Fukuda, T.; Moad, G.; Rizzardo, E.; Thang, S. H. *Macromolecules* **2001,** 34, 402-408.

159. Sumerlin, B. S.; Donovan, M. S.; Mitsukami, Y.; Lowe, A. B.; McCormick, C. L. *Macromolecules* **2001,** 34, 6561-6564.

160. Donovan, M. S.; Lowe, A. B.; Sumerlin, B. S.; McCormick, C. L. *Macromolecules* **2002,** 35, 4123-4132.

161. Donovan, M. S.; Sanford, T. A.; Lowe, A. B.; Sumerlin, B. S.; Mitsukami, Y.; McCormick, C. L. *Macromolecules* **2002,** 35, 4570-4572.

162. Vana, P.; Davis, T. P.; Barner-Kowollik, C. *Macromol. Theory. Simul.* **2002,** 11, 823-835.

163. Moad, G.; Solomon, D. H., *The Chemistry of Radical Polymerization*. Elsevier: Amsterdam, **2006**; p 505.

164. Moad, G.; Chiefari, J.; Chong, Y. K.; Kristina, J.; Postma, A.; Mayadunne, R. T. A.; Rizzardo, E.; Thang, S. H. *Polym. Int.* **2000,** 49, 931-936.

165. Tsujii, Y.; Ejaz, M.; Sato, K.; Goto, A.; Fukuda, T. *Macromolecules* **2001,** 34, 8872-8878.

166. Perrier, S.; Takolpuckdee, P.; Mars, C. A. *Macromolecules* **2005,** 38, 6770-6774.

167. Hao, X. J.; Nilsson, C.; Jesberger, M.; Stenzel, M. H.; Malmstrom, E.; Davis, T. P.; Östmark, E.; Barner-Kowollik, C. *J. Polym. Sci., Part A: Polym. Chem.* **2004,** 42, 5877-5890.

168. Quinn, J. F.; Chaplin, R. P.; Davis, T. P. *J. Polym. Sci., Part A: Polym. Chem.* **2002,** 40, 2956-2966.

169. Bernard, J.; Favier, A.; Davis, T. P.; Barner-Kowollik, C.; Stenzel, M. H. *Polymer* **2006,** 27, 1121-1126.

170. Perrier, S.; Barner-Kowollik, C.; Quinn, J. F.; Vana, P.; Davis, T. P. *Macromolecules* **2002,** 35, 8300-8306.

171. Chernikova, E.; Morozovo, A.; Leonova, E.; Garina, E.; Golubev, V.; Bui, C.; Charleux, B. *Macromolecules* **2004,** 37, 6329-6339.

172. McLeary, J. B.; Calitz, F. M.; McKenzie, J. M.; Tonge, M. P.; Sanderson, R. D.; Klumperman, B. *Macromolecules* **2005,** 38, 3151-3161.

173. Barner-Kowollik, C.; Quinn, J. F.; Nguyen, T. L. U.; Heuts, J. P. A.; Davis, T. P. *Macromolecules* **2001,** 34, 7849-7857.

174. Monteiro, M. J.; de Brouwer, H. *Macromolecules* **2001,** 34, 349-352.

175. Kwak, Y.; Goto, A.; Fukuda, T. *Macromolecules* **2004,** 37, 1219-1225.

176. Kwak, Y.; Goto, A.; Tsujii, Y.; Murata, Y.; Komatsu, K.; Fukuda, T. *Macromolecules* **2002,** 35, 3026-3029.

177. Feldermann, A.; Coote, M. L.; Stenzel, M. H.; Davis, T. P.; Barner-Kowollik, C. *J. Am. Chem. Soc.* **2004,** 126, 15915-15923.

178. Barner-Kowollik, C.; Quinn, J. F.; Morsley, D. R.; Davis, T. P. *J. Polym. Sci., Part A: Polym. Chem.* **2001,** 39, 1353-1365.

Chapter 3: Synthesis of RAFT agents, and nitroxide and free radical initiators

Abstract: This chapter details the experimental conditions and the synthesis procedures of the Reversible Addition-Fragmentation Chain Transfer (RAFT) agents, Nitroxide Mediated Polymerization (NMP) initiators, and free radical initiators, which are used in the course of this study. Nuclear Magnetic Resonance (NMR) spectroscopy, Ultraviolet/visible (UV/Vis) spectroscopy and Fourier Transform-Infrared (FT-IR) spectroscopy are the characterization techniques used in this chapter.

3.1 Introduction

3.1.1 Synthesis of dithioester RAFT agents

Interest in the synthesis of RAFT agents emerged after it was found that they could be used in Controlled/"Living" Radical Polymerization (CLRP) to produce polymers with narrow molecular weight distributions and well-defined structures.[1-3]

One of the early methods that was used in the synthesis of dithioester RAFT agents is the Grignard reaction.[4,5] The Grignard salts used in the synthesis of dithioesters is shown in Scheme 3.1. Arylmagnesiumhalide reacts with carbon disulfide in dry solvents such as tetrahydrofuran (THF) or ether to form the magnesiumhalide salt of the dithioacid (dithioester salt). The dithioester salt can then be transformed directly into a dithioester RAFT agent by addition of suitable alkyl halide, or alkyl sulphate, into the reaction contents.[5,6] It has been reported in the literature that the dithioester yield improved drastically when dry THF was used as solvent instead of dry ether.[7] Therefore, THF was chosen as the solvent for this study.

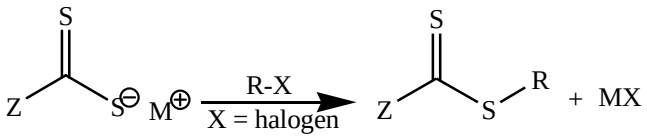

Scheme 3.1: Preparation of a dithioester using a Grignard salt.[5]

Although Grignard synthesis is one of the most versatile synthesis methods, however, its sensitivity to oxygen, water, amides, thio-compounds and carboxylic acids limits its application in some specific cases.[8]

To be able to attach a RAFT agent to the surface of MNPs, a RAFT agent with an interacting group to the surface of the MNPs, such as carboxylic or phosphate group, is needed. As starting material for the Grignard reaction in this study, 4-Bromomethyl benzoic acid was used. The protection of the carboxylic acid group was successfully performed using 2-amino-2-methyl-1-propanol, in a procedure described in the

literature.[9] A yield of 90% of 2-(4-bromophenyl)-4,4-dimethyl-4,5-dihydro-oxazole was achieved and the purity was 98%, as determined by ^{1}H-NMR. However, the Grignard reaction of the 2-(4-bromophenyl)-4,4-dimethyl-4,5-dihydro-oxazole was deemed not successful because of its poor solubility in the Grignard solvent (THF). An alternative method therefore was used for the preparation of benzyl-(4-carboxydithiobenzoate). The alternate method is based on substitution reactions. These reactions were widely used for the synthesis of thio-organic compounds.[10] The bromo methyl group of the 4-bromomethyl benzoic acid (Scheme 3.2) was substituted with a dithio group using elemental sulphur (S_8) in the presence of strong base (sodium methoxide). The substituted compound acts as a nucleophile for the substitution reaction with alkyl halides.

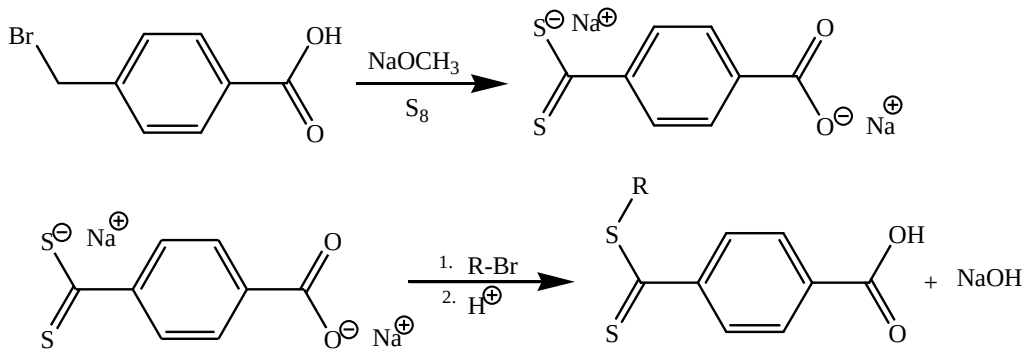

Scheme 3.2: Preparation of a dithio acid via addition of elemental sulphur.

Addition of dithioacid in its protonated form to olefins has also been reported for synthesis of various dithioesters.[11] However this method will not be discussed in details, as it is not to be used in this study.

Trithiocarbonate RAFT agents can be prepared by the alkylation of potassium or sodium salt of trithiocarbonic acid. The reaction is described in Scheme 3.3.[12]

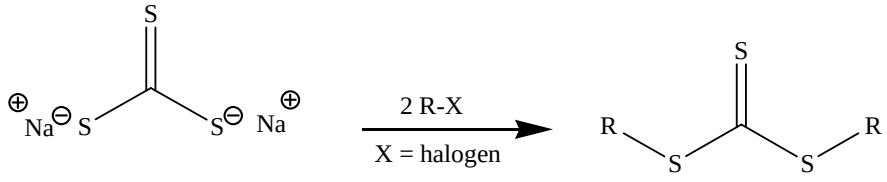

Scheme 3.3: Preparation of trithiocarbonates.[12]

There are however other synthetic methods available in the literature for synthesis of tritiocarbonates involving reactions of thiols with thiophosgene,[13] chlorodithioformates,[14] or diethyl azodicarboxylate/ triphenylphosphine.[15] Reactions of thiols with sodium/or potassium t-butoxide , carbon disulphide, and iodineare new developed methods that have also been recently used for synthesis of various trithiocarbonates.[16] These methods will not be discussed in detail in this study, since they will not be used.

Most of the methods used in this work are based on substitution reactions using alkyl halides.

3.1.2 Synthesis of alkylhalides

One of the most common types of reagents used in the synthesis of certain RAFT agents are bromoalkyls, which can be prepared by the allylbromination method (also called allylic substitution).[17] The method is based on a radical substitution reaction of the hydrogen in the allylic position, using N-bromosuccinimide (NBS). The NBS is the most important reagent in the bromination process (it generates the bromine). [18-21] A low bromine concentration is however necessary for the success of allylic bromination.[22]

3.1.3 Synthesis of unimolecular NMP agents

One of the successful contributions of the NMP process was the development and the synthesis of single molecule NMP agent, which permits control over molecular weight, molecular architecture and end-group functionality of the produced polymers.[23,24]

The synthesis of such a unimolecular NMP agent (used in this study) is based on the radical addition between a tertiary radical (produced by the thermal decomposition of azo initiator compounds) and the nitroxide mediating radical, to produce an unimolecular NMP agent. The NMP agent is normally stable at the reaction temperature (e.g. 85 °C), but should be fairly unstable at the elevated polymerization temperature (e.g. 135 °C).

3.1.4 Synthesis of phosphoric esters

The phosphoric ester compounds have strong affinity towards metal hydroxides, such as iron oxides, which made these compounds attractive in many industrial applications (as

emulsifier, lubricants, and metal-chelating agents).[25] It is the strong affinity of the phosphate group towards iron oxides that prompted the author to prepare and use them as extractable attaching groups to the surface of MNPs. The synthesis of mono-, di- and tri-phosphoric esters has been described in the literature.[26,27] In a substitution reaction the phosphorous oxyhalide reacts with an organic hydroxyl compound to produce a phosphoric ester in the presence of triethylamine (metal salt with pK_a values from -5 to 3 could also be used).

3.2 Materials

The following materials were used as received: p-toluic acid (98%; Fluka), N-bromosuccinimide (99%; Aldrich), benzoyl peroxide (98%; Merck), sodium metal (Merck), ethanol (HPLC grade, BDH; 99.70%), sulphur powder (98%; Merck), hydrochloric acid (32%; Merck), benzyl bromide (98%; Fluka), magnesium turnings (Merck), carbon disulphide (99%; Labchem), bromobenzene (99%; Aldrich), 11-bromo-1-undecanol (99%; Fluka), phosphorus(V)-oxychloride (99%; Merck), α-toluenethiol (99%; Across Organics), anhydrous magnesium sulphate (Merck), sodium hydroxide (Merck), sodium cyanide (95+%; Aldrich), hydrazine sulphate (99%; Analar), bromine (99%; Merck), 5-hydroxy-pentane-2-one (96%; Aldrich), 2,2'-azobis(isobutyronitrile) (AIBN) (98%; Fluka), potassium hydroxide (Merck), carbon tetrachloride (99.5%; Saarchem), 2-amino-2-methyl-1-propanol (95%; Riedel-deHaen), 2,2,6,6-tetramethyl piperidine hydroxyl TEMPO (98%; Aldrich), triethylamine (99%; Across), toluene (99.9%; Aldrich), dimethyl sulphoxide (DMSO) (99%; Merck), chloroform (99%; Saarchem), pentane (99%; Saarchem), hexane (99.5%; Saarchem), dichloromethane (DCM) (98%; Saarchem), and ethyl acetate (99%; Saarchem).

Tetrahydrofurane (THF) (99%; Aldrich) was freshly distilled from lithium aluminium hydride (95%; Aldrich).

3.3 Characterization techniques

The prepared RAFT and NMP agents, and free radical initiators, were characterized by Nuclear Magnetic Resonance (NMR) and Fourier-Transform Infrared (FT-IR) spectroscopy. The UV absorptions by the C=S bond of RAFT agents, phosphate group of NMP agents and free radical initiators were measured using Ultraviolet/Visible (UV/Vis) spectroscopy.

3.3.1 Nuclear Magnetic Resonance spectroscopy

^{1}H-NMR (300 MHz) and ^{13}C-NMR (75 MHz) spectra were recorded on a Varian mercury 300 spectrometer.

3.3.2 Fourier-Transform Infrared spectroscopy

Structural information of the prepared RAFT agents was determined by FT-IR spectroscopy. Samples of the RAFT agents (in a form of powder/ crystals) were first dried for 24 hours under reduced pressure to remove any solvent or moisture traces. Each solid sample of the RAFT agent was then mixed with potassium bromide (KBr) in a mass ratio of 1:250, and then ground into a fine powder. A small portion of the powder was placed in a cylinder and pressed with a hydraulic pump to form a small round KBr disk. The disk was placed in the instrument and the IR spectra recorded using a ThermoNicolet Nexus FT-IR spectrometer. Each spectrum was scanned 32 times and data analysis was performed with Omnic Software version 7.2.

Samples of RAFT agents (in an oil form) were dried and then a small drop of each RAFT agent was put onto a sodium plate. The sodium plate containing a sample of the RAFT agent was placed in the instrument and the IR spectra recorded using a PerkinElmer instrument. Each spectrum was scanned 32 times and data analysis was performed with Omnic Software version 7.2.

3.3.3 UV/visible spectroscopy

The UV absorption spectra of the prepared RAFT agents, NMP and free radical initiators were recorded using a Perkin Elmer Lambda 20 UV/visible spectrometer. All samples were dissolved in dichloromethane and then 1.5 mL of each sample transferred into quartz cuvettes, and the spectra recorded.

3.4 Experimental

3.4.1 Synthesis of 4-bromomethyl benzoic acid

p-Toluic acid (68 g; 500 mmol), NBS (89 g; 500 mmol) and benzoyl peroxide (4 g; 16.5 mmol) were mixed in dry carbon tetrachloride (400 mL) and refluxed for 1.5 h. After cooling, the solvent was evaporated and the residue washed with pentane (3 × 100 mL). The remaining solid was then mixed with water (600 mL) for 1 h to dissolve any succinimide, and filtered. The residue was washed with water (3 × 100 mL) and pentane (3 ×100 mL) to yield a solid white product. The product was recrystallized from methanol and dried to give white crystals (62.3 g, 58% yield), T_m = 219 °C. ^{1}H-NMR, $(CD_3)_2SO$ δ (ppm): 4.7 (2H, Br–CH_2); 7.5–7.9 (H; H–aromatic). ^{13}C-NMR, $(CD_3)_2SO$ δ (ppm): 62.28 (C; –CH_2); 126.37, 129.37, 129.59, 129.84 (C; C–aromatic); 167.70 (C=O). (The ^{1}H-NMR and ^{13}C-NMR spectra of the 4-bromomethyl benzoic acid are shown in Appendix A, Figures A.1 and A.2, respectively)

3.4.2 Synthesis of benzyl-(4-carboxydithiobenzoate) RAFT agent

A 500 mL 3-necked round-bottom flask was fitted with two 500 mL dropping funnels. An absolute ethanol (300 mL) was put in one of the dropping funnels. Sodium metal (3.6 g; 200 mmol) was placed in the flask and ethanol was allowed to flow dropwise until complete dissolution of sodium metal occurred (the reaction was very exothermic). 4-bromomethyl benzoic acid (20.5 g; 100 mmol) and sulphur powder (9.6 g; 300 mmoL) were then added and the mixture heated to 90 °C. After 3.5 h the reaction was cooled to room temperature. Benzyl bromide (17 g, 100 mmoL) was put into the other dropping funnel and added dropwise, to form a pinkish coloured mixture. The reaction mixture was then warmed to 60 °C for 1 h. The mixture was stirred overnight at room temperature.

Water (400 mL) was added, followed by acidification with HCl (32%). The organic layer was then extracted with chloroform (3 × 150 mL) and dried over anhydrous magnesium sulphate for 30 min. The $MgSO_4$ solid was then filtered off and the solvent evaporated from the filtrate to yield a red solid. The product was then stirred with toluene for 30 min and the solid product filtered. The solid product was purified through a silica chromatography column, using ethyl acetate and hexane (4:1) as eluent. The concentrated product was isolated after evaporating the solvent and drying under reduced pressure. The product was a red powder (17.5 g, 60% yield), T_m = 68–70 °C. ^{1}H-NMR, $(CD_3)_2SO$ δ (ppm): 4.65 (s, 2H; S–CH_2), 7.3– 7.45 (m, 5H; H–aromatic), 8–8.5 (m, 4H; H–aromatic). ^{13}C-NMR, $(CD_3)_2SO$ δ (ppm): 41.26 (C; S–CH_2), 126.79, 127.90, 128.80, 129.46, 129.83 (C; C–aromatic); 166.76 (C=O), 226.74 (C=S). FT-IR (KBr pellets) cm^{-1}: 644–680 (CH; aromatic), 1057 (C=S), 1599 (C=C; aromatic), 1687 (C=O) and 3432 (OH). UV maxima (nm), dichloromethane: λ = 307 ($\pi \rightarrow \pi^*$) and λ = 505 ($n \rightarrow \pi^*$). The preparation of benzyl-(4-carboxydithiobenzoate) is shown in Scheme 3.4. (The ^{1}H-NMR and ^{13}C-NMR spectra of the benzyl-(4-carboxyldithiobenzoate) are shown in Appendix A, Figures A.3 and A.4, respectively)

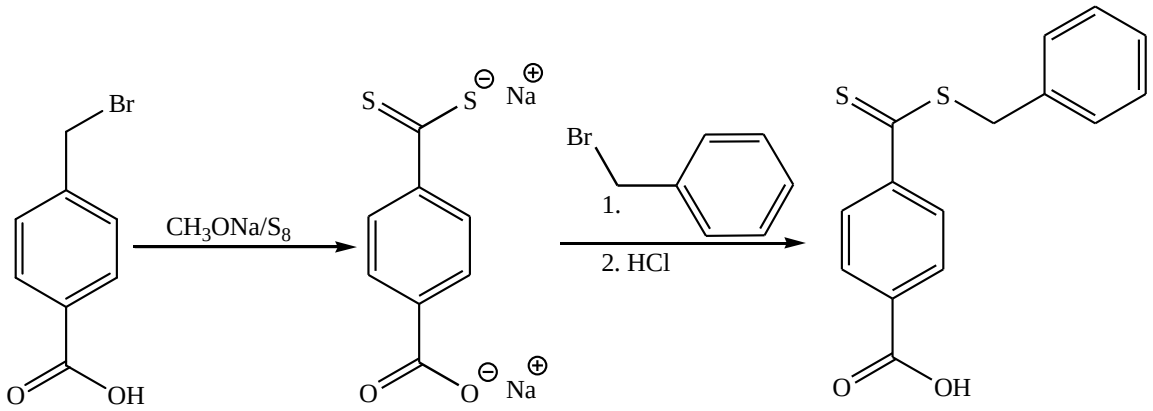

Scheme 3.4: Preparation of benzyl-(4-carboxydithiobenzoate).

3.4.3 Synthesis of benzyl dithiobenzoate RAFT agent

The benzyl dithiobenzoate RAFT agent was synthesized via a Grignard reaction (see Scheme 3.5). A 250-ML 3-necked round-bottom flask was fitted with a 150mL dropping

funnel. 5 mL THF was put in the flask. Magnesium turnings (1.6 g, 63.3 mmol) and a small iodine crystal were put in the flask and stirred with the dry THF. Ten millilitres of a solution of bromobenzene (10.10 g, 63.3 mmol) in dry THF (100 mL) (was put in the dropping funnel) was allowed to flow into the magnesium/THF mixture. The contents in the flask were then carefully warmed with a heat gun (Skill, F015 8000, 1600W) until the reaction started. This is indicated by the disappearance of the brownish iodine colour. The remaining solution of bromobenzene was then added dropwise at such rate to keep the reaction temperature below 40 °C. An ice bath was used to remove the heat of the reaction. Upon the completion of the solution addition, the reaction was then allowed to stir for 2 h at room temperature. Carbon disulphide (4.85 g, 63.3 mmol) was put in the empty dropping funnel and added dropwise over 20 min (a red mixture was formed) while keeping the reaction temperature below 40 °C. Upon complete addition, the contents in the flask were allowed to stir for 30 min at room temperature (the reaction mixture turned to dark opaque brown due to formation of dithiobenzoate salt). Benzyl bromide (10.9 g, 63.7 mmol) was put in the other dropping funnel and added dropwise. After complete addition, the contents were stirred at room temperature overnight. The mixture was poured into water (200 mL) and acidified with HCl (32%). The aqueous layer was extracted with ether (3 × 100 mL) and dried over anhydrous magnesium sulphate. The $MgSO_4$ was removed by filtration, the solvent was evaporated off and the remaining oil was purified through a silica chromatography column, using pentane as eluent. The product was a red oil (5.40 g, 35% yield). ^{1}H-NMR, $CDCl_3$ δ (ppm): 4.55 (s, 2H; S–CH_2), 7.3–7.52 (m, 7H; H–aromatic), 7.54-8.01 (m, 1H; H–aromatic), 8.01–8.25 (m, 1H; H–aromatic). ^{13}C-NMR, $CDCl_3$ δ (ppm): 41.92 (C; S–CH_2), 126.94, 127.69, 128.28, 128.66, 129.29, 129.79 (C; C–aromatic), 227.62 (C=S). FT-IR (NaCl) cm^{-1}: 640-880 (CH; aromatic), 1444cm^{-1} (C=S), 1654 cm^{-1} (C=C; aromatic). UV maxima (nm), dichloromethane: λ = 302 ($\pi \rightarrow \pi^*$) and λ = 507 ($n \rightarrow \pi^*$). (The ^{1}H-NMR and ^{13}C-NMR spectra of the benzyl dithiobenzoate RAFT agent are given in Appendix A, Figures A.5 and A.6, respectively.)

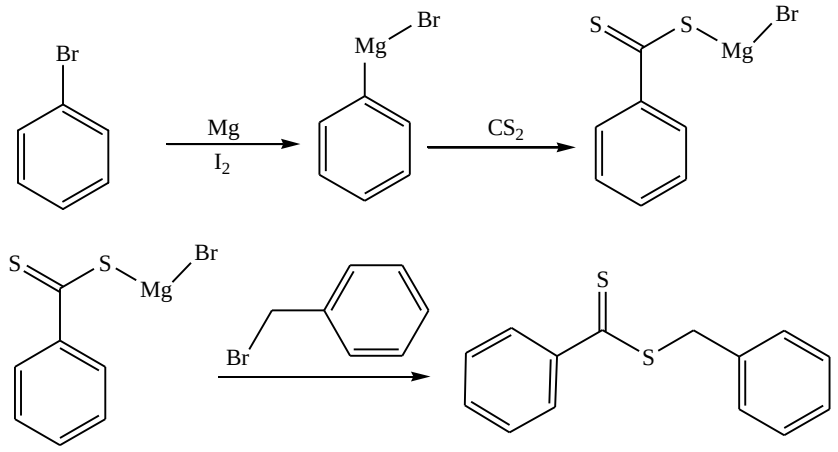

Scheme 3.5: Preparation of benzyl dithiobenzoate.

3.4.4 Synthesis of bis(thiocarbonyl)disulphide RAFT agent

The bis(thiocarbonyl)disulphide (Scheme 3.6) was prepared using a method described in the literature.[28] A 250-ML 3-necked round-bottom flask was fitted with a 150mL dropping funnel. 5 mL THF was put in the flask. Magnesium turnings (1.6 g, 63.3 mmol) and a small iodine crystal were put in the flask and stirred with the dry THF. Ten milliliters of a solution of bromobenzene (10.10 g, 63.3 mmol) in dry THF (100 mL) (was put in the dropping funnel) was allowed to flow into the magnesium/THF mixture. Commencement of the reaction was indicated by the iodine colour disappearing. The remaining solution of bromobenzene was then added dropwise and the reaction temperature was kept below 40 °C (using an ice bath). Upon the complete addition of the solution, the mixture in the flask was then allowed to stir for 2 h at room temperature. Carbon disulphide (4.85 g, 63.3 mmol) was put in the empty dropping funnel and added dropwise over 20 min with keeping the reaction mixture below 40 °C. An ice bath was used to remove the heat of the reaction. After complete addition of carbon disulphide, the mixture was stirred for 30 min. Water (200 mL) was added slowly to the cooled reaction mixture. The mixture was filtered to remove insoluble magnesium salt and subsequently treated with HCl (32%) until the brown colour of dithiobenzoate salt had disappeared completely. The aqueous layer was extracted with ether (3 × 100 mL) and dried over anhydrous magnesium sulphate. The $MgSO_4$ was removed by filtration and the solvent

was evaporated off to give a purple/red oil product. The product was then transferred to 150-mL round-bottom flask and stirred with 2 mol equivalent of DMSO in absolute methanol (50 mL), using iodine as catalyst. The reaction was stopped after 2 hours (red crystals had formed, indicating of completion of the reaction), and the mixture was stored in a refrigerator overnight to promote further crystallization. The crystals were collected by filtration and recrystalized from methanol, filtered, and dried to give 9 g (50% yield). ^{1}H-NMR, $CDCl_3$ δ (ppm): 7.45 (m, 4H; H–aromatic); 7.61 (m, 2H; H–aromatic); 8.09 (d, 4H; H–aromatic). ^{13}C-NMR, ($CDCl_3$) δ (ppm): 127.81, 128.89, 133.38, 143.95, (C; C–aromatic); 219.84 (C=S). FT-IR (KBr) cm^{-1}: 458 cm^{-1} (S–S), 640–880 (CH; aromatic), 1043cm^{-1} (C=S), 1639–1644 cm^{-1} (C=C; aromatic). UV maxima (nm), dichloromethane: λ = 3025 ($\pi \rightarrow \pi^*$) and λ = 524 ($n \rightarrow \pi^*$). (The ^{1}H-NMR and ^{13}C-NMR spectra of this RAFT agent are given in Appendix A, Figures A.7 and A.8, respectively.)

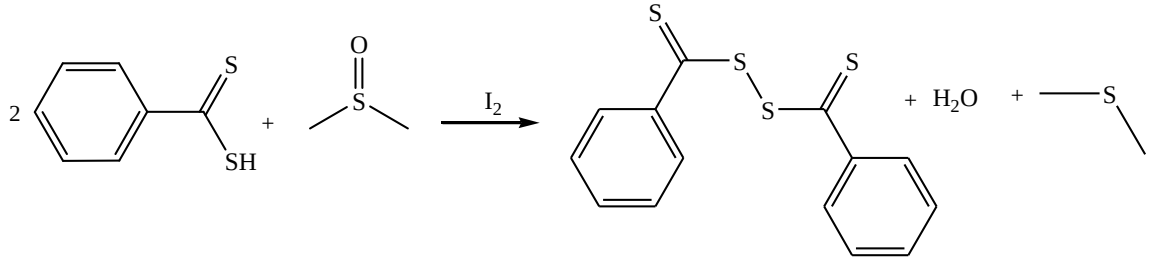

Scheme 3.6: Preparation of bis(carbonyldithio)benzoate.

3.4.5 Synthesis of 2-cyanoprop-2-yl dithiobenzoate RAFT agent

2-Cyanoprop-2-yl dithiobenzoate (Scheme 3.7) was prepared according to a method described in literature.[29] One-to-one ratios of bis(carbonyldithio)benzoate (4 g; 13 mmol) and 2,2'-azobis(isobutyrolnitrile) (1.78 g; 13 mmol) were refluxed in a medium of ethyl acetate (80 mL) at 85 °C for 8 h. The reaction was stopped by placing the flask and contents in an ice bath and the solvent was evaporated. The residual (red oil) was purified via column chromatography using hexane/chloroform (1:1) as eluent, to afford a red oil as product (4.3 g; 75% yield). ^{1}H-NMR, $CDCl_3$ δ (ppm): 7.39 (t, 2H; H–aromatic); 7.56 (t, 1H; H–aromatic); 1.94 (s, 6H; CN–$(CH_3)_2$); 7.92 (d, 2H; H–aromatic). ^{13}C-NMR, ($CDCl_3$) δ (ppm): 26.33 (C; CN–$(CH_3)_2$); 41.62 (C; C– $(CH_3)_2$); 120 (C; C–N); 126.59, 28.69, 133, 144.83 (C; C–aromatic); 223.59 (C=S). FT-IR (NaCl) cm^{-1}: 640–880 cm^{-1}

(CH; aromatic), 1048cm^{-1} (C=S), 1590 cm^{-1} (C=C; aromatic), 2231 cm^{-1} (CN), 3075 (CH_3-stretching). UV maxima (nm), dichloromethane: λ = 302 ($\pi \rightarrow \pi^*$) and λ = 514 ($n \rightarrow \pi^*$). (The ^{1}H-NMR and ^{13}C-NMR spectra of this RAFT agent are given in Appendix A, Figures A.9 and A.10, respectively.)

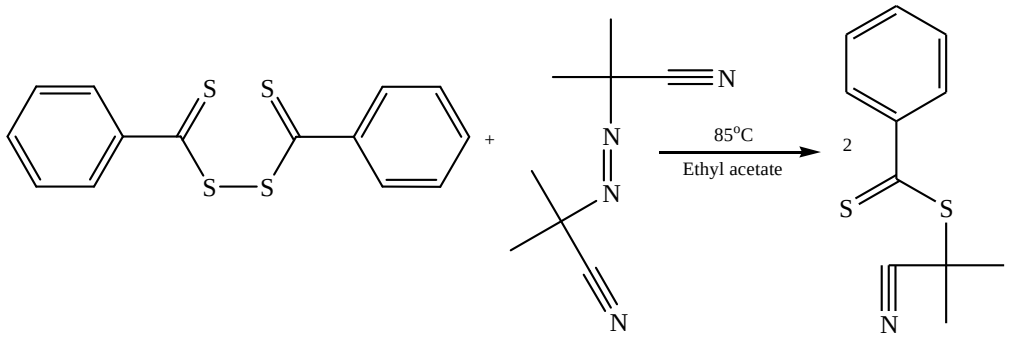

Scheme 3.7: Preparation of 2-cyanoprop-2-yl dithiobenzoate RAFT agent.

3.4.6 Synthesis of 11-bromo-undecyl-oxyphosphate

11-Bromo-undecyl-oxyphosphate (Scheme 3.8) was prepared by a modified procedure described in the literature.[26] 11-bromo-1-undecanol (12 g, 47.7 mmol) and sodium bicarbonate (4.80 g, 57.3 mmol) were suspended in distilled hexane (80 mL) in a 250-ml round-bottom flask at -10 °C (using an ice/NaCl mixture). Phosphorus(V)-oxychloride (12 g, 97.3 mmol) was added dropwise at a rate that was sufficient to maintain the above mentioned temperature for 5 h. The mixture was stirred overnight at room temperature. A solution of sodium hydroxide (7.8 g, 19.5 mmol) and water (10 mL) was then added dropwise into the flask (the contents of which was stirred at -10 °C), followed by acidification using HCl (32%), to yield a white precipitate. The precipitate was filtered and washed with water (2 × 200 mL) and then with hexane (2 × 200 mL). The remaining product was dried in a vacuum oven to yield a white solid (13 g, 81% yield). ^{1}H-NMR, ($CDCl_3$) δ (ppm), 1.21–1.50 (m, 6H; –CH_2–CH_2–), 1.67 (m, 2H; –CH_2–CH_2–), 1.86 (q, 2H; –CH_2–CH_2–), 3.42 (t, 2H; Br–CH_2), 4.05 (m, 2H; O–CH_2).

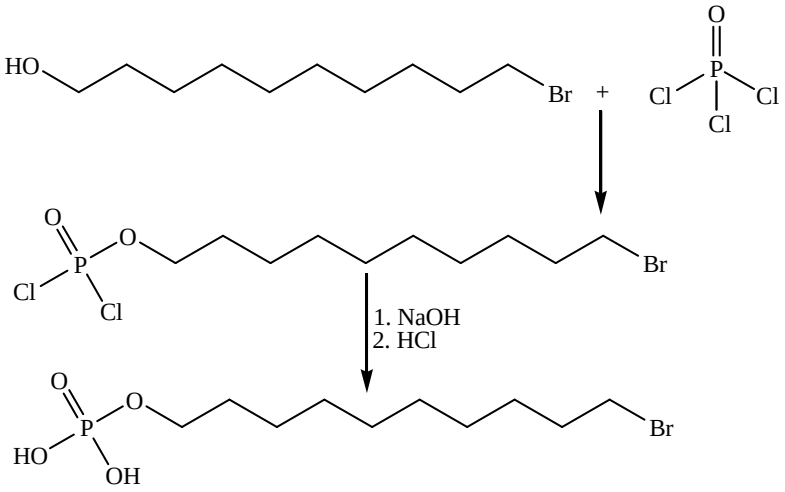

Scheme 3.8: Preparation of 11-bromo-undecyl-oxyphosphate.

3.4.7 Synthesis of S-benzyl-S′-(11-phosphonoxy-undecyl) trithiocarbonate RAFT agent

α-Toluenethiol (4 g, 32.2 mmol) and a solution of potassium hydroxide (1.78 g, 32.2 mmol) in water (70 mL) were placed in a 250-mL 3-necked round-bottom flask and stirred for 5 min. Carbon disulphide (2.45 g, 32.2 mmol) was added dropwise into the solution and stirred for 30 min (a yellow solution was observed). A prepared solution of 11-bromo-undecyl-oxyphosphate (7.4 g, 22.3 mmol) and potassium hydroxide (2.45 g, 32.2 mmol) in water (100 mL) was then added dropwise into the solution over 20 min, and the mixture heated to 70 °C for 2 h. The mixture was then cooled, and acidified using HCl (32%) to yield a yellow solid. The solid was filtered, washed with water (4 × 100 mL) and stirred with hexane (100 mL) for 1 h. The remaining solid (after filtration) was then dissolved in dichloromethane and precipitated using hexane (10/90 v/v). The product was filtrated off and dried in a vacuum oven, to yield a yellow powder (11.50 g, 60% yield). T_m = 53–55 °C. ^{1}H-NMR, $CDCl_3$ δ (ppm): 1.14–1.77 (m, 10H; –CH_2–CH_2–), 2.04 (t, 2H; CH_2–S), 4.02 (2H; O–CH_2), 7.20–7.36 (m, 5H; CH–aromatic). ^{13}C-NMR, ($CDCl_3$) δ (ppm): 24.40; 25.19; 28.18; 28.69; 29.04; 29.32; 29.97; 31.25; 36.15 (C; –CH_2–CH_2–), 33.85 (C; CH_2–CH_2–S), 41.18 (C; –S–CH_2–aromatic), 67.94 (C; CH_2–O), 126.95; 128.53; 128.94 (C; CH–aromatic), 223.98 (C=S). ^{13}P NMR, $CDCl_3$ δ (ppm): 199.75 (P–mono-phosphate). FT-IR (KBr pellets) cm^{-1}: 1060 (C=S, P–O and P=O), 1269

(P=O), 1453 (C=C; aromatic), 3444 (OH). UV maxima (nm), dichloromethane: $\lambda = 309$, ($\pi \rightarrow \pi^*$) and $\lambda = 434$ ($n \rightarrow \pi^*$). The reaction is shown in Scheme 3.9. (The ^{1}H-NMR, ^{13}C-NMR, and ^{13}P-NMR spectra of this RAFT agent are given in Appendix A, Figures A.11, A.12, and A.13, respectively.)

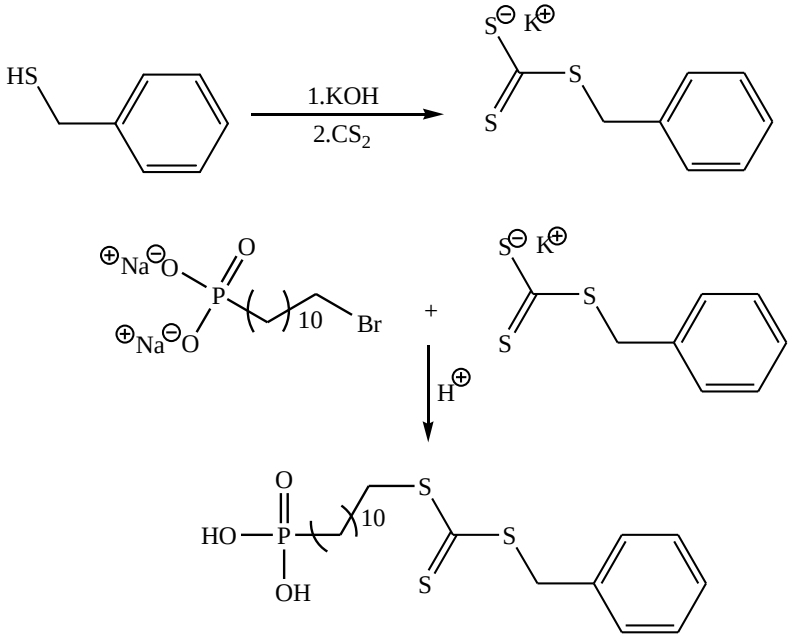

Scheme 3.9: Preparation of S-benzyl-S′-(11-phosphonoxy-undecyl) trithiocarbonate.

3.4.8 Synthesis of 4,4′-azobis(4-cyanopentanol) (hydroxyl free radical initiator)

The hydroxyl free radical initiator (Scheme 3.10a) was synthesized according to a procedure described in the literature.[30] Hydrazine sulphate (14.3 g; 110 mmol) was dissolved in water (150 mL) in a 500-mL 3-necked round-bottom flask. 5-Hydroxy-pentane-2-one (22.5 g; 220 mmol) was added and the mixture was stirred for 5 min. An aqueous sodium cyanide solution (10.8 g; 220 mmol in 100 mL water) was slowly added and the mixture was stirred overnight at room temperature. Bromine (32 g, 200 mmol) was then added dropwise over a period of 5 h (the reaction mixture turned yellow) while the temperature was kept at around 0 °C (by placing the contents in ice bath). The mixture was then acidified by slow addition of dilute HCl (32%; 50 mL /50 mL water),

keeping the reaction mixture at 0 °C. After complete addition of HCl the flask and contents were allowed to stand overnight. A white precipitate formed. This was filtered off, washed several times with water and then with pentane, and dried in a vacuum oven overnight to yield 5 g product. The filtrate was also washed with several portions of a DCM/acetone mixture (2:1). The aqueous phase was discarded and the organic portions were combined. The solvent was evaporated off and the solid residue obtained was dried in a vacuum oven to yield 3 g product. The combined yield of the two fractions was 8g (30% yield). T_{m1} = 93–95 °C, T_{m2} = 80–83 °C. ^{1}H-NMR, $(CD_3)_2SO$ δ (ppm): 1.50–1.64(m, 2H, $–CH_2–CH_2–CH_2–$), 1.72(s, 3H, $–CH_3$), 1.74–1.83 (m, 2H; $–CH_2–C(CH_3)$ –(CN)–), 2.05–2.19(m, 2H; $–CH_2–CH_2–CH_2$), 2.20–2.32(m, 2H; $–CH_2–C(CH_3)(CN)–$), 3.70(t, 2H; $–CH_2–OH$). ^{13}C-NMR, $(CD_3)_2SO$ δ (ppm): 23.20, 27.75 (C; $–CH_3$), 34.40 (C; $–CH_2–CH_2$), 60.10 (C–C), 72.45 (C; $–CH_2–OH$), 118.50 (C; CN). (The ^{1}H-NMR and ^{13}C-NMR spectra of the hydroxyl free radical initiator are shown in Appendix A, Figures A.14 and A.15, respectively.)

3.4.9 Synthesis of (E)-diazene-1,2-diylbis-3- cyanobutane-3,1-diylbis(dihydrogen phosphate) (phosphate free radical initiator)

The synthesis of phosphate free radical initiator is shown in Scheme 3.10. Phosphorus(V)-oxychloride (20 g; 130 mmol) was placed in 150-mL 3-necked round-bottom flask, and placed in an ice/ammonium chloride bath. Hydroxyl free radical initiator (4.5 g; 20 mmol) and triethylamine (5 g) were mixed and dissolved in dry THF (40 mL) and added dropwise to the contents of the flask, while the temperature was kept at -10 °C. The reaction mixture was allowed to stand overnight. An aqueous sodium hydroxide solution (20g/60 mL water) was added dropwise to the reaction mixture, while keeping the temperature at 0 °C. The solvent was evaporated off, and the water phase was washed several times with DCM. The organic portions were combined; the DCM was evaporated off to afford a solid product. The product was dissolved in DCM and precipitated in hexane (1:9 v/v) to yield a white powder (60% yield). T_m = 72 °C. ^{1}H-NMR, $(CD_3)_2SO$ δ (ppm): 1.59–1.65 (m, 2H; $–CH_2–CH_2–CH_2$), 1.70(s, 3H; $CH_3–$), 1.74-1.90 (m, 2H;$–CH_2–C(CH_3)(CN)–$), 2.05–2.19 (m, 2H; $–CH_2–CH_2–CH_2$), 2.20–2.32 (m, 2H;$–CH_2–C(CH_3)(CN)$ –), 3.70 (t, 2H; $–CH_2–OH$). ^{13}C-NMR, $(CD_3)_2SO$ δ (ppm):

23.30, 26.90 (C; - CH_3), 34.40 (C; -–CH_2–CH_2), 44.10 (C–C), 72.10 (C; –CH_2–OH), 118.15 (C; CN). (The ^{1}H-NMR, ^{13}C-NMR, and ^{13}P-NMR spectra of the phosphate free radical initiator are given in Appendix A, Figures A.16, A.17, and A.18, respectively.)

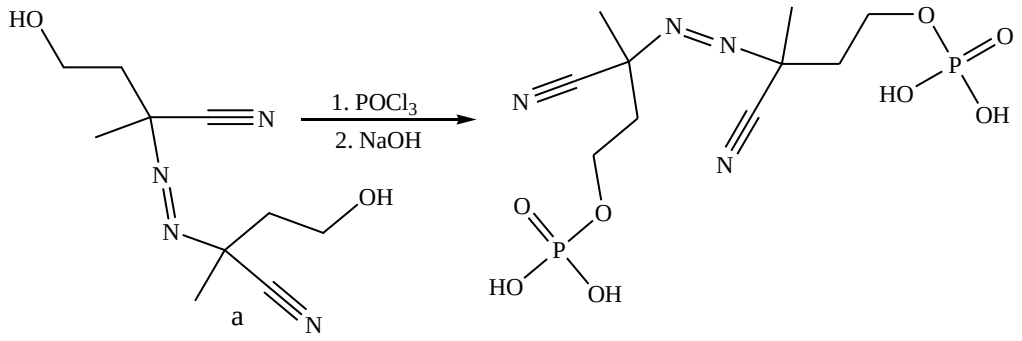

Scheme 3.10: Synthesis of phosphate free radical initiator.

3.4.10 Synthesis of 1-(1-cyano-1-methylethoxy)-2,2,6,6-tetramethylpiperidine-4-yl-hydroxyl (hydroxyl NMP initiator)

The synthesis of 1-(1-cyano-1-methylethoxy)-2,2,6,6-tetramethylpiperidine-4-yl-hydroxyl is shown in Scheme 3.11. A tube was charged with 4-hydroxy-2,2,6,6-tetramethylpiperidinyl-1-oxyl (4-hydroxyl TEMPO) (5 g; 29 mmol), AIBN (2.30 g; 29 mmol) and ethyl acetate (50 mL), then sealed, and placed in an oil bath preheated at 85°C for 8 h. The solvent was evaporated off and the residue was dissolved in DCM and precipitated using hexane (DCM/hexane was 2:8 v/v). The precipitate was filtrated off, dried in a vacuum oven to yield 5.3 g yellowish product (75%). ^{1}H-NMR, $CD_3(SO)_2$ δ (ppm): 1.16, 1.25 (m, 12H; –CH_3); 1.40–1.60 (m, 2H; –CH_2); 1.70 (s, 6H, $(CH_3)_2$–CN); 4.13 (q, H; –CH). ^{13}C-NMR, $CD_3(SO)_2$ δ (ppm): 23.30 (C; C–CH_3); 26.90 (C; C–CH_3), 34.40 (C; –CH_2–CH_2), 44.10 (C; C$(CH_3)_2$–CN); 72.10 (C; –CH_2–OH), 118.15 (C; CN). (Appendix A, Figures A.19 and A.20 are showing the ^{1}H-NMR and ^{13}C-NMR spectra of the hydroxyl NMP initiator, respectively.)

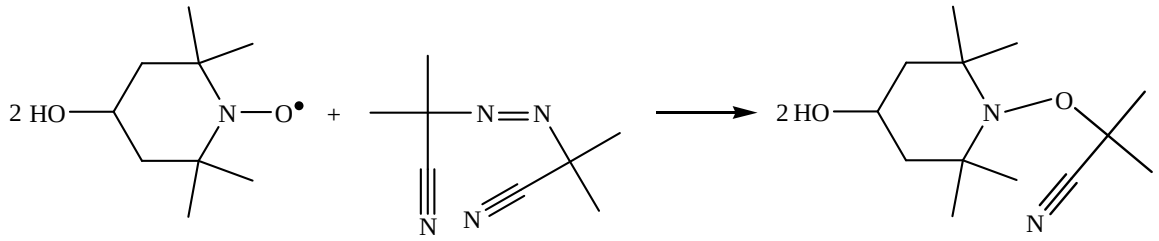

Scheme 3.11: Synthesis of 1-(1-cyano-1-methylethoxy)-2,2,6,6-tetramethylpiperidine-4-yl-hydroxyl.

3.4.11 Synthesis of 1-(1-cyano-1-methylethoxy)-2,2,6,6-tetramethylpiperidine-4-yl-dihydrogen phosphate (phosphate NMP initiator)

A typical procedure for the synthesis of 1-(1-cyano-1-methylethoxy)-2,2,6,6-tetramethylpiperidine-4-yl-dihydrogen phosphate is shown in Scheme 3.12. Phosphorus(V)-oxychloride (15 g; 98 mmol) was added to a dry 150-mL a 3-necked round-bottom flask, and placed in a ice/ ammonium chloride bath to keep the temperature at -10 °C. A solution of triethylamine (5 g) and 1-(1-cyano-1-methylethoxy)-2,2,6,6-tetramethylpiperidine-4-yl-hydroxyl (5.0 g; 20.80 mmol) in dry THF (15 mL) was then added dropwise to the flask, while the flask and contents were kept at below 0 °C. The mixture was stirred overnight at room temperature. Sodium hydroxide solution (15 g/20 mL water) was slowly added to the flask, still keeping the mixture's temperature below 0 °C. The solvent was then evaporated off, and the aqueous layer was washed with DCM (5 × 150 mL). The organic layers were combined, the solvent was evaporated off and the product was dried in a vacuum oven to afford a brownish produce (6 g). In the case where the extraction of the product was difficult, the water and organic phases were placed in a wide pan and left in a fume hood to allow the solvent and water to evaporate slowly. The residue was collected, dissolved in fresh DCM, filtered off, and the solution was treated as before to afford the product. ^{1}H-NMR, $CD_3(SO)_2$ δ (ppm): 1.12, 1.17, 1.20, 1.22 (s, 12H; $-CH_3$); 1.40-1.60 (m, 2H; $-CH_2$); 1.70(s, 6H, $(CH_3)_2$–CN); 4.13 (q, H; –CH). ^{13}C-NMR, $CD_3(SO)_2$ δ (ppm): 23.30 (C; CH_3–); 26.90 (C; C–CH_3), 34.40 (C; –CH_2–CH_2), 44.10 (C; C$(CH_3)_2$–CN); 72.10 (C; –CH_2–OH), 118.15 (C; CN). (Appendix A, Figures A.21, A.22, and A.23 are showing the ^{1}H-NMR, ^{13}C-NMR, and ^{13}P-NMR spectra of the phosphate NMP initiator, respectively.)

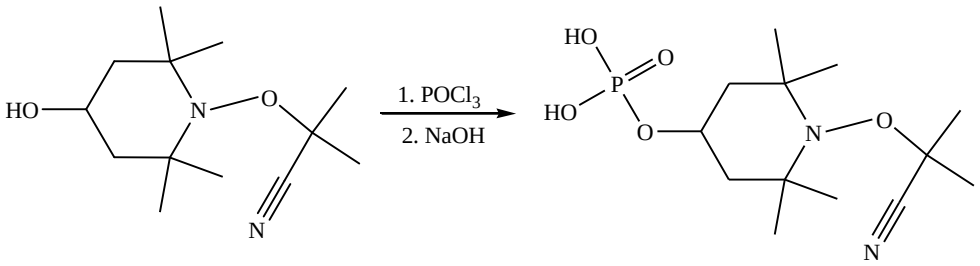

Scheme 3.12: Synthesis of 1-(1-cyano-1-methylethoxy)-2,2,6,6-tetramethylpiperidine-4-yl-dihydrogen phosphate.

3.5 Discussion

Benzyl-(4-carboxydithiobenzaote) RAFT agent was successfully prepared using the substitution reaction of 4-bromomethyl benzoic acid with a dithio group using elementry sulphur (S_8) in the presence of strong base (sodium methoxide). The substituted compound acts as a nucleophile for the substitution reaction with alkyl halides. This method was found to be efficient and yields 60% of benzyl-(4-carboxyldithiobenzoate) RAFT agent. The purity of the RAFT agent was 97%, as determined by ^{1}H-NMR.

It was however not possible to prepare the benzyl-(4-carboxydithiobenzaote) RAFT agent using the Grignard reaction. This is because of the poor solubility of the 2-(4-bromophenyl)-4,4-dimethyl-4,5-dihydro-oxazole with its protected acid group in the Grignard reaction solvent (THF).

Benzyl dithiobenzoate RAFT agent was prepared by the Grignard reaction. The Grignard reaction with carbon disulphide proceeds via a similar pathway to that of ketones. A yield of 35% of benzyl dithiobenzoate RAFT agent with purity > 98% (as determined by 1H-NMR) were obtained using the Grignard reaction.

It was not easy to prepare mono phosphate S-benzyl-S′-(11-phosphonoxy-undecyl) trithiocarbonate RAFT agent in this study, as the di-phosphate RAFT agent also forms. This is possibly because of high reactivity and valency of the phosphate. The RAFT agent was also contaminated by unreacted 11-bromo-undecyl-oxyphosphate, from which

the phosphate RAFT agent was synthesized. These impurities could not be totally removed using column chromatography. This is because the phosphate group interacts with the silica used to pack the column. Therefore, the product was purified using a simple precipitation method, which involved dissolving the product in DCM, and then adding hexane in a ratio of 1:9, v/v. Although this purification method was simple, the purity of the RAFT agent was about 75%, as determined by ^{1}H-NMR with a yield of 60%. The associated side products were 11-bromo-undecyl-oxyphosphate and di-substituted phosphate, as indicated by the ^{1}H-NMR signal at 3.34 ppm and ^{13}P-NMR signal at 198.86 ppm, (Figures A.11 and A.13), respective. In this stage of the research the purity of the product was not of the highest priority, compared with the screening investigation of the interaction efficiency of the phosphate group towards the surface of MNPs. Further investigation into improving the purity should be part of future work.

Bis(thiocarbonyl)disulphide RAFT agent was prepared by oxidizing the dithiobenzoic acid using catalytic amounts of iodine and double molar ratio of dimethyl sulphoxide in a medium of absolute methanol. The bis(thiocarbonyl)disulphide was used as intermediate for the synthesis of 2-cyanoprop-2-yl dithiobenzoate RAFT agent. This was achieved by reacting the bis(thiocarbonyl)disulphide with AIBN. The reaction proceeds by radical addition (the radical formed by the thermal decomposition of AIBN), with bis(thiocarbonyl)disulphide to form 2-cyanoprop-2-yl dithiobenzoate. Possible side products are the self reactions by combination of two radicals of 2-cyanoprop-2-yl or self disproportionations of these two radicals. The side products can be separated from the desired RAFT agent product using column chromatography on silica gel. This is indicated by the high purity of the prepared 2-cyanoprop-2-yl dithiobenzoate RAFT agent: 97%, as determined by ^{1}H-NMR. The reaction also proceeds with high efficiency yielding 81% of a 2-cyanoprop-2-yl dithiobenzoate RAFT agent.

The 4,4′-azobis(4-cyanopentanol) exists in two isomer forms with different melting temperatures.[30] Its reaction proceeds well, although the yield was as low as 30%. The later could however be due to the loss of the product during the extraction of the product from the water phase using DCM, and also from the crystallization process. The purity of

the product was reasonable good (98%), as determined by ^{1}H-NMR. The hydroxyl groups of 4,4′-azobis(4-cyanopentanol) were readily converted to phosphate groups. This was achieved by reacting the 4,4′-azobis(4-cyanopentanol) with a major excess of phosphorus(V)-oxychloride. Mono phosphate functional free radical initiator was confirmed by ^{13}P-NMR (see appendix A, Figure A.18). The product was easy to purify by precipitation using dichloromethane/hexane (1:9 v/v). The product purity was 98%, as determined by ^{1}H-NMR.

1-(1-cyano-1-methylethoxy)-2,2,6,6-tetramethylpiperidine-4-yl-hydroxyl (hydroxyl NMP initiator) was prepared by the radical addition method. A probable mechanism for its formation is shown in Scheme 3.13. 2-Cyanoprop-2-yl radical formed from the thermal decomposition of AIBN reacts with 4-hydroxy TEMPO (commercially available) to form the hydroxyl NMP initiator. This NMP initiator is expected to be fairly stable at the addition reaction temperature (80 °C), but should undergo thermal decomposition at elevated temperature. Possible by-products that might arise from the self reaction of 2-cyanoprop-2-yl radicals by combination or disproportionation, or other reactions involving this type of radicals, as discussed above. This reaction affords 75% of hydroxyl NMP initiator with 97% purity (which was determined by ^{1}H-NMR).

.

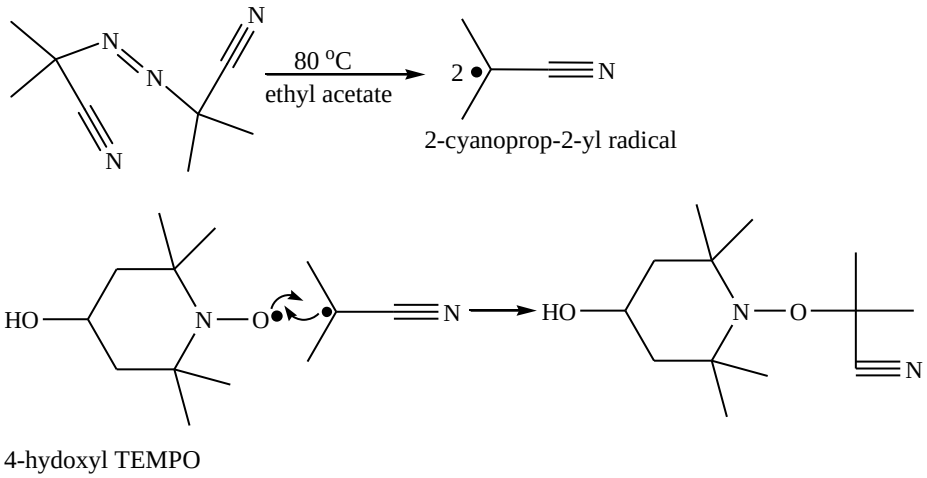

Scheme 3.13: Radical addition reaction of 2-cyanoprop-2-yl radical and 4-hydroxyl TEMPO to form 1-(1-cyano-1-methylethoxy)-2,2,6,6-tetramethylpiperidine-4-yl-hydroxyl.

1-(1-Cyano-1-methylethoxy)-2,2,6,6-tetramethylpiperidine-4-yl-dihydrogen phosphate (phosphate NMP initiator) was prepared by the reaction of the hydroxyl NMP initiator with a major excess of phosphorus(V)-oxychloride. The use of an excess amount of the phosphorus(V)-oxychloride in this reaction helps in reducing the formation of di and tri-phosphate NMP initiators. This is consistent with ^{13}P-NMR of the phosphate NMP initiator (Appendix A, Figure A.23), which shows that this NMP initiator contains one phosphate peak. The reaction yields 55% of the NMP initiator with 55% purity (as determined by ^{1}H-NMR). The product will be used after synthesis in the polymerization reaction, and the reason for this will be discussed in Chapter 6.

3.6 Conclusions

A number of RAFT agents, free radicals and NMP initiators each of which had different synthetic aspects were addressed.

Benzyl-(4-carboxydithiobenzoate), 2-cyanoprop-2-yl dithiobenzoate, and benzyl dithiobenzoate were successfully prepared in satisfactory yields, characterized by NMR, UV/Vis and FT-IR spectroscopy. S-benzyl-S′-(11-phosphonoxy-undecyl) trithiocarbonate RAFT agent was also prepared and characterized by NMR, UV/Vis and FT-IR spectroscopy. This RAFT agent contaminated with unreacted 11-bromo-undecyl-oxyphosphate, and contained di-substituted phosphate RAFT agent. The separation of the contaminants was not possible using the available separation processes including column chromatography, or crystallization processes.

The 4,4′-azobis(4-cyanopentanol) and thus (E)-diazene-1,2-diylbis-3- cyanobutane-3,1-diylbis(dihydrogen phosphate) free radical initiators were successfully prepared and characterized by NMR spectroscopy.

1-(1-cyano-1-methylethoxy)-2,2,6,6-tetramethylpiperidine-4-yl-hydroxyl and 1-(1-Cyano-1-methylethoxy)-2,2,6,6-tetramethylpiperidine-4-yl-dihydrogen phosphate NMP initiators were prepared and characterized by NMR.

3.7 References

1. Chiefari, J.; Chong, Y. K.; Ercole, F.; Krstina, J.; Jeffery, J.; Le, T. P. T.; Mayadunne, R. T. A.; Meijs, G. F.; Moad, C. L.; Moad, G.; Rizzardo, E.; Thang, S. H. *Macromolecules* **1998,** 31, 5559-5562.

2. Mayadunne, R. T. A.; Rizzardo, E.; Chiefari, J.; Moad, G.; Thang, S. H. *Macromolecules* **1999,** 32, 6977-6980.

3. Mayadunne, R. T. A.; Rizzardo, E.; Chiefari, J.; Krstina, J.; Moad, G.; Postma, A.; Thang, S. H. *Macromolecules* **2000,** 33, 243-245.

4. Chong, Y. K.; Krstina, J.; Le, T. P. T.; Moad, G.; Postma, A.; Rizzardo, E.; Thang, S. H. *Macromolecules* **2003,** *36*, 2256-2272.

5. Houben, J. *Ber.* **1906,** 39, 3219-3233.

6. Houben, J. *Ber.* **1910,** 43, 2481-2485.

7. Meijer, J.; Vermeer, P.; Brandsma, L. *Recl. Trav. Chim. Pays-Bas.* **1973,** 92, 601.

8. Solomons, T. W. G., *Organic Chemistry*; John Wiley & Sons: USA, **1988**; p 702.

9. Greene, T. W.; Wuts, P. G. M., *Protective Groups in Organic Synthesis;* John Wiley & Sons: Canada, **1991**; p 265-266.

10. Mikloweit, U.; Mattes, R. *Z. Anorg. Allg. Chem.* **1986,** 532, 145-149.

11. Oae, S.; Yaghihara, T.; Okabe, T. *Tetrahedron* **1972,** 28, 3203-3216.

12. Sugawara, A.; Shirahata, M.; Sato, S.; Sato, R. *Bull. Chem. Soc. Jpn.* **1984,** 57, 3353-3354.

13. El-Hewehi, Z. *J. Prakt. Chem.* **1962,** 16, 201-206.

14. Godt, H. C.; Wann, R. E. *J. Org. Chem.* **1961,** 26, 4047-4051.

15. Chaturvedi, D.; Chaturvedi, A. K.; Mishra, N.; Mishra, V. *Tetrahedron Lett.* **2008,** 49, 4886-4888.

16. Farnham, W. B. US2007123729/A1, **2005**.

17. Harwood, L. M.; Moody, C. J.; Percy, J. M., *Experimental Organic Chemistry;* Blackwell Science: UK, **1999**; p 468-471.

18. Pearson, E. R.; Martin, C. J. *J. Am. Chem. Soc.* **1963,** 85, 345, 3142.

19. Russell, G. A.; DeBoer, C.; Desmone, K. M. *J. Am. Chem. Soc.* **1963,** 85, 365-366.

20. Incremona, J. H.; Martin, J. C. *J. Am. Chem. Soc.* **1970,** 92, 627-634.

21. Day, J. C.; Lindstorm, M. J.; Skell, P. S. *J. Am. Chem. Soc.* **1974,** 96, 5616-5617.

22. Cary, F. A.; Sundberg, R. J., *Advanced Organic Chemistry, Part A: Structure and Mechanisims*; Plenum: New York, **1991**; p 692.

23. Hawker, C. J. *J. Am. Chem. Soc.* **1994,** 116, 11185-11186.

24. Hawker, C. J.; Barclay, G. G.; Orellana, A.; Dao, J.; Devonport, W. *Macromolecules* **1996,** 29, 5245-5254.

25. Daou, J. T.; Begin-Colin, S.; Grene`che, M. J.; Thomas, F.; Derory, A.; Bernhardt, P.; Legare´, P.; Pourroy, G. *Chem. Mater.* **2007,** 19, 4494-4505.

26. Ihara, T.; Shinji, Y.; Katsumi, K. C07F009/09, **1996**.

27. Matsuno, R.; Yamamoto, K.; Otsuka, H.; Takahara, A. *Macromolecules* **2004,** 37, 2203-2209.

28. Rizzardo, E.; Thang, S. H.; Moad, G. 98-AU569 **1999**.

29. Thang, S. H.; Chong, Y. K. B.; Mayadunne, R. T. A.; Moad, G.; Rizzardo, E. *Tetrahedron Lett.* **1999,** 40, 2435-2438.

30. Clouet, G.; Knipper, M.; Brossas, J. *Polym. Bull.* **1984,** 11, 171-174.

Chapter 4:
Synthesis, stabilization and functionalization of magnetic nanoparticles

Abstract: In this chapter experimental conditions and details for the synthesis of superparamagnetic nanoparticles (MNPs), used in this study are discussed. Steric stabilization of MNPs using oleic and decanoic acid surfactants for comparison as well as the attachment of Z-functional RAFT agents (e.g. benzyl-(4-carboxyldithiobenzoate) and S-benzyl-S′-(11-phosphonoxy-undecyl) trithiocarbonate) to the surface of MNPs by means of the ligand exchange and isothermal adsorption methods are also discussed. Fourier Transform-Infrared (FT-IR), Ultraviolet/Visible (UV/Vis) spectroscopy and Transmission Electron Microscopy (TEM) are the characterization techniques used in this study.

4.1 Introduction

Many different methods are described, or reviewed in the literature for the synthesis of magnetic nanoparticles (MNPs), including co-precipitation, microemulsion, thermal decomposition, and hydrothermal methods.[1-9] These were discussed in Sections 2.1.2.2 – 2.1.2.5. Thermal decomposition and co-precipitaion are regraded the most applicable methods for the synthesis of MNPs on a large scale.[8] Co-precipitaion is a simple, convenient and inexpensive method; it proceeds at ambient conditions in few minutes.[8] Thermal decomposition (considered the best method for the synthesis of monodisperse MNPs), involves the use of high temperatures over several days. This makes it an expensive method compared to the co-precipitation method.[8,9] The co-precipitation method was therefore selected to produce a large quantity of nanosized (10 – 20 nm) MNPs.

An unavoidable problem associated with nanosized MNPs is the instability of the MNPs over a long period of time.[10] This is possibly because of the tendency of MNPs to form large aggregation clusters, to reduce the energy associated with high surface area to volume ratio of these MNPs. Naked (uncoated) MNPs are chemically reactive; they can oxidize to form hematite.[7] The instability and chemical reactions of MNPs result in loss of magnetism of the MNPs. To passivate the surface of MNPs and in order to avoid the aggregation problem, it is necessary to stabilize the MNPs. Electrostatic stabilization using ionic surfactants in aqueous medium can be used. This type of stabilization however cannot provide adequate stability to MNPs in organic solvents (to meet the goals in this study).[5] Steric stabilization, on the other hand, using surfactants[11,12] or polymers[5] provides stabilization of these MNPs in organic solvents.

One of the aims in this section of this study is to determine suitable methods for the attachment of RAFT agents to the surface of MNPs. If successful, these RAFT agents attached to the surface of MNPs can then be used for the synthesis of polystyrene (PSt) grafted to the surface of MNPs. The methods that are used for the attachment of the RAFT agents to the surface of MNPs include:

- An isothermal adsorption process, where hydroxyl groups on the surface of MNPs exerts electrostatic forces towards the attachment group to the surface of MNPs of the RAFT agent, which leads to attachment of this RAFT agent to the surface of MNPs.

- A ligand exchange process (chemical transformation process) has been widely used for the modification of nanoparticle surfaces to produce organic-and water-soluble nanoparticles.[13,14] The process is based on the exchange of oleic acid (used to stabilize MNPs) on the surface of MNPs with other molecules which then attach to the surface of MNPs. The exchange of oleic acid on the surface of MNPs by galactaric and citric acids have been reported in literature.[15]

Benzyl-(4-carboxydithiobenzoate) (Z-carboxylate RAFT agent), and S-benzyl-S′-(11-phosphonoxy-undecyl) trithiocarbonate (Z-phosphate RAFT agent), used in this study are shown in Scheme 4.1.

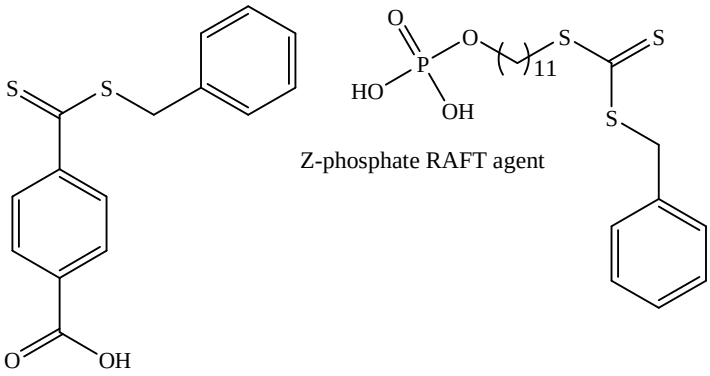

Scheme 4.1: Benzyl-(4-carboxydithiobenzoate) (Z-carboxylate), and S-benzyl-S′-(11-phosphonoxy-undecyl) trithiocarbonate (Z-phosphate) RAFT agents.

4.2 Characterization

The size and distribution of MNPs were determined by Transmission Electron Microscopy (TEM). Fourier Transform-Infrared (FT-IR) spectroscopy was used for the structure characterization of MNPs RAFT agents and to study and confirm the structure

of the RAFT agents attached to the surface of MNPs (RAFT–MNPs). UV/Vis spectroscopy was used to determine the amounts of the RAFT agents attached to the surface of MNPs.

4.2.1 Transmission Electron Microscopy

Particle morphology, size, and size distribution of MNPs was determined using TEM. The image analysis was performed using a JEOL 200 CX instrument. Magnetite samples were first diluted with water and stained with the negative staining agent uranyl acetate (UAc). A small portion of the diluted magnetite sample was then mixed with a drop of UAc solution (2%). A small drop of the magnetite/UAc mixture was placed on 200-mesh copper grid. The grid was left for few minutes at room temperature to dry before being placed in the instrument.

4.2.2 Fourier Transform-Infrared spectroscopy

Structures of MNPs, RAFT agents and RAFT–MNPs were determined by FT-IR. All MNPs, RAFT agents and RAFT–MNPs samples were first dried for 24 h in a vacuum oven to remove any traces of solvent or moisture. The solid samples were then mixed with potassium bromide (KBr) in a ratio of 1:250, and ground into a fine powder. A small portion of each sample was placed in a cylinder and pressed with a hydraulic pump to form a small round KBr disk. The disk was placed in the instrument and the IR spectra recorded. The spectra were recorded using a Thermo Nicolet instrument. Thirty-two scans were used. All recordings were done under nitrogen.

4.2.3 UV/visible spectroscopy

The UV absorbance of the RAFT agent groups were recorded using a Perkin Elmer Lamba 20 UV/Visible spectrometer. All samples of the RAFT agents used to create UV calibration curves were dissolved in dichloromethane (DCM) and then 1.5 mL of each sample transferred into quartz cuvettes, and the spectra were recorded. A sample of each decanted methanol solution containing RAFT agents that did not attach to the surface of the MNPs (1.5 mL) was also transferred into quartz cuvettes. The spectrum of each decanted solution was then recorded in the same manner.

4.3 Experimental

4.3.1 Materials

Ferric chloride hexahydrate (99%; Merck), ferrous sulphate heptahydrate (98%; Merck), ammonia solution (25%; Merck), decanoic acid (99%; Merck), oleic acid (99%; Merck), pH 4 buffer solution (BDH), DCM (98%; Saarchem), and methanol (99%; Merk) were used as received.

4.3.2 Synthesis of magnetic nanoparticles

A typical batch of MNPs was synthesized as follows: Ferric chloride hexahydrate (2.34 g, 6.8 mmol) and ferrous sulphate heptahydrate (1.2 g, 3.4 mmol) were dissolved in deionized water (100 mL) in a 250-mL 3-necked round-bottom flask. After purging the mixture with nitrogen for 5 min, ammonia solution (4 mL) was added through syringe under vigorous mixing. A black dispersion was immediately formed. It was stirred for another 15 min at room temperature. Magnetic nanoparticles were then separated by applying an external magnetic field (provided by a Neodymium (NdFeB) magnet, at a measured magnetic field intensity of 4.5×10^5 A/m) and washed several times with deionized water until the pH of the decanted solution reached ~7.0. The particles were thereafter dried in a vacuum oven to give 0.98 g of a black powder (98% yield). The chemical reactions involved in the co-precipitation method for the synthesis of MNPs are shown in Scheme 4.2.

$$Fe^{2+} + 2Fe^{3+} + 8\ OH^- \longrightarrow Fe_3O_4 + 4H_2O$$

Scheme 4.2: Chemical reaction involved in the co-precipitation method for the synthesis of MNPs of (Fe_3O_4 structure).[7]

4.3.3 Stabilization of magnetic nanoparticles

Stabilization of a typical batch of MNPs was carried out as follows: Freshly washed and prepared MNPs (4.0 g; 17 mmol) were dispersed in deionized water (150 mL) at pH 4 – 5 (a buffer solution of pH 4 was used (4 mL)) and 0.5 M NaCl. Oleic acid/ or decanoic acid (4.5 g, 16 mmol and 4.5 g, 26 mmol, respectively) in DCM (150 mL) was added and the

dispersion stirred for 18 h. The stabilized dispersed particles were separated from the aqueous layer. Methanol (150 mL) was then added into the separated dispersed particles and the contents stirred for 5 min. The MNPs was isolated by applying an external magnetic field (provided by an NdFeB magnet, at a magnetic field intensity of 4.5 × 105 A/m), and then washed several times with methanol to remove the excess oleic acid. The particles were then dispersed again in a sufficient volume of DCM (e.g. 100 mL) for the attachment of the RAFT agents. Scheme 4.3 shows the stabilization of the MNPs using oleic acid surfactant.

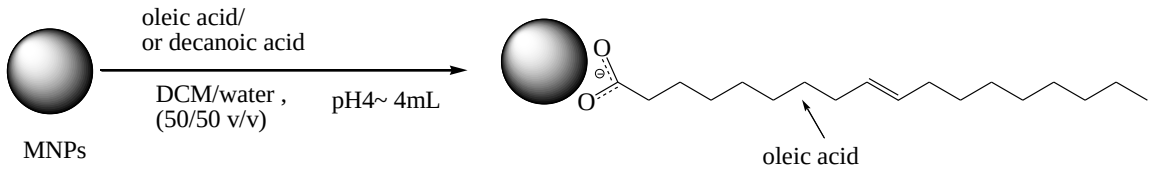

Scheme 4.3: Stabilization of MNPs using oleic acid surfactant.

4.3.4 Attachment of the RAFT agents to the surface of MNPs by means of the isothermal adsorption process

The attachment of Z-carboxylate RAFT agent to the surface of MNPs by means of the isothermal adsorption process is shown in Scheme 4.4. A dispersion of MNPs in water (1g/ 50 mL) (was made acidic (pH 4–5) by addition of pH 4 buffer solution (4 mL)) and 5 g NaCl were mixed and placed in a 150 mL round-bottom flask. A solution of Z-carboxylate RAFT agent (0.25g) in DCM (50 mL) was added to the contents in the flask, and stirred at room temperature for 18 h. An equivalent weight quantity of decanoic acid to MNPs was added, and the mixture stirred for another 24 h. The organic layer was separated from the aqueous layer. A strong, external magnetic field (provided by an NdFeB magnet, at a magnetic field intensity of 4.5 × 105 A/m) was then applied to the MNPs dispersion, which attracted the MNPs and any attached RAFT agent, thus separating the MNPs from the remaining solution. The remaining solution (the solution containing the free unattached RAFT agent) was decanted and collected. The MNPs dispersion and attached RAFT agents were dispersed in methanol (20 mL), stirred for 5

min, separated in the same manner as discussed above, decanted, and placed in a separate tube. The decanted methanol in the tube was transferred into UV/Vis spectroscopy lab to determine the quantity of unattached RAFT agent by measuring the UV absorbance of this decanted solution

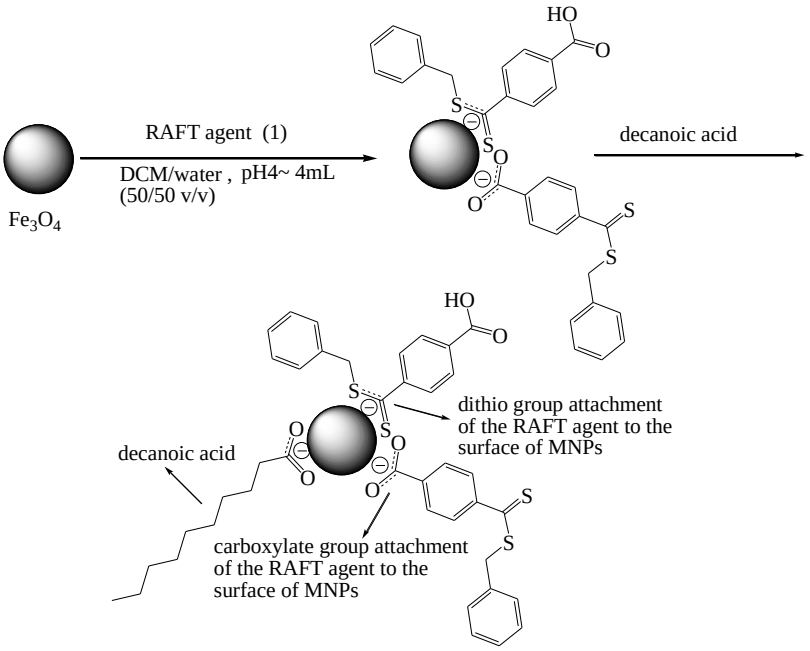

Scheme 4.4: Attachment of Z-carboxylate RAFT agent to the surface of MNPs by means of the isothermal adsorption process.

The procedure was repeated several times until the UV/Vis spectroscopy could detect no UV absorbance peak of the RAFT groups in the decanted methanol, indicating that the methanol contained no unattached RAFT agent. The quantities of the Z-carboxylate RAFT agent attached to the surface of MNPs using the isothermal adsorption process, at two different concentrations of Z-carboxylate RAFT agent/ magnetite (g), are given in Table 4.1

Table 4.1: Quantity of the Z-carboxylate RAFT agent attached to the surface of the MNPs, achieved using the isothermal adsorption process.

Experiment	RAFT agent (g)	MNPs (g)
1	0.1	1
2	0.05	4.5

4.3.5 Attachment of the RAFT agents to the surface of magnetic nanoparticles by means of the ligand exchange process

The attachment of Z-carboxylate RAFT agent to the surface of MNPs by means of the ligand exchange process is shown in Scheme 4.5. The Z-carboxylate or Z-phosphate RAFT agents were attached to the surface of MNPs by thoroughly mixing and stirring the RAFT agent of choice (e.g. 0.3 mmol), DCM (70 mL), and stabilized MNPs (4.5 g) at room temperature for 24 h. The Z groups of the RAFT agents attached to the surface of the MNPs, concurrently displacing a fraction of the oleic acid used to stabilize the MNPs. A strong, external magnetic field (provided by an NdFeB magnet, at a magnetic field intensity of 4.5 × 105 A/m) was applied to the MNPs dispersion, which attracted the MNPs and any attached RAFT agents, thus separating the MNPs from the remaining solution. The remaining solution (the solution containing the free unattached RAFT agents) was decanted, collected, and placed in a separate tube. The dispersion of MNPs and attached RAFT agent were then treated in the same way, as discussed earlier in Section 4.3.4.

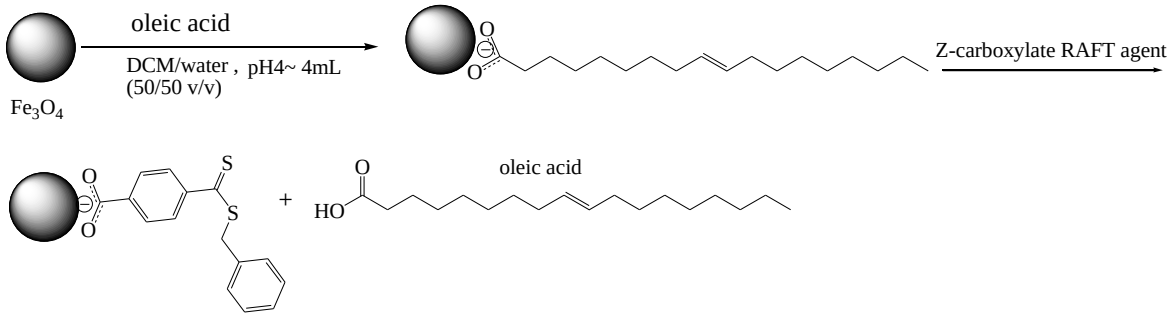

Scheme 4.5: Attachment of the Z-carboxylate RAFT agent to the surface of MNPs by means of the ligand exchange process.

The quantities of the attached Z-carboxylate and Z-phosphate RAFT agents to the surface of the MNPs are given in Table 4.2.

Table 4.2: Quantities of the Z-carboxylate and Z-phosphate RAFT agents attached to the surface of MNPs, achieved using the ligand exchange process.

Experiment	RAFT agent	RAFT agent (g)	MNPs (g)
1	Z-carboxylate	0.06	4.5
2	Z-phosphate	0.11	4.5

4.4 Results and discussion

4.4.1 FT-IR characterization of the MNPs, stabilized MNPs and RAFT agent attached to the surface of the MNPs

Figure 4.1 shows the FT-IR spectra of (a) MNPs, (b) the unattached Z-carboxylate RAFT agent (free Z-carboxylate RAFT agent), and (c) the Z-carboxylate RAFT agent attached to the surface of the MNPs (Z-carboxylate RAFT-MNPs) by means of the isothermal adsorption process.

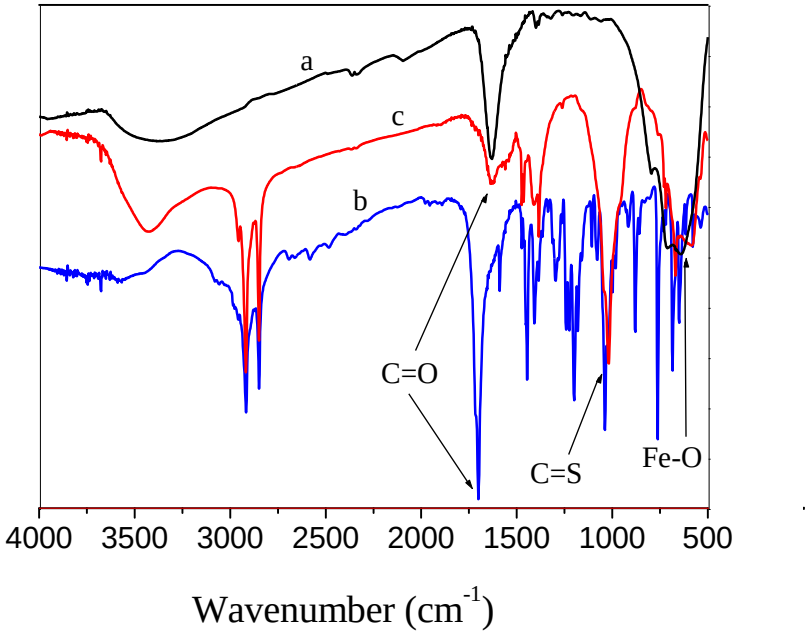

Figure 4.1: FT-IR spectra of (a) MNPs, (b) the Z-carboxylate RAFT agent (unattached Z-carboxylate RAFT agent), and (c) the Z-carboxylate RAFT-MNPs (attached by isothermal adsorption process).

(a) Figure 4.1 a shows that MNPs have absorption bands at 639 cm^{-1} and 1635 cm^{-1} due to vibration and stretching of the Fe–O, respectively

(b) Figure 4.1b shows the unattached Z-carboxylate RAFT agent has absorption bands at 1036 cm^{-1} and 1704 cm^{-1} due to C=S and C=O of the unattached Z-carboxylate RAFT agent.

(c) Figure 4.1c shows that the Z-carboxylate RAFT-MNPs have absorption bands at 1015 cm^{-1} and 1635 cm^{-1} due to C=S and C=O of the Z-carboxylate RAFT agent attached to the surface of MNPs, respectively. It also shows absorption bands at 639 cm^{-1} and 1635 cm^{-1} due to vibration and stretching of (Fe–O), respectively.

These results show that the absorption bands of the C=S and C=O of the Z-carboxylate RAFT-MNPs clearly shifted from the bands of the C=S and C=O of the Z-carboxylate RAFT agent (unattached Z-carboxylate RAFT agent). These results indicate that the Z-carboxylate RAFT agent was attached to the surface of the MNPs by means of the isothermal adsorption process. They also indicate that the Z-carboxylate RAFT agent attaches to the surface of the MNPs by its carboxylate and dithio groups

Figure 4.2 shows the FT-IR spectra of (a) MNPs, (b) stabilized MNPs with oleic acid (oleic acid attached to the surface of the MNPs), and (c) the Z-carboxylate RAFT-MNPs by means of the ligand exchange process.

(a) Figure 4.2a shows that MNPs have absorption bands at 639 cm^{-1} and 1635 cm^{-1} due to vibration and stretching of the Fe–O, respectively.

(b) Figure 4.2b shows that the stabilized MNPs with oleic acid has absorption band at 1530 cm^{-1} due to C=O of the oleic acid. It also has absorption bands at 639 cm^{-1} and 1635 cm^{-1} due to vibration and stretching of the Fe–O, respectively, as expected when oleic acid used to stabilize the MNPs.

(c) Figure 4.2c shows that the Z-carboxylate RAFT-MNPs have absorption bands at 1036 cm^{-1} and 1650 cm^{-1} due to C=S and C=O of the Z-carboxylate RAFT-MNPs, respectively. They also have absorption bands at 639 cm^{-1}, 1635 cm^{-1}, and 1605 cm^{-1} due to stretching and vibrating of the Fe–O and C=O of the oleic acid, respectively.

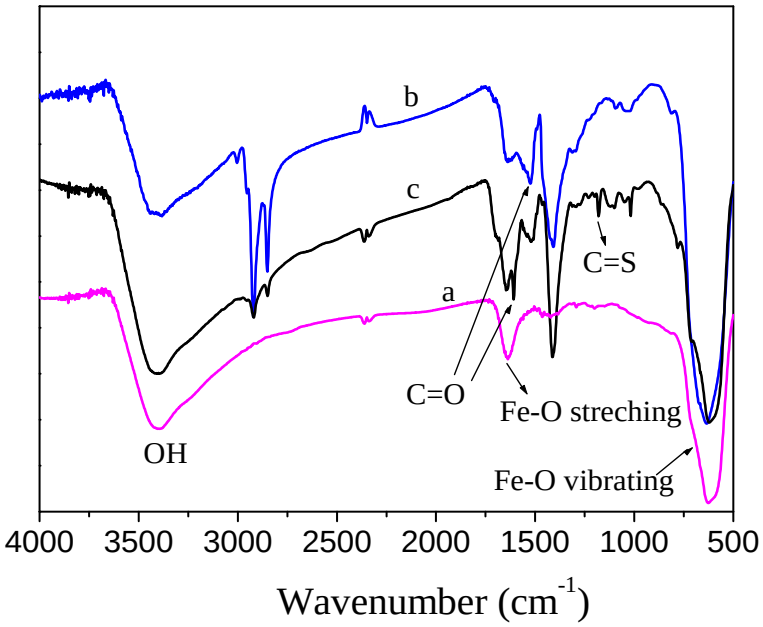

Figure 4.2: FT-IR spectra of (a) MNPs, (b) stabilized MNPs with oleic acid, and (c) the Z-carboxylate RAFT-MNPs (attached by means of the ligand exchange process).

These results show that the absorption band of the C=O of the Z-carboxylate RAFT-MNPs shifted from that of the C=O of the unattached Z-carboxylate RAFT agent (see Figure 4.1b). The absorption band of the C=S of the Z-carboxylate RAFT-MNPs however, did not shift from that of the C=S of the unattached RAFT agent. These results indicate therefore, that the Z-carboxylate RAFT agent was attached to the surface of the MNPs by means of the ligand exchange process. They also indicate that the Z-carboxylate RAFT agent was most probably attached to the surface of the MNPs via its carboxylate group.

Figure 4.3 shows the FT-IR spectra of (a) MNPs, (b) the unattached Z-phosphate RAFT agent, (c) stabilized MNPs with oleic acid, and (d) the Z-phosphate RAFT-MNPs by means of the ligand exchange process.

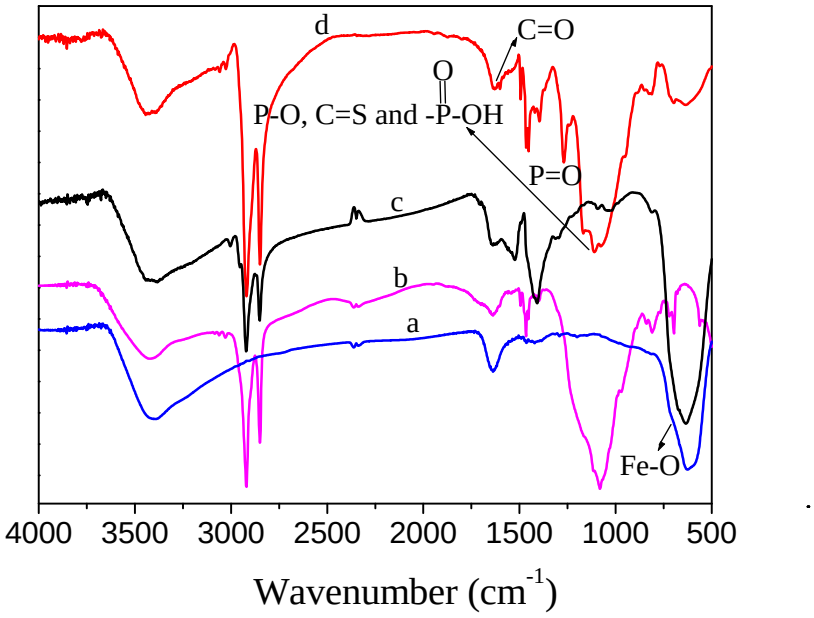

Figure 4.3: FT-IR spectra of (a) MNPs, (b) the Z-phosphate RAFT agent (unattached Z-phosphate RAFT agent), (c) MNPs surface modified by oleic acid, and (d) the Z-phosphate RAFT-MNPs (attached by the ligand exchange process).

(a) Figure 4.3a shows that MNPs have absorption bands at 639 cm^{-1} and 1635 cm^{-1} due to vibration and stretching of the Fe–O, respectively.

(b) Figure 4.3b shows the unattached Z-phosphate RAFT agent has strong and broad absorption band at 1098 cm^{-1}, 1456 cm^{-1} due to C=S band overlapped with that of P–O and P=O, and CH binding of the unattached Z-phosphate RAFT agent, respectively.

(c) Figure 4.3c shows that the stabilized MNPs with oleic acid has an absorption band at 1530 cm^{-1} due to the C=O of the oleic acid. It also has absorption bands at 639 cm^{-1} and 1635 cm^{-1} due to vibration and stretching of the Fe–O, respectively. This result indicates that the MNPs were stabilized with oleic acid.

(d) Figure 4.3d shows that the Z-phosphate RAFT-MNPs have absorption bands at 1114 cm^{-1}, 1273 cm^{-1} , and 1456 cm^{-1} due to C=S, P=O, and CH of the Z-phosphate RAFT-MNPs, respectively. It also shows that they have absorption bands at 1530 cm^{-1} due to the C=O of oleic acid, and that at 639 cm^{-1} and 1635 cm^{-1}due to stretching and vibrating of the Fe–O, respectively.

These results show that the absorption band at 1114 cm^{-1} of C=S and P–O of the Z-phosphate RAFT-MNPs shifted from that at 1098 cm^{-1} of C=S and P–O of the unattached Z-phosphate RAFT agent. They also show that the absorption band at 1273 cm^{-1} of P=O of the Z-phosphate RAFT-MNPs separated and shifted from that broad band at 1098 cm^{-1} of the unattached Z-phosphate RAFT agent. These indicate that the Z-phosphate RAFT agent was attached to the surface of the MNPs.

4.4.2 Attachment of the Z-carboxylate RAFT agent to the surface of the MNPs (ligand exchange vs isothermal adsorption process)

The Z-carboxylate RAFT agent was attached to the surface of MNPs using the isothermal adsorption process. The attachment efficiency of the Z-carboxylate RAFT-MNPs was as low as 40% (by weight) (1.80 RAFT agent molecule/ nm^2, based on 5.20 g/cm^3 density of MNP and 10 nm average diameter size of each MNP). This low grafting efficiency (by weight with respect to the total amount of RAFT agent used in the attachment process (0.25 g)) of the Z-carboxylate RAFT to the surface of MNPs, is probably due to poor diffusion of the RAFT agent between the water and organic phases, before it reaches the surface of MNPs and became attached. However, the process is efficient for the attachment of a large number of RAFT agent molecules per nm of magnetite. This process also led to the attachment of the Z-carboxylate RAFT agent to the surface of MNPs by its dithio and carboxylate groups (illustrated in Scheme 4.4). The structure of the Z-carboxylate RAFT-MNPs by means of the isothermal adsorption process was determined by FT-IR. The FT-IR result showed that the Z-carboxylate RAFT agent was attached to the surface of the MNPs by its dithio and carboxylate groups (see Figure 4.1).

The hydroxyl groups on the surface of MNPs may exert electrostatic forces towards the dithio groups of the RAFT agents, leading thus to RAFT agents to attach to the surface of

MNPs via dithio groups, as observed in this study. The idea that the hydroxyl groups on the surface of MNPs exert electrostatic forces towards dithio groups of RAFT agents has been used as explanation for RAFT agents attached to the surface of gold nanoparticles (they also have hydroxyl groups, similar to MNPs).[16]

The Z-carboxylate RAFT agent was attached to the surface of MNPs via a chemisorptions exchange process. In this process the Z-carboxylate RAFT agent attach to the surface of MNPs by displacing some fraction of oleic acid (illustrated in Scheme 4.5). The attachment efficiency of the Z-carboxylate RAFT agent to the surface of MNPs reached 75% (by weight) (0.24 RAFT agent molecule/nm^2 magnetite, based on 5.20 g/cm^3 MNP and 10 nm average diameter size of each MNP). This result indicates that the ligand exchange process is also efficient for the attachment of the Z-carboxylate RAFT agent to the surface of MNPs.

In the ligand exchange process, MNPs are protected by oleic acid prior to the attachment of the RAFT agent to the surface of MNPs. Oleic acids most probably reacted by displacing hydroxyl groups on the surface of MNPs. Thus, there will probably be a negligible fraction of hydroxyl groups on the surface of MNPs, resulting in less significant interaction between the MNPs and dithio groups of the Z-carboxylate RAFT agents. The structure of the Z-carboxylate RAFT-MNPs by means of the ligand exchange process was determined by FT-IR (Figure 4.2), which shows that the Z-carboxylate RAFT agent attached to the surface of the MNPs by its carboxylate groups.

4.4.3 Attachment of the Z-phosphate RAFT agent to the surface of the MNPs

The Z-phosphate RAFT agent was also attached to the surface of MNPs using the ligand exchange process. The results show that the attachment efficiency was 85% (by weight) (0.28 RAFT agent molecule/ nm2 magnetite, based on 5.2 g/ cm3 density of MNP and 10 nm average diameter size of each MNP), indicating efficient exchange between the oleic acid on the surface of MNPs and the phosphate group of the RAFT agent. This result indicates that the phosphate group of the RAFT agent has better affinity for exchangeability of oleic acid on the surface of MNPs than that of the carboxylate group

of the RAFT agent. This is probably because of the higher acidity and polarity of the phosphate group than the carboxylate group, resulting in more oleic acid fraction on the surface of MNPs to be replaced by the phosphate group of the RAFT agent, as was observed in this study.

4.4.4 Determination of the quantities of the RAFT agents attached to the surface of the MNPs using UV/Vis spectroscopy

The quantities of the Z-carboxylate RAFT-MNPs and Z-phosphate RAFT-MNPs were determined using UV/Vis spectroscopy and gravimetric analysis. UV/vis spectroscopy was first used to create UV calibration curves using each of RAFT agents. In the UV calibration curves, the RAFT agents were used free. Each RAFT agent (to be attached to the surface of MNPs) was therefore dissolved in DCM to prepare solutions of this RAFT agent at known concentrations. Different solutions of each RAFT agent, at different concentrations, were prepared, and then the UV absorbancies of the RAFT groups of each solution were determined by UV/Vis spectroscopy. The UV calibration curves were then created by plotting these UV absorbancies of each solution of known concentration of the RAFT agent against the concentrations of this RAFT agent in this each solution, resulting in the UV calibration curves shown in Figures 4.4 and 4.5. Because of the two wavelengths at which the RAFT groups absorb UV radiations (e.g., λ_{505} and λ_{249} for the Z-carboxylate RAFT agent, Figure 4.4), each RAFT agent therefore has two UV calibration curves: one corresponds to absorbance at high wavelength, the other one corresponds to that at low wavelength (e.g. Figures 4.4a and 4.4b).

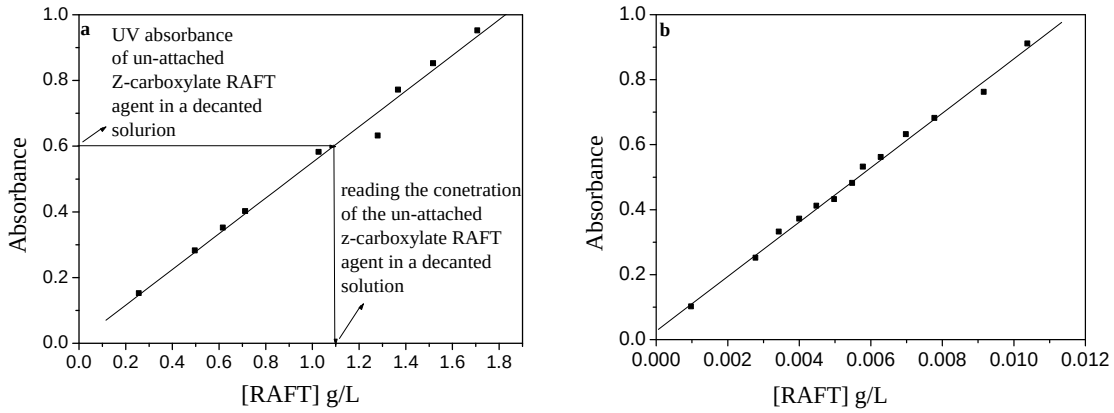

Figure 4.4: UV calibration curves of the Z-carboxylate RAFT agent in dichloromethane: (a) ($n \rightarrow \pi^*$) at λ_{505}, ε_{505} (160.95 l/mol/cm) and (b) ($\pi \rightarrow \pi^*$) at λ_{249}, ε_{249} (26560 l/mol/cm).

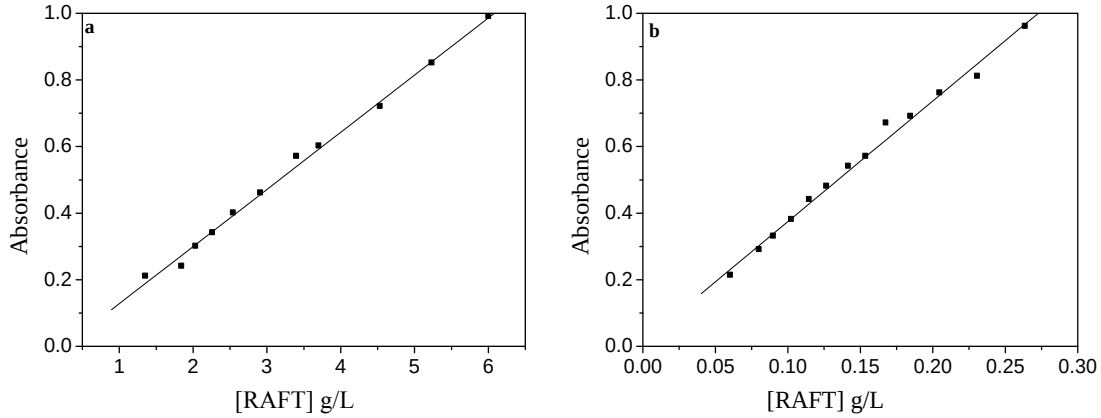

Figure 4.5: UV calibration curves of the Z-phosphate RAFT agent in dichloromethane: (a) ($n \rightarrow \pi^*$) at λ_{434} ε_{434} (73.64 l/mol/cm) and (b) ($\pi \rightarrow \pi^*$) at λ_{309}, ε_{309} (1687.50 l/mol/cm).

The UV calibration curves were then used to determine the quantities of the unattached Z-carboxylate and unattached Z-phosphate RAFT agents to the surface of the MNPs after the attachment process. This was done first by measuring the UV absorbance of each collected decanted solution (containing quantities of unattached RAFT agents to the surface of MNPs after the attachment process, as discussed in Section 4.3.4), and secondly determining the concentration of the RAFT agents in each decanted solution, which can be obtained from the UV calibration curve (see example illustrated in Figure 4.4a).

The quantities of the Z-carboxylate and Z-phosphate RAFT agents attached to the surface of MNPs were then determined gravimetrically using Equation 4.1:

$$W_{attached} = W_{total} - W_{unattached} \quad (4.1)$$

where $W_{attached}$ is the weight amount of the RAFT agent attached to the surface of MNPs, W_{total} is the total amount of the RAFT agent initially used in the attachment process of this RAFT agent to the surface of MNPs, and $W_{unattached}$ is the remaining quantity of the unattached RAFT agent after the attachment process.

4.4.5 TEM results of the MNPs and dispersion of stabilized MNPs by decanoic and oleic acid surfactants

Figure 4.6 (a – c) shows the TEM images of the MNPs, dispersion of stabilized MNPs with decanoic acid, and dispersion of stabilized MNPs with oleic acid, respectively. Typical aggregation of the MNPs can be clearly seen in Figure 4.6a.

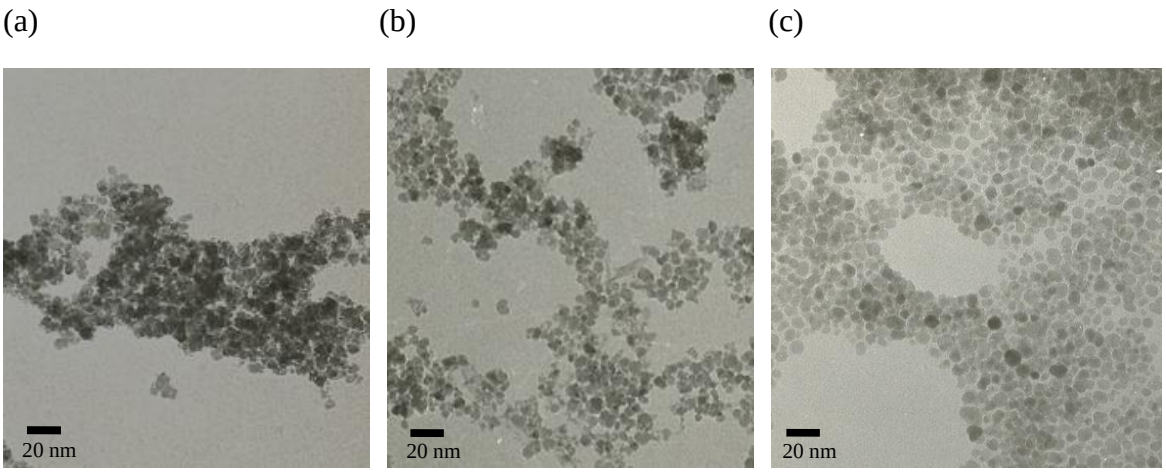

Figure 4.6: TEM analysis of (a) MNPs, (b) dispersion of stabilized MNPs magnetite with decanoic acid and (c) dispersion of stabilized MNPs with oleic acid.

Aggregation occurs mainly due to the surface interaction between MNPs to decrease their surface energies. This renders the MNPs less useful for many applications. This is because the actual size and size distribution of these MNPs is disrupted by the large aggregation cluster, as observed in this TEM analysis of the MNPs (Figure 4.7a). This

result therefore indicates that MNPs stabilization is necessary to prevent their aggregation and to improve the solubility of these MNPs in organic solvents. Figure 4.6b shows the TEM image of a dispersion of stabilized MNPs with decanoic acid surfactant. Decanoic acid clearly stabilizes the MNPs to an extent, but not so totally that it prevents particle aggregations. This is illustrated by the large amount of MNPs aggregations in Figure 4.6b. In the case of oleic acid used to stabilize the MNPs, there were no observed aggregations of MNPs (see Figure 4.6c). This result indicates that oleic acid is a better candidate for the stabilization of MNPs than the decanoic acid. This is possibly because of the longer chain of oleic acid compared to that of decanoic acid, which might provide better steric stability to the MNPs, as was observed in this study.
TEM results also showed that the average size of the dispersion of stabilized MNPs with oleic acid was 10 nm in all three dimensions (considering the spherical shape).

4.5 Conclusions

MNPs were successfully synthesized by a co-precipitation method in alkaline medium and characterized by TEM and FT-IR. The method was found to be efficient for the synthesis of MNPs and yielded >98% of MNPs. The average particle size of the dispersion of stabilized MNPs was 10 nm in all three dimensions (assuming spherical shape and excluding particle aggregation). The MNPs prior to stabilization are colloidally unstable and interact strongly with each other to form large clusters of aggregated particles. However, less aggregation occurred when the MNPs were stabilized by decanoic acid, and no significant aggregation was observed when they were stabilized by oleic acid.

Z-carboxylate and Z-phosphate RAFT agents were successfully attached to the surface of the MNPs. The attachment structures of these RAFT agents were determined using FT-IR spectroscopy. The quantities of these RAFT agents that were attached to the surface of MNPs were determined using UV/Vis spectroscopy.

The attachment efficiency of the RAFT agents to the surface of the MNPs was based on the attachment force of the RAFT agent to the surface of the MNPs, and also on the

attachment method used to attach the RAFT agents to the surface of the MNPs. Both the ligand exchange and isothermal adsorption processes were found to be efficient for the attachment of the Z-carboxylate and Z-phosphate RAFT agents to the surface of the MNPs in this study. Table 4.3 is summerizing all the grafting efficiencies of Z-carboxylate and Z-phosphate RAFT agents onto the surface of MNPs via ligand exchange and isothermal adsorption processes.

The phosphate group has better affinity towards the surface of the MNPs compared to that of the carboxylate group.

Table 4.3: Grafting effecincies of the Z-carboxylate and Z-phosphate RAFT agents attached to the surface of MNPs, achieved using the ligand exchange and isothermal adsorption processes.

Method used	RAFT agent	Number of RAFT molecules/ nm^2 magnetite
isothermal	Z-carboxylate	1.80
ligand exchange	Z-carboxylate	0.24
ligand exchange	Z-phosphate	0.28

4.6 References

1. Pich, A.; Bahattacharya, S.; Ghosh, A.; Alder, P. *Polymer* **2005,** 46, 4596-4603.

2. Yamaura, M.; Camilo, R.; Sampaio, L.; Macedo, M.; Nakamura, M.; Toma, H. *J. Magn. Magn. Mater.* **2004,** 279, 210-217.

3. LaConte, L.; Nitin, N.; Bao, G. *Nanotoday* **2005,** 8, 32-38.

4. Asmatulu, R.; Zalich, M.; Claus, R.; Riffle, J. *J. Magn. Magn. Mater.* **2004,** 292, 108-119.

5. Harris, L.; Goff, J.; Carmichael, A.; Riffle, J.; Harburn, J.; Pierre, T.; Saunders, M. *Chem. Mater.* **2003,** 15, 1367-1377.

6. Dresco, A. P.; Zaitsev, S. V.; Gambino, J. R.; Chu, B. *Langmuir* **1999,** 15, 1945-1951.

7. Kim, D.; Mikhaylova, M.; Zhang, Y.; Mohamed, M. *Chem. Mater.* **2003,** 15, 1617-1627.

8. Lu, A.-H.; Salabas, E. L.; Shüth, F. *Angew. Chem. Int. Ed.* **2007,** 46, 1222-1244.

9. Cary, A. F.; Sundberg, J. R., *Advanced Organic Chemistry, Part A: Structure and Mechanisms*; Plennum Press: New York, **1991**; p 688-692.

10. Tartaj, P.; Morales, M. D. P.; Veintemillas-Verdaguer, S.; Gonzalez-Carreno, T.; Serna, C. J. *J. Phys. D: Appl. Phys.* **2003,** 36, R182-R197.

11. Shen, L.; Stachowiak, A.; Hatton, T. A.; Laibinis, P. E. *Langmuir* **2000,** 16, 9907-9911.

12. Shen, L.; Stachowiak, A.; Seif-Eddeen, K. F.; Laibinis, P. E.; Hatton, T. A. *Langmuir* **2001,** 17, 288-299.

13. Warner, M. G.; Hutchison, J. E., *Functionalization and Surface Treatment of Nanoparticles; Baraton, M. -I,* Ed;. American Scientific Publishers: San Francisco, **2003**; p 67-89.

14. Hostetler, M. J.; Green, S. J.; Stokes, J. J.; Murray, R. W. *J. Am. Chem. Soc.* **1996,** 118, 4212-4213.

15. Lattuada, M.; Hatton, T. A. *Langmuir* **2007,** 23, 2158-2168.

16. Duwez, A.-S.; Guillet, P.; Colard, C.; Gohy, J.-F.; Fustin, C.-A. *Macromolecules* **2006,** 39, 2729-2731.

Chapter 5:
Use of magnetic nanoparticles for purification of polymers prepared via the RAFT process

Abstract: Living chains prepared by RAFT-mediated polymerization reactions using Z-carboxylate and Z-phosphate RAFT agents were attached to the surface of superparamagnetic nanoparticles (MNPs) and have been used for separation of all dead chains formed in polymerization reactions using these RAFT agents prior to the attachment. All living chains attached to the surface of MNPs were separated from the remainder of solution by the presence of an external magnetic field. All chains that attached selectively to the surface of MNPs contained the RAFT functionality, showed low polydispersity index (PDI), and could be reactivated to form a new polymer extension or block copolymers with no detectable deviation from 100% efficiency.

Living chains prepared by a RAFT-mediated miniemulsion polymerization reaction using Z-carboxylate RAFT agent have been attached to the surface of MNPs and this was then used for separation of all dead chains and secondary particle formation formed in the medium of the miniemulsion polymerization reaction prior to the attachment. Separated dead chains that remained after the separation process in the remainder (decanted) of the polymer solution contained low RAFT functionality, showed broad PDI, and contained a significant amount of uncontrolled high molecular weight polymer, most probably formed as a result of secondary particle formation.

RAFT chains prepared by a RAFT-mediated polymerization reaction using Z-carboxylate RAFT agent and an excess of free radical initiator have been attached to the surface of MNPs and separated in the presence of an external magnetic field. Separated RAFT-functional chains were highly accentuated after separation of all dead chains using MNPs. These chains contained a substantial amount of cross-terminated by product, and showed a significant deviation between UV absorbance at 320 nm and the corresponding DRI signal.

Initiator derived chains formed in RAFT-mediated polymerization reactions of styrene (St) and methyl methacrylate (MMA) using phosphate free radical (PFR) initiator have been attached to the surface of MNPs and separated from the remainder of the polymer solution in the presence of an external magnetic field. The remainder of the polymer

solution contained a large fraction of RAFT chains, a small fraction of R group (leaving group of the RAFT agent) derived dead chains, and showed low PDI in the polymerization of St, but high PDI in the polymerization of MMA. Separated initiator derived chains contained low RAFT functionality, showed higher PDI than the as-prepared polymer in the polymerization of St, but lower PDI than the as-prepared polymer in the polymerization of MMA.

5.1 Introduction

5.1.1 Reversible Addition-Fragmentation Chain Transfer

Reversible Addition-Fragmentation chain Transfer (RAFT) polymerization has been shown to be versatile for the synthesis of a wide range of homopolymers and block copolymers with desired molecular weights, molecular architecture and polydispersity indexes (PDIs).[1,2] The RAFT process provides well defined predictable polymer structures with a good degree of control over the molecular weight, compared to the products of conventional radical polymerization. It does however not afford 100% living polymers. This is because termination and transfer reactions are also taking place during RAFT-mediated polymerization reactions, which yield dead chains. The expected fraction of these chains is generally small compared to that of living chains formed in efficient RAFT-mediated polymerization reactions. However, the quantity of dead chains progressively increases throughout the polymerization reaction due to the accumulation of terminated polymer species. Separation of dead chains from living chains formed in RAFT-mediated polymerization reactions is therefore a great advantage for making ultra high quality pure RAFT polymer products.

5.1.2 Water-borne polymerizations

Water-borne polymerization is a preferred method of polymer synthesis, particularly on an industrial scale. This is because it eliminates the need for organic solvents, provides products with low viscosity that are easy to handle, and also makes it relatively easy to remove the heat of reaction.[3] Numerous industrial applications might be enhanced by conducting water-borne polymerization with Controlled/"Living" Radical Polymerizations (CLRP). Miniemulsion polymerization is an important class of water-borne polymerization. It has been widely used in conjunction with the RAFT process.[4-6] Miniemulsion polymerization is widely described in the literature[7] (it will not be described here in more detail, as the details are beyond the scope of this study). One of the problems that might occur in RAFT-mediated miniemulsion polymerization reactions is secondary particle nucleation, resulting in secondary particle formation in the aqueous phase. The extent to which the secondary nucleation process can occur depends on

number of factors. The most important factors are the amounts and types of initiator and surfactant, and the amount of monomer present in aqueous phase.[3] Surfactants, initiator, impurities, and side processes might also affect particle stability.

Secondary particle nucleation is not a desired process in RAFT-mediated miniemulsion polymerization. This is because the newly formed particle will not usually contain any RAFT agent and thus, the polymerization in these particles will be conventional (uncontrolled) free radical polymerization. This also applies to RAFT in emulsion polymerization.

5.1.3 Separation of by-products from living chains formed in the RAFT process

By-products have been separated from living chains formed in RAFT-mediated polymerization reactions by anchoring growing polymer chains to a solid substrate.[8-11] Most previous studies have however involved attachment by a non-living chain end (R groups of the RAFT agents)[12-18], that does not selectively attach living chains and/or involves the requirement of difficult extraction/separation processes.[14,19] Superparamagnetic nanoparticles (MNPs) that exhibit strong magnetic properties are effectively used for separation and purification of biomolecules in the presence of an external magnetic field.[20-22] They have not yet been used for purification of RAFT polymers.

Colloidally stable dispersions of small sized MNPs, each containing only a single magnetic domain, have no net magnetism in the absence of a magnetic field, but the MNPs will be attracted to an external magnet. This phenomenon allows for the convenient separation of the MNPs from the remainder of a mixture, with much higher efficiency than conventionally achieved with processes such as sedimentation or ultracentrifugation. Hence, polymers containing groups capable of strong attraction to the surface of MNPs can be separated together with the MNPs.

The RAFT process[23] mainly produces living polymer chains and only a small fraction of cross-termination products[24] that contain the RAFT group (living functionalities),

whereas dead and polymer chains formed by secondary particle formation (non living chains) do not contain any RAFT groups. RAFT agents contain activating (Z) and leaving (R) groups. It is to be noted that not all chains will contain the R group, since the initiator (I) group could exchange in many cases during the RAFT polymerization reactions.

5.2 Methodology

In this study a strong attachment force to the surface of MNPs was incorporated into the Z group of the RAFT agent (see Scheme 5.1).

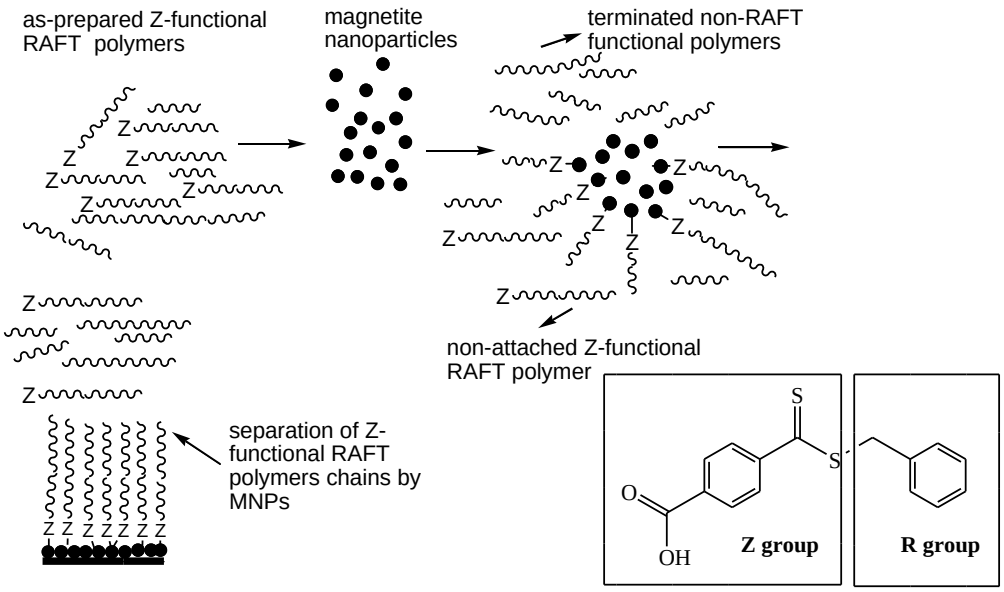

Scheme 5.1: Separation of Z-functional RAFT polymer chains by attachment to the surface of MNPs in the presence of an external magnetic field.

Thus, the living chains were strongly attracted to the surface of MNPs, whereas dead chains were not. This method is only effective when the functional moiety is part of the Z group; in the case of an R-functional RAFT agent, dead chains (which also usually contain at least one R group) will also be attracted to the surface of MNPs, thus invalidating the procedure. By analogy, such functional polymers produced by any CLRP method require the functional moiety to be on the living chains for selective attraction of living chains to the MNP surfaces. Thus, of the commonly used CLRP methods, only the RAFT(/MADIX) and nitroxide mediated polymerization (NMP) techniques are likely to

be efficient for this extraction method, since ATRP and degenerative transfer techniques do not involve groups, that are strongly attracted to MNPs, exclusively on the living chains.

A functional moiety that is strongly attracted to the surface of MNPs was also incorporated into free radical initiator in this study. Thus, in that case, the initiator derived chains were strongly attracted to the surface of MNPs.

5.3 Objectives

The objectives of this part of the study were the following:

1. To investigate the use of a separation (extraction) process using MNPs for separation of all dead chains from living chains formed in RAFT-mediated polymerization reactions.

2. To investigate improvement of the extraction process for the separation of all dead chains from living chains formed during RAFT-mediated polymerization reactions using Z-phosphate RAFT agents.

3. To investigate the effect of non-functional polymer chains in the attachment process of living chains to the surface of MNPs.

4. To investigate the possible use of the extraction process using MNPs to determine the existence of secondary particle nucleation formed during RAFT-mediated miniemulsion polymerization reactions

5. To investigate the separation of living chains and by-product RAFT chains formed in RAFT-mediated polymerization reaction using an excess of free radical initiator by attachment to the surface of MNPs in the presence of an external magnetic field.

6. To investigate the separation of all initiator derived chains formed in RAFT-mediated polymerization reactions of St and MMA.

5.4 Layout of this chapter

For the sake of simplicity this includes also the abbreviations of RAFT agents, free radical initiators, monomers, and polymers used in this study, which are given in Table 5.1:

Table 5.1: The RAFT agents, free radical initiators, monomers, and polymers used in this study.

compound	**abbreviation**
benzyl-(4-carboxyldithiobenzoate) RAFT agent	Z-carboxylate RAFT agent
S-benzyl-S′-(11-phosphonexy-undecyl) trithiocarbnate RAFT agent	Z-phosphate RAFT agent
2-cyanoprop-2-yl dithiobenzoate RAFT agent	blank RAFT agent
2,2′-azobis(isobutyronitrile) free radical initiator	AIBN
(E)-diazen-1,2-diylbis-3-cyanobutane-3,1-diylbis(dihydrogen phosphate) free radical initiator	PFR
Styrene monomer	St
methyl methacrylate monomer	MMA
polystyrene	PSt
poly methyl methacrylate	PMMA

The structures of the RAFT agents and free radical initiators used in the course of this study are given in Scheme 5.2.

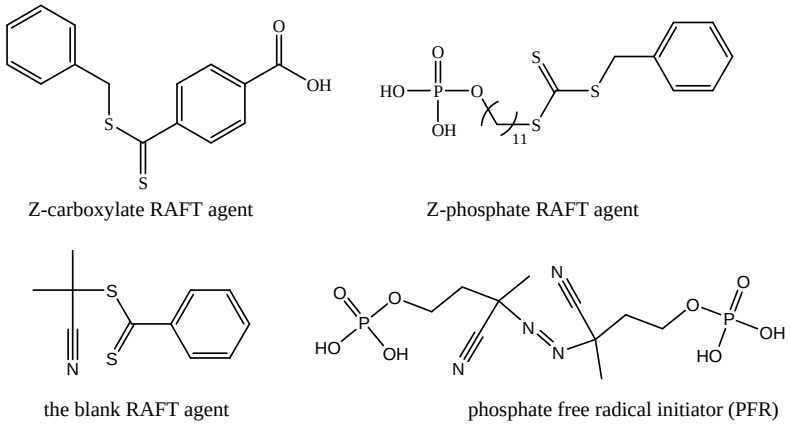

Scheme 5.2: Z-carboxylate, Z-phosphate, and blank RAFT agents and PFR initiator.

This chapter comprises three sections (Section 5.4–5.6).

Section 5.5 Experimental

In this section the experimental conditions used for the synthesis of various RAFT agents and free radical initiators, and the synthesis and stabilization of MNPs, which are used in the course of this study, are given. The polymerization conditions of all RAFT-mediated polymerization reactions using the various RAFT agents in the presence of different free radical initiators that are used in this study are described. The use of MNPs for the separation of functional polymer chains by attachment to the surface of MNPs in the presence of an external magnetic field is given in this section.

Section 5.6 Characterization techniques

Characterization techniques used in this study are described in this section.

Section 5.7 Results and discussions

The results of the following areas of investigation are described and discussed in this section.

Section 5.7.1: *Use of MNPs for synthesis of ultra pure RAFT polymers*

Describes and discusses the use of polymer products of RAFT-mediated polymerization reactions of St using Z-carboxylate RAFT agent in the extraction process using MNPs (illustrated in Scheme 5.1). This is to separate all dead chains from living chains formed in this RAFT-mediated polymerization reactions.

Section 5.7.2: *Effect of attachment force in the extraction process*

Describes and discusses the separation of living chains from dead chains formed in RAFT-mediated polymerization using Z-phosphate RAFT agent. Improvement to the extraction efficiency by using polymers containing phosphate groups compared with that of polymers containing carboxylate groups is also described and discussed in this section. This study was primarily based on the stability of iron to phosphate links, which is

expected to be generally higher than that of the iron-carbonyl complex, which possibly relies on the basis of the valency of the attachment. Therefore the phosphate is expected to be an excellent compound to study if the separation of the attached polymer to the surface of MNPs in the presence of an external magnetic field can be improved. Unfortunately, pure phosphate RAFT agent was not easy to prepare due to some reasons that were already discussed in Section 3.5. Thus, the extraction process was conducted in this study based on the 75% pure mono phosphate RAFT agent.

Section 5.7.3: *Effect of non-functional polymers in the extraction process*

Describes and discusses the effect of non-functional polymers in the attachment process of living chains to the surface of MNPs. It thus describes the selective attachment of living chains to the surface of MNPs and the use of this process for the separation of all non-functional polymers (which comprises dead chains formed in RAFT-mediated polymerization reaction and non-functional polymer standard obtained from Gel Permeation Chromatography) prior to the attachment.

Section 5.7.4: *Use of MNPs to determine the existence of secondary particle formation*

Describes and discusses the use of the extraction process using MNPs to determine the existence of secondary particle formation formed in a RAFT-mediated miniemulsion polymerization reaction of St using the Z-carboxylate RAFT agent.

Section 5.7.5: *Use of MNPs for separation of by-products formed in RAFT process*

Discusses the results of the investigation of using MNPs for separation of by-products formed in RAFT-mediated polymerization reaction of St using the Z-carboxylate RAFT agent and an excess of AIBN initiator.

Section 5.7.6: *Separation of initiator derived chains formed in RAFT process*

Describes and discusses results of the separation process of initiator derived chains formed in RAFT-mediated polymerization reactions of St and MMA using the blank RAFT agent and PFR initiator.

5.5 Experimental

5.5.1 Materials

The following materials were used as received: ferric chloride hexahydrate (98%; Fluka), ferrous sulphate heptahydrate (98%; Fluka), ammonium solution (25%; Merk), oleic acid (99%; Merk), pH 4 buffer solution (BDH), dichloromethane (DCM) (98%; Saarchem), methanol (99%; Merck), toluene (99.9%; Aldrich), ethyl acetate (99%; Saarchem), hexadecane (99%; Aldrich), sodium dodecyl sulphate (99%; biochemical grade (BDH)).

St (98%; Aldrich) was purified by washing with potassium hydroxide solution (KOH) (0.03 M) and distilling under reduced pressure prior to use. AIBN (98%; Aldrich) was recrystallized twice from methanol and dried prior to use. Hexane (99.5%; Saarchem) was distilled prior to use. Tetrahydrofuran (THF) (99%; R&S Enterprises) was distilled prior to use. MMA (98%; Aldrich) was distilled prior to use.

5.5.2 Synthesis of Z-carboxylate and Z-phosphate and blank RAFT agents, and PFR initiator

The Z-carboxylate, Z-phosphate, and blank RAFT agents were synthesized using the same procedures as described in Sections 3.4.2, 3.4.7 and 3.4.5, respectively. The PFR initiator was synthesized using the procedure that was described in Section 3.4.9.

5.5.3 RAFT-mediated polymerization reactions of St and MMA

All RAFT-mediated polymerization reaction conditions of St and MMA are tabulated in Table 5.2. The polymerization reactions were carried out using St or MMA monomers; in THF solution or bulk reaction media; using AIBN or PFR free radical initiators; and using Z-carboxylate or Z-phosphate or blank RAFT agents. In a typical polymerization reaction: the monomer, RAFT agent, free radical initiator, and solvent (if used) were

placed in a tube containing a stir bar. The contents in the tube were stirred at room temperature for 5 min, and then purged with N_2 for 15 min to remove the oxygen from the system, and sealed. The tube was then placed in an oil bath at 70 °C for reaction times of between 5 and 20 h. The polymerization was quenched by placing the tube in ice water, and the polymer (as-prepared polymer) was obtained after precipitation in methanol, and dried in a vacuum oven for 24 h. The as-prepared polymer was then characterized, and used in the extraction process.

Table 5.2: Formulations and reaction conditions used for St and MMA RAFT (solution/bulk) polymerizations

exp	monomer	medium	time (h)	[monomer] (mol/L)	[RAFT] (mmol/L)	[initiator] (mmol/L)	monomer conversion (C%)
1[a]	St	THF (50 mL)	7	3.2	4.6	0.57	6
2[a]	St	THF (50 mL)	20	3.2	4.6	0.57	17
3[b]	St	bulk	8	9.6	66.67	-	45
4[a]	St	bulk	6.5	9.4	59.9	29.47	16.2
5[c]	St	bulk	10	9.3	110	14.15	22
6[c]	MMA	bulk	5	9.7	130	28.2	20

[a]The polymerization reaction was carried out at 70 °C, using Z-carboxylate RAFT agent, and AIBN initiator

[b]The polymerization was carried out at 100 °C, using Z-phosphate RAFT agent, and thermal initiation of styrene

[c]The polymerization was carried out at 70 °C, using a blank RAFT agent, and PFR initiator

5.5.4 RAFT-mediated miniemulsion polymerization reaction of St

The organic phase was prepared by dissolving the Z-carboxylate RAFT agent (0.15 g; 0.52 mmol), AIBN (0.01 g; 0.06 mmol) and costabilizer (hexadecane) (0.3 g) in St monomer (10 g; 0.97 mmol) by stirring for 30 min. The aqueous phase was prepared by

dissolving the surfactant (sodium dodecylsulphate) (0.3 g) in deionized water (DDI) (40 g). Both phases were then mixed together and stirred using a magnetic stirrer at 700 rpm for 15 min, to form the pre-emulsion. The pre-emulsion was then sonified for 20 min using a Sonics and Material Vibra Cell 750VCX ultrasonicator. The sonication process was carried out for 20 min at 90% amplitude and a cut-off probe temperature of 40 °C. The latex was then placed in a sealed tube where the contents were purged with N_2 for 15 min to remove the oxygen from the system. The tube was then sealed and placed in an oil bath at 70 °C for 6 h. The contents were then cooled, using an ice bath, and precipitated in methanol to afford 1 g of polymer (10 % monomer conversion).

5.5.5 Synthesis and stabilization of MNPs

MNPs were synthesized and stabilized using the procedures described in Sections 4.3.2 and 4.3.3, respectively.

5.5.6 Extraction/separation of functional chains by attachment to the surface of MNPs in the presence of an external magnetic field from non-functional chains

The extraction process used here is illustrated in Scheme 5.1. Typically, the functional polymer chains (functional chains are all chains containing an attachment force to the surface of the MNPs (in this study they are living or initiator derived chains)) was separated from the remaining polymer chains by mixing and stirring (at ca. 300 – 400 rpm) a solution of the as-prepared polymer chains in DCM (a good solvent for the polymer; typically 100 mL of DCM was used for 4.0 g of MNPs to extract 0.7 g of polymer) with a freshly stabilized MNP dispersion for 24 h at room temperature. The functional chains attached to the surface of MNPs (by displacing a fraction of oleic acid) were separated together with MNPs from the remaining solution by applying an external magnetic field, with magnetic intensity of 4.5×10^5 A/m). The remaining solution (the unextracted solution, which contained the unextracted polymer) was decanted and collected. The MNP dispersion was then mixed at room temperature (by stirring at ca. 300 – 400 rpm) with a 32% HCl solution (20 mL for 4.0 g of MNPs) until the MNPs completely dissolved (which took less than 5 minutes), as indicated by the disappearance of the black colour of the MNPs. The organic phase (containing the oleic acid and the extracted polymer) was separated from the aqueous phase, and the aqueous phase

extracted with DCM (15 mL × 2). The solvent was evaporated to afford the extracted polymer. In the case of MNPs remaining in the unextracted solution, this solution was also washed and extracted as above. The final extracted and unextracted polymers were characterized and used whenever necessary for chain extension reactions.

5.5.7 Chain extension reactions

The extracted and unextracted PSt polymers were tested for living behavior by chain extension. A sample of each polymer was dissolved in St, and the solution heated to 100 °C for *ca*. 12 h. The resulting polymers were characterized by SEC and evaluated for chain extension efficiency.

5.6 Characterization of PSt and PMMA polymers

5.6.1 Determination of the molecular weights and molecular weight distributions

The synthesized PSt and PMMA molecular weights and molecular weight distributions were determined using Size Exclusion Chromatography (SEC). Polymer samples were dissolved in stabilized THF (HPLC grade) at a concentration of 5 mg/mL, and filtered through a 0.45 μm nylon filter prior to injection into the SEC columns. The SEC apparatus comprised a Waters 1515 isocratic HPLC pump, Waters 717 plus autosampler, Waters 24141 refractive index detector, two pLgel 5 μm Mixed-C (300 × 7.5 mm) columns, and one pLgel 5 μm guard column (50 × 7.5mm). The samples were eluted using THF (HPLC grade) at 30 °C, using a flow rate of 1 mL/min. The instrument was calibrated using nine Polymer Laboratories Easyvial PSt standards with narrow molecular weight distributions in the range 580 – 9 × 10^5g mol^{-1} (Polymer Laboratories).

The living distribution of each polymer sample was determined by comparing of the UV absorbance at 320 nm (dominated by the absorption of the RAFT group plus a small fraction by the aromatic group of the St repeat unit) and the differential refractive index (DRI) SEC traces of the polymer sample. The UV detector detects only one chromophore per RAFT group per polymer chain (it normally contains approximately one functional RAFT group). The DRI detector however detects one signal per monomer unit of the

polymer chain. Therefore for a more sensible comparison of the UV and DRI data, each UV data set was multiplied by *M* at each point of the UV chromatograms. The UV corrected data were applied for all polymer samples and used for all comparisons here. It should be noted that the term UV absorbance will be used for simplicity to indicate the corrected UV absorbance at 320 nm (unless otherwise stated).

5.6.2 Transmission Electron Microscopy (TEM)

PSt polymer latex was analyzed using TEM to visualize the particle morphology on a nanometer scale. A sample of PSt latex was prepared by diluting it in water. The diluted latex sample was then stained with 2% uranyl acetate solution and mounted on a copper grid. The PSt latex TEM analysis was carried out on a Leo 912 microscope, attached to a digital camera.

5.7 Results and discussion

Most of the results presented in this chapter were reproducible.

5.7.1 Use of MNPs for synthesis of ultra pure RAFT polymers

A PSt polymer produced by RAFT-mediated polymerization of St using Z-carboxylate RAFT agent and AIBN initiator at 70 °C was used in the extraction process. The DRI and UV absorbance SEC traces of the as-prepared polymer (the unmodified polymer initially synthesized), extracted polymer (the polymer that was separated by the attachment to the surface of MNPs in the presence of an external magnetic field), and unextracted polymer (the polymer that remained in solution after the extraction process) are shown in Figure 5.1. The DRI signal comparison (Figure 5.1a), shows distinct differences between these PSt polymers with respect to the molecular weight distribution (MWD), molecular weight (*M*), and UV absorbance. The PDI values of the unextracted and the as-prepared polymers were the highest (1.20, $\overline{M}_n$ = 2900, 4170), and the extracted polymer had a significantly better PDI (1.14, $\overline{M}_n$= 4700). For as-prepared polymers of high PDI, the order of PDI values was unextracted polymer > as-prepared polymer > extracted

polymer, as expected for the separation of all dead chains from living polymer chains formed in the RAFT-mediated polymerization reactions.

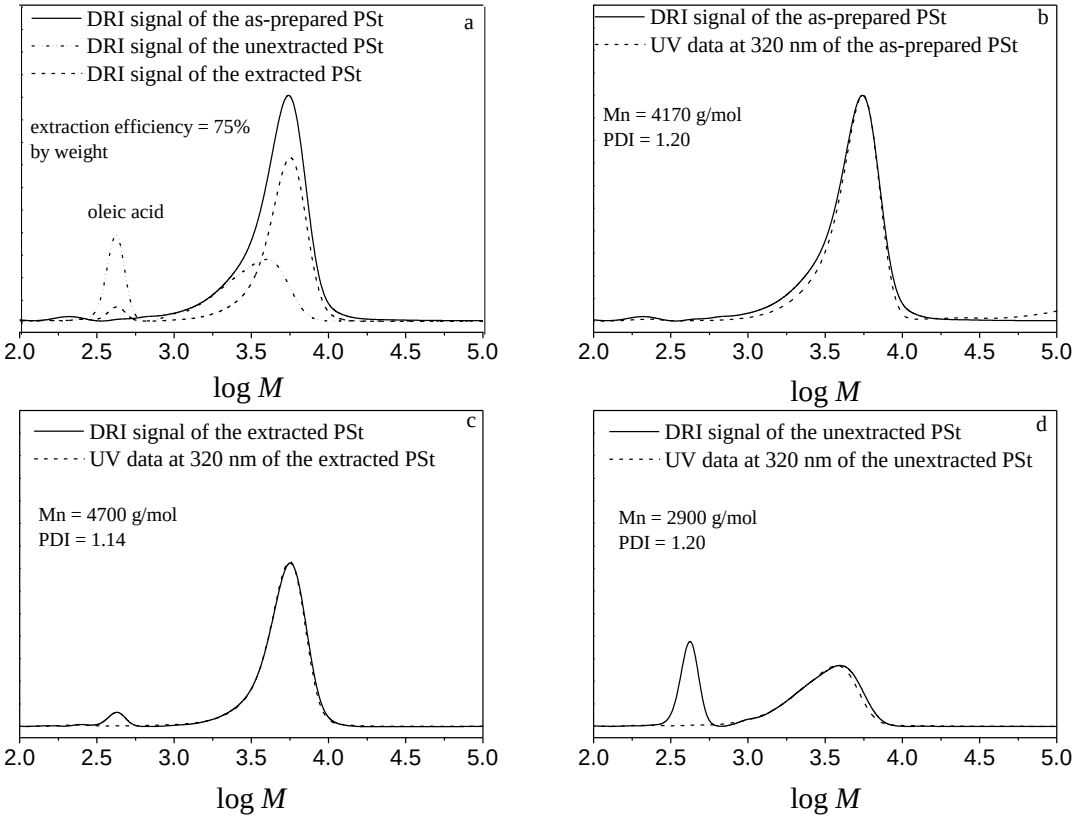

Figure 5.1: DRI signal and UV absorbance SEC traces of PSt polymers produced by RAFT-mediated polymerization of St using Z-carboxylate RAFT agent and AIBN initiator: (a) comparisons of the as-prepared, extracted and unextracted polymers, (b) the as-prepared polymer, (c) the extracted polymer, and (d) the unextracted polymer.

Dead chains are normally formed by termination events throughout RAFT-mediated polymerization reactions with high PDI, and are possibly of lower *M* than the living polymer chains. This is because a large fraction of the termination products are formed earlier in the reaction due to the generation of radicals at the early stage of free radical polymerization, which will therefore give shorter chains on average. It is expected that the higher molecular weight polymer chains will tend to be the well-controlled polymer and the low molecular weight will tend to be due to the formation of impurities, as observed in this study.

The unextracted polymer is expected to contain a large fraction of dead chains. These dead chains lack RAFT functionality, and absorb little UV radiation, as observed from the deviation between the UV absorbance and the DRI signal in Figure 5.1d. There is a minimal deviation between the UV absorbance and DRI signal of the extracted polymer (Figure 5.1c), indicating that the extracted polymer apparently contains 100% RAFT functionality. The extracted polymer should therefore undergo complete reinitiation for chain extension.

The RAFT functional chains in the unextracted polymer probably result from the ligand exchange process in the extraction step, which does not attach all RAFT functional chains to the surface of MNPs in the first extraction, thus leaving unattached RAFT chains to be decanted with the unextracted solution. This is consistent with the amount of polymer extracted, which was 75% by weight and 65% by number of chains; although only about 5% dead chains are expected here. Thus, a substantial fraction of living chains are in the unextracted polymer. These chains could be removed from this fraction by further extractions with MNPs, if desired.

Figure 5.2a and 5.2b show the DRI signal and UV absorbance SEC traces of the extracted and unextracted polymer extension tests (extension tests are based on the use of the extracted and unextracted polymers as macroinitiators), respectively. The insets magnify the region where the initial polymer was found, to demonstrate the fraction of chains that did not reinitiate. The extracted polymer in Figure 5.2a apparently underwent virtually complete reinitiation, since there is no measurable initial polymer remaining, which would correspond to dead chains. Thus, the separation process is extremely efficient in terms of removing dead chains. The PDI of 1.84 ($\overline{M}_n$ = 212000) is rather (but understandably) high here due to the very high target *M* (ca. 500000) resulting in less control, but still good living behaviour, as clearly indicated by the UV absorbance with respect to the DRI signal of this polymer.

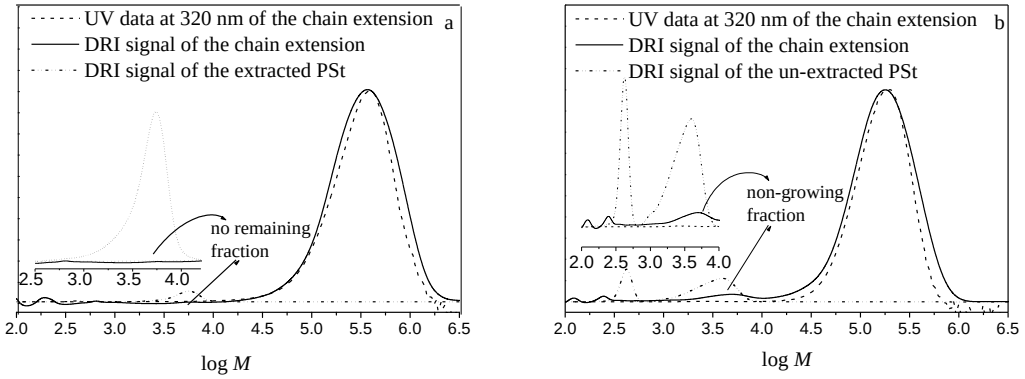

Figure 5.2: DRI signal and UV absorbance SEC traces of the chain extension tests: (a) chain extension of the extracted polymer, and (b) chain extension of the unextracted polymer.

The extension test of the unextracted polymer showed a significant fraction of high *M* polymer contained some RAFT group, as expected. A large fraction of the chains were not however reactivated (reinitiated) (Figure 5.2b); these apparently (about 30%) shows no UV absorbance, indicating the absence of the RAFT functionality, as expected of dead chains. The PDI of 1.80 ($\overline{M}_n$ = 240000) is similar to that of the PDI of the chain extended of the extracted polymer in this case, due to the high target *M* dominating the degree of PDI control.

5.7.2 Effect of the attachment force in the extraction process

The PSt polymer prepared by RAFT-mediated polymerization reaction of St using the Z-phosphate RAFT agent and thermal initiation of St at 100 °C (exp 3, Table 5.2), was used in the extraction process. Figure 5.3 shows the DRI signal and UV absorbance SEC traces of the as-prepared, extracted, and unextracted polymers. These SEC traces indicate that there are large differences between these polymers with respect to *M*, MWD, and UV absorbance. The extracted polymer has the highest *M* and lowest PDI ($\overline{M}_n$ = 38160, PDI = 1.45), while the unextracted and as-prepared polymers have the highest PDIs (2.5, 1.70 and $\overline{M}_n$ = 11260, 13570, respectively).

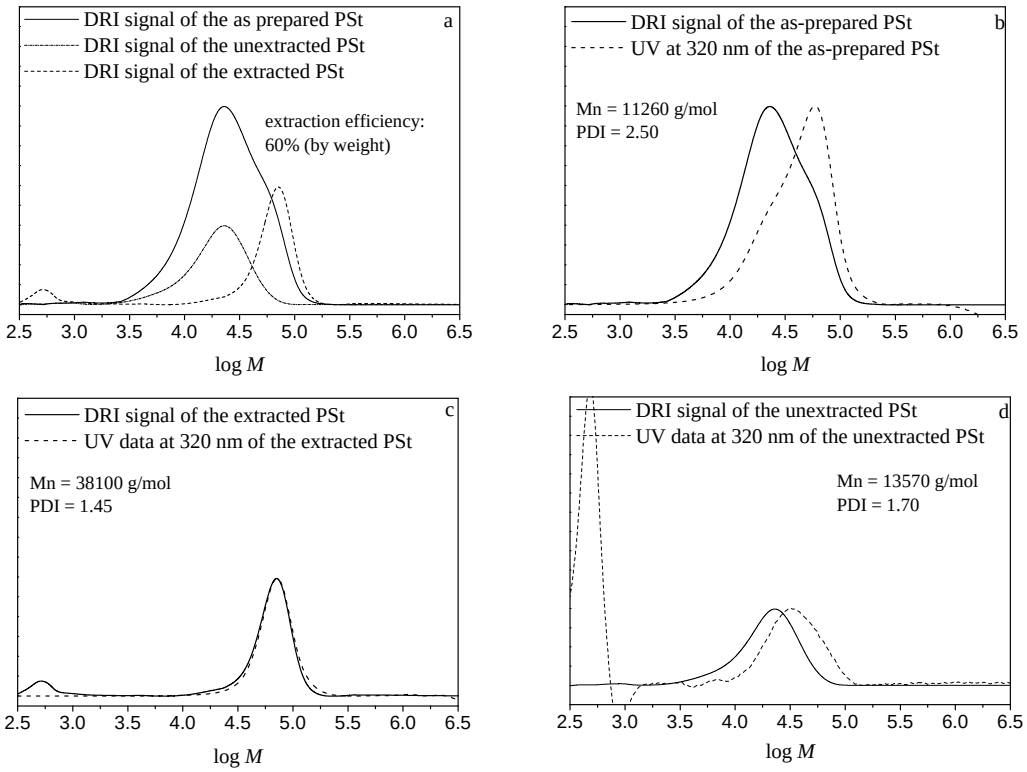

Figure 5.3: DRI signal and UV absorbance SEC traces of the PSt polymers prepared by RAFT-mediated polymerization of St using the Z-phosphate RAFT agent and thermal initiation of St: (a) comparison of the as-prepared, extracted and unextracted polymers, (b) the as-prepared polymer, (c) the extracted polymer, and (d) the unextracted polymer.

The unextracted polymer in this experiment is expected to contain large fractions of by-products. These by-products have a high PDI, lack RAFT functionality, and absorb little UV radiation with respect to the DRI signal, as observed in Figure 5.3d. The UV absorbance of the unextracted and as-prepared polymers is biased to high *M* polymers (see Figures 5.3b and 5.3d). This is because the high *M* polymer consists of living chains. This is also consistent with the extracted polymer containing living chains with high *M* and a minimal deviation between UV absorbance and DRI signal (see Figure 5.3c). These results indicate efficient separation of by-products from living chains formed in this RAFT-mediated polymerization reaction.

The *M* difference of extracted polymer and those of the as-prepared and unextracted polymers was large, as observed in Figure 5.3a. This is quite unexpected of polymers prepared by efficient RAFT-mediated polymerization reactions (see DRI signal

comparisons Figure 5.3a). This is possibly because of excessive termination reactions and unexpected side reactions taking place during this polymerization reaction. These termination reactions and other side reactions may produce a large number of by-products (comprising dead chains and any other unknown products) with shorter *M* than the normal living chains. This possibly happened here because of the initial impurities in this RAFT agent. It also should be noted that the measured *M* is normally governed by the total number of chains, thus, if a large number of dead chains are short and a small number of them are large, the average *M* of the dead chains will be lower than otherwise expected, as observed in this experiment.

The amount of the living chains that was separated by attachment to the surface of MNPs in the presence of an external magnetic field was 60% by weight. Since the purity of the Z-phosphate RAFT agent was 70% of phosphate groups, this means that the amount of the living chains would be 85% by weight (0.6/0.7) and 67% by number, of the pure RAFT agent. This result is highly significant as one can see how the attachment efficiency of a functional RAFT agent to the surface of MNPs was improved when the Z-phosphate RAFT agent was used, compared to the Z-carboxylate RAFT agent.

5.7.3 Effect of non-functional polymers in the extraction process

The PSt polymer mixture [PSt polymer [$\overline{M}_n$ = 11800, PDI = 1.29] prepared by RAFT-mediated polymerization reaction of St using the Z-carboxylate RAFT agent and AIBN initiator at 70 °C (exp 2, Table 5.2), and non-functional PSt polymer standard [$\overline{M}_n$ = 415,000, PDI = 1.04]), at ratios of 80/20 w/w, respectively] was used in the extraction process.

The PSt polymer mixture is expected to contain functional and non-functional polymer chains. These different polymer chains are illustrated in Figure 5.4.

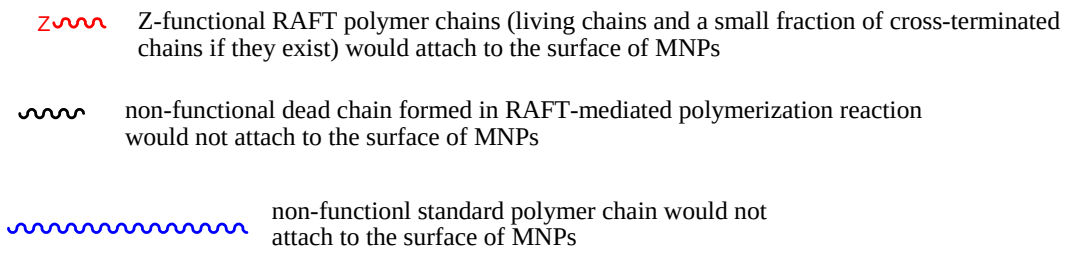

Figure 5.4: A polymer mixture containing functional and non-functional polymer chains.

Figure 5.5 shows the DRI signal and UV absorbance data SEC traces of the polymer mixture, unextracted and extracted polymers. This result indicates that there are significant differences between these polymers with respect to the *M*, MWD, and UV absorbance.

The polymer mixture contains two polymer fractions: a low *M* polymer peak [$\overline{M}_n$ = 11800, PDI =1.29] (corresponding to the PSt polymer prepared by RAFT-mediated polymerization reaction of St using the Z-carboxylate RAFT agent), and a high *M* polymer peak [$\overline{M}_n$ = 415,000, PDI =1.04] (corresponding to PSt polymer standard). This is expected upon mixing of these two polymers. The unextracted polymer is also expected to contain two polymer fractions. It contains a polymer of low *M* [$\overline{M}_n$= 10800, PDI = 1.34], and that of high *M* [$\overline{M}_n$ = 415,000, PDI = 1.04], as observed in Figure 5.5a. The low *M* polymer peak corresponds to dead chains (also includes small fraction of RAFT chains) with broad PDI, lacks RAFT functionality, and a small UV absorbance, as observed in Figure 5.5d. The high *M* polymer peak corresponds to the unextracted non-functional polymer standard with no RAFT functionality and weak UV absorbance, as observed in Figure 5.5d. The UV absorbance of the high *M* polymer peak is due to the small UV absorbance of the St monomer units of the PSt backbone, of which they are many per chain for high *M* polymer. This is expected of separation of all non-functional polymer and dead chains from living chains. The extracted polymer however only contains one polymer peak [$\overline{M}_n$ = 12800, PDI = 1.19]. This polymer contains living chains, with low PDI, RAFT functionality, and shows minimal deviation between the UV absorbance and DRI signal (see Figure 5.5c). This result indicates that only living chains

have been selectively attached to the surface of MNPs and efficiently separated from the remainder of the solution polymer mixture in the presence of an external magnetic field. It also indicates that non-functional polymer has no interaction with the surface of MNPs in the extraction process.

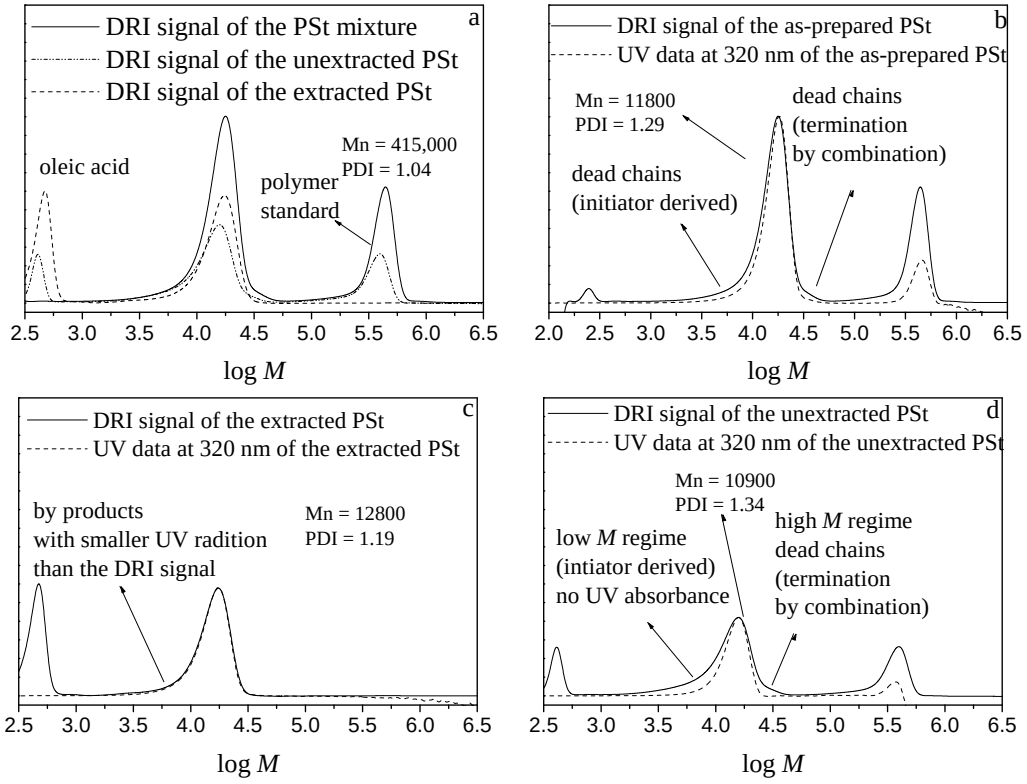

Figure 5.5: DRI signal and UV absorbance SEC traces of the polymer mixture (contains PSt polymer prepared by Z-carboxylate RAFT-mediated polymerization of St at 70 °C using AIBN, and non-functional PSt polymer standard at ratios of 80/20 w/w, respectively): (a) comparison of the polymer mixture, unextracted, and extracted polymers, (b) the polymer mixture, (c) the extracted polymer, and (d) the unextracted polymer.

Inspection of Figures 5.5b and 5.5c and 5.5d indicate that the PDI of the extracted polymer was the lowest (PDI = 1.19), while PDIs of the as-prepared and unextracted polymers were the highest (1.29 and 1.34 (based on the low *M* peak), respectively). This indicates efficient separation of all dead chains (high PDI) from living chains (low PDI) formed in RAFT-mediated polymerization reactions. The order of PDI values of these polymers was unextracted polymer > as-prepared polymer > extracted polymer, which is consistent with the previous results.

The unextracted polymer contains dead chains formed continuously by termination reactions during the RAFT-mediated polymerization reaction with different and comparable chain lengths to chain lengths of living chains, and lack of RAFT functionality, as observed in Figure 5.5d. It also contains dead chains that are formed by combination with chain length being double the chain length of living chains and minimal UV absorbance compared to the DRI signal (see high *M* regime in Figure 5.5d).

Figure 5.5c shows the comparison of the UV absorbance and DRI signal of the extracted polymer. It shows that there is minimal deviation between the UV absorbance and DRI signal of this polymer. These results indicate therefore that this polymer apparently contains 100% RAFT functionality and maybe a small fraction of cross-terminated polymer by-products that cause very little deviation between the UV absorbance and DRI signal.

5.7.4 Use of MNPs to determine the existence of secondary particle formation

Since the separation of all non-functional chains from functional living chains was successful (Section 5.7.3), it was considered that the extraction process using MNPs could be useful to determine the existence of secondary particle formation in RAFT-mediated miniemulsion polymerization reactions.

5.7.4.1 SEC analysis of the as-prepared, extracted and unextracted PSt polymer latex prepared by RAFT-mediated miniemulsion polymerization reaction of St using the Z-functional RAFT agent

The PSt polymer prepared by a RAFT-mediated miniemulsion polymerization reaction of St using the Z-carboxylate RAFT agent and AIBN initiator at 70 °C was used in the extraction process. Figure 5.6 shows the DRI signal and UV absorbance at 320 nm and that at 254 nm of the as-prepared, extracted and unextracted polymers.

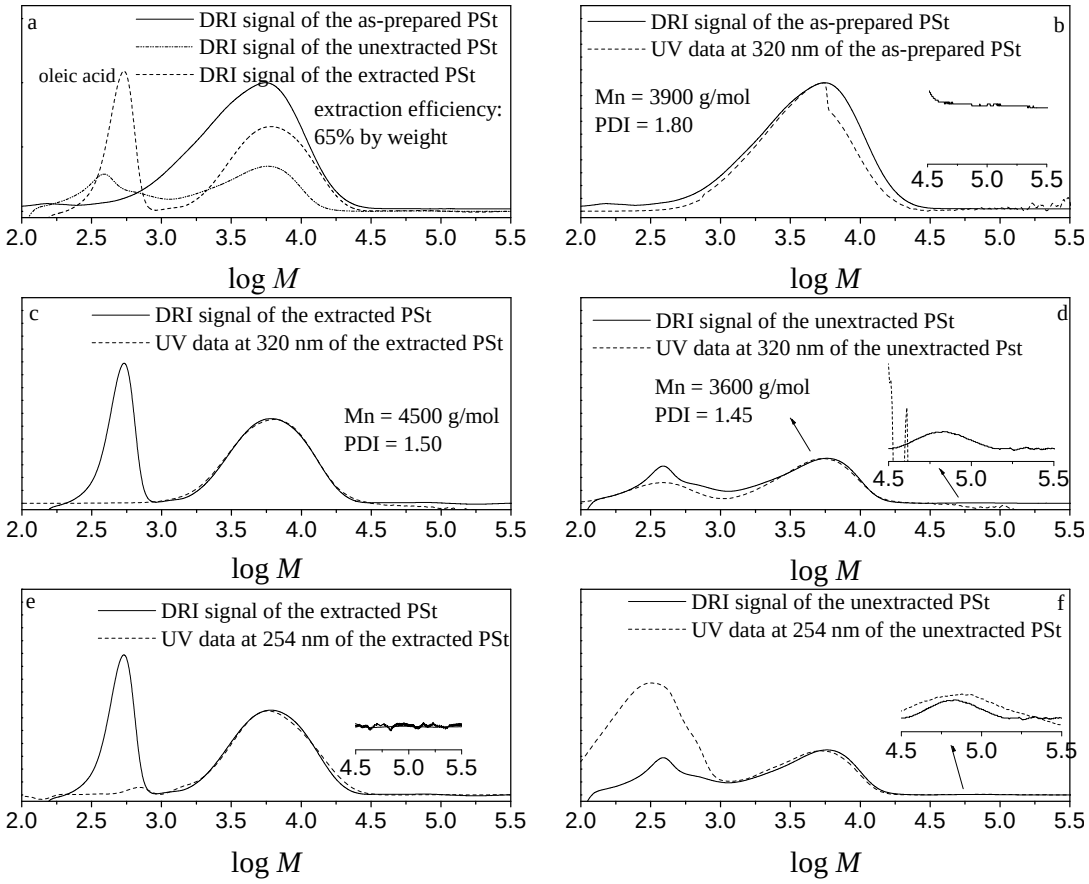

Figure 5.6: DRI signal and UV absorbance at 320 nm and at 254 nm of the PSt polymer prepared by a RAFT-mediated miniemulsion polymerization reaction of St using the Z-carboxylate RAFT agent and AIBN initiator: (a) comparison of the as-prepared, extracted, and unextracted polymers, (b) the as-prepared polymer, (c and e) the extracted polymer, and (d and f) the unextracted polymer.

The magnified inset in Figure 5.6d of the DRI signal comparison with the UV absorbance at 320 nm of the unextracted polymer functions to show that the high *M* polymer contains no UV radiation at 320 nm, indicating that this polymer contains no RAFT groups. The magnified insets in Figures 5.6e and 5.6f of the DRI signal comparison with the UV absorbance at 254 nm of the extracted and unextracted polymers serves to show that the unextracted polymer contains a negligible amount of uncontrolled high *M* polymer with UV radiation at 254 nm. This indicates that the unextracted high *M* polymer is a PSt polymer and that it might be formed due to secondary particle formation. They also show that the extracted polymer does not contain uncontrolled high *M* polymer. The UV absorbance at 254 nm is dominated by that of the St. These results show that these

polymer are different with respect to *M*, MWD, and UV absorbances. Inspection of Figures 5.6b and 5.6c and 5.6d indicates that the PDIs of the as-prepared, extracted, and unextracted polymers were high (1.80, 1.55, 1.45, and $\overline{M}_n$ = 3900, 4500, 3200, respectively). This is expected of polymers prepared by RAFT-mediated miniemulsion polymerization reactions when different polymer particles are being with different MWDs. This is possibly because of different initial particle sizes. Different initial particle sizes in miniemulsion systems might happen as a result of the particle formation process when the RAFT agent is unable to transport between particles because of its limited solubility in the continuous phase, while monomer is able. This therefore will result in strong fluctuations in the ratios of monomer/RAFT agent throughout the polymerization reaction time, and thus, different particles will have different *M*.

Figure 5.6d shows that the unextracted polymer contains dead chains with a large deviation between the UV absorbance and DRI signal and thus low RAFT functionality. The extracted polymer however contains living chains with a minimal deviation between the UV absorbance and DRI signal, as observed in Figure 5.6c. The extracted polymer should therefore contain 100% RAFT functionality and it should thus undergo complete chain reactivation for chain extension.

The unextracted polymer contains a small fraction of high *M* polymer, which could probably be a secondary particle formation with minimal UV absorbance at 320 nm and thus, lacks RAFT functionality, but shows strong UV absorbance at 254 nm, as observed in the magnified insets in Figures 5.6d and 5.6f. This is expected, since secondary particles formed in RAFT-mediated miniemulsion polymerization reactions are expected to produce uncontrolled high *M* polymer and lack RAFT functionality. It was reported in the literature that RAFT-mediated miniemulsion polymerization of St using phenyl 2-propyl phenyl dithioacetate (PPPDTA) RAFT agent in the presence of AIBN initiator produced uncontrolled high *M* polymer due to secondary particle formation.[25] It should be noted that the RAFT agent and reaction conditions used in this miniemulsion polymerization reaction and those used in the reported literature are different. The data that was reported in the literature and that of this experiment show the existence of

uncontrolled high *M* polymer. The number of the uncontrolled high *M* polymer chains in this experiment however is small possibly due to low monomer conversion compared to reported data in the literature.

The extracted polymer contains no uncontrolled high *M* polymer which would correspond to secondary particle formation, or otherwise impurities (see inset of Figure 5.6e). This result clearly indicates separation of all dead chains and uncontrolled high *M* polymer from living chains formed in RAFT-mediated miniemulsion polymerization reactions. It also shows that MNPs can be used to determine the existence of secondary particles that could form in miniemulsion and emulsion systems.

The magnified inset in Figure 5.6b shows that as-prepared polymer contains a small high *M* polymer tail around the same region where secondary particle formation is expected. This polymer was visible in the unextracted polymer, as observed in the magnified inset in Figure 5.6d. A possibly reason for the uncontrolled high *M* polymer being hardly visible (or to measure) in the as-prepared polymer could be due to that the number of the high *M* polymer chains is very small compared to the total number of the as-prepared polymer chains. This may be because SEC is very sensitive to a large number of chains and less sensitive to a small number of chains. On the other hand the number of uncontrolled high *M* polymer chains is visible compared to the total number of the unextracted polymer chains. Thus, uncontrolled high *M* polymer chains, which could possibly be due to secondary particle formation, were detected in the unextracted polymer. This indicates that the extraction process using MNPs accentuated the visibility of products in the remainder of the solution polymer after separation of living chains formed during this RAFT-mediated miniemulsion polymerization reaction. It is to be noted that the lack of visibility of the uncontrolled high *M* polymer in the as-prepared polymer might suggest that the high *M* polymer could be due to contamination in the unextracted polymer distribution. Repeated experiments showed however similar distribution, indicating that uncontrolled high *M* polymer (although it is a negligible fraction, as observed in this experiment) in the unextracted polymer is indeed due to secondary particle formation.

5.7.4.2 TEM analysis of the PSt polymer latex prepared by RAFT-mediated miniemulsion polymerization reaction of St using the Z functional RAFT agent

Figure 5.7 shows the particle size, size distribution, and particle morphology in the TEM image of the PSt polymer latex prepared by the above RAFT-mediated miniemulsion polymerization of St using the Z-carboxylate RAFT agent in the presence of AIBN initiator. It clearly shows that these particles are not monodisperse, which implies that each particle should develop a different MWD. This result also shows a population of small particles, which is possibly due to the secondary particle formation. It is also possible that small particles might be present at the start of the polymerization. This is especially important, since particle morphology at the start of the polymerization was not determined using TEM microscopy. This might suggest then that small particles could be a result of the initial conditions, as possibility.

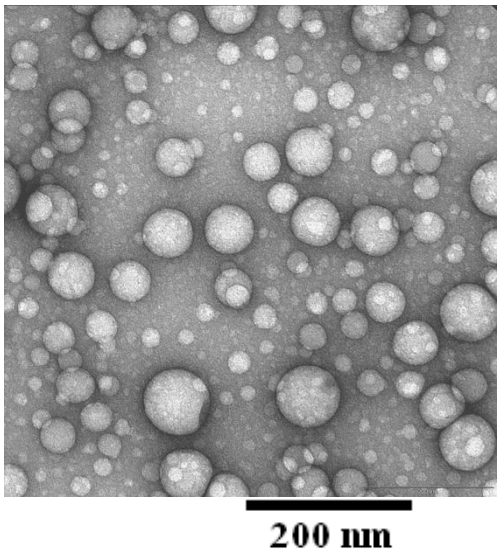

Figure 5.7: TEM image of the PSt polymer latex prepared by RAFT-mediated miniemulsion polymerization of St using the Z-carboxylate RAFT agent in the presence of AIBN initiator.

5.7.4.3 Chain extension tests of the extracted and unextracted PSt polymers prepared by RAFT-mediated miniemulsion polymerization of St using the Z-functional RAFT agent

Figures 5.8a and 5.8b show the DRI signal and UV absorbance SEC traces of the extension tests of the extracted and unextracted polymers prepared by RAFT-mediated miniemulsion polymerization of St using the Z-carboxylate RAFT agent in the presence of AIBN initiator, respectively. The extracted polymer in Figure 5.8a apparently underwent almost complete reinitiation, since there is no detectable initial polymer remaining that would correspond to dead chains. The extension test of the extracted polymer indicates that this polymer contains 100% RAFT agents. Thus, the separation process is extremely efficient in terms of removing dead chains from living chains formed in RAFT-mediated miniemulsion polymerization reactions.

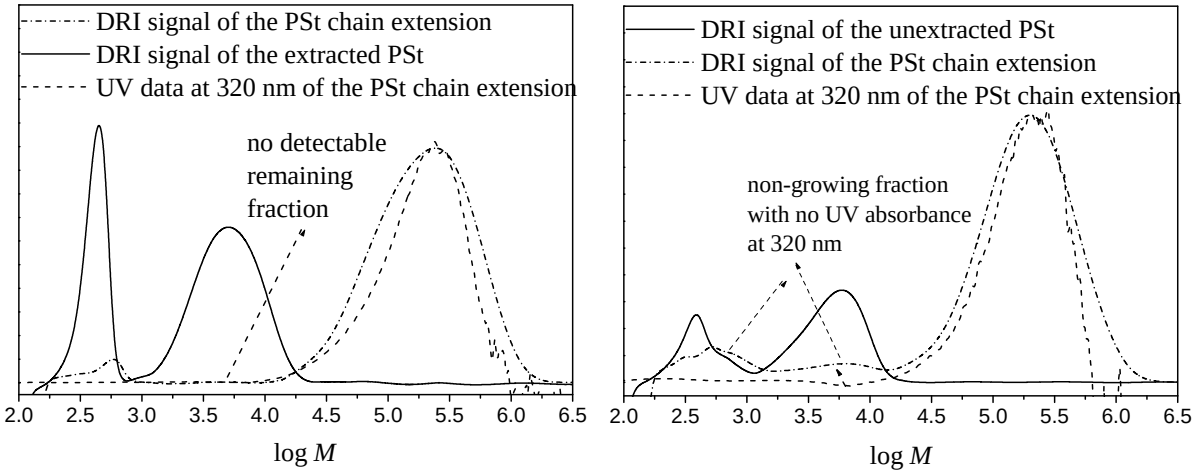

Figure 5.8: SEC traces of the DRI signal and UV absorbance at 320 nm for the chain extension tests of the extracted and unextracted PSt polymers prepared by RAFT-mediated miniemulsion polymerization of St using the Z-carboxylate RAFT agent in the presence of AIBN initiator: (a) chain extension of the extracted polymer, and (b) chain extension of the unextracted polymer.

The extension test of the unextracted polymer shows however a significant fraction of high *M* polymer containing some RAFT agents, as expected. A large fraction of low *M* polymer was not reinitiated (Figure 5.8b). This low *M* polymer is apparently about 40%

of the unextracted polymer and shows no UV absorbance, which indicates absence of RAFT functionality, as is expected of dead chains.

5.7.5 Use of MNPs for separation of by-products formed in RAFT process

The PSt polymer prepared by a RAFT-mediated polymerization reaction of St using the Z-carboxylate RAFT agents using an excess of AIBN initiator at 70 °C (exp 4, Table 5.2) was used in the extraction process. Figure 5.9 illustrates polymer products expected to be formed during RAFT-mediated polymerization reactions using an excess of free radical initiator. There might be however other by-products formed in this polymerization reaction other than those illustrated in Figure 5.9. These are not included in this study.

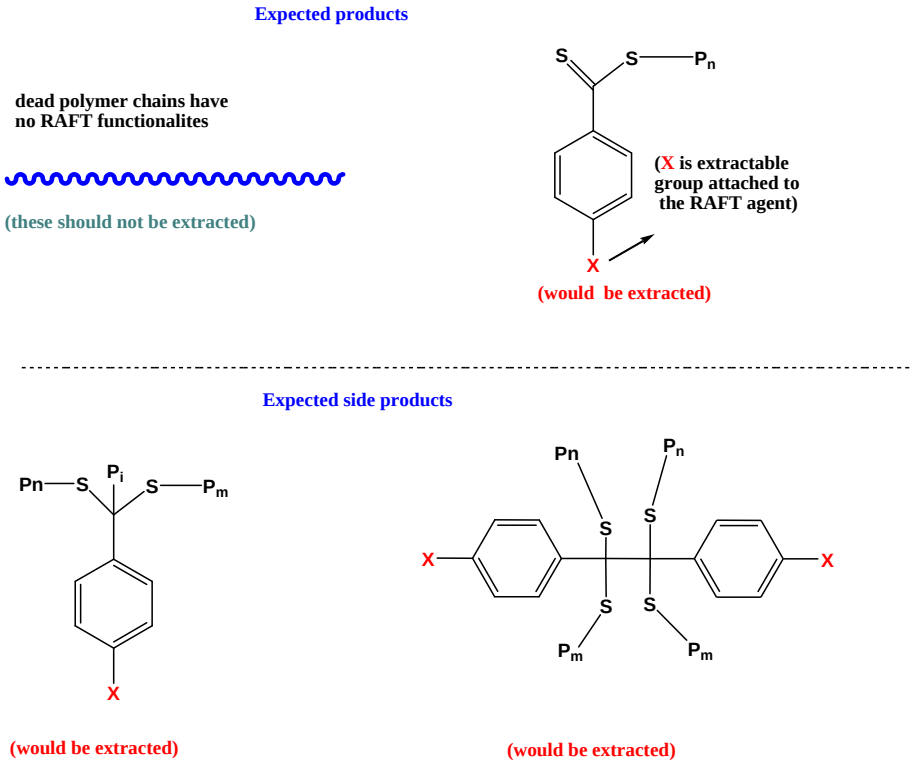

Figure 5.9: Polymer products expected to be formed during a RAFT-mediated polymerization reaction.

5.7.5.1 SEC analysis of the as-prepared, extracted and unextracted PSt polymers prepared by RAFT-mediated polymerization reaction of St at a high free radical concentration

Figure 5.10 shows the DRI signal and UV absorbance of the as-prepared, extracted and unextracted polymers. This indicates that these polymers are different with respect to *M*, MWD, and UV absorbance.

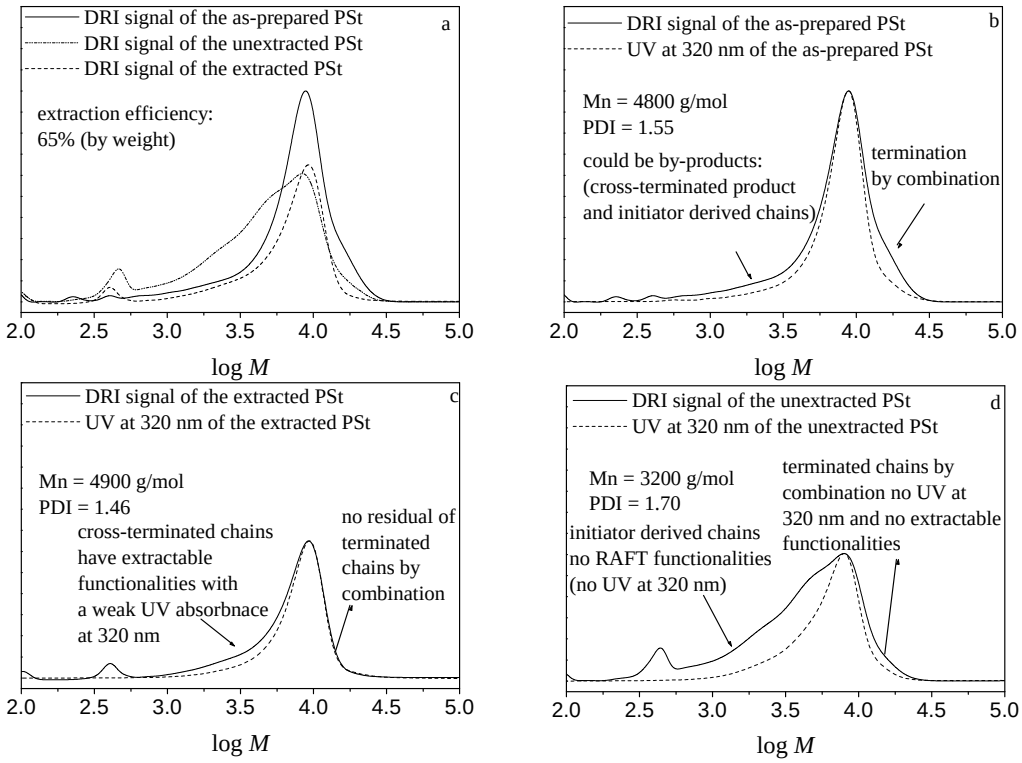

Figure 5.10: DRI signal and UV absorbance at 320 nm SEC traces of the PSt polymers prepared by the RAFT-mediated polymerization reaction of St using the Z-carboxylate RAFT agent and an excess of AIBN initiator: (a) comparison of as-prepared, extracted, and unextracted polymers, (b) the as-prepared polymer, (c) the extracted polymer, and (d) the unextracted polymer.

Inspection of Figures 5.10b and 5.10c and 5.10d indicates that PDIs of the as-prepared, extracted and unextracted polymers are high (PDIs = 1.55, 1.46, 1.70, and $\overline{M}_n$ = 4800, 4900, 3200, respectively). The PDIs of these polymers are larger than the normally expected PDIs of polymers prepared by RAFT-mediated polymerization reactions using a

low concentration of AIBN (see PDIs of the as-prepared, extracted and unextracted polymers in Figures 5.1b and 5.1c and 5.1d). This shows the effect of an excess of free radical initiator on RAFT-mediated polymerization reactions. It is possibly because a high free radical concentration increases radical concentrations (there are both propagating and intermediate radicals) during this RAFT-mediated polymerization reaction. Thus the expected number of dead chains and by-products will result in a broad PDI and many chains will lack RAFT functionality.

The as-prepared polymer contains a long low *M* polymer tail with a large deviation between the UV absorbance and DRI signal and therefore lacks RAFT functionality, as observed in Figure 5.10b. It also contains a high *M* polymer shoulder with weak UV absorbance, which also lacks RAFT functionality.

The low *M* polymer tail possibly results from early and extensive termination and transfer reactions. Termination reactions produce dead chains and maybe cross-terminate by-products, both of which weakly absorb UV radiation with respect to the DRI signal. Transfer reactions produce long dead chains and short radicals. The short radicals can react with the RAFT agents to then produce living chains with shorter *M* than that of living chains that have not experienced chain transfer reactions. This is observed in this experiment.

The extracted polymer which was separated by attachment to the surface of MNPs from the remainder of solution polymer in the presence of an external magnetic field contains a large fraction of polymer with a small UV absorbance, as observed in Figure 5.10c. This polymer fraction is the extractable product, yet it has a small UV absorbance with respect to the DRI signal. This indicates that this polymer fraction is possibly cross-terminated by-product formed by irreversible cross-termination reactions between propagating and intermediate radical species during this RAFT-mediated polymerization reaction. Evidence of cross-termination reactions occurring in RAFT-mediated polymerization reactions, which produce cross-terminated products with small UV absorbance at 320 nm with respect to DRI signals, are reported in the literature.[24,26,27] Those experimental data and that obtained in this experiment are identical in that respect.

Figure 5.10c also shows that there is no deviation between the UV absorbance and DRI signal of the extracted polymer at the high *M* polymer regime which would correspond to dead chains formed by combination reactions. It clearly shows that MNPs successfully separate dead chains from living chains formed in this polymerization reaction.

The unextracted polymer contains a large fraction of dead chains with a broad PDI and a large deviation between the UV absorbance and DRI signal, as observed in Figure 5.10d. It is to be noted that the use of a high AIBN concentration in RAFT-mediated polymerization reactions should not change the actual RAFT mechanism. It does lead however to an increase in the actual concentration of all radical derived polymer by-products formed during this RAFT-mediated polymerization reaction. The results obtained in this experiment indicate therefore that irreversible cross-termination reactions might take place in RAFT-mediated polymerization reactions.

5.7.5.2 ^{1}H-NMR and ^{13}C-NMR spectra of the extracted and as-prepared PSt polymers prepared by RAFT-mediated polymerization of St using a high free radical concentration

Figure 5.11 shows the comparison of the ^{1}H-NMR spectra of the extracted (top spectrum) and as-prepared (lower spectrum) polymers prepared by RAFT-mediated polymerization reaction of St using the Z-carboxylate RAFT agent in the presence of an excess of AIBN initiator. The ^{1}H-NMR spectrum of the as-prepared polymer clearly shows that the as-prepared polymer exhibits signals at around 4.8 and 5.3 ppm. These signals correspond to unsaturated dead polymer chains formed due to disproportion and (maybe) transfer to monomer reactions. The extracted polymer exhibits however no signal that would correspond to unsaturated dead polymer chains. Thus, this indicates successful separation of unsaturated dead chains from RAFT chains using the extraction process.

The as-prepared polymer also exhibits a significant signal at 3.14 ppm. This signal most probably corresponds to dead chains formed by combination during this polymerization reaction. This is consistent with the SEC result of the as-prepared polymer (see Figure 5.10b), which shows that this polymer contains a large fraction of high *M* polymer

shoulder with a small UV absorbance compared to the DRI signal. The *M* of this polymer fraction is double the *M* of the main polymer peak (the main polymer peak is around log *M* = 3.90, in Figure 5.10b). This indicates that this polymer fraction is possibly formed by combination reactions.

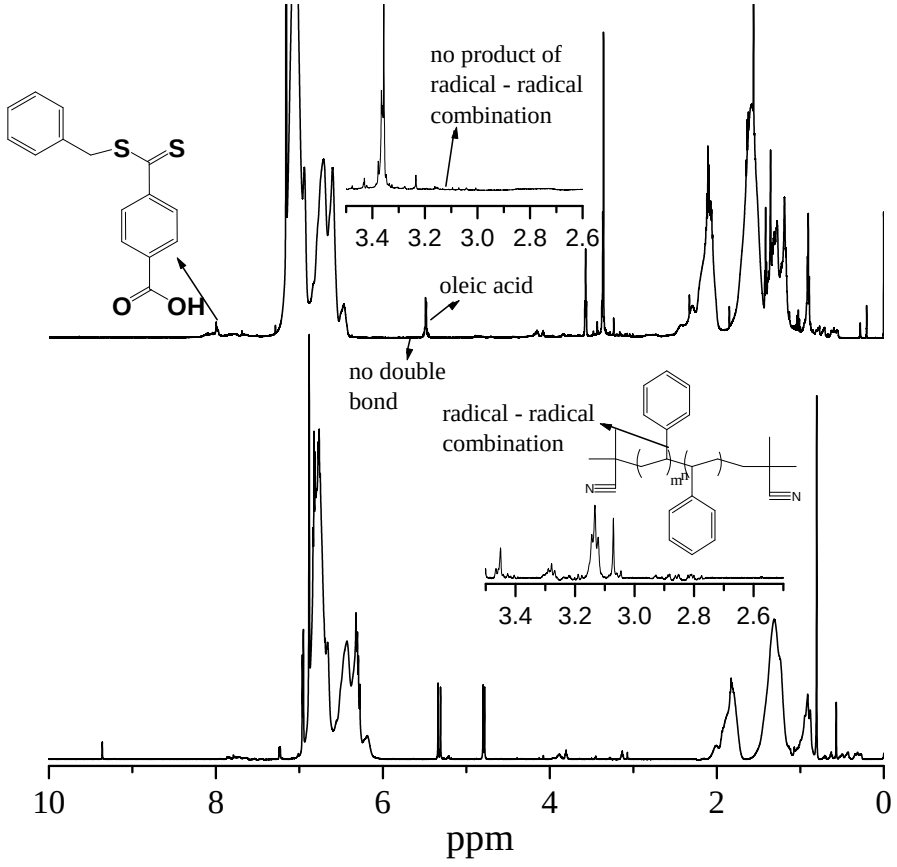

Figure 5.11: ^{1}H-NMR spectra of the as-prepared (lower spectrum) and extracted (top spectrum) PSt polymers prepared by a RAFT-mediated polymerization reaction using the Z-carboxylate RAFT agent and an excess of AIBN initiator. (Reaction conditions: [styrene]: [RAFT]: [AIBN] = 160: 1: 0.5, 70 °C.)

The extracted polymer contains no signal at 3.14 ppm that would correspond to dead chains formed by combination reactions. This is also consistent with the extracted polymer SEC data (Figure 5.10d), which shows that this polymer contains no detectable dead chains formed by combination reactions. This clearly shows efficient separation of dead chains formed by combination reactions from functional RAFT chains.

Figure 5.12 shows the comparison ^{13}C-NMR spectra of the extracted polymer (top spectrum) and as-prepared polymer (lower spectrum).

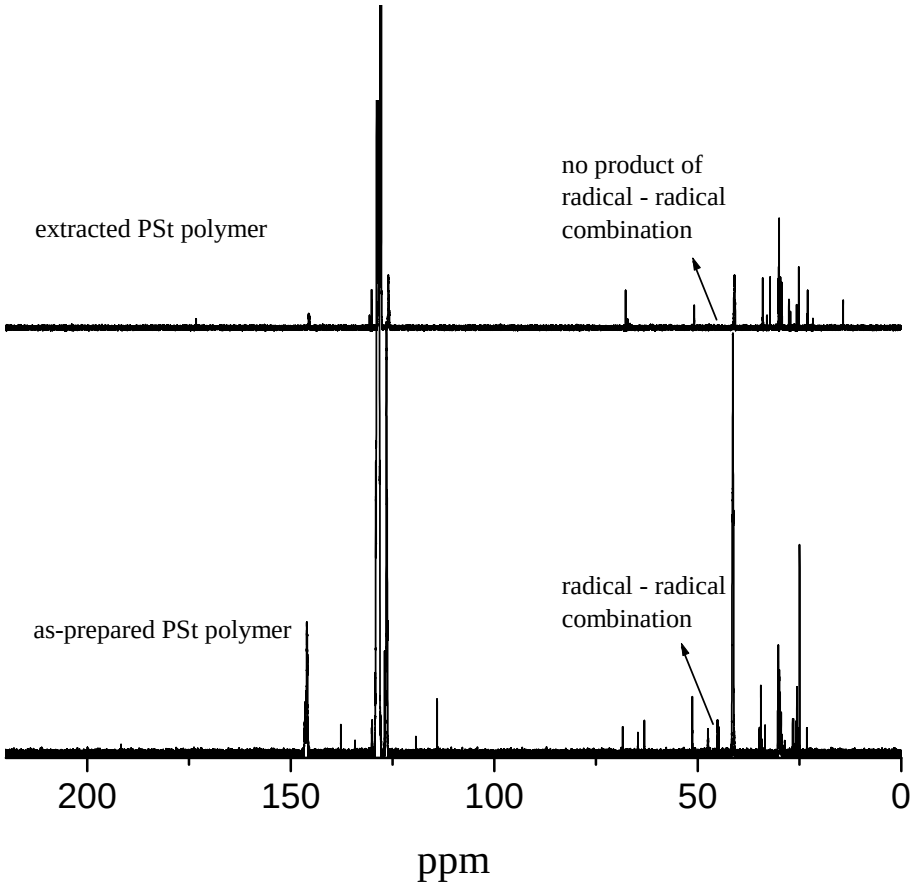

Figure 5.12: ^{13}C-NMR spectra of the as-prepared (lower spectrum) and extracted (top spectrum) PSt polymers prepared by a RAFT-mediated polymerization reaction of St using the Z-carboxylate RAFT agent and an excess of AIBN initiator. (Reaction conditions: [styrene]: [RAFT]: [AIBN] = 160: 1: 0.5, 70 °C.)

The carbon signal which corresponds to a double bond formed due to disproportionation reactions is clearly visible in the ^{13}C-NMR spectrum (lower) of the as-prepared polymer. This signal it is not visible in the ^{13}C-NMR spectrum (top) of the extracted polymer, as expected of separation of all dead chains from living chains. The ^{13}C-NMR spectrum of the as-prepared polymer also exhibits significant signals at 44.82 and 45.14 ppm. These signals correspond to the methylene carbons of polymer products formed by combination reactions. Although some polymer structures that result from head-to-head propagation

reactions have similar structures to those formed by combination reactions, the two structures should however have different chemical shifts. The ^{13}C-NMR signals due to structures from random head-to-head propagation reactions should also be of the same relative intensity in spectra of all the other polymer signals. Therefore signals due to random-to-random propagation reactions are much easier to be distinguished than signals due to structures of combination reactions. The signal at 51.33 ppm of ^{13}C-NMR spectrum of the as-prepared polymer could possibly be due polymer structures of head-to-head propagation reactions formed during this RAFT-mediated polymerization reaction. The methylene carbon signals at 44.8 and 45.14 ppm in the ^{13}C-NMR spectrum of the as-prepared polymer are not visible in the ^{13}C-NMR spectrum of the extracted polymer. This indicates that the extracted polymer contains no dead chains formed by combination reactions.

The ^{1}H-NMR and ^{13}C-NMR comparison spectra of the extracted and as-prepared polymers indicate that extraction process using MNPs efficiently separates all dead chains from functional RAFT chains formed in RAFT-mediated polymerization reactions.

5.7.6 Use of MNPs for separation of initiator derived chains formed in the RAFT process

5.7.6.1 Separation of initiator derived chains of RAFT-mediated polymerization of St

The PSt polymer produced by RAFT-mediated polymerization of St using the blank RAFT agent and PFR initiator at 70 °C (exp 5, Table 5.2) was used in the extraction process. Figure 5.12 shows the DRI signal and UV absorbance SEC traces of the as-prepared, extracted, and unextracted polymers. This indicates that these polymers are different with respect to *M* and MWD. The unextracted polymer has the lowest PDI (1.08, $\overline{M}_{\mathrm{n}}$ = 3300), while the PDIs of the as-prepared and extracted polymers are the highest (1.13, 1.15 and $\overline{M}_{\mathrm{n}}$ = 2900, 2700, respectively). The order of PDIs of these polymers is the unextracted > as-prepared > extracted polymers. This result indicates that

the separation of initiator derived chains formed during the RAFT-mediated polymerization reaction of St has a dramatic effect on the PDI of the prepared polymer.

Figure 5.13b shows that there is a minimal deviation between UV absorbance and DRI signal of the as-prepared polymer. This might indicate that this polymer contains a small fraction of dead chains. Figure 5.13d also shows that the unextracted polymer contains a small fraction of dead chains (possibly R group derived chains) with a minimal deviation between UV absorbance and DRI signal.

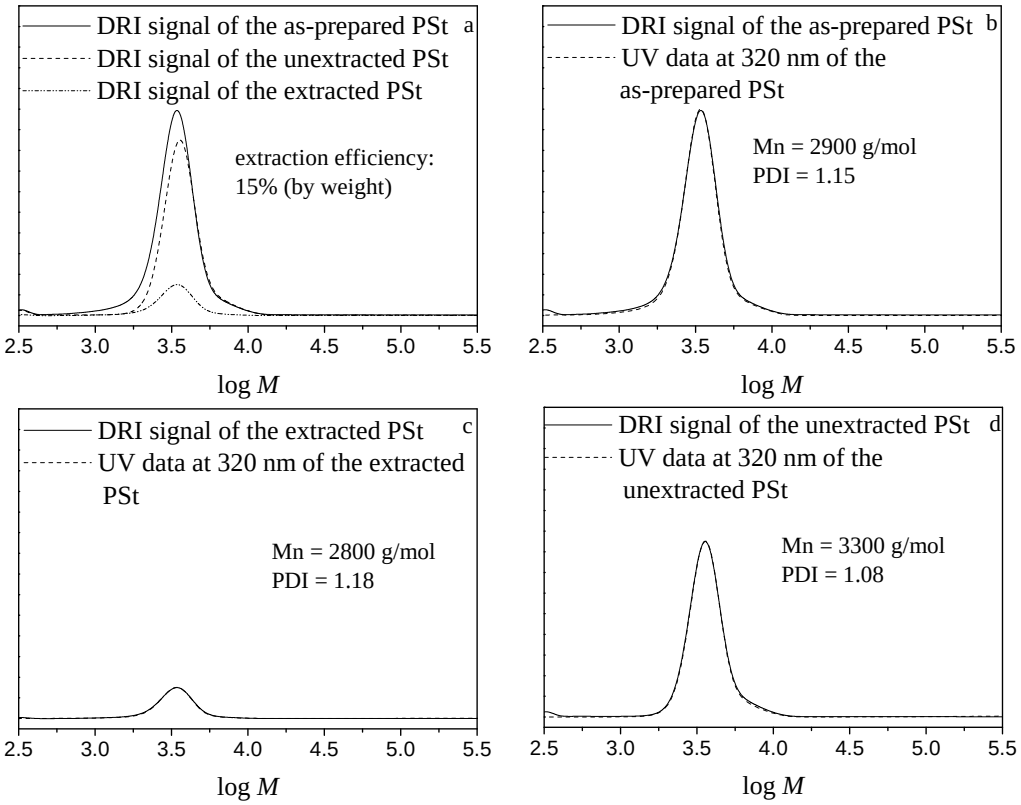

Figure 5.13: SEC traces of the DRI signal and UV absorbance at 320 nm of the PSt polymers prepared by RAFT-mediated polymerization of St using the blank RAFT agent in the presence of PFR initiator: (a) comparison of the as-prepared, extracted and unextracted polymers, (b) the as-prepared polymer, (c) the extracted polymer, and (d) the unextracted polymer.

The extracted polymer contains polymer chains with a minimal deviation between UV absorbance and DRI signal of this polymer, as observed in Figure 5.13c. This is not

expected, since the extracted polymer should contain a small fraction of initiator derived living chains (which produces by some exchange of initiator and R groups during this polymerization reaction). This polymer should however contain a large fraction of dead chains with a broad PDI and partially lack RAFT functionality. Thus, it is expected to see a large deviation between UV absorbance and DRI signal of this polymer, which is not observed in Figure 5.13c. After investigating the UV absorbance of the extracted polymer it was found that the PFR initiator also absorbs UV radiation strongly at 320 nm. The UV absorbance of the PFR initiator was measured using UV/Vis spectroscopy (see Appendix A, Figure A.24). This indicates that the comparison between the UV absorbance at 320 nm and DRI signal of these polymers does not provide enough information about the different polymer species in each polymer product. It was therefore necessary to determine various UV wavelengths where the UV absorbance by the RAFT agent and that by PFR initiator do not overlap.

Figure 5.14 (a – d) shows the DRI signal and UV absorbance at 520 nm (which is due solely to absorption by the RAFT agent) SEC traces of the as-prepared, extracted, and unextracted polymers. These results clearly show that there are large differences between these polymers with respect to *M*, MWD, and UV absorbance at 520 nm. The extracted polymer contains a low *M* polymer tail with a small UV absorbance which lacks RAFT functionality, as observed in Figure 5.14c. The low *M* polymer tail in the extracted polymer could be initiator derived dead chains with at least one initiator group. This is consistent with the unextracted polymer containing no low *M* polymer tail, indicating that the low *M* polymer tail in the extracted polymer is extractable and it is most probably initiator derived dead chains. Initiator decomposition at start of polymerization is high, thus it is expected to see a large number of initiator derived dead chains at start of polymerization reaction, as observed in this study.

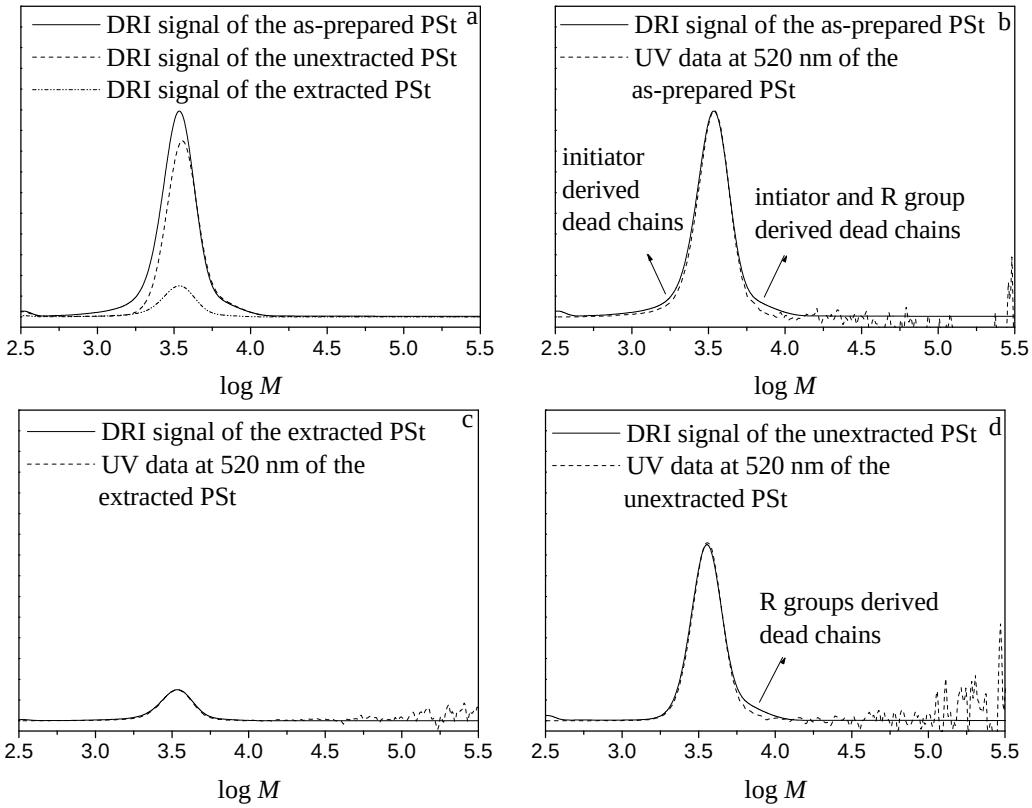

Figure 5.14: SEC traces of the DRI signal and UV absorbance at 520 nm for PSt polymers prepared by RAFT-mediated polymerization of St using the blank RAFT agent in the presence of PFR initiator (same sample as in Figure 5.13): (a) comparison of the as-prepared, extracted and unextracted polymers, (b) the as-prepared polymer, (c) the extracted polymer, and (d) the unextracted polymer.

The unextracted polymer contains high *M* tail with a small UV absorbance, as observed in Figure 5.14d. This is in contrast to the extracted polymer containing no tail at high *M* polymer (see Figure 5.14c). This indicates that the high *M* polymer tail in the unextracted polymer consists mostly of R derived chains and maybe some initiator derived chains, but since no signal is seen in the same region in the extracted polymer (see Figure 5.14c) that probably implies that there are no initiator derived chains in the unextracted polymer distribution at the high *M* polymer tail. The high *M* polymer tail consists of most recently terminated dead chains including cross-terminated chains, since the *M* of this polymer is around twice than that of the living polymer peak of the unextracted polymer with a small UV absorbance at 520 nm. This polymer would be mostly R group derived dead chains

formed by combination (RR), cross-terminated polymer chains between intermediate and polymeric radicals with R end-groups (RRR). It could also contain H-terminated intermediate radicals with R end-groups (RRH) that could be formed by disproportionation reactions producing polymer chains with *M* being twice that of the living polymer peak of the unextracted polymer distribution.

The extracted polymer also contains some living chains with a significant UV absorbance at 520 nm. The living chains in the extracted polymer formed by some exchange of initiator with R groups during this polymerization reaction (the maximum fraction of these chains could be statistically determined by how much initiator has decomposed during this polymerization reaction). The unextracted polymer contains however a large fraction of living chains, as observed in Figure 5.14d, which shows that most of the distribution of this polymer contains a UV absorbance at 520 nm.

5.7.6.2 Use of MNPs for separation of initiator derived chains formed in RAFT-mediated polymerization of MMA

Figure 5.15 shows the DRI signal and UV absorbance SEC traces of the as-prepared, extracted and unextracted PMMA polymers prepared by a RAFT-mediated polymerization reaction of MMA using the blank RAFT agent in the presence of PFR initiator (exp 6, Table 5.2). The magnified inset in Figure 5.15a shows the as-prepared and extracted low *M* polymers. The magnified inset in Figure 5.15b shows the comparison between the UV absorbance at 320 nm and DRI signal of the as-prepared low *M* polymer tail, and that in Figure 5.15c shows the extracted high *M* polymer. These results show significant differences between the as-prepared, extracted, and unextracted PMMA polymers with respect to *M*, MWDs, and UV absorbance. The as-prepared polymer has the highest *M* (PDI = 1.18, $\overline{M}_n$ = 6000), while the unextracted and extracted polymers *M* were the lowest (PDI = 1.5, 1.05 and $\overline{M}_n$ = 4000, 500, respectively). It is to be noted that 1.05 would not normally be considered possible at *M* = 500, for cases when random, even growth was the cause. This might imply that the mechanism for the formation of this polymer is not normal statistical, living process. However, it may be

that the rate coefficients for the first few steps are biased, thus, this becomes possible in such unusual conditions. However, 1.05 could indicate that this might not be a normal polymer peak, which could be formed by chain transfer to initiator, as possibility. This is speculative at this stage, since no more evidence available, but further investigation would be needed to make this clear.

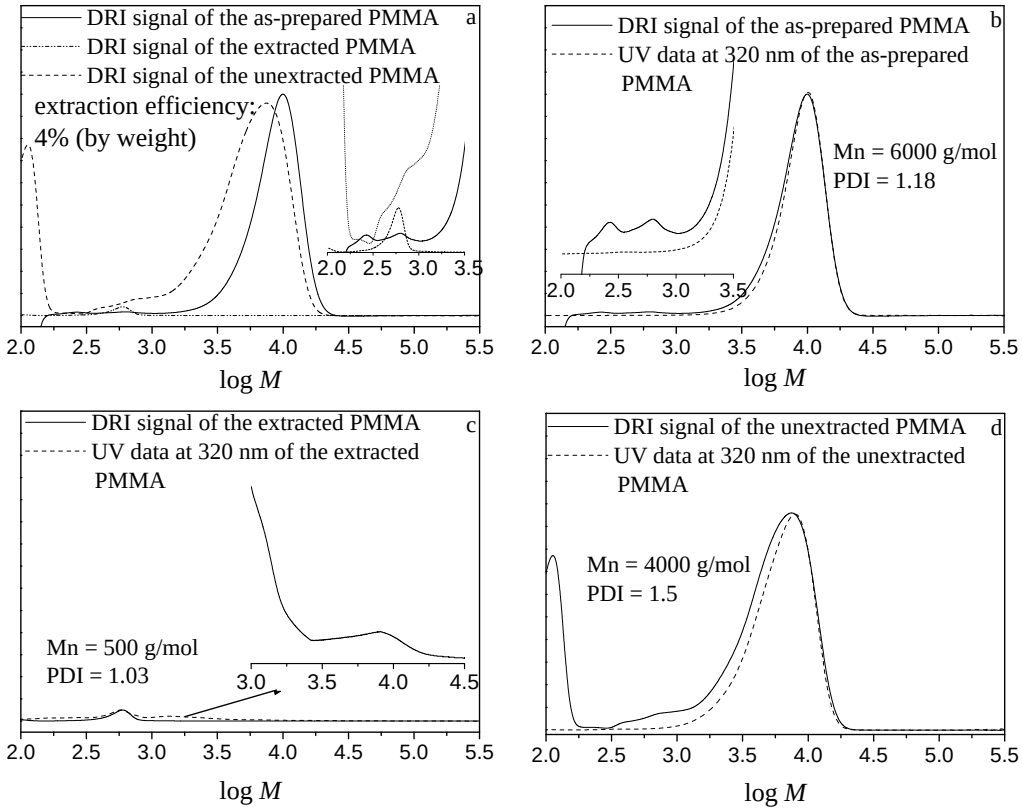

Figure 5.15: DRI signal and UV absorbance SEC traces of the PMMA polymers prepared by RAFT-mediated polymerization reaction of MMA using the blank RAFT agent and PFR initiator: (a) comparison of the as-prepared, extracted and unextracted polymers, (b) the as-prepared polymer, (c) the extracted polymer, and (d) the unextracted polymer.

The as-prepared polymer has a low *M* polymer tail with a small UV absorbance at 320 nm, as observed in the magnified inset in Figure 5.15b. This polymer tail possibly comprises R group derived dead chains that lack both RAFT and initiator groups. This is also consistent with the unextracted polymer containing a low *M* polymer tail with no UV absorbance at 320 nm, as observed in Figure 5.15d. This implies that this polymer tail is

most probably R group derived dead chains which lack RAFT and initiator functionalities.

Figure 5.15b shows that the PDI of the as-prepared polymer is 1.18, which was measured on the basis the as-prepared *M* polymer peak (log *M* = 3.25 – 4.50). However the measured PDI of the as-prepared polymer (including the low *M* polymer tail, as observed in the magnified inset in Figure 5.15) is 1.32. The low *M* polymer tail was not intentionally neglected during the measurement of the PDI of the as-prepared polymer, but it happened due to difficulty in seeing that polymer tail in the GPC original data (as being saved in the GPC instrument). Figure 5.15d clearly demonstrates the effect of such polymer tail on the PDI of the unextracted polymer, which is 1.5. This polymer tail of the unextracted polymer contains dead chains with small UV radiation and lack of RAFT and initiator groups in this case. The PDI of the unextracted polymer was however 1.23 ($\overline{M}_n$ = 5000), when the unextracted low *M* polymer tail was neglected. This clearly indicates the effect of small fraction of dead chains on the PDI value of the prepared polymer.

It is to be noted that the unextracted polymer of this experiment was obtained after removing a number of initiator derived dead chains from this polymer using MNPs. This result indicates however that the separation of initiator derived chains formed in this RAFT-mediated polymerization reaction of MMA has no large effect on the PDI value of the prepared PMMA polymer. This is in contrast to the effect of these chains on the PDI of the prepared PSt polymer, observed in Figure 5.13d.

Figure 5.15d shows that the unextracted PMMA polymer (monomer conversion = 20%) has a bimodal distribution, with a small polymer fraction of about log *M* = 2.80 and a large polymer fraction of about log *M* = 3.80, respectively. The literature reported that RAFT-mediated polymerization of MMA using cumyl phenyldithioacetate RAFT agent and AIBN initiator at 60 °C produced PMMA polymer with bimodal character at a monomer conversion < 25%.[28] Although their RAFT agent and reaction conditions are different from those used in this experiment, their experimental data and that of this experiment are similar. This might indicate that the bimodal distribution of the PMMA

polymer prepared by RAFT-mediated polymerization reactions is possibly attributed to a large extent to a hybrid mechanism, and the living history of MMA itself (MMA may exhibit a hybrid of conventional chain transfer and living characteristic, resulting in bimodal distribution, which could be at low monomer conversion, as observed in this study). Thus, in MMA polymerization, a chain propagates a few steps (adds few monomer units) within each period when the chain is activated by fragmentation. This fast propagation of MMA and it being a good leaving group leads to a relatively uncontrolled *M* and broadened MWD. This was observed in this experiment, as one can see that the unextracted polymer (should contain most of the living chains with RAFT groups) exhibits a large deviation between the UV absorbance and DRI signal at the low *M* unextracted polymer peak (see Figure 5.15d). This indicates that the unextracted polymer contains a fraction of dead chains with a high PDI, that lacks both RAFT and initiator groups.

The DRI signal comparison in Figure 5.15a shows that there is a large difference between the *M* of the extracted and unextracted polymers. This is quite unexpected; since in efficient RAFT-mediated polymerization reactions recently dead chains and living chains should be of comparable chain lengths. However, earlier dead chains should leave a low *M* tail. This result suggests drastically different kinetics for the formation of two distributions as a possibility. It could be that all initiator derived chains propagate very slowly and that they undergo extensive transfer to MMA during this polymerization reaction. This leads to a large number of dead chains with lower *M* than normally expected of living chains formed in RAFT-mediated polymerization reactions. This is consistent with the amount of the extracted polymer, which was 4% (by weight) and 15% by number of chains, suggesting that the unextracted polymer contains a large number of low *M* dead chains.

Figure 5.15a shows a little problem, which is that the high *M* polymer component in the as-prepared polymer is not seen in the extracted or either in the unextracted polymer distributions. There may be a possibility that some of the high *M* polymer chains are being lost during the extraction process, or it might be a problem from the SEC

calibration. This suggests that more extraction work of PMMA using MNPs, would be needed for future investigating this problem.

Figure 5.16 shows the SEC traces of the DRI signal and UV absorbance at 520 nm of the extracted and unextracted polymers. The extracted polymer contains a significant low *M* polymer with small UV absorbance at 520 nm, and a small fraction of high *M* polymer with minimal deviation between UV absorbance at 520 nm and the DRI signal. The extracted polymer appears to contain therefore a large number of initiator derived dead chains and a small number of living chains.

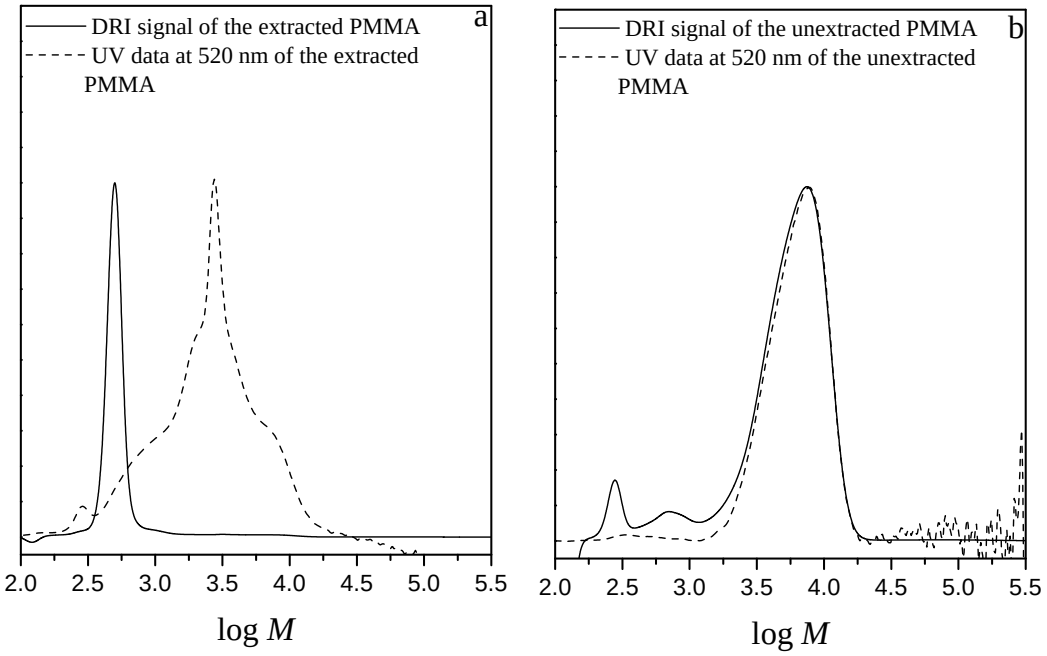

Figure 5.16: SEC traces of the DRI signal and UV absorbance at 520 nm for the PMMA polymers prepared by the RAFT-mediated polymerization reaction of MMA using the blank RAFT agent and PFR initiator (same sample as in Figure 5.15): (a) the extracted polymer, and (b) the unextracted polymer.

Figure 5.16b shows that there is a significant deviation between the UV absorbance at 520 nm and DRI signal at the low *M* of the unextracted polymer, but this is not the case for most of the distribution. This is also consistent with the deviation between the UV absorbance at 320 nm and the DRI signal of the unextracted polymer, as observed in

Figure 5.15d. This indicates that the unextracted polymer contains a large number of living chains with a strong UV absorbance and a significant fraction of dead chains with no RAFT and initiator groups. These dead chains are most probably R group derived and MMA dead chains. The observation that the extracted polymer containing initiator derived chains (see Figure 5.15b) clearly indicates that there are few to no initiator derived chains in the unextracted polymer.

5.8 Conclusions

(1) MNPs were successfully used to separate living chains from dead chains formed in RAFT process using Z-functional RAFT agents with very high efficiency. Separated living chains were efficiently recovered from MNPs and showed apparently 100% RAFT functionality, a lower PDI than the as-prepared polymer, and no detectable dead chains. Chains extension of extracted living chains showed no deviation from 100% extension efficiency, whereas the remaining unextracted chains showed poor extension efficiency.

(2) Non functional polymer chains have no effect in the extraction process. All dead chains formed in RAFT-mediated polymerization reactions and non-functional polymer standard were successfully separated from living chains using MNPs. Separated living chains showed low PDI, 100% RAFT functionality, and contained no detectable fraction of dead and non-functional polymer chains. The remaining polymer after the separation process showed high PDI, less RAFT functionality, and contained a large fraction of non-functional chains.

(3) MNPs were successfully used to separate all dead chains and uncontrolled high molecular weight polymer might be produced by secondary particle formation from living chains formed in RAFT-mediated miniemulsion polymerization reaction using a Z-functional RAFT agent. Separated living chains showed high RAFT functionality, broad PDI, and no uncontrolled high molecular weight polymer. Chain extension of the separated living chains showed no deviation from 100% chain extension. The remaining polymer after the extraction process contained low RAFT functionality, a small amount

of uncontrolled high molecular weight polymer, and showed high PDI and poor chain extension efficiency.

(4) MNPs were used to separate all dead chains from RAFT polymer chains formed in RAFT-mediated polymerization reaction using Z-functional RAFT agent and excess of free radical initiator. Separated RAFT chains were successfully accentuated after separation of all dead chain using MNPs. The separated RAFT polymer chains showed a broad PDI and contained by-products with a significant deviation between UV absorbance at 320 nm and the DRI signal. This polymer contained no detectable fraction of dead chains formed by termination reactions such as combination or disproportionation or transfer reactions. The remaining polymer after the extraction process and the as-prepared polymer showed broader PDI than the separated RAFT polymer chains and contained significant fractions of dead chains formed by combination and disproportionation reactions.

(5) Initiator derived chains formed in RAFT-mediated polymerization reactions of styrene and methyl methacrylate using a phosphate functional free radical initiator were successfully attached to the surface of MNPs and separated from R group derived polymer chains in the presence of an external magnetic field. Separated initiator derived chains contained a large fraction of initiator dead chains and a small amount of RAFT-functional polymer chains. Separated initiator derived dead chains (in the RAFT polymerization of styrene) showed broader PDI than the as-prepared polystyrene polymer. Separated initiator derived dead chains (in the RAFT polymerization of MMA) showed a narrower PDI than the as-prepared polymethyl methacrylate polymer.

5.9 References

1. Matyjaszewski, K., *In Controlled/"Living" Radical Polymerization*; ACS Symposium Series 768; American Chemical Society: Washington, DC, **2000**.
2. Perrier, S.; Takolpuckdee, P.; Westwood, J.; Lewis, D. M. *Macromolecules* **2004,** 37, 2709-2717.
3. de Brouwer, H.; Tsavalas, J. G.; Schork, F. J.; Monteiro, M. J. *Macromolecules* **2000,** 33, 9239-9246.
4. Monteiro, M. J.; de Barbeyrac, J. *Macromolecules* **2001,** 34, 4416-4423.
5. Lansalot, M.; Davis, T. P.; Heuts, J. P. A. *Macromolecules* **2002,** 35, 7582-7591.
6. Prescott, S. W.; Ballard, M. J.; Rizzardo, E.; Gilbert, R. G. *Macromolecules* **2002,** 35, 5417-5425.
7. Landfester, K. *Macromol. Rapid Commun.* **2001,** 22, 897-936.
8. Nguyen, D., H ; Vana, P. *Polym. Adv. Technol.* **2006,** 17, 625–633.
9. Nguyen, D. H.; Wood, M. R.; Zhao, Y.; Perrier, S.; Vana, P. *Macromolecules* **2008,** 41, 7071-7078.
10. Takolpukdee, P.; Mars, C. A.; Perrier, S. *Org. Lett.* **2005,** 7, 3449-3452.
11. Zhao, Y.; Perrier, S. *Macromolecules* **2006,** 39, 8603-8608.
12. Baum, M.; Brittain, W. J. *Macromolecules* **2002,** 35, 610-615.
13. Ejaz, M.; Yamamoto, S.; Ohno, K.; Tsujii, Y.; Fukuda, T. *Macromolecules* **1998,** 31, 5934-5936.
14. Li, C.; Han, J.; Ryu, C. Y.; Benicewicz, B. C. *Macromolecules* **2006,** 39, 3175-3183.
15. Matsuno, R.; Yamamoto, K.; Otsuka, H.; Takahara, A. *Macromolecules* **2004,** 37, 2203-2209.
16. Ohno, K.; Koh, K.-M.; Tsujii, Y.; Fukuda, T. *Macromolecules* **2002,** 35, 8989-8993.
17. Raula, J.; Shan, J.; Nuopponen, M.; Niskanen, A.; Jiang, H.; Kauppinen, E. I.; Tenhu, H. *Langmuir* **2003,** 19, 3499-3504.
18. Wang, W.-C.; Neoh, K.-G.; Kang, E.-T. *Macromol. Rapid Comm.* **2006,** 27, 1665-1669.

19. Li, C.; Benicewicz, B. C. *Macromolecules* **2005,** 38, 5929-5936.
20. Elaïssari, A.; Bourrel, V. J. *J. Magn. Magn. Mater.* **2001,** 225, 151-155.
21. Koneracká, M.; Kopcanský, P.; Antalík, M.; Timko, M.; Ramchand, C. N.; Lobo, D.; Mehta, R. V.; Upadhyay, R. V. *J. Magn. Magn. Mater.* **1999,** 201, 427-430.
22. Roath, S. *J. Magn. Magn. Mater.* **1993,** 122, 329-334.
23. Chiefari, J.; Chong, Y. K. B.; Ercole, F.; Krstina, J.; Jeffery, J.; Le, T. P. T.; Mayadunne, R. T. A.; Meijs, G. F.; Moad, C. L.; Moad, G.; Rizzardo, E.; Thang, S. H. *Macromolecules* **1998,** 131, 5559-5562.
24. Calitz, F. M.; McLeary, J. B.; McKenzie, J.; Tonge, M. P.; Klumperman, B.; Sanderson, R. D. *Macromolecules* **2003,** 36, 9687-9690.
25. van Zyl, A. J. P; Bosch, R. F. B.; McLeary, J. B.; Sanderson, R. D.; Klumperman, b. *Polymer* **2005,** 46, 3607-3615.
26. Kwak, Y.; Goto, A.; Tsujii, Y.; Murata, Y.; Komatsu, K.; Fukuda, T. *Macromolecules* **2002,** 35, 3026-3029.
27. Geelen, P.; Klumperman, B. *Macromolecules* **2007,** 40, 3914-3920.
28. Barner-Kowollik, C.; Quinn, J. F.; Uyen Nguyen, T. L.; Heuts, J. P. A.; Davis, T. P. *Macromolecules* **2001,** 34, 7849-7857.

Chapter 6:
Use of magnetic nanoparticles for purification of polymers prepared via the NMP process

Abstract: Living chains formed in Nitroxide-Mediated Polymerization reactions using X-functional NMP initiator were attached to the surface of MNPs and have been used to separate all dead chains formed in these polymerization reactions prior to the attachment. All living chains attached to the surface of MNPs were then separated from the remainder of solution polymer by applying an external magnetic field. Separated living chains showed lower polydispersity index (PDI) than the as-prepared polymer (the polymer that has not been extracted using MNPs) and contained 100% NMP groups also they could be reactivated to form block copolymers with no deviation from 100% efficiency. The polymer that remained after the separation process using MNPs contained a large fraction of dead chains, showed a broad PDI and poor reactivation efficiency.

6.1 Introduction

6.1.1 Nitroxide-mediated polymerization

One of the important and first achievements in Controlled/"Living" Radical Polymerization (CLRP) is the Nitroxide-Mediated Polymerization (NMP) process.[1,2] The process is widely used for the production of polymers with predetermined and controlled molecular weights, low polydispersity indexes (PDIs), and complex molecular architectures.[3] Although the NMP process produces polymers with a high degree of livingness based on the persistent radical effect (PRE),[4,5] it must be emphasized that termination also plays a crucial role in this process, and that this process is therefore not a true living process. This is because chain termination reactions produce dead chains. Therefore, separation of all dead chains from living chains formed in the NMP process is required for the synthesis of ultra pure high quality polymer standards, or otherwise for any other applications when high purity polymers is required.

6.1.2 Separation of dead chains from living chains in the NMP process

Immobilization of NMP agents onto solid substrates/or particles has been used for synthesis of polymers grafted onto the surface of particles.[6-10] Attachment of NMP agents to the surface of particles is a convenient way for separating all dead chains from living chains formed in the NMP process. In all of the studies reported, the NMP agents were however attached to the surface of particles by their initiating (R) groups. This has been used for the synthesis of polymer grafted onto solid particles, but has not been used yet for separation of by-products from living chains.

It was reported in the literature that the phosphate group strongly interacted and attached to the surface of MNPs[7,8,11] A phosphate group was therefore incorporated into the X group of the NMP agent used in this study (see X-phosphate NMP initiator in Scheme 6.1). Thus all living chains interact and attach to the surface of MNPs, whereas dead chains do not. This allows separation of the attached living chains to the surface of MNPs from the remainder of solution polymer by applying an external magnetic field (Scheme 6.2). This separation (extraction) of all dead chains from living chains formed in NMP

reactions is only effective if the attachment force of the NMP agents to the surface of MNPs is incorporated into the X group of the NMP agents.

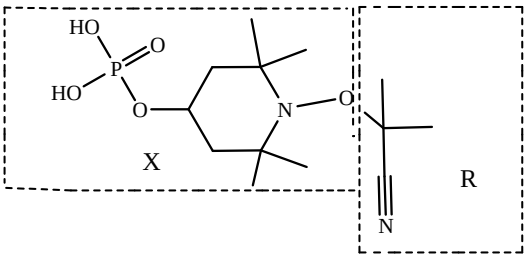

X-phosphate NMP initiator

Scheme 6.1: 1-(1-cyano-1-methylethoxy)-2,2,6,6-tetramethylpiperidine-4-yl-dihydrogen phosphate (X-phosphate) NMP initiator.

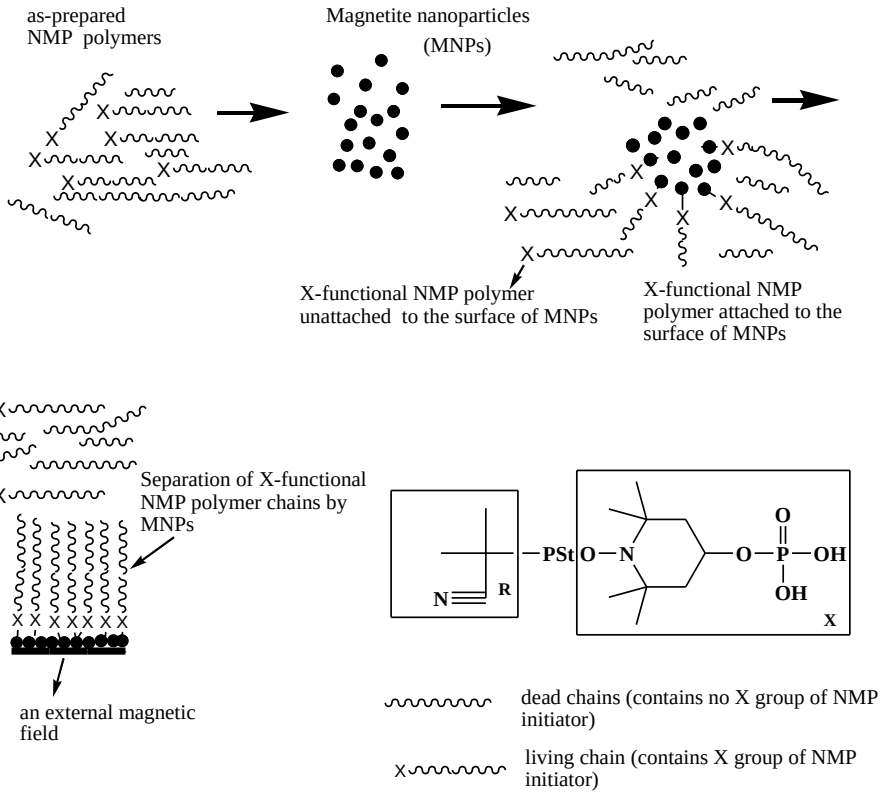

Scheme 6.2: Attachment of X-functional NMP polymer living chains to the surface of MNPs and separation of all living chains attached to the surface of MNPs from dead chains formed in the NMP process by applying an external magnetic field.

In this study, MNPs and the application of a strong external magnetic field are used to separate all dead chains from living chains formed in NMP reactions mediated using X-phosphate NMP initiators. Separated living chains are of much higher purity and NMP functionality than the "as-prepared" polymer chains that have not undergone the extraction process. This allows access to higher purity NMP functional polymers based on the range of monomers available to the NMP process.

It is to be noted that the X-phosphate NMP initiator (which will be used in all NMP reactions during this study) was used after synthesis with no purification. The reason for this is to investigate the use of the extraction process to improve the PDI and MWD quality of modified polymers using this extraction process, when the as-prepared polymers contains an unusually large fraction of by-products, high PDIs and a bimodal MWD.

6.2 Experimental

6.2.1 Materials

The following materials were used as received: hydrochloric acid (32 wt%; Merck), dichloromethane (DCM) (98%; Saarchem), dimethyl sulphoxide (DMSO) (99%; Merck), methanol (99%; Saarchem), and tetrahydrofuran (THF) (99%; Sigma Aldrich).

Styrene monomer (St) (98%; Aldrich) was purified by washing with potassium hydroxide solution (KOH) (0.03M) and distilled under reduced pressure prior to use.

6.2.2 Synthesis of X-phosphate NMP initiator

The X-phosphate NMP initiator was synthesized using the procedure described in Section 3.4.11.

6.2.3 Synthesis and stabilization of MNPs

The synthesis and stabilization of MNPs used in this study are described in Sections 4.3.2 and 4.3.3, respectively.

6.2.4 Nitroxide-mediated solution polymerization of St using X-phosphate NMP initiator

St (10 g; 96 mmol) and X-phosphate NMP initiator (0.24 g; 1 mmol) were dissolved in dimethyl sulphoxide (20 mL), and added to a 150 mL 3-necked round-bottom flask. The flask was purged with N_2 for 15 min to remove the oxygen and placed into an oil bath at 135 °C for 24 h. The polymerization was then quenched by putting the flask into ice water, and the polystyrene polymer was precipitated in methanol (100 mL), filtered off, and dried in a vacuum oven to yield 8.2 g of PSt polymer (yield = 80%).

6.2.5 Nitroxide-mediated bulk polymerization of St using X-phosphate NMP initiator

St (10 g; 96 mmol) and X-phosphate NMP initiator (0.24 g; 1 mmol) were added to a 150 mL 3-necked round-bottom flask. The flask was purged with N_2 for 15 min to remove the oxygen, and then placed into an oil bath at 135 °C for 10 h. The polymerization was quenched by putting the flask into ice water. THF was added to the flask (20 mL) to dissolve the PSt polymer and the polymer solution was then added to methanol (100 mL). The PSt polymer was precipitated in methanol, filtered off, and dried in a vacuum oven to afford 5.5g of the as-prepared PSt polymer (yield = 55%).

6.2.6 Separation of all dead chains from living chains formed in the NMP process using MNPs

The living NMP polymer was separated from the remaining chains by thoroughly mixing and stirring (at ca. 300 – 400 rpm) a solution of the as-prepared polymer chains in dichloromethane (a good solvent for the polymer; typically 100 mL of dichloromethane (DCM) was used for 4.0 g of MNPs to extract 0.8 g of polymer) with a freshly synthesized MNP for 24 h at room temperature. The phosphate groups of living polymer chains competes on the surface of MNPs and replaces some fraction of oleic acid (used to stabilize MNPs). This led to a significant fraction of living polymer chains attached to the surface of MNPs and probably provided additional steric stabilization to the MNPs. A strong, external magnetic field (provided by an NdFeB magnet, with magnetic field intensity of 4.5×10^5 A/m) was applied to the MNP dispersion, which attracted the MNPs and any attached chains to the magnet, thus separating the MNPs from the

remaining solution. The remaining solution (the unextracted solution, which contained the unextracted polymer) was decanted and collected. The MNP dispersion was then mixed at room temperature (by stirring at ca. 300 – 400 rpm) with a 32% HCl solution (typically 15 mL for 4.0 g of MNPs) until the MNPs completely dissolved (which took less than 5 minutes), which was indicated by the disappearance of the black color of the MNPs. The organic phase containing the oleic acid and the extracted polymer was separated from the aqueous phase, and the aqueous phase extracted with DCM. The solvent was evaporated from the combined organic phase to give the extracted polymer. In the case of MNPs remaining in the unextracted solution, this solution was also washed and extracted as above. The final extracted and unextracted polymers were characterized and used for polymer chain extension studies.

6.3 Analytical techniques

6.3.1 Determination of the molecular weight of PSt polymers

The molecular weight distributions of the PSt polymers prepared in this study were determined by Size Exclusion Chromatography (SEC). Polymer samples were dissolved in stabilized THF (HPLC-grade) at a concentration of 5 mg/mL and filtered through a 0.45 nm nylon filter prior to injection. The SEC apparatus comprised a Waters 1515 isocratic HPLC pump, Waters 717 plus autosampler, Waters 24141 refractive index detector, Waters 2487 dual wavelength absorbance detector, two pLgel 5 μm Mixed-C (300 × 7.5 mm) columns, and one pLgel 5 μm guard column (50 × 7.5mm). The samples were eluted using THF (HPLC-grade) at 30 °C and a flow rate of 1 mL/min. The instrument was calibrated using 9 Polymer Laboratories Easyvial polystyrene standards with narrow molar mass distributions in the range 580 – 9 × 10^5g mol^{-1}, supplied by Polymer Laboratories.

6.3.2 Determination of the living functionality

The NMP groups (living functionality) of all PSt polymers prepared by NMP reactions using X-phosphate NMP initiator were determined by the comparison of Ultra Violet (UV) absorbance at 320 nm and Differential Refractive Index (DRI). The wavelength at 320 nm was found to be a suitable wavelength at which the X-phosphate NMP initiator

groups absorb UV radiation strongly. This was measured in our lab using UV/Vis spectroscopy. All UV data was corrected as in the previous studies (see Section 5.6.1) and used for all UV/DRI comparisons during this study.

6.4 Results and discussion

6.4.1 Separation of dead chains from living chains formed in nitroxide-mediated solution polymerization of St using X-phosphate NMP initiator

The PSt polymer prepared by nitroxide-mediated solution polymerization of St using the X-phosphate NMP initiator at 135 °C was used in the extraction process. It is to be noted that DMSO was a good solvent for all the components used in this polymerization reaction. However, the reactivity of the solvent during the polymerization reaction was not tested, as it is beyond the objectives of this study. It should keep in mind that if it is reactive, it might cause problems and produce by-products that will affect the as-prepared polymer distributions, thus it is a good idea to investigate the reactivity of the solvent DMSO in future studies.

Figure 6.1 shows the DRI signal and UV absorbance SEC traces of the as-prepared polymer (the polymer that was not modified by the extraction process), unextracted polymer (the polymer that remains in solution after the extraction process), and extracted polymer (the polymer that was attached to the surface of MNPs and separated from a mixture of solution polymer by applying an external magnetic field). The insets in Figure 6.1a shows the comparison of the DRI signals of the as-prepared and unextracted polymers, to show that the intensity of the high molecular weight (*M*) polymer peak of the unextracted polymer increased after the separation using MNPs.

The SEC traces of the as-prepared, extracted, and unextracted polymers show that there are large differences between these polymers with respect to (*M*), molecular weight distribution (MWD), and UV absorbance (which is dominated by absorption by the phosphate (X) group of the X-phosphate NMP initiator (plus a small contribution from the aromatic rings of each styrene unit)).

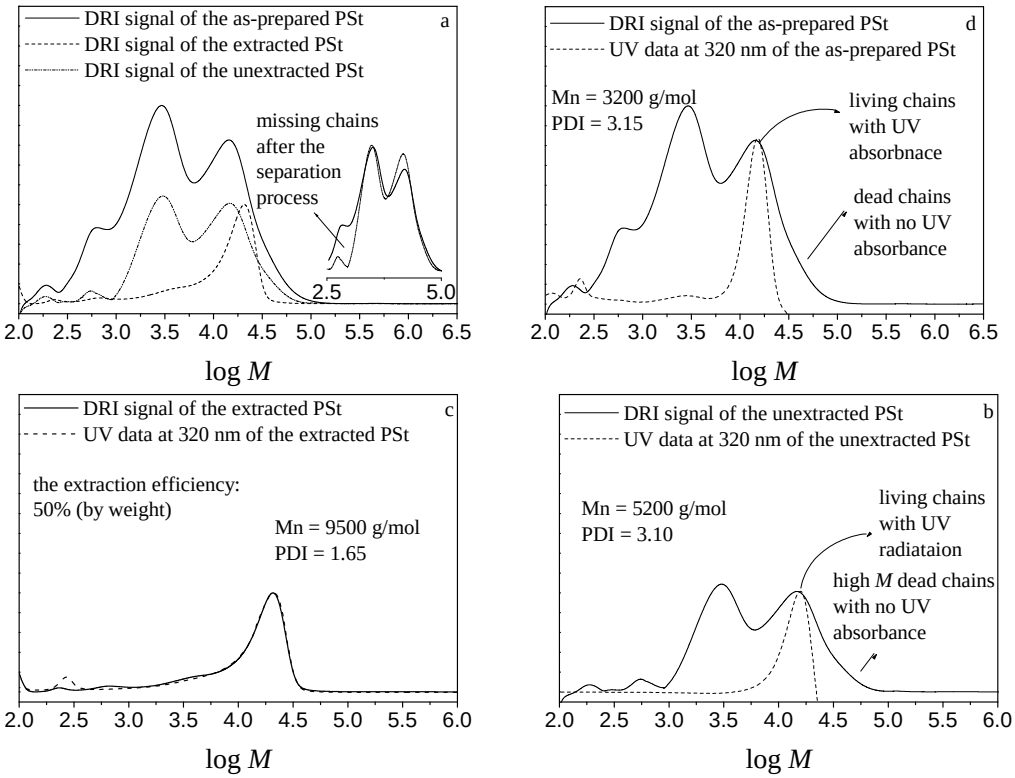

Figure 6.1: DRI signal and UV absorbance SEC traces of the PSt polymers prepared by nitroxide-mediated solution polymerization of St using X-phosphate NMP initiator at 135 °C, (a) the comparison of as-prepared, extracted and unextracted polymers, (b) the as-prepared polymer, (c) the extracted polymer, and (d) the unextracted polymer.

The DRI signal comparison in Figure 6.1a shows that the extracted polymer exhibits a symmetrical shape (based on the main part of the polymer peak) with a monomodal MWD. The overall distribution of the extracted polymer shows that there is also a long *M* tail possibly due to a large amount of thermal initiation producing chains that start growing later, but are controlled. The as-prepared and unextracted polymers exhibit a bimodal MWD (neglecting the low *M* polymer peaks). The extracted polymer is of higher molecular weight ($\overline{M}_n$ = 9500) and it shows better PDI (1.65) than the as-prepared and unextracted polymers ($\overline{M}_n$ = 3200, 5200, PDI = 3.1, 3.15, respectively). The extracted polymer contains living chains with strong UV absorbance and NMP functionality, as observed in Figure 6.1c. The as-prepared and unextracted polymers however contain a

large fraction of dead chains with weak UV absorbance and lack NMP functionality, and a small fraction of living chains with UV absorbance, as observed in Figures 6.1b and d, respectively. This indicates separation of all dead chains (weak UV absorbance and lack NMP functionality) from living chains formed in this NMP reaction. Therefore, the extracted polymer should contain dormant NMP polymer chains, and is expected to undergo complete chain reactivation (reinitiation) for the extension polymerization test.

The as-prepared polymer exhibits mainly a bimodal (it might also be considered multimodal) MWD, as observed in Figure 6.1b. It contains a large number of dead chains with low *M* and weak UV absorbance. It also contains a large fraction of high *M* polymer; this polymer contains living and dead chains. The observation of as-prepared polymer exhibiting mainly a bimodal MWD suggests the occurrence of different polymerization reaction periods or maybe two environments taking place during this polymerization reaction of St using X-phosphate NMP initiator. The low *M* polymer possibly originates from an extensive auto polymerization due to thermal self-initiation of St (thermal self-initiation will occur throughout the reaction, but expected to become slower as the St concentration decreases) and termination reaction and by-product formation taking place during the early stage of this NMP polymerization reaction. The high *M* polymer possibly originates from activation and deactivation reactions taking place during the NMP polymerization reactions, which normally are expected to produce living and dead chains.

A proposed explanation of this reaction follows: in the NMP process, initiating and mediating (R and X groups, respectively) radicals are formed by decomposition of the NMP initiator. The concentration of the mediating and initiating radicals should normally increase with time until steady state equilibrium concentration is reached (R reaches its maximum), while the mediating radicals are still increasing with time. During the early stage of the polymerization reaction initiating radicals are gradually consumed in self-termination reactions (i.e. the overall termination rate is high during this polymerization stage). The polymerization reaction will then gradually change to another period where the total termination rate normally decreases, while the overall deactivation rate

increases. Therefore the activation/deactivation process dominates other competing processes, and with associated equilibrium constant, means that the propagating radical concentration is low, and thus, termination rates will be low. This makes other side reactions such as termination by combination to be negligible. However, the above mentioned reactions taking place during NMP polymerization reactions might be a little different when the NMP initiator contains a large fraction of impurities, as in this experiment. This is because impurities are expected to interrupt/ or affect the actual NMP polymerization reactions. Therefore in this NMP reaction, which was mediated by an NMP initiator containing a large fraction of impurities, a large number of side reactions might take place. Initiating radicals might be consumed by extra termination reactions with impurities, or their by-products, and thus produce dead chains with weak UV absorbance that lack NMP functionality, as observed in Figure 6.1b. Mediating radicals at the early stage of the NMP reaction could also react with unknown impurities, and thus could produce by-products such as very stable NMP initiators. This might lead to a small number of those by-product species being present, due to consumption in side reaction, or low mediating radical efficiency at the early stage of the NMP reaction, and thus a small number of living chains, as was observed in this experiment.

A significant amount of the active mediating radicals became however available for equilibration at a later stage of this NMP reaction, and thus a significant fraction of living chains with strong UV absorbance and NMP functionality formed during this stage, as observed in Figure 6.1b. This however does not preclude other termination reactions taking place during this stage of the NMP reaction, which produced a fraction of dead chains with weak UV absorbance that lack NMP functionality, as was observed in this experiment (see the high *M* polymer peak in Figure 6.1b). Although knowing all different polymer species involved during this polymerization reaction is important in order to better understand the reaction mechanism, this will not however be further discussed, as it is beyond the objectives of this study.

It is also to be noted that the polymerization reaction temperature of this experiment was high (135 °C), thus the probability of the thermal self-initiation of St is also high.[12] This

leads to a higher radical concentration than normally expected, which will also increase the probability of chain transfer and termination reactions, resulting thus in a large number of dead chains, as was observed in this study. There is also probability of alkoxyamine disproportionation rate at the polymerization reaction temperature (135 °C). This would produce unsaturated terminated chains by the loss of one TEMPO molecule in each disproportionation event.[13] This should also have an effect on the degree of control and livingness of this polymerization reaction system.

The living chains in the unextracted polymer probably result from the ligand exchange process in the extraction step, which does not attach all NMP functional chains to the MNP surface, thus leaving unattached NMP chains to be decanted with the unextracted solution of polymer. This is consistent with the amount of polymer extracted, which was 50% by weight and 38% by number of chains. The total number of living chains is expected to be 55%, or even less since the NMP initiator was 55% pure and due to an expected large amount of thermal self-initiation of St producing a large number of extra chains. Thus, a substantial fraction of living chains are in the unextracted polymer.

The PDI of the extracted polymer was higher than normally expected of polymers prepared via CLRP. This indicates that the extracted polymer is less controlled in this case, but apparently contains dormant chains with UV radiation and NMP functionality, as observed in Figure 6.1c. Dead chains are normally produced by termination, and transfer reactions throughout the NMP polymerization reactions. Therefore, the PDI of dead chains is expected to be high, as was observed in this experiment.

Although the as-prepared and unextracted polymers showed high PDIs, the PDI of the extracted polymer was much lower, which clearly indicates efficient removal of all dead chains (high PDI) from living chains (low PDI).

The high M polymer peak of the unextracted polymer (see log M ~ 4.4) contains living chains with UV absorbance and dead chains (see the very high M component of the unextracted polymer shows no UV absorbance, so these are likely to be dead chains some

of these are more than twice the living chains, which suggests a possibly different mechanism, impurities, side reactions, or (dead) polymer forming away from the living chains, such as in heterogeneous system). The magnified inset in Figure 6.1a shows that the intensity of the high *M* polymer peak of the unextracted polymer (log *M* ~ 4.4, which contains living chains) increased after the separation process. This was not expected, since the separation process using MNPs separates living chains from dead chains of the as-prepared polymer. Thus, the DRI intensity (amounts) of high *M* unextracted polymer peak should be lower than the as-prepared polymer DRI intensity in that region.

The observation of the amount of high *M* polymer peak of the unextracted polymer increasing after the separation process suggests that the total number of the unextracted polymer chains somehow decreased after the separation process. Thus, the number of the high *M* polymer chains maybe increased because the total number of the unextracted polymer chains decreased, as was observed in this study. This is consistent with DRI signal comparison of the as-prepared and unextracted polymers (insets in Figure 6.1a), which shows that the low *M* of the as-prepared polymer (see log *M* ~ 3.1) exhibits higher DRI intensity than that of the unextracted polymer. It indicates that a large fraction of chains in the as-prepared polymer. This strongly suggests the idea that the total number of the unextracted polymer chains decrease after the extraction process.

The chains that do not exist in the unextracted polymer after the extraction process, which was observed in the insets in Figure 6.1a, are probably absent because these chains were soluble in methanol. This might happen, since these chains are short and that the unextracted polymers were obtained by precipitation in methanol. Thus, the total amount of the unextracted polymer was less than otherwise expected. This will be discussed in detail later.

6.4.2 Chain extension tests of the extracted and unextracted PSt polymers

The extracted and unextracted polymers prepared using nitroxide-mediated solution polymerization of St using the X-phosphate NMP initiator at 135 °C were used for chain extension tests to investigate chain livingness of these polymers. Chain extensions are

based on the use of the extracted and unextracted polymers as macroinitiators. Figures 6.2a and b show the DRI signal and UV absorbance SEC traces of the chain extension experiments of the unextracted and extracted polymers, respectively.

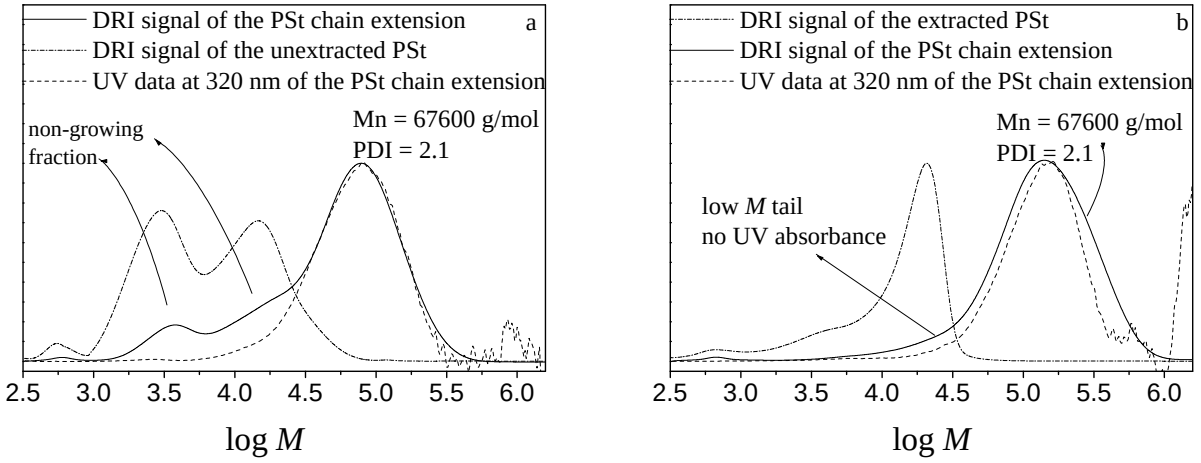

Figure 6.2: DRI signals and UV absorbance SEC traces of the extracted and unextracted PSt chain extension polymers prepared using nitroxide-mediated solution polymerization of St using X-phosphate NMP initiator at 135 °C, (a) the unextracted polymer, and (b) the extracted polymer.

The extracted polymer apparently underwent complete chain reinitiation with a minor new low *M* polymer tail (a small fraction of this polymer tail shows UV absorbance) (again, the low *M* tail polymer is almost certainly due to new chains being formed by thermal self-initiation of St, giving living chains with low *M*, plus the dead chains formed will also exhibit a similar distribution to that of the living chains), as observed in Figure 6.2b. The newly formed polymeric tail consists of dead chains with weak UV absorbance that lacks NMP functionality. These dead chains are formed during the extension test of the extracted polymer. This is consistent with the SEC traces of extracted polymer before chain extension experiment (Figure 6.1c), which shows that there is no deviation between the UV absorbance and the DRI signal, indicating that this polymer contains no detectable dead chains prior to the chain extension test. Therefore, the low *M* extracted polymer tail after chain extension is probably dead chains newly formed during the extension polymerization test. Thus, the extraction process using MNPs is highly efficient in removing all dead chains from living chains formed in NMP reactions. The

PDI of the extracted polymer after chain extension (2.10, $\overline{M}_n$ = 67,000) is possibly due to high target *M* (ca 480,000), resulting in less control and also thermal self-initiation of St adding more short chains, but good living behaviour.

The unextracted polymer after chain extension shows however two distinct polymer fractions: (i) A significant fraction of high *M* polymer peak, that, as expected, underwent almost complete chain extension with UV absorbance and NMP functionality, indicating that this fraction consists of living chains. (ii) A large fraction of low *M* polymer with weak UV absorbance that lacks NMP functionality. This polymer fraction underwent almost no chain reinitiation, as observed in Figure 6.2a. This suggests that the low *M* polymer peak consists of dead chains which lack NMP functionality, as expected of separation of all dead chains from living chains formed in the NMP process.

The observation that the extracted polymer after chain extension exhibited a large fraction of dead chains with weak UV absorbance that lack NMP functionality is possibly due to the low macroinitiator concentration (this is the concentration of the extracted polymer used for the extension test). If the concentration of the macroinitiator is low, chain transfer to monomer might give rise to large number of dead chains with a long low *M* tail, as observed in this experiment. The ratio of [P$^{\bullet}$]/[deactivator] also increases with decreasing the initial concentration of the macroinitiator, resulting thus in significant amounts of termination. Inspection of Figure 6.2b shows that the extracted polymer after chain extension contains a significant fraction of dead chains with a significant deviation between the UV and DRI signals.

The extension polymerization tests of the unextracted and extracted polymers show that the extracted polymer contains living polymer chains, while the unextracted polymer contains a large fraction of dead chains and a significant fraction of living polymer chains. This shows the extraction process using MNPs is very efficient process for separation of all dead chains from living chains formed in NMP reactions.

The extracted polymer after chain extension exhibits a monomodal MWD, as observed in Figure 6.2b. This is in contrast to the SEC traces of the as-prepared polymer (Figure 6.1b), which shows that this polymer exhibits a bimodal MWD. These observations clearly indicate that impurities have a dramatic effect on the actual NMP polymerization reactions and MWD of the prepared polymers.

6.4.3 Separation of dead chains from living chains formed in nitroxide-mediated bulk polymerization of St using X-phosphate NMP initiator

The earlier proposed idea, that suggested that a large number of dead chains and a small fraction of living chains are formed during the NMP of St using the X-phosphate NMP initiator containing a large fraction of impurities, was further investigated. Therefore, the PSt polymer prepared by nitroxide-mediated bulk polymerization of St using the X-phosphate NMP initiator at 135 °C (yield 55%), which is lower than the previous case (80%) was used in the extraction process for supporting and comparison. Figure 6.3 shows the DRI signal and UV absorbance of the as-prepared, extracted and unextracted polymers. The comparison Figures 6.3a – d show distinct differences between these polymers with respect to *M*, MWDs, and UV absorbance. The extracted polymer exhibits a fairly symmetrical shape and low PDI (1.25, $\overline{M}_n$ = 22500), as expected of polymers prepared by well controlled polymerization reactions. The as-prepared and unextracted polymers have however high PDIs (1.95, 2.7, $\overline{M}_n$ = 3000, 3780, respectively).

The as-prepared polymer contains a large fraction of low *M* dead chains with minimal UV absorbance that lack NMP functionality and a smaller fraction of high *M* living chains with UV absorbance and NMP functionality, as observed in Figure 6.3b. The unextracted polymer contains dead chains with low *M* and weak UV absorbance and lack NMP functionality, and a fraction of living chains with high *M* and UV absorbance and have NMP functionality, as observed in Figure 6.3d. However, the extracted polymer contains living chains with UV absorbance and NMP functionality, as observed in Figure 6.3c. This indicates that the separation process is highly efficient in terms of removing all dead chains (that lack NMP functionality) from living chains (that contain NMP

functionality) formed in the NMP reactions. The extraction process could therefore be used for the synthesis of pure NMP polymers.

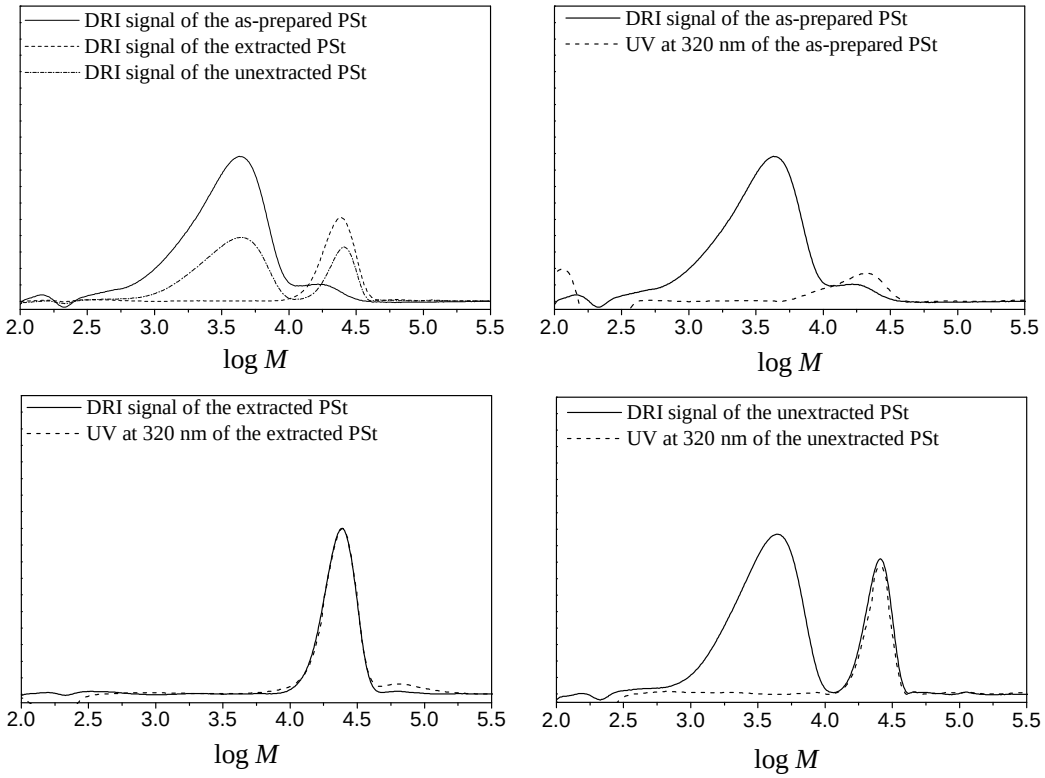

Figure 6.3: DRI signal and UV absorbance SEC traces of the PSt polymers prepared by nitroxide-mediated bulk polymerization of St using X-phosphate NMP initiator at 135 °C, (a) the comparison of the as-prepared, extracted and unextracted polymers, (b) the as-prepared polymer, (c) the extracted polymer, and (d) the unextracted polymer.

The observation that the as-prepared polymer exhibits a very small fraction of living chains compared to dead chains indicates that the amount of the living chains decreased as the reaction yield decreased. This supports the idea that at lower yield the efficiency of the X-phosphate NMP initiator could be low, but more importantly this shows the effect of extensive thermal initiation, as was discussed in Section 6.4.2. The effect of thermal initiation clearly is being much more prevalent in this polymerization reaction (in bulk), compared to solution, reaction. If the number of dead chains (in a tail) is large, it will appear as broad peak, as seen here. Thus the production of dead chains will be much higher than living chains, as was observed in this study.

The fraction of living chains in the unextracted polymer is higher than that in the as-prepared polymer, as observed in Figure 6.3a. The observation that the number living chains is increasing after the separation process is also observed in the previous experiment (see insets in Figure 6.1a). This was because the total number of the unextracted polymer chains decreased after the separation process, which was attributed to the loss of a significant fraction of dead chains form the unextracted polymer during the precipitation in methanol.

The observation that the DRI peak intensity of the high *M* polymer of the unextracted polymer, which contains living chains and dead chains is being increased after the extraction process and the idea that this was because of the loss of a significant number of the unextracted polymer chains in methanol during the precipitation of this polymer, was further investigated. Thus, the unextracted polymer (prepared by nitroxide-mediated bulk polymerization of St using the low purity X-phosphate NMP initiator at 135 °C) was used in a second extraction using MNPs. This is also to show that living chains that left in the unextracted polymer after the first extraction can possibly be removed in a multiple extraction. In order to prevent a possible loss of the unextracted polymer chains, this polymer was not precipitated in methanol.

Figure 6.4 shows the comparison of the DRI signals SEC traces of the unextracted polymers (after first extraction process (unextracted polymer 1) and that after the second extraction process (unextracted polymer 2)). The unextracted polymer (2) contains a lower number of high *M* polymer (log *M* ~ 4.4, comprises dead and living chains) than the unextracted polymer (1). This is indicated by the much lower DRI signal intensity of the unextracted polymer (2) than that of the unextracted polymer (1), as observed in Figure 6.4. The observation that the intensity of the high *M* polymer peak of the unextracted polymer decreased after the second extraction indicates that living chains in the unextracted polymer can be removed by further extractions using MNPs. This shows that the extraction process using MNPs is very efficient in terms of removing a small fraction of living chains from a large fraction of dead chains, as observed in this study. Figure 6.4 also shows that the unextracted polymers contain a comparable number of

dead chains based on the low *M* polymer (log *M* ~ 3.60), as indicated by the small deviation between DRI SEC signals of the unextracted polymers at that low *M* polymer peaks. This supports the idea the loss of low *M* polymer chains in the unextracted polymer, as observed in the magnified inset in Figure 6.1a, is due to the precipitation of the unextracted polymer in methanol.

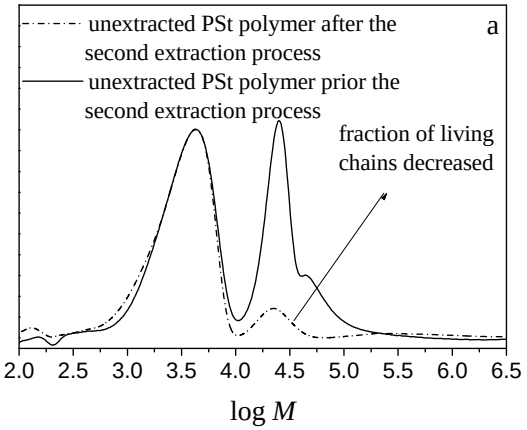

Figure 6.4: The DRI signal and UV absorbance SEC traces of the unextracted PSt polymers prior and after the second extraction process prepared by nitroxide-mediated bulk polymerization of St using the X-phosphate NMP initiator at 135 °C.

6.5 Conclusions

MNPs were successfully used to separate living chains from dead chains formed in the NMP process using X-functional NMP initiators with a very high efficiency. Separated living chains were effectively recovered from MNPs and used successfully in chain extension tests. All separated living chains exhibited monomodal molecular weight distributions and contained NMP functionality and showed lower PDIs than the as-prepared polymers. The separated living chains can be extended to produce block polymers with a good living behaviour and high extension efficiency.

The as-prepared polymers using X-functional NMP initiator showed broad PDIs, and bimodal MWDs with large fractions of dead chains and a small fraction of living chains. The as-prepared polymer prepared using the bulk polymerization reaction contained a lower number of living chains than that prepared using the solution polymerization

reaction. This was attributed to an extensive termination due to the more prevalent thermal initiation effect in the bulk polymerization reaction at lower yield (the ratios of [P$^{\bullet}$]/[deactivator] may be high, thus average termination is also high) than that in the solution polymerization reaction at a higher yield (the ratios of [P$^{\bullet}$]/[deactivator] may be lower, thus average termination is also lower). This could also be attributed to the lower efficiency of the X-phosphate NMP initiator at a lower reaction yield than that at higher reaction yield.

The remaining polymer chains after the extraction process showed broad PDIs, bimodal molecular weight distributions, and poor chain extension efficiency. The observed fraction of living polymer chains in this polymer increased after the extraction process. This was because the total number of the remaining polymer chains after the extraction process decreased. It possibly decreased due to loss of a significant fraction of unextracted polymer chains during the precipitation of this polymer using methanol.

6.6 References

1. Georges, M. K.; Veregin, R. P. N.; Kazmaier, P. M.; Hamer, G. K. *Macromolecules* **1993,** 26, 2987-2988.
2. Solomon, D. H.; Rizzardo, E.; Cacioli, P. US Patent. 4581429, **1986**.
3. Matyjaszewski, K., *In Controlled/"Living" Radical Polymerization;* ACS Symposium Series 768; American Chemical Society: Washington, DC, **2000**.
4. Fischer, H. *J. Polym. Sci., Part A: Polym. Chem.* **1999,** 37, 1885-1901.
5. Tang, W.; Fukuda, T.; Matyjaszewski, K. *Macromolecules* **2006,** 39, 4332-4337.
6. Husseman, M.; Malmstrom, E. E.; McNamara, M.; Mate, M.; Mecerryes, D.; Benoit, D. G.; Hedrick, J. L.; Mansky, P.; Huang, E.; Russel, T. P.; Hawker, C. J. *Macromolecules* **1999,** 32, 1424-1431.
7. Matsuno, R.; Yamamoto, K.; Otsuka, H.; Takahara, A. *Chem. Mater.* **2003,** 15, 3-5.
8. Matsuno, R.; Yamamoto, K.; Otsuka, H.; Takahara, A. *Macromolecules* **2004,** 37, 2203-2209.
9. Hawker, C. *J. Angew. Chem., Int. Ed. Engl.* **1995,** 34, 1456-1459.
10. Bartholome, C.; Beyou, E.; Bourgeat-Lami, E.; Chaumont, P.; Lefebvre, F.; Zydowicz, N. *Macromolecules* **2005,** 38, 1099-1106.
11. Daou, T. J.; Begin-Colin, S.; Grene`che, J. M.; Thomas, F.; Derory, A.; Bernhardt, P.; Legare´, P.; Pourroy, G. *Chem. Mater.* **2007,** 19, 4494-4505.
12. Greszta, D.; Matyjaszewski, K. *Macromolecules* **1996,** 29, 7661-7670.
13. Ohno, K.; Tsujii, Y.; Fukuda, T. *Macromolecules* **1997,** 30, 2503-2506.

Chapter 7:
Use of magnetic nanoparticles for purification of by-products formed in a RAFT/ATRP model reaction

Abstract: The cross-termination of the intermediate radical formed in the reversible addition-fragmentation chain transfer (RAFT) process has been investigated in the monomer excluded free radical reaction model of polystyryl benzyl-(4-carboxyl dithiobenzoate) and polystyryl ethyl-2-bromoisobutyrate. The 3- and 4-arms star polymers, possibly produced by the irreversible cross-termination between intermediate radical and propagating radical species or intermediate-intermediate radicals, were efficiently separated using magnetite nanoparticles (MNPs) from any other non-functional RAFT terminated chains (those produced by termination reactions involving no intermediate radicals, including termination by combination). Z-carboxylate 3- and 4-arm stars (those produced by irreversible cross- termination reactions) strongly interacted with and attached to MNPs magnetic nanoparticles surfaces by replacing some fraction of the oleic acid (used to stabilize the MNPs), while other non- functional terminated chains that contained no group that could interact with the MNPs did not. This allows selective separation of the 3- and 4-arm star polymers together with MNPs by applying a strong external magnetic field. The 3- and 4-arm star polymers were separated from MNPs and characterized by ^{1}H and ^{13}C Nuclear Magnetic Resonance spectroscopies and Matrix Assisted Laser Desorption Ionization-time of flight Mass Spectroscopy.

7.1 Introduction

Reversible addition-fragmentation chain transfer (RAFT) polymerization process involves the equilibrium reaction (Scheme 7.1)[1,2] in which the dormant chain (P'-Y) reacts with a growing polymeric radical (P•) to produce an intermediate radical (P'-Y•-P). The intermediate radical, which is clearly observed by electron spin resonance (ESR) spectroscopy[3], fragments at either of its two arms or can also undergo cross-termination with another radical species (R•). If the addition and fragmentation reactions in the RAFT process occur at a fast rate and there are no by-products formed, there should not be any influence of the RAFT process on the propagation rate, and thus the retardation should be negligible. A significant retardation rate has however been clearly observed in some RAFT studies, particularly in reactions mediated by dithioester RAFT agents.[2,4-7]

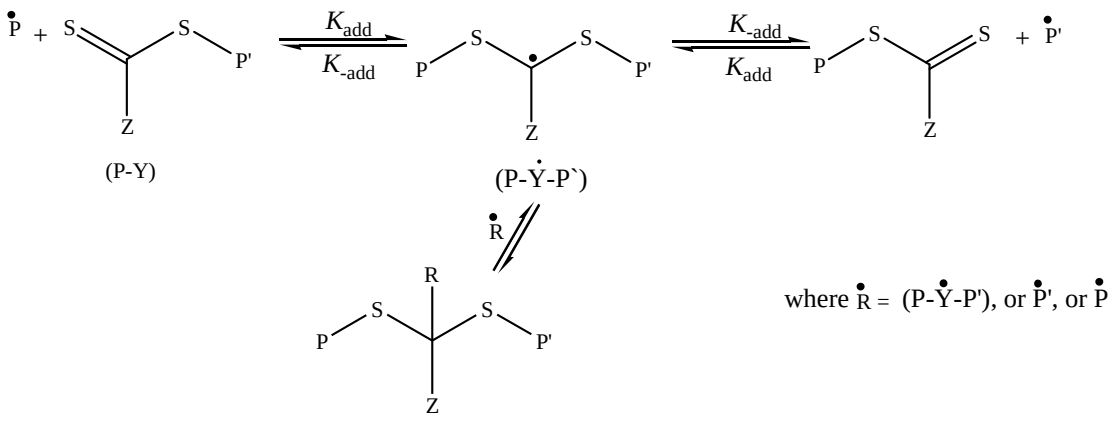

Scheme7.1: The central equilibrium of the RAFT process (top), and expected cross-termination reaction (below).[1]

In the ongoing debate of the rate retardation in RAFT polymerization, there is the argument by several authors including de Brouwer and Monteiro,[6,7]Kwak ,[8,9] Calitz,[10] and Buback[11,12] that regard rate retardation to be caused by cross-termination of the intermediate radical model. There are even indications that the other possibilities, namely slow fragmentation (long life time) of intermediate radical model, can be complimentary and therefore an additive contribution in terms of rate retardation.[4,5]

The slow fragmentation model suggests that the intermediate radicals are rather stable and have long lifetimes. To explain this phenomenon, the Centre for Advanced Macromolecular Design CAMD group have used a commercial kinetics simulation package (PREDICI) to correlate monomer conversion and molecular weight data of St bulk polymerization mediated by cumyl dithiobenzoate at 60 °C, they reported the fragmentation rate coefficient (k_f) of the intermediate radical of this system is typically in order of 10^{-2} s^{-1}.[4] However in polymerization of St mediated by polystyryl dithiobenzoate also at 60 °C, Kwak found that the rate coefficient of fragmentation of the intermediate radicals is 7×10^{4} s^{-1},[9] which is much faster than the predicted rate coefficient as determined by the CAMD group (~10^{-2} s^{-1}), indicating that intermediate radicals fragments at a faster rate in this specific system. The same experimental system was carried out by Calitz (St polymerization mediated by polystyryl dithiobenzoate (PSt–SCSPh)) at 70 and 90 °C and also obtained a similar fragmentation rate coefficient to that determined by Kwak.[3] Monteiro group also reported k_f of 10^{5} s^{-1} of RAFT polymerization of St mediated by dithiobenzoate at 80 °C.[7]

The rate coefficient of fragmentation is very dependent on the Z and R groups of the RAFT agent as well as reaction conditions.[13-15] It is therefore well recognized that the rate coefficient of fragmentation can vary dramatically with the RAFT agent. However it is not feasible that the k_f can vary by six-order-of magnitude in a similar RAFT polymerization reaction systems (PSt–S–C$^{\bullet}$–Ph–S–PSt), as determined by CAMD[4], which contradict those determined by de Brouwer and Monterio[6,7], Kwak[9], and Calitz[3] groups. Thus there should be other mechanistic factors that need to be considered as well as lots of work to investigate all of the RAFT phenomenon.

There have been very good studies by Monteiro and Kwak providing 3-arm stars when a radical (propagating radical) reacts with the intermediate radical formed in RAFT process. Monteiro's group shows the evidence of this when they create free radical polymer species by UV irradiation of the PSt–SCSPh system in the absence of monomer, in this case they observe a polymer of triple molecular weight (*M*) in Size Exclusion

Chromatography (SEC), which is a strong indication of the formation of 3-arm star polymers as they have assumed.[6] In the experiment repeated by the CAMD group however, they have claimed that such a 3-arm star polymer was not detected as a product.[16] The evidence of 3-arm star has also been shown by Kwak when he excluded monomer and created free radical polymer species by ATRP catalysts at 60 °C in the presence of short RAFT chains, when he used an equal RAFT chain length to the bromo-end group chain length, SEC shows two peaks (namely the peak for the single polymer chain and the peak with triple *M*, highly indicative of a 3-arm star).[9] Calitz also carried out St polymerization mediated by ^{13}C-labeled cumyl dithiobenzoate RAFT agent and using ^{13}C-NMR detected quaternary carbon at the branch point, which they assigned to 3- and 4-arm stars.[10]

In Kwak's second report, the reactions of polystyryl radical (PSt$^{\bullet}$) and (PSt–SCSPh) were modeled and studied by using shorter molecules (those of 1-phenylethyl (PE$^{\bullet}$) radical and 1-phenylethyl dithiobenzoate (PE–SCSPh)). He used these small molecules again in the absence of monomer to mimic the RAFT polymerization reaction. Because of the high concentration of the branch point of the small molecules, NMR spectroscopy was effective to prove the presence of quaternary carbons (the necessary prerequisite for 3-arm star species). Because this model reaction generates only PE$^{\bullet}$ free radicals, the Matrix Assisted Laser Desorption Ionization Time-of-Flight Mass Spectroscopy (MALDI-ToF-MS) and elemental analysis were also very useful in obtaining clear structural information on the 3-arm products. It should however kept in mind that the reaction model using small molecules might not necessarily present the actual RAFT polymerization reaction due to factors such as the higher propagation and termination rate of these small radicals compared to polymeric radicals, which might be expected to show major steric hindrance effects.

Kwak measured the (average) cross-termination rate coefficient (k_t') of the intermediate radical into 3-arm star formed during the heating of the mixture of PSt–SCSPSt [$\overline{M}_n$ =

2400, PDI = 1.07], PSt–Br [$\overline{M}_n$ = 2450, PDI = 1.09], CuBr, Cu(0), and tris[2-dimethylamino) ethyl]amine (ME_6TREN) at 60 °C in the absence of monomer.[17] This k_t' of intermediate radical was deduced from the relative amount of 3-arm star formed in the abovementioned model reaction. Kwak also measured the k_t' of the intermediate radical deduced from the polymerization rate (R_p) of St polymerization mediated by PSt–SCS–PSt [$\overline{M}_n$ = 1100, PDI = 1.08] using AIBN at 60 °C for comparison.[17] He found that the estimated cross-termination rate coefficient deduced from the relative amount of 3-arm star and that deduced from the actual polymerization rate, using the simple model for rate retardation as a result of this cross-termination reaction, were comparable. Thus, the estimated rate coefficient was in accord with the observed (experimental) product distribution, indicating internal consistency. More importantly, the value of k_t', which was obtained in these experiments was half of the self-termination rate coefficient (k_t) of PSt$^\bullet$ (under those reaction conditions). These results were highly indicative of firstly, that the model and actual polymerization reactions, as mentioned above are equivalent in terms of radical reactions, and secondly that the rate retardation in these reactions was quantitatively in accord with irreversible cross-termination. As in the case of the Kwak reaction model, we have used the situation when conversion is complete (no monomer) and radicals are then generated, and therefore we carry out reactions of the polystyryl benzyl-(4-carboxydithiobenzoate) (PSt-carboxylate) and polystyryl ethyl-2-bromoisobutyrate (PSt-Br) in toluene at 60 °C using copper catalyst in the absence of monomer to mimic the RAFT polymerization reaction. This makes it easier to monitor the relative amounts of cross-terminated products and improves analysis of products due to concentration enrichment.

Kwak has shown advances, as if this product were purer it would be much easier to analyze. Thus if we enhance concentrations, we should also can see species using advanced characterization techniques. From theses analysis, contributions from various processes can be identified.

We have been investigating advanced purification concentration technique in living polymerization (including RAFT and Nitroxide-Mediate polymerization (NMP)). We have been able to separate pure "living" polymer chains (i.e. dormant RAFT and dormant NMP chains) from dead chains (initiator derived species) formed in the RAFT-mediated polymerization and NMP reactions using superparamagnetic nanoparticles (MNPs). This was illustrated in Chapter 5 and 6, respectively.

Adding this purification technique using nanomagnets and tracking the carboxyl group as Z-functionality on the RAFT agent, we can improve analytical detection. Through this we can measure the relative amount of the cross-terminated polymer product more accurately, and thus it should be possible to deduce the cross-termination rate coefficient from the relative amount of these cross-terminated products more readily. Also we can look at the different products more easily as 3-arm stars contain one carboxylate group and 4-arm star contain two carboxylate groups (extractability can be thus explored).

This paper therefore discusses the experimental setup, isolation and concentration of products, as well as NMR, SEC and MALDI-ToF-MS of the products, and ends with discussion of these results showing firstly confirmation of 3 and 4-arm stars at higher molar masses (i.e. polymers) and secondary that of the use of nanomagnets as a product enrichment technique can be useful in mechanistic investigations of living polymerization (including RAFT).

7.2 Experimental

7.2.1 Materials

The following materials were used as received: hydrochloric acid (32 wt%; Merck), ferric chloride hexahydrate (98%; Fluka), ferrous sulfate heptahydrate (98%; Fluka), ammonia solution (25%; Merck), oleic acid (99%; Merck), pH 4 buffer solution (BDH), sodium metal (Merck), absolute ethanol (98.8%; Sigma Aldrich), sulfur powder (98%; Merck), benzyl bromide (98%; Fluka), anhydrous magnesium sulfate (Merck), ethyl-2-bromoisobutyrate (98%; Alfa Aesar), 2,2'-bipyridyl (99%; Sigma Aldrich), copper (I) bromide (99%; Sigma Aldrich), copper (II) bromide (99%; Sigma Aldrich), anisole

(99%; Acros Organics), dichloromethane (98%; Across Organics) and toluene (99.7%; Riedel-deHäen).

Styrene monomer (98%; Aldrich) was purified by washing with potassium hydroxide solution (KOH) (0.03M) and distilling under reduced pressure prior to use. 2,2'-Azobis(isobutyronitrile) (AIBN) (98%; Aldrich) was recrystallized twice from methanol and dried prior to use. Hexane (99.5%; Saarchem) was distilled prior to use.

7.2.2 Synthesis of benzyl-(4-carboxyldithiobenzoate) RAFT agent

The benzyl (4-carboxyldithiobenzoate) (Z-carboxylate) RAFT agent was synthesized using the procedure described in Section 3.4.2.

7.2.3 Synthesis of PSt-carboxylate

St (10 g; 96 mmol), Z-carboxylate RAFT agent (0.40 g; 1.3 mmol) and AIBN (0.028 g; 0.17 mmol) were added to a 150 mL 3-neck round-bottom flask. The oxygen was removed by purging the flask using N_2 for 15 min, and the flask was then placed into an oil bath preheated at 70 °C, and the mixture stirred for 6 h. The polymerization was then quenched by putting the flask into ice water, and the polymer solution was poured into 250 mL methanol. The precipitate was filtered off, dried in a vacuum oven to yield 0.5 g of PSt-carboxylate (5% yield). The *M* and molecular weight distributions (MWDs) were then determined using SEC.

7.2.4 Synthesis of PSt-Br

St monomer (20 g; 192 mmol), ethyl-2-bromoisobutyrate (EBiB) (0.30 g; 1.50 mmol), copper (I) bromide (0.22 g; 1.50 mmol), copper (II) bromide (0.03 g; 0.15 mmol) and 2,2'-bipyridyl (0.48 g; 3 mmol) were dissolved in anisole (10 g) and added to a sealed tube. The oxygen was then removed by four freeze-thaw cycles; the tube was placed into an oil bath at 70 °C and stirred for 8 h. The product was cooled by placing the tube into ice water, diluted with THF (10 mL), and the resulting solution passed through an aluminum oxide column to remove copper bromide. The solvent was allowed to evaporate slowly in a fume hood, dried in vacuum oven and was collected to yield the

polymer product (PSt-Br; 2.80 g, 14%). The polymer molar mass distribution was determined using size exclusion chromatography.

7.2.5 Model termination Reaction (PSt-Br and PSt-carboxylate)

PSt-Br [$\overline{M}_n$ = 2300 g/mol, PDI = 1.19], (1.0 g; 0.44 mmol), PSt-carboxylate [$\overline{M}_n$ = 1700 g/mol, PDI = 1.21], (0.37 g; 0.22 mmol), copper (I) bromide (0.12 g; 0.88 mmol) and copper (0) (used in the form of copper wire) were dissolved in toluene (3 g) and added to a sealed tube. The oxygen was removed by four freeze-thaw cycles, and the tube was placed into a preheated oil bath at 60 °C for 16 h. The reaction was stopped by placing the tube into ice water, and the product was diluted with THF (10 mL), and passed through aluminum oxide column to remove the copper bromide. The product was obtained after allowing the solvent to evaporate in a fume hood and drying under vacuum. The *M* and MWD of the polymer was determined using size exclusion chromatography.

7.2.6 Synthesis and stabilization of MNPs

MNPs were synthesized and stabilized using procedures described in Sections 4.3.2 and 4.3.3, respectively.

7.2.7 Extraction of 3-and 4-arm PSt star polymers using MNPs

The cross-terminated polymer containing the RAFT groups (3- and 4-arm stars) was separated from the remaining chains by thoroughly mixing and stirring (at ca. 300 – 400 rpm) a solution of the obtained polymer after the heat treatment of PSt-Br and PSt-carboxylate (Section 7.2.6) in dichloromethane (DCM). DCM is a good solvent for the polymer; typically 50 mL of DCM was used for 4.0 g of MNPs to extract 0.5 g of polymer. This was stirred for 24 h at room temperature. The Z groups of the 3- and 4-arm PSt and any unreacted RAFT agents attached to the MNP surface, concurrently displacing some fraction of the oleic acid stabilizer. A strong, external magnetic field (provided by an NdFeB magnet, with magnetic field intensity of 4.5×10^5 A/m) was applied to the MNP dispersion, which attracted the MNPs and any attached chains to the magnet, thus separating the MNPs from the remaining solution. The remaining solution

(the unextracted solution that contained the unextracted polymer) was decanted and collected. The MNP dispersion was then mixed with 32% HCl solution (typically 20 mL for 4.0 g of MNPs) at room temperature until the MNPs completely dissolved (which took less than 5 minutes), as indicated by the disappearance of the black color of the MNPs. The organic phase containing the oleic acid and the extracted polymer was separated from the aqueous phase. The aqueous phase was extracted with DCM. The solvent was evaporated from the combined organic phases to afford the extracted polymer. In the case of MNPs remaining in the unextracted solution, this solution was also washed and extracted as described above. The final extracted polymer (expected to be mainly a cross-terminated product) was characterized by ^{1}H and ^{13}C-NMR and MALDI-ToF-MS.

7.3 Characterization of PSt polymers

7.3.1 Determination of the molecular weight and molecular weight distribution of PSt polymers

Determination of the *M* and MWDs of the polymers prepared in this study was carried out by SEC. Samples were dissolved in stabilized THF (HPLC-grade) at a concentration of 5 mg/mL and filtered through a 0.45 μm nylon filter prior to injection into the apparatus. The SEC apparatus comprised a Waters 1515 isocratic HPLC pump, Waters 717 plus autosampler, Waters 24141 refractive index detector, Waters 2487 dual wavelength absorbance detector, two pLgel 5 μm Mixed-C (300 × 7.5 mm) columns, and one pLgel 5 μm guard column (50 × 7.5 mm). The samples were eluted using THF (HPLC-grade) at 30 °C and a flow rate of 1 mL/min. The instrument was calibrated using nine Polymer Laboratories Easyvial polystyrene standards with narrow molar mass distributions in the range 580 – 9 × 10^{5}g mol^{-1}, supplied by Polymer Laboratories.

The comparison of the DRI signal and UV absorbance at 320 nm was used in this study to determine the distribution of RAFT groups of each polymer product. The UV absorbance data were modified to match the DRI data using the molecular weight correction described in Section 5.6.1. This was used for all UV comparison in this study.

7.3.2 Nuclear Magnetic Resonance Spectroscopy

The Nuclear Magnetic Resonance (NMR) spectra were measured in benzene-d_6 (Aldrich; 99.90%) as solvent using a Varian Unity Inova spectrometer operating at 600 MHz. A 5 mm inverse detection PFG probe was used for the experiments, and the probe temperature was calibrated using an ethylene glycol sample in the manner suggested by the manufacturer using the method of Van Geet.[18] Conditions: ^{1}H: spectral acquisition time 4 s, number of transits 128, and pulse delay 1 s. ^{13}C: spectral acquisition time 1.3s, number of transits 11000, and pulse delay 1 s. DEPT (Distortionless Enhancement by Polarization Transfer): spectral acquisition time 1 s, number of transits 16576, and pulse delay 1 s. ^{1}H-H COSY: 0.19 s, 8, and 1.30 s. pulse delay. gHSQC (Heteronuclear Single Quantum Coherance): spectral acquisition time 0.19 s, number of transits 64, and pulse delay 1 s.

7.3.3 Matrix Assisted Laser Desorption Ionization-Time of Flight Mass Spectroscopy

All mass spectra were recorded with a Voyager-DE STR (Applied Biosystems, Framingham, MA) instrument equipped with a 337 nm nitrogen laser. The instrument was operated in reflectron and linear modes. The ions were accelerated at a potential of 20 kV and the positive ions were detected in all cases. *Trans*-2-[3-(4-*tert*-butylphenyl)-2-methyl-2-propenylidene] malononitrile (MM) was chosen as the matrix for the reflectron mode while 1,8,9-anthracenetriol (dithranol) was used for the linear mode (both matrixes were purchased from Aldrich). Silver trifluoroacetate (AgTFA; Aldrich, 98%) was added as the cationic ionization agent. Matrixes, polymer samples and AgTFA were pre-dissolved in THF at concentrations 40 mg/mL, 1 mg/mL, and 1 mg/mL respectively. Samples were prepared by mixing 5 μL of the matrixes with 5 μL of the polymer and 0.5 μL of the salt (AgTFA). The obtained mixture was hand-spotted on the target plate. For each spectrum 1000 laser shots were accumulated for the reflectron mode and 300 for the linear mode.

7.4 Results and discussion

The termination model reaction of PSt-Br and PSt-carboxylate using copper complex was performed in the absence of monomer at 60 °C for 16 h. As Kwak explains,[9] in this reaction PSt-Br is activated by the Cu(I) complex to yield a polymeric radical (P•). The polymeric radical (P•) reacts with the dormant chain (P'-X) to afford an intermediate radical adduct (P′-X•-P), or reacts with another radical (either P• (to give a conventional 2-arm linear termination product) or an intermediate radical Y•). The formed intermediate radical (Y•) can fragment, or react with another propagating (P•) or intermediate radical (P′-X•-P) via a cross-termination reaction to yield a 3-arm or 4-arm product, respectively. The intermediate radical could also undergo a disproportionation reaction with (P•) to yield two linear chains (P'-YH-P, and P= (which contains a terminal double bond)). The obtained polymer after the heat treatment of PSt-Br and PSt-carboxylate was then primarily characterized using SEC.

Figure 7.1 shows the DRI signal and UV data SEC traces of the PSt-Br and PSt-carboxylate polymers before the heat treatment, and the polymer obtained after the heat treatment. The comparison Figure (7.1a) shows distinct differences between these polymers with respect to the *M*, MWDs, and UV absorbance. The UV absorbance at 320 nm is dominated by the absorption by the RAFT group, but a very weak contribution from the aromatic rings of the St repeating units is also expected. The PSt polymer obtained after the heat treatment has a different MWD ($\overline{M}_n$ = 2000, PDI = 1.44) compared to the PSt-Br ($\overline{M}_n$ = 2100, PDI = 1.22) and PSt-carboxylate ($\overline{M}_n$ = 1700, PDI = 1.21) polymers. The obtained polymer after the heat treatment contains a large fraction of high *M* polymer chains, with a significant amount of higher than would be formed by combination reactions, and that these are extractable and contain RAFT groups (see Figure 7.2c). This strongly suggests that the obtained polymer after the heat treatment contained a large fraction of cross-terminated product with a small UV absorbance, as observed in Figure 7.1c. This is because cross-terminated polymer chains are expected to

show significantly less UV absorbance at 320 nm (due to loss of the conjugation of the C=S bond with the aromatic ring when in the intermediate radical/cross-terminated forms) than the DRI signal.

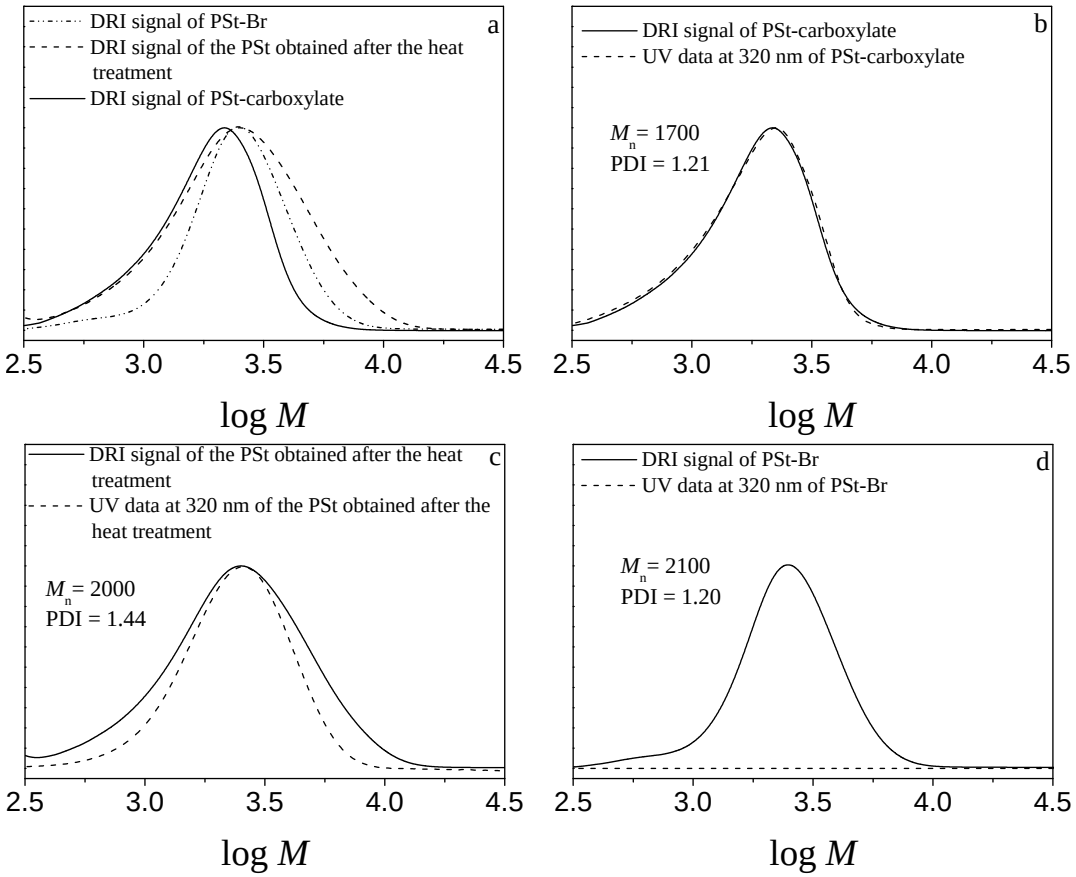

Figure 7.1: SEC results showing the DRI signal and UV data at 320 nm of PSt polymers: (a) comparison of PSt-Br, PSt-carboxylate and PSt obtained after the heat treatment, (b) PSt-carboxylate, (c) the PSt obtained after the heat treatment, and (d) PSt-Br.

The PSt-Br contains polymer with no UV absorbance, as observed in Figure 7.1d. This indicates that this polymer contains no RAFT functionality. It also shows that there was no significant UV absorbance due to the contribution of the aromatic ring here, which is probably because of the low *M* of this polymer (i.e small number of repeating units). PSt-carboxylate contains living chains with UV absorbance and RAFT functionality, and maybe a small fraction of dead chains with minimal UV absorbance, as observed in Figure 7.1b.

The polymer obtained after the heat treatment was used in the extraction process using MNPs (Scheme 7.2).

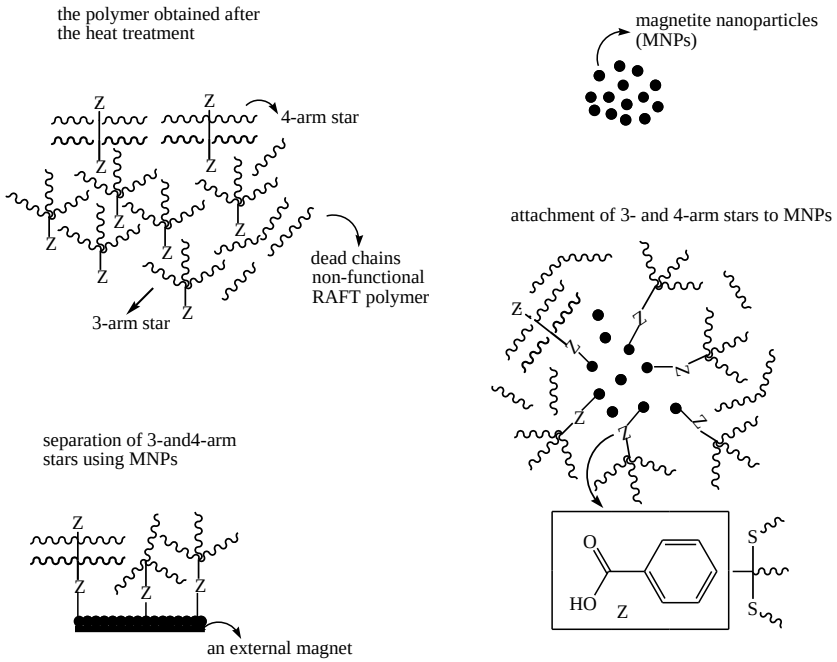

Scheme 7.2: Separation of 3-and 4-arm star polymers by attachment to the surface of MNPs in the presence of an external magnetic field.

The extraction process using MNPs is expected to separate all cross-terminated chains and any unreacted RAFT agents from other terminated polymers (those obtained by termination reactions other than the cross-termination). This is because all cross-terminated polymer chains contain carboxylate groups with a strong affinity to MNP surfaces, while other terminated chains lack such functional groups.

Figure 7.2 shows the DRI signal and UV absorbance SEC traces of the various polymer species: the polymer obtained after the heat treatment (Figure 7.2b), the unextracted polymer (the polymer that remains in solution after the extraction process; Figure 7.2d) and the extracted polymer (the polymer attached to the surface of MNPs and separated by the extraction process; Figure 7.2c).

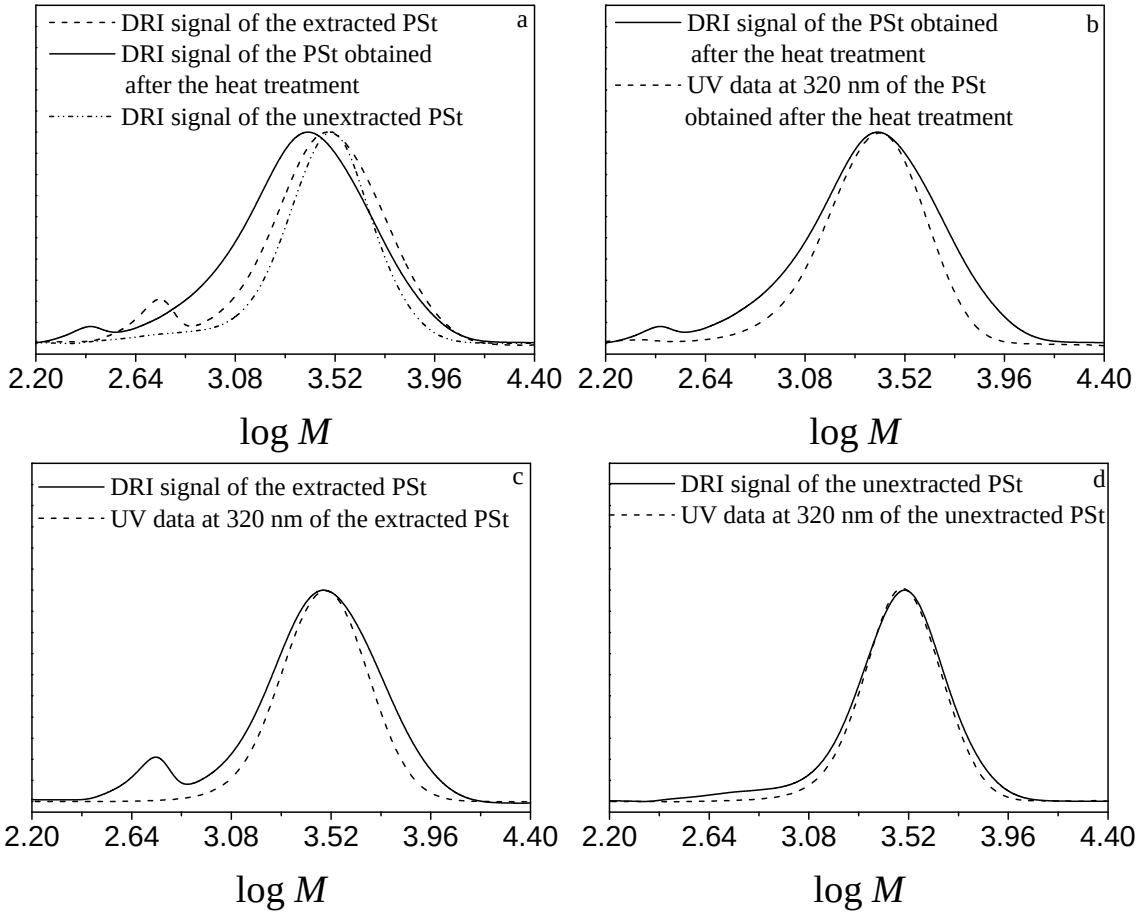

Figure 7.2: SEC results showing DRI signal and UV data at 320 nm of PSt polymers: (a) comparison of the PSt obtained after the heat treatment, extracted and unextracted PSt polymers, (b) the PSt obtained after the heat treatment, (c) the unextracted PSt, and (d) the extracted PSt.

The DRI signal and UV absorbance comparison Figures 7.2 a – d show that there are large differences between these polymers with respect to the *M*, MWDs, and UV absorbance. The extracted polymer ($\overline{M}_n$ = 2600, PDI = 1.33) contains a fraction of polymer chains with small UV absorbance, and another fraction of living chains with UV absorbance, as observed in Figure 7.2c. This indicates that the extracted polymer contains by-products with small UV absorbance, yet this product can be extracted using MNPs. It strongly suggests that this polymer contains a large fraction of cross-terminated polymer by-product.

The *M* of the extracted polymer clearly shifts from the original PSt-carboxylate (RAFT chains) before the heat treatment, as observed in Figure 7.3a (which shows the DRI signal comparison of the extracted and original PSt-carboxylate polymers). This is possibly because of ATRP-derived (EBiB end groups) being exchanged with original RAFT chains during the heat treatment reaction. This can happen when ATRP-derived EBiB end-groups react with the RAFT chains to produce intermediate radicals with fragmentation probabilities are expected to be the same here. Thus, an intermediate radical with at least one EBiB end-groups will then fragment to give an ATRP-derived (EBiB-end groups) RAFT chain. This exchange reaction seems to be common during the heat treatment reaction, and, since the extraction group is incorporated into the Z group of the RAFT agent, means that these ATRP based RAFT chains are also extractable and contain EBiB end-groups, which were observed in this study.

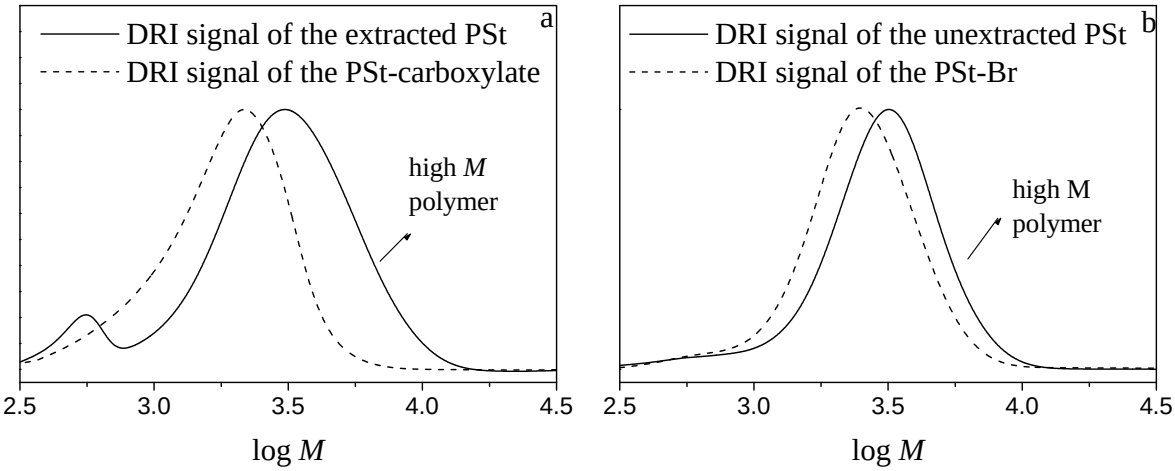

Figure 7.3: DRI signal comparison SEC traces of the PSt-carboxylate and PSt-Br (original polymers) and extracted and unextracted polymers obtained after the heat treatment of the original polymers: (a) the PSt-carboxylate and extracted polymers, and (b) the PSt-Br and unextracted polymers.

The unextracted polymer ($\overline{M}_n$ = 3200, PDI = 1.38) contains a large fraction of living chains with minimal UV radiation and RAFT functionality, as observed in Figure 7.2d. This polymer also contains a small fraction of terminated chains by combination and maybe fractions of 3- and 4-arm stars with small UV radiation. The fraction of living chains and cross-terminated polymer product in the unextracted polymer, which appear to remain in solution after the extraction process, are probably due to the ligand exchange

process. The extraction process (Scheme 7.2) is based on ligand exchange, which is likely to have less than 100% efficiency. Thus some of the living chains and cross-terminated polymer chains (3-and 4-arm stars) might not attach to MNPs, resulting in these unattached polymer chains being decanted with the unextracted solution.

The *M* of the unextracted polymer also shifts from the original PSt-Br (see DRI signal comparison Figure 7.3b). This indicates that this polymer should contain new polymer species formed during the heat treatment reaction. This molecular weight polymer shift of the unextracted polymer can be due to the following reasons: (i) it can be due to unextracted ATRP-derived EBiB end groups becoming capped RAFT chains. This is also consistent with SEC trace of the unextracted polymer (Figure 7.2d), which shows that this polymer contains RAFT functionality with UV absorbance. (ii) It can also be due dead chains formed by combination reactions with *M* being higher than normal PSt-Br chains, as these chains expected to remain in the unextracted solution after the separation process using MNPs. (iii) It can be due to unextracted cross-terminated polymer product, with *M* being higher than normal formed chains by combination and other termination reactions. This is also consistent with SEC trace of the unextracted polymer (see Figure 7.3b), which shows that this polymer contains high *M* polymer with *M* being higher than that of dead chains formed by combination. Unextracted cross-terminated polymer products such as those might be formed by disproportionation with a small UV absorbance and *M* being similar to terminated chains formed by combination, would also be in the unextracted polymer.

In conclusion the extracted and unextracted polymers and the polymer obtained after the heat treatment contain a significant fraction of high *M* polymer with small UV absorbance. This polymer does not correspond to dead chains formed by combination, and it can be extracted using MNPs, indicating that this polymer contains an extractable group that is incorporated into the Z group of the RAFT agent. This again suggests that these polymers contain cross-terminated products.

7.4.1 NMR analysis of the extracted PSt polymer that was obtained after the heat treatment of the PSt-carboxylate and PSt-Br in the absence of monomer

A typical ^{1}H-NMR spectrum of the extracted polymer (the polymer obtained after the heat treatment and extracted using the extraction process) is shown in Figure 7.4. It shows that this polymer contains a significant signal at δ = 3.88 assigned to the methylene protons of the EBiB end-group. This indicates that the extracted polymer contains a large fraction of polymer with EBiB end-groups. This polymer also contains significant signals at δ = 7.40 and 7.70 (Figure 7.4) (due to the protons of the aromatic ring of the RAFT agent) and signal at δ = 177.50 in the ^{13}C-NMR spectrum (Figure 7.5; due to the carbonyl group of the RAFT agent). This indicates that the extracted polymer contains the carboxylate group (extractable group).

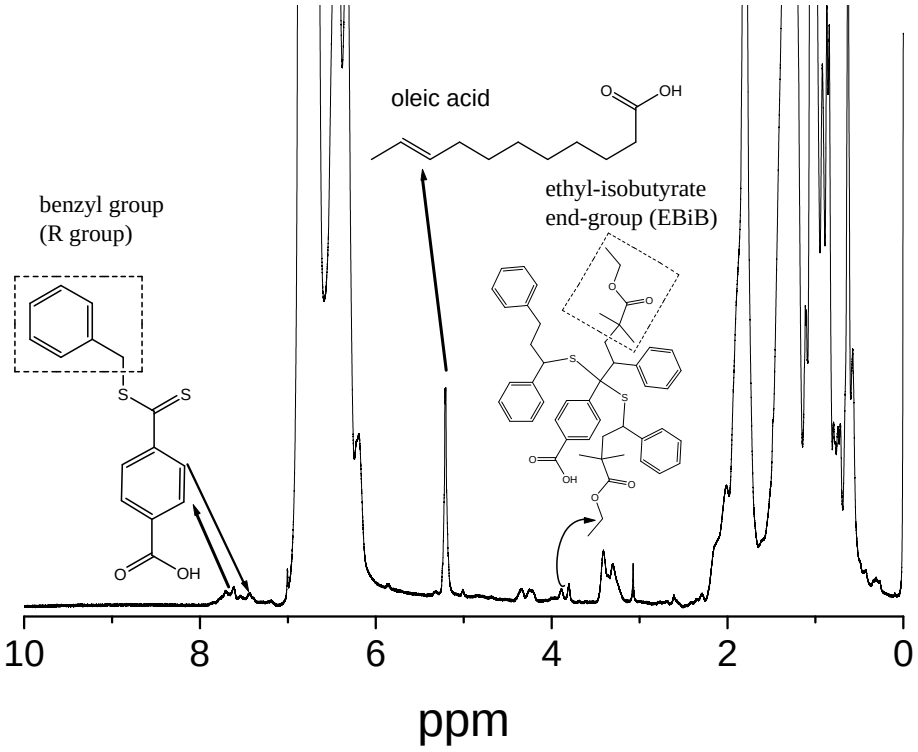

Figure 7.4: A typical ^{1}H-NMR spectrum of the extracted PSt polymer (obtained after the heat treatment and extraction) showing the peaks corresponding to several important groups: methylene protons of EBiB, indicating the presence of EBiB in the extracted polymer, aromatic protons of the RAFT agent, and protons of the double bond of the oleic acid.

This NMR spectrum of the extracted polymer shows that the EBiB end-groups that originate from ATRP-derived chains are present in the extracted polymer. The presence of EBiB end-groups in the extracted polymer can be either due to above mentioned exchange reaction (an ATRP-derived chains with original RAFT chains), and/or due to 3- and 4-arm star polymers formed during the heat treatment reaction with EBiB end-groups (see e.g. 3-arm star polymer in Figure 7.4). This is consistent with SEC trace of the extracted polymer (Figure 7.2d), which shows that the extracted polymer *M* shifts from the original PSt-carboxylate (see Figure 7.3a) due to ATRP-derived EBiB end-groups being exchanged with RAFT chains forming polymer chains with UV absorbance, as observed in this experiment. It also shows that this polymer contains a large fraction of high *M* polymer with a small UV absorbance, which corresponds to cross-terminated polymer products.

The extracted polymer also contains a significant signal at $\delta = 5.15$, as observed in Figure 7.4. This signal was assigned to the double bond of the oleic acid used to stabilize MNPs. The fraction of the oleic acid in the extracted polymer results from the exchange process, which does not replace all oleic acid with RAFT chains during the extraction process.

The ^{13}C-NMR spectrum of the extracted polymer is shown in Figure 7.5. It shows that the extracted polymer contains a large fraction of polymer chains with EBiB end-groups, as indicates by the strong carbon signal that appears at $\delta = 60.30$ assigned to the methylene carbon of the EBiB groups. This is also consistent with Heteronuclear Multiple-Bond Correlation (HMBC) spectrum of the extracted polymer (see Appendix A Figure A.25), which shows that the signal at $\delta = 3.88$ ppm (which was assigned to the methylene protons) corresponds to the significant carbon signal at $\delta = 60.30$ ppm. This indicates that the ^{13}C-NMR signal at $\delta = 60.30$ ppm is due to the methylene carbon of the EBiB end group. HSQC NMR measurement detects every chemical shift of the protons (plotted on one axis) and their bonded carbon (plotted on another axis).

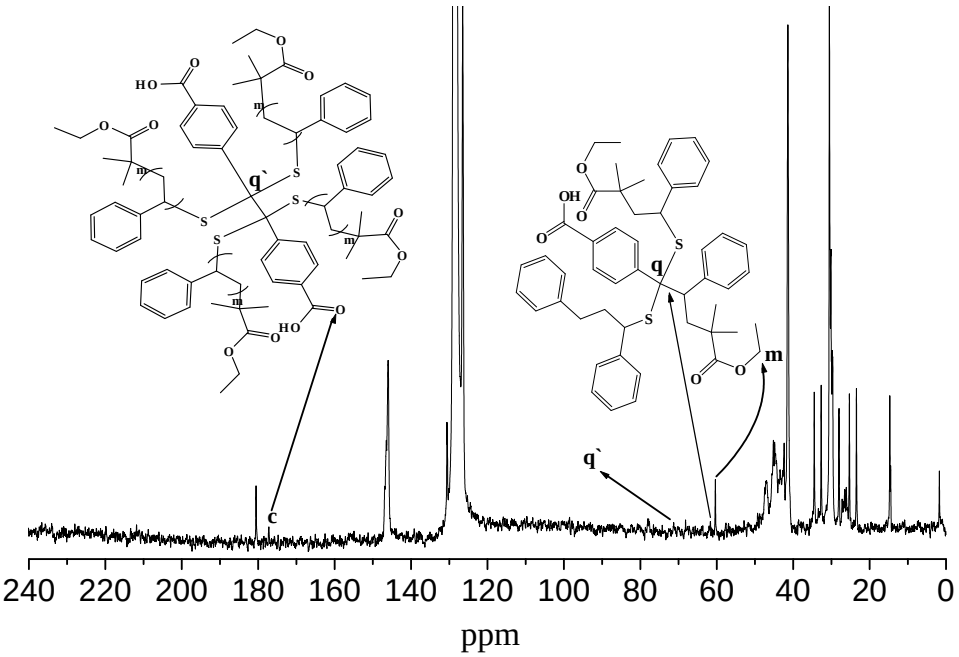

Figure 7.5: ^{13}C-NMR spectrum of the extracted PSt polymer (obtained after the heat treatment and extraction) showing the important carbon atoms: methylene carbon of the EBiB end-group (m signal), quaternary carbon of 3-arm star polymer (q signal), quaternary carbon of the 4-arm star (q` signal) and carbonyl group of the RAFT agent (c signal).

A very weak signal appears at δ = 61.6 ppm, which crossponds to the characteristic carbon (q) of the 3-arm stars formed by cross-termination reaction (e.g., right handside structures, Figure 7.5). The quaternary carbon is expected to have a weak signal for the following reasons: (i) since no hydrogen is attached to this carbon, there is very little Nuclear Overhauser Effect (NOE) enhancement; (ii) The concentration of the quaternary carbon at the branch point of 3-arm star polymer chains is very low, which makes the ^{13}C-NMR signal weak. The quaternary nature of the carbon at δ = 61.60 was further confirmed by Distortionless Enhancement by Polarization Transfer (DEPT (45°)) NMR measurements. DEPT NMR only detects carbons that are bonded to protons. The signal appearing at δ = 61.60 ppm was only detected by ^{13}C-NMR, not with DEPT-NMR (see Appendix A, Figure A.26).

The other weak signal at δ = 70.5 ppm (Figure 7.5) appears to be in the expected region of the characteristic quaternary carbon (q`) of the 4-arm star polymer (e.g., left handside structures, Figure 7.5). This signal shifts from the quaternary carbon of 3-arm polymer, possibly due to this quaternary carbon being attached to four sulphur species and two carbonyl groups in contrast to the 3-arm star polymer. This quaternary carbon was formed after the cross- termination reaction between two intermediate radicals. DEPT (45°) NMR measurements (Figure A.25) detects no signal at 70.5 ppm, thus confirming the quaternary nature of this carbon signal.

The ^{13}C-NMR spectrum of the extracted polymer shows that there are quaternary signals in the expected regions of 3 and 4-arm polymer chains. This supports the idea proposed in the SEC analysis of the extracted polymer, which suggests that the extracted polymer contains a large fraction of cross-terminated polymer product with high *M* and small UV absorbance.

The ^{1}H-NMR and ^{13}C-NMR and SEC data suggest the formation of cross-terminated polymer products. The identity of end-groups of these products was further investigated using MALDI-ToF-MS.

7.4.2 MALDI-ToF-MS analysis of the extracted PSt polymer that was obtained after the heat treatment of the PSt-carboxylate and PSt-Br in the absence of monomer

All of the MALDI-ToF mass spectra of the extracted polymer that was obtained from the extraction process were recorded using linear and reflectron modes. The linear mode (has larger sensitivity for larger polymer molecules) allows us to determine the *M* and MWDs of all of the different polymer species, while information on chemical structure and end groups of each polymer species can be achieved using the reflectron mode, which has a higher resolution than the linear mode.[19,20] The higher resolution in the reflectron mode could be achieved by a reflecting field located at the end of the flight tube of the instrument. Thus ions with same mass to charge ratios, but different velocities cause peak broadening with small resolution in the linear mode, while these ions can be time focused and resolved more clearly using the reflectron mode.[20] This possibly because ions with

different velocities reflect and travel along the tube according to their velocities in the reflectron mode (ions that have faster velocities travel a longer time path than ions with lower velocities).

7.4.2.1 MALDI-ToF-MS analysis of the extracted PSt polymer using the linear mode

Figure 7.6 shows an expanded section of the mass spectrum of the extracted PSt polymer as detected by MALDI-ToF-MS using the linear mode.

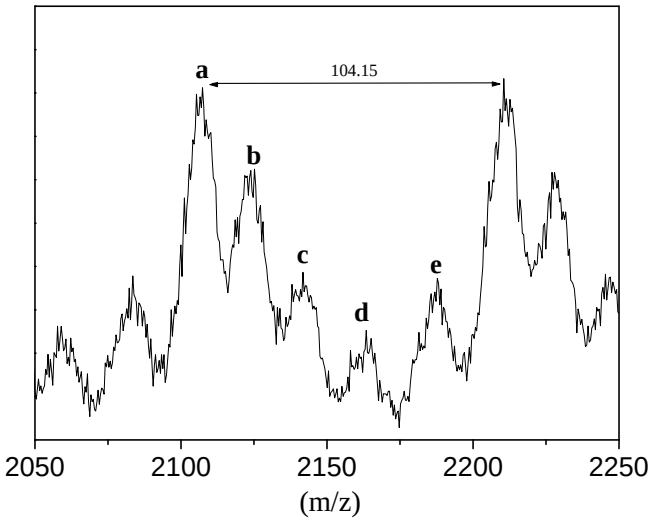

Figure 7.6: Enlarged section of the mass spectrum of the extracted PSt polymer acquired by MALDI-ToF-MS using the linear mode with AgTFA salt/dithranol matrix showing the different repeating PSt chain populations (a – e).

There are at least five distinguishable chain populations (distributions) (a – e, Figure 7.6), with (a) having the highest peak intensity. All of the various chain populations are equivalent to PSt chain populations with Δm =104.15 Da, which is equivalent to a St monomer unit.

Figure 7.7 shows enlarged sections of the mass spectra that correspond to the different chain populations, as detected by MALDI-ToF-MS using the linear mode (observed (above) and calculated (below)). The mass structures, which were assigned for the different chain populations, are also given in Figure 7.7 (right-hand column). A large fraction of the mass structure (a) (top spectrum in Figure 7.7) was assigned to 3-arm PSt star polymer produced by the cross-termination reaction between a propagating radical

with an EBiB end-group and intermediate radical with two PSt arms bearing an EBiB end-group each. A small fraction of the mass structure (b) (Figure 7.7), was assigned to a 3-arm PSt star polymer also produced by the cross-termination between a propagating radical with a benzyl group (benzyl group = R group of the RAFT agent) and an intermediate radical with two PSt arms, each of which has an EBiB end-group.

The mass corresponding to the mass structure (c) was assigned to a 3-arm PSt star polymer. This polymer formed by the cross-termination reaction between an intermediate radical that has two PSt arms bearing R and EBiB end-groups, and a PSt propagating radical terminated by an R end-group. A significant fraction of the mass structure (d) (Figure 7.7) corresponds to a 3-arm PSt star polymer each arm of which has an R end-group.

PSt mass structures derived from MALDI-ToF-MS distributions	Extracted PSt mass spectra detected by MALDI-ToF-MS: observed (above) and calculated (below)
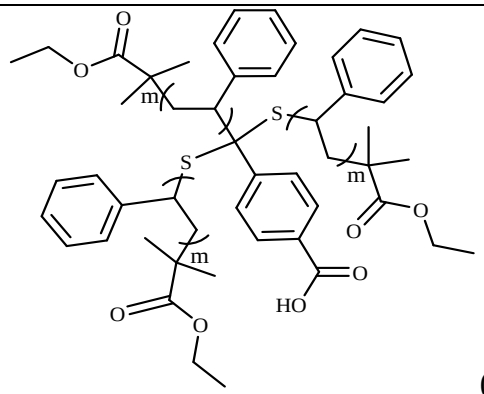 (**a**)	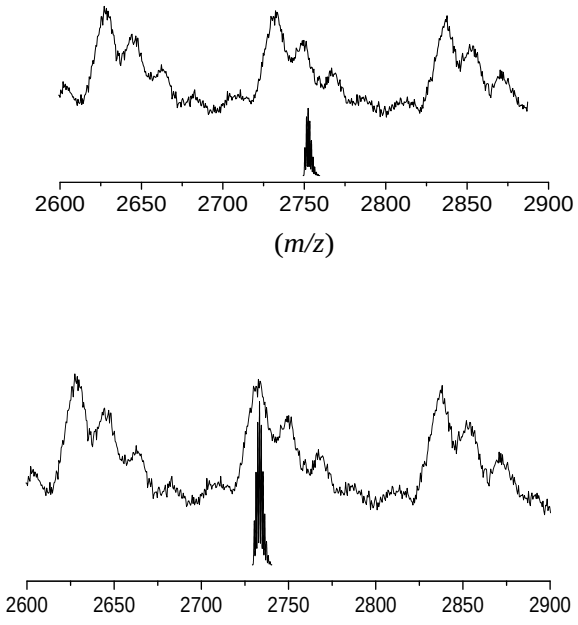

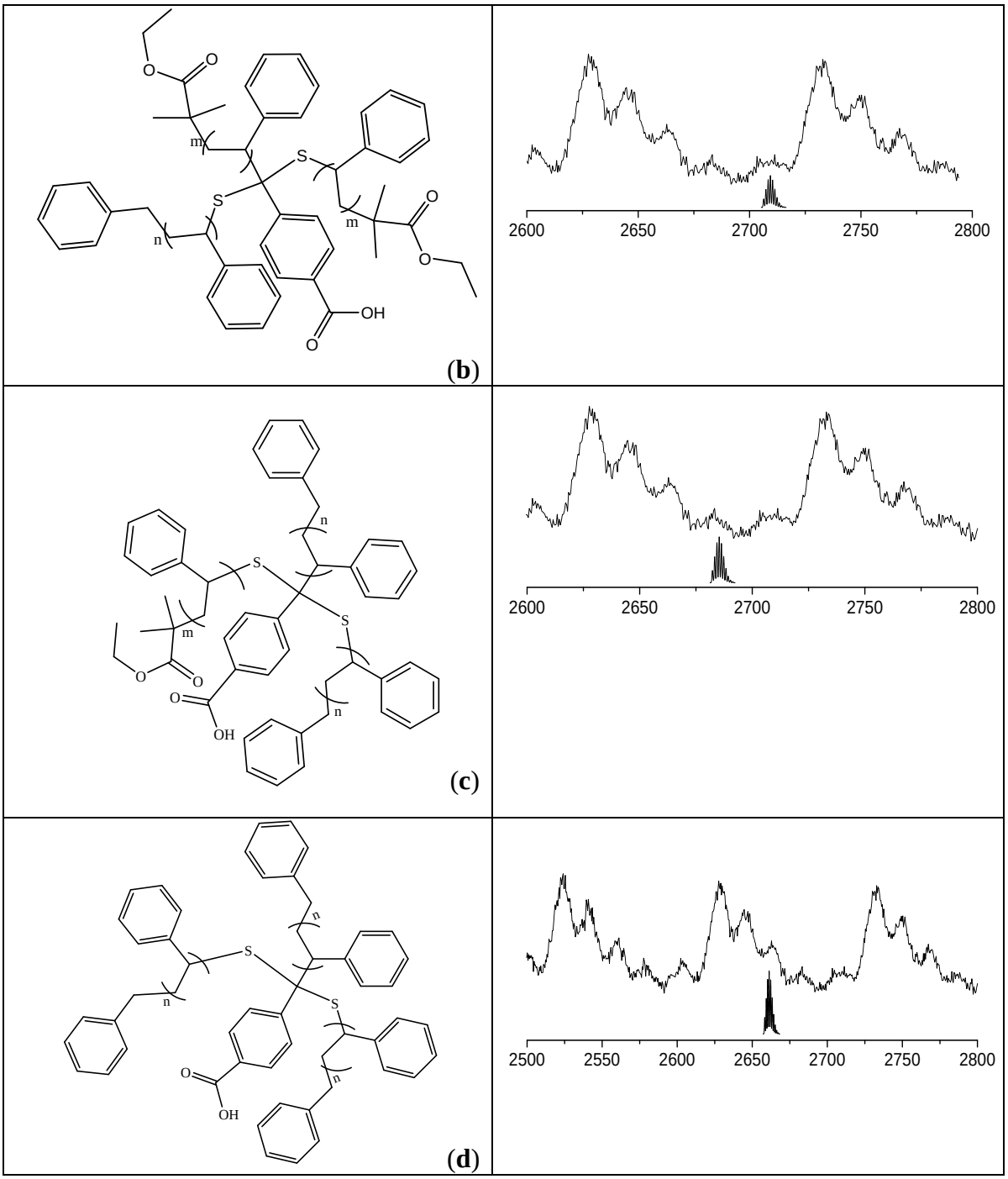
O
O
m
S
S
n
m
O
O
OH
O
(b)
2600
2650
2700
2750
2800
n
S
m
S
O
O
O
OH
n
(c)
2600
2650
2700
2750
2800
n
S
n
S
O
OH
n
(d)
2500
2550
2600
2650
2700
2750
2800

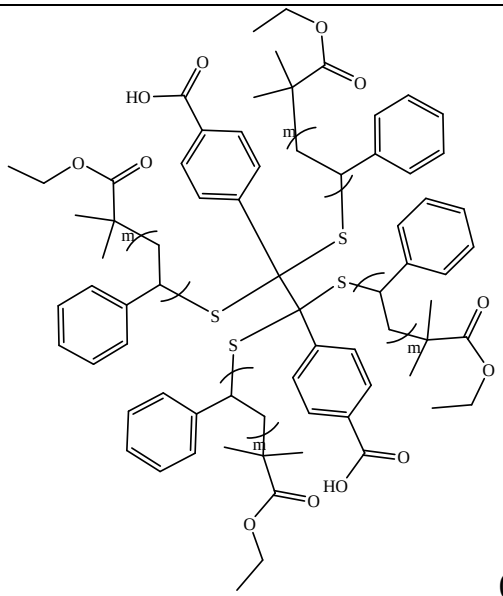

(**e**)

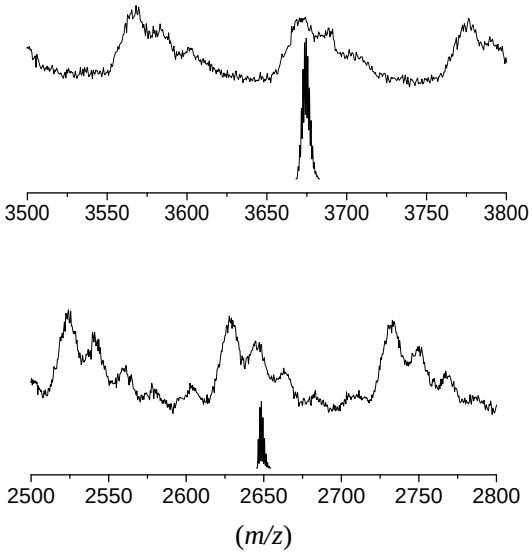
3500
3550
3600
3650
3700
3750
3800
2500
2550
2600
2650
2700
2750
2800
(*m/z*)

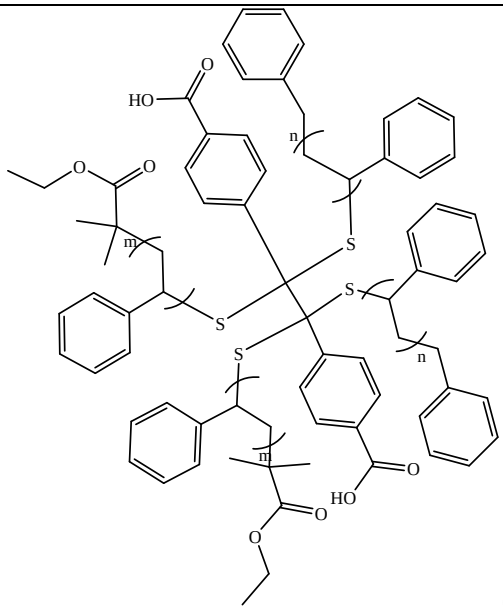

(**f**)

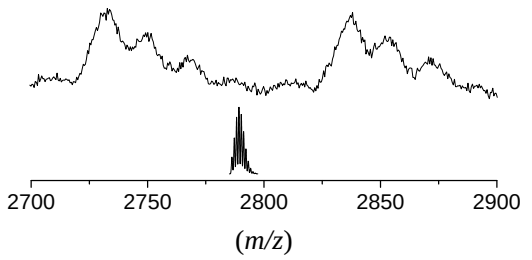
2700
2750
2800
2850
2900
(*m/z*)

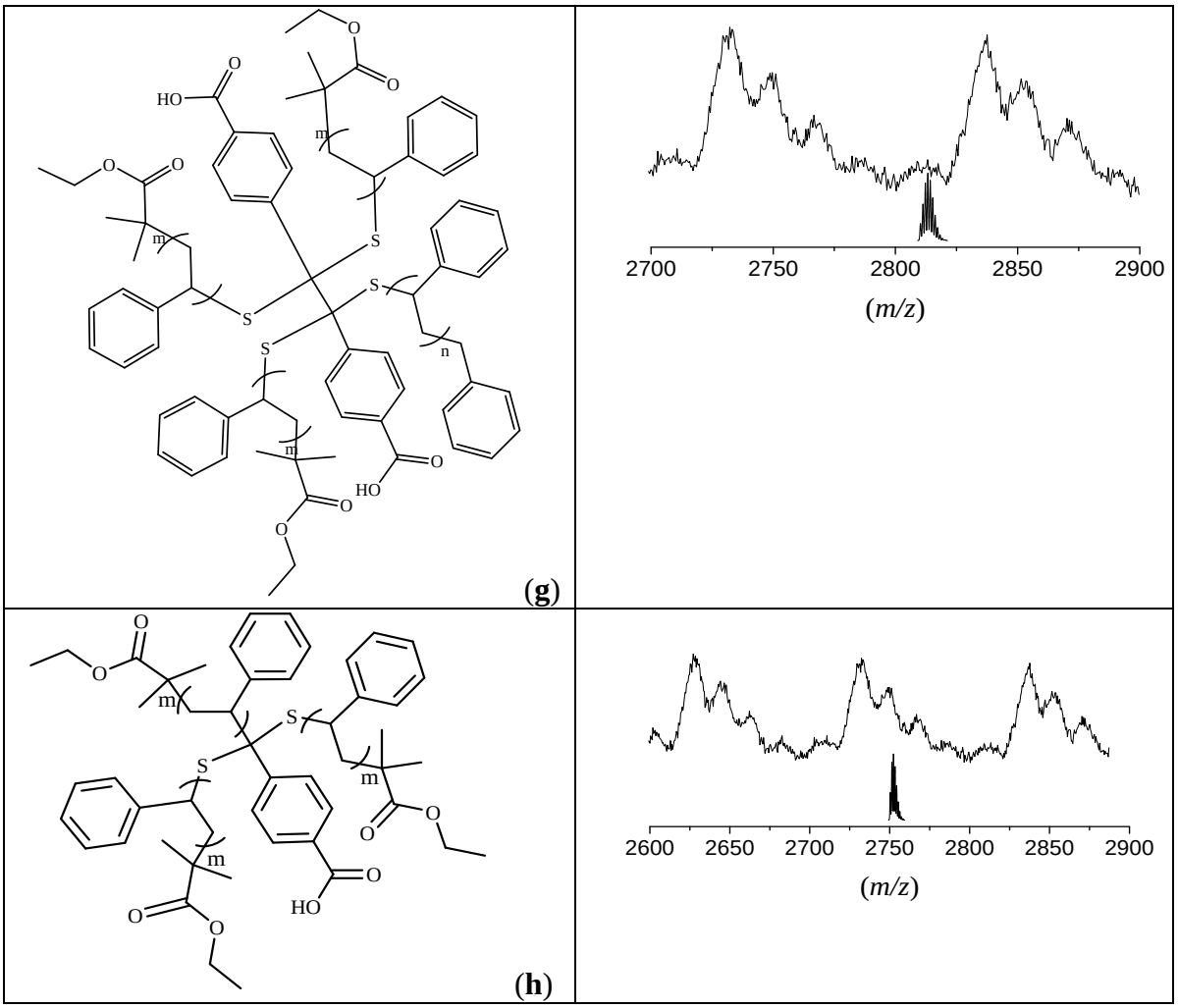

Figure 7.7: Enlarged sections of the mass spectra that correspond to the extracted PSt chain populations detected by MALDI-ToF-MS using the linear mode observed (above) and calculated (below) with AgTFA salt/dithranol matrix, and the corresponding PSt mass structures of the different chain populations (left-hand column).

The mass structure (e) (Figure 7.7) (which overlapped with the mass structure (a)), was assigned to a 4-arm PSt star polymer formed by cross-termination between two intermediate radicals containing EBiB end-groups. The mass structure (f) in Figure 7.7 corresponds to a 4-arm star PSt polymer with two R end-groups and two EBiB end-groups. There is also a small fraction of 4-arm PSt star polymer formed by cross-termination reaction between an intermediate radical with R and EBiB end-groups and that with EBiB end-groups, as observed in Figure 7.7, mass structure (g).

A fraction of PSt chain population (b in Figure 7.6) being cationized by sodium (Na) was assigned to 3-arm star PSt polymer with the mass structure (a) (lower spectrum in Figure 7.7) and 4-arm PSt star polymer with the mass structure (e) (lower spectrum in Figure 7.7).

Although the linear mode mass spectra of the extracted PSt polymer analysis allowed us to determine the different distributions of each chain population, the exact chemical structure (end-group) of each chain population requires optimal resolution. This can not be achieved using the linear mode, but is possible using the reflectron mode. Therefore the extracted PSt polymer was further characterized using the reflectron mode.

7.4.2.2 MALDI-ToF-MS analysis of the extracted PSt polymer using the reflectron mode

Figure 7.8 shows an enlarged section of the mass spectrum of the extracted PSt polymer as detected by the MALDI-ToF-MS using the reflectron mode.

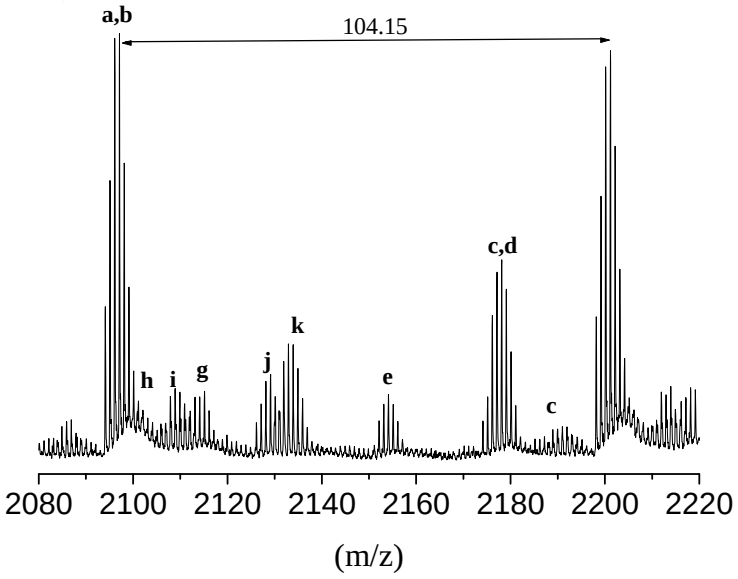

Figure 7.8: Expanded section of the mass spectrum that corresponds to the extracted PSt polymer acquired by MALD-ToF-MS using the reflectron mode with AgTFA salt/MM matrix showing the different PSt chain populations (a – k).

This mass spectrum displays a larger number of chain populations (a – k) than those observed in the mass spectrum (Figure 7.6) obtained by linear mode. The large number of chain populations detected by the reflectron mode are probably due to chain cleavage (fragmentation) reactions, which normally occur during MALDI-ToF-MS analysis of RAFT polymers.[21,22] The fragmentation reaction occurring during sample analysis by MALD-ToF-MS is due to the weakness of the C-S bond of the RAFT polymer.[23] MALDI-ToF-MS analysis uses a high laser intensity, with a wavelength about 337 nm, which is very close to the absorption wavelength of the C=S bond of the RAFT agent. Thus there is a large chance for chain cleavage to occur upon the sample ionization.

The literature describes a number of attempts to prevent the chain cleavage during the MALDI-ToF-MS analysis of RAFT polymers, by changing the laser intensity, matrix and cationization salt.[22] Although it was successful to detect the dormant chain population (initiated by the R and terminated by the SCS-Z groups of that RAFT agent), a number of fragmentation species were observed.[22]

The mass spectra of all different PSt chain populations of the extracted polymer, as detected by MALDI-ToF-MS using the reflectron mode (observed (above) and calculated (below)) are given in Figure (9). The mass structures, which correspond to each PSt chain population, as detected by MALDI-ToF-MS, are also presented (left-hand column).

It has to be noted that Figure 7.9 shows that all the mass structures of possible PSt RAFT polymer chains formed by fragmentation reactions with chain scission which being occurred at the C=S bond. The results in this study will be discussed on the basis of the chain scission of at the C=S bond. This does not however mean that other scission of C–S bonds are excluded and does not occur (these produce PSt arms with radicals being on the S). Thus all the mass structures in Figure 7.9 could also be linked in different ways.

PSt mass structures derived from MALDI-ToF-MS distributions	Extracted PSt mass spectra detected by MALDI-ToF-MS using the reflectron mode: observed (above) and calculated (below)
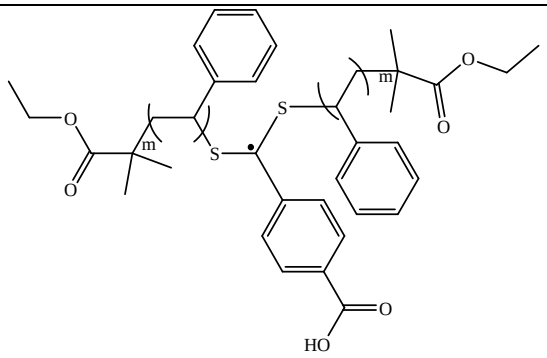 (**a**)	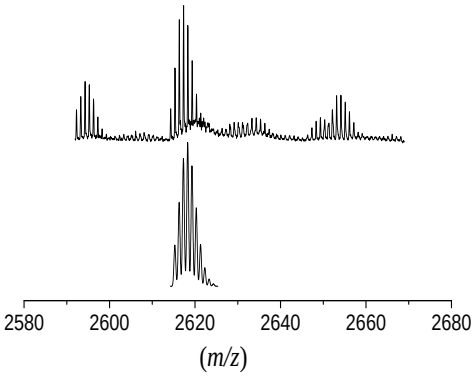
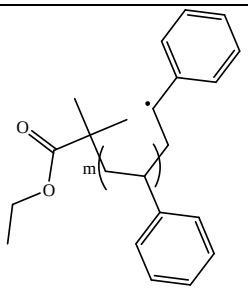 (**b**)	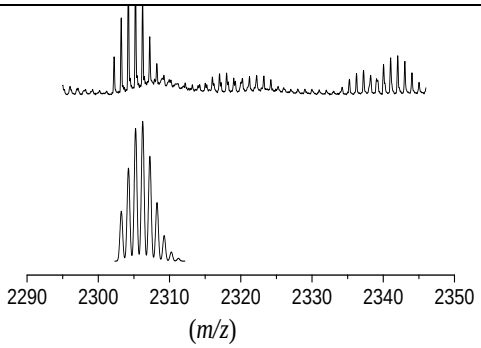
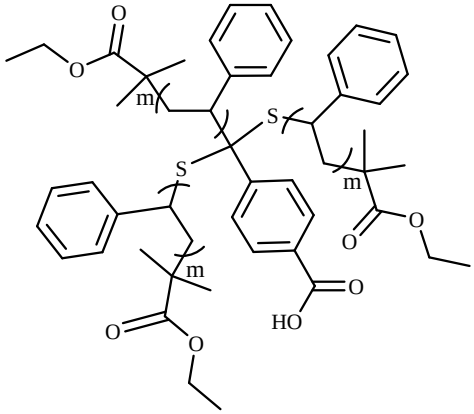 (**c**)	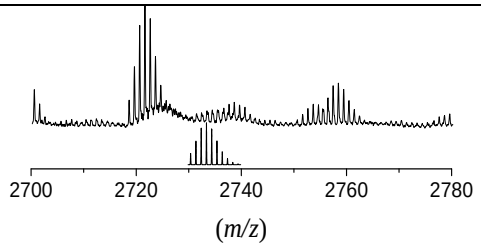

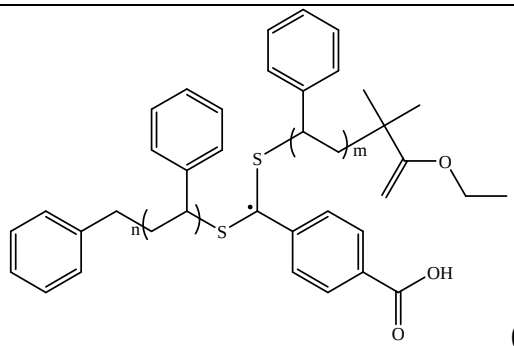
S
m
O
n
S
OH
O

(**d**)

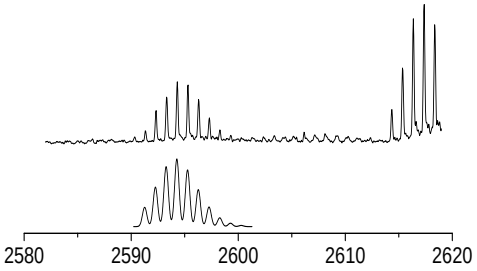
2580
2590
2600
2610
2620
(m/z)

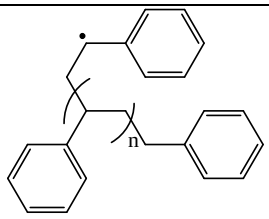
n

(**e**)

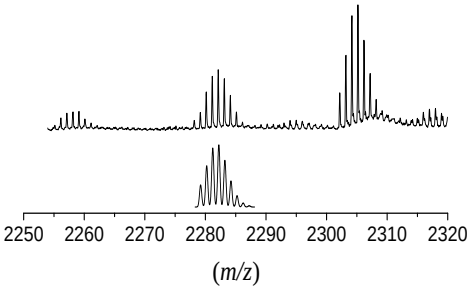
2250
2260
2270
2280
2290
2300
2310
2320
(m/z)

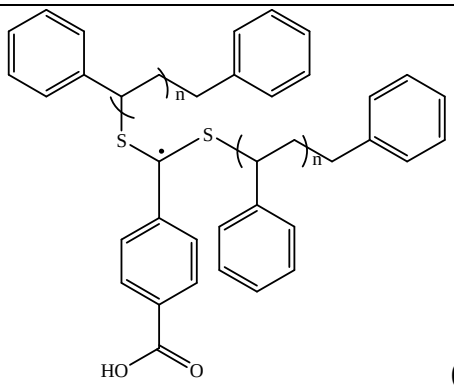
n
S
S
n
HO
O

(**f**)

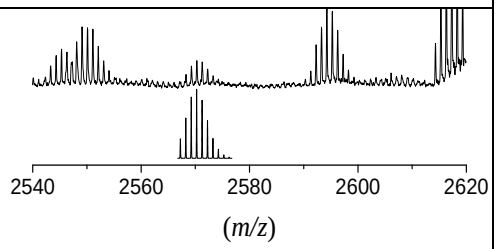
2540
2560
2580
2600
2620
(m/z)

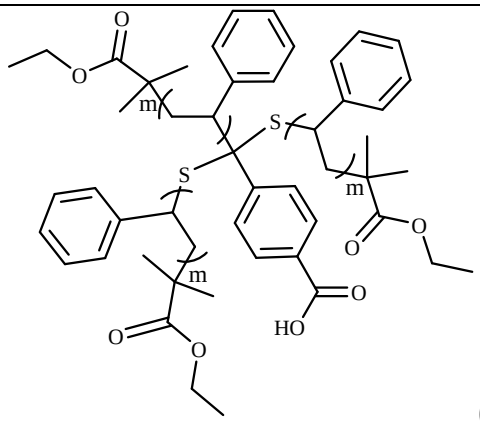
O
O
m
S
S
m
O
O
m
O
HO
O
O

(**g**)

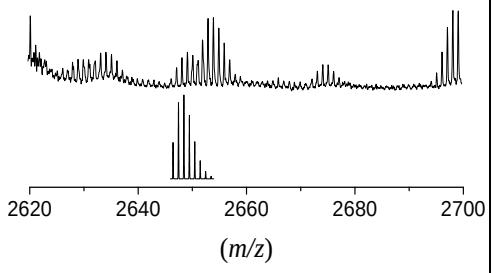
2620
2640
2660
2680
2700
(m/z)

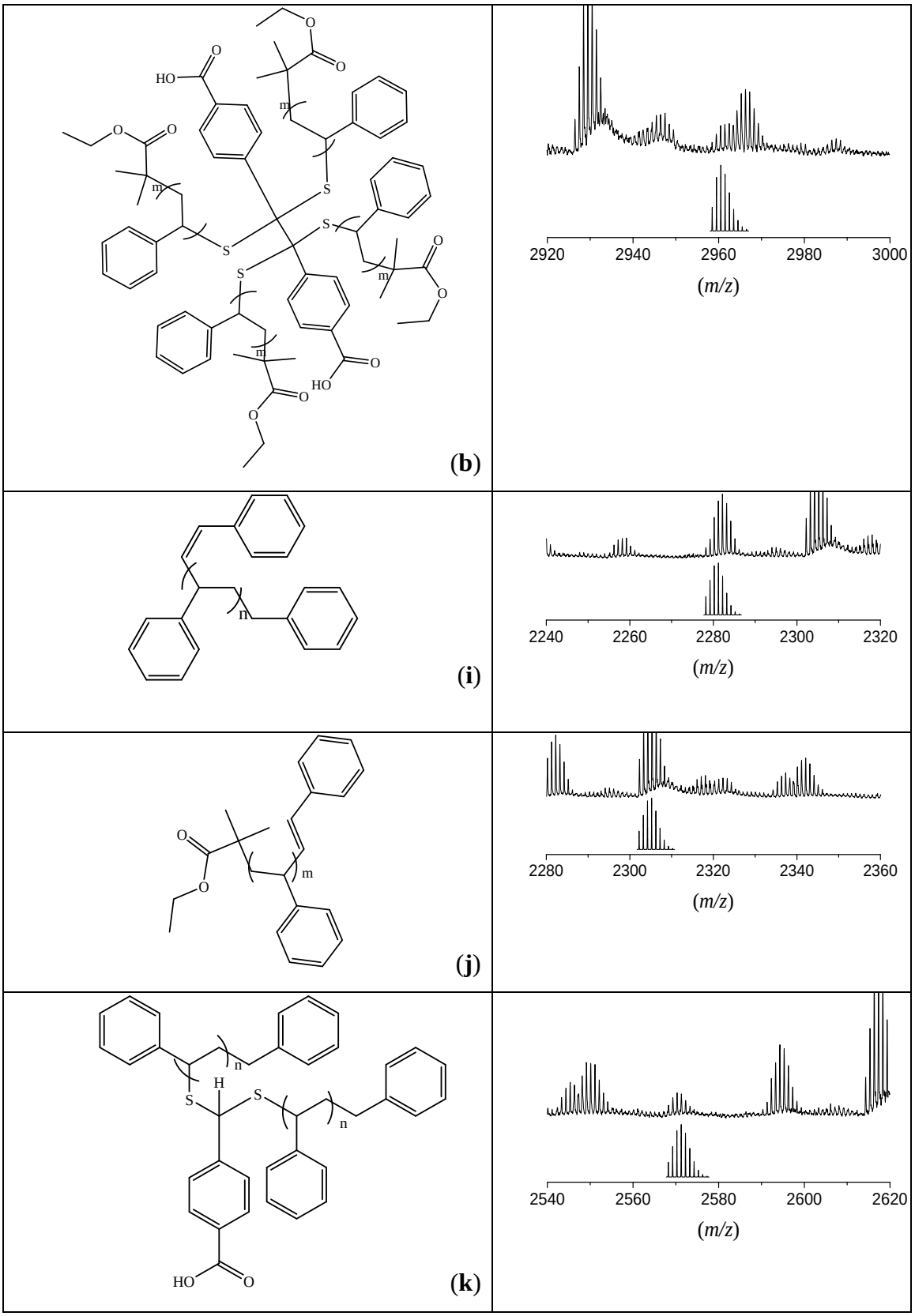
(b)
2920
2940
2960
2980
3000
(m/z)
(i)
2240
2260
2280
2300
2320
(m/z)
(j)
2280
2300
2320
2340
2360
(m/z)
(k)
2540
2560
2580
2600
2620
(m/z)

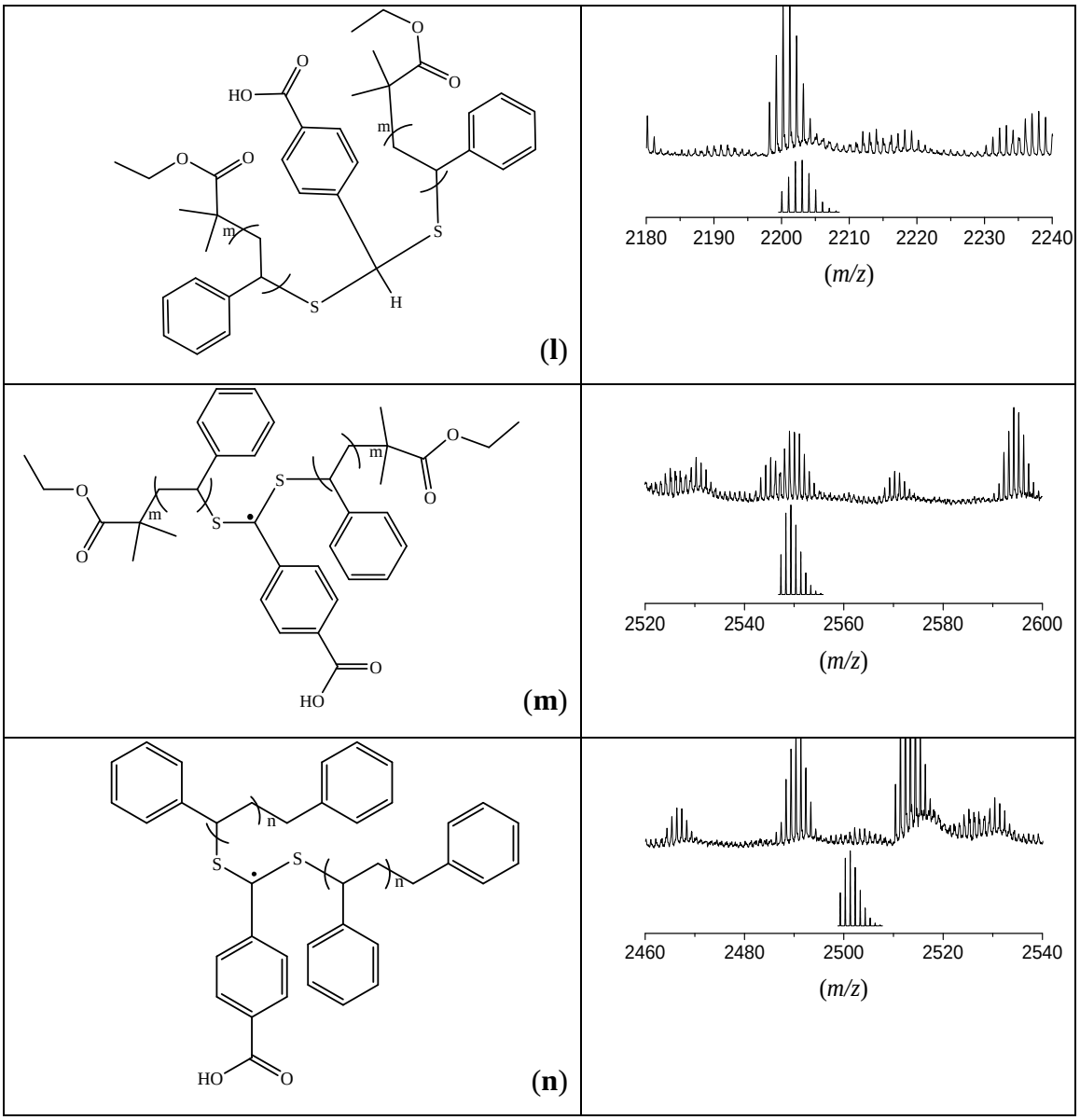

Figure 7.9: PSt chain populations of the extracted polymer (obtained after heat treatment and extracted using the extraction process): as detected by MALDI-ToF-MS using the reflectron mode (above spectra) with AgTFA salt/MM matrix, as theoretically calculated spectra (below spectra) and the corresponding mass structures of each chain population (left hand side column).

Table 7.1 provides all of the details of the observed and theoretical (calculated) monoisotopic mass differences of the extracted PSt chain populations.

Table 7.1: Monoisotopic masses of the different chain population of the extracted PSt detected by MALDI-ToF-MS analysis using the reflectron mode (AgTFA salt/MM matrix).

Structures derived from the MALDI-ToF-MS	Units of styrene (*n*)	Theoretical mass (Da)	Observed mass (Da)	Cationized agent
$C_8H_5S_2O_2(C_6H_{11}O_2)_3$ - $(styrene)_n$	20	2733.24	2733.36	Ag^+
$C_8H_5S_2O_2(C_6H_{11}O_2)_2$- $(styrene)^{\bullet}_n$	20	2617.28	2617.28	Ag^+
$C_6H_{11}O_2$-(styrene)$^{\bullet}_n$	20	2305.24	2305.22	Ag^+
$C_8H_5S_2O_2$-$(C_7H_7)_2$- (styrene)$^{\bullet}_n$	20	2570.24	2570.33	Ag^+
$C_8H_5S_2O_2$-$(styrene)^{\bullet}_n$- $(C_6H_{11}O_2)(C_7H_7)$	20	2594.27	2594.33	Ag^+
C_7H_7-$(styrene)^{\bullet}_n$	20	2282.22	2282.17	Ag^+
$C_8H_5S_2O_2)_2(C_6H_{11}O_2)_4$ $(styrene)_n$	20	2960.50	2960.54	Na^+
$C_8H_5S_2O_2)_2(C_6H_{11}O_2)_3$ $(styrene)_n$	20	2648.45	2648.39	Na^+
$C_8H_5S_2O_2(C_6H_{11}O_2)_2$- $(styrene)^{\bullet}_n$	20	2549.35	2549.15	K^+
$(C_8H_5S_2O_2)_2(C_6H_{11}O_2)_4$- $(styrene)_n$	20	3045.41	3045.52	Ag^+
$(C_8H_5S_2O_2)_2(C_6H_{11}O_2)_2$ - $(C_7H_7)_2$-$(styrene)_n$	20	2928.43	2928.53	K^+
$C_8H_5S_2O_2$-($C_7H_7)_2$- (styrene)$^{\bullet}_n$	20	2501.30	2501.14	K^+

The mass structures (a) in Figure 7.9 assigned to a two PSt arm chain with an EBiB end-group each. This mass structure possibly formed by the chain cleavage of the C=S/C–S bond of the 3-arm PSt star polymer (a) in Figure 7.7. Our results confirmed this fragmentation reaction for the following reasons: (i) Only a small fraction of 3-arm star polymeric species with PSt arms bearing EBiB end-groups (see intensity of the species c in Figure 7.8) was detected using the reflectron mode in contrast to its much higher fraction detected by the linear mode (it is possible that the linear mode experienced fewer fragmentation reactions): see Figure 7.7, first right-hand spectrum). (ii) Detection of PSt

chain populations with monoisotopic peaks at 2305.23 and 2617.28 *m*/*z*, matching (b) and (a) in Figure 7.9, which are assigned for PSt• with EBiB end-group, and a polymeric RAFT chain with two PSt arms bearing EBiB end-group each, respectively.

The mass structure (a) in Figure 7.9 could also formed by the chain scission of the C=S/C–S bond of 4-arm PSt star polymers with the mass structures (e), (g) and (i) in Figure 7.7. The chain scission of the mass structures (e) and (i) in Figure 7.7 results in a formation of 2-arm PSt polymers with EBiB end-groups. On the other hand the chain scission of the mass structure (g) in Figure 7.7 affords 2-arm PSt polymer with EBiB end-groups and 2-arm PSt polymer with R and EBiB end-groups. This is consistent with the MALDI-ToF-MS analysis of the extracted PSt (Figure 7.9), which shows that there are monoisotopic peaks at 2617.28 *m*/*z* and at 2570.33 *m*/*z* assigned to the 2-arm PSt polymer bearing EBiB end-groups with the mass structures (a) and that with R and EBiB end-groups with the mass structure (d), respectively.

The mass structure (d) in Figure 7.9 assigned to a 2-arm PSt polymer with an EBiB and R end-groups. This mass structure can be formed by fragmentation reactions at C=S/C–S bond of different polymer species. It can be formed by the fragmentation reaction of the 3-arm PSt star polymer with the mass structure (b) in Figure 7.7. This fragmentation reaction produced a 2-arm PSt polymer with a monoisotopic peak at 2594.33 *m*/*z* and PSt• chain population with a monoisotopic peak at 2305.23 *m*/*z*, as observed in Figure 7.9. It can be due to the fragmentation reaction of the 3-arm PSt star polymer with the mass structure (c) in Figure 7.7. This fragmentation reaction produces the 2-arm PSt polymer with the mass structure (d) and PSt• chain population with a mass structure (e) in Figure 7.9. This is consistent with the MALDI-ToF-MS results of the extracted PSt polymer (Figure 7.9) showing that there is a monoisotopic peak at 2282.17 *m*/*z* corresponds to the PSt• chain population with R end-group. It can also be due to fragmentation reaction of the 4-arm PSt star polymer with the mass structure (f) in Figure 7.7.

The mass structure (f) in Figure 7.9 formed by chain cleavage of the 3-arm PSt star polymer with the mass structure (d) in Figure 7.7. This chain cleavage produced a 2-arm PSt polymer and PSt• chain population terminated with R-end-groups. Figure 7.9 shows that there are monoisotopic peaks at 2570.33 *m*/*z* and at 2282.17 *m*/*z* assigned to 2-arm PSt polymer with the mass structure (f) and PSt• chain population with the mass structure (e), respectively.

There is monoisotopic peak at 2648.39 *m*/*z* assigned to sodium species of a 3-arm PSt star polymer with the mass structure (g) in Figure 7.9. This mass structure was formed by cross-termination reaction between an intermediate radical with two PSt arms being terminated with an EBiB end-group each and a PSt• with an EBiB end-group. The mass structure (g) in Figure 7.9 (overlaps with the mass structure (h) in Figure 7.9), which corresponds to a sodium specie of a 4-arm PSt star polymer. This 4-arm PSt star polymer formed by cross-termination of intermediate–intermediate radicals bearing EBiB end-groups. The MALDI-ToF-MS analysis (Figure 7.9) confirms this cross-termination reaction, showing that there is a monoisotopic peak at 2960.54 *m*/*z* assigned to the 4-arm PSt star polymer with EBiB end-groups.

The monoisotopic peaks at 2281.21 *m*/*z* and that at 2305.22 *m*/*z* assigned to unsaturated PSt polymeric chains with R and EBiB end-groups with the mass structures (i) and (j), as observed in Figure 7.9, respectively. Unsaturated polymeric chains could have resulted from termination reactions by a disproportionation mode during the free radical polymerization reactions. These mass structures being in the extracted polymer that obtained after the heat treatment reaction cannot however be due to termination reaction via disproportionation between propagating radicals that might occur during the heat treatment reaction for the following reasons: (i) The extraction process (Scheme 7.2), selectively separates all polymeric RAFT chains bearing at least one carboxylate group that can strongly interact and attach to the surface of MNPs. Thus any terminated chains (that have no RAFT functionality (carboxylate group)), will not be extracted using MNPs. (ii) These unsaturated species are not observed in the ^{1}H-NMR, or ^{13}C-NMR spectra of the corresponding extracted PSt polymer. This indicates that the mass

structures (i) and (j) in the extracted polymer most probably formed by disproportionation reactions that have occurred during the MALDI-ToF-MS analysis of the extracted polymer. The MALDI-ToF-MS analysis shows that there are monoisotopic peaks at 2571.32 *m*/*z* and at 2619.39 *m*/*z*, as observed in Figure 7.9. These monoisotopic peaks assigned to the mass structures (k) and (l) in Figure 7.9, respectively. These mass structures possible formed by disproportionation reactions between intermediate and propagating radicals.

The observation that the extracted polymer containing unsaturated PSt chain populations and the idea that these unsaturated PSt chains might be due to disproportionation reactions occurred during the MALDI-ToF-MS analysis of the extracted polymer is consistent with the literature reported data..[21,22] This data shows that there is a significant fraction of unsaturated PSt chains formed during the MALDI-ToF-MS analysis of PSt polymer prepared via RAFT process.

A significant fraction of potassium species of a 2-arm PSt polymer chain with a monoisotopic peak at 2549.15 *m*/*z* assigned to the mass structure (m), as observed in Figure 7.9. The mass structure (m) formed by fragmentation reactions of the mass structures (a), (e), (g) and (i) in Figure 7.7. This was discussed earlier in this section. There is also a small fraction of potassium species of 2-arm PSt polymer with a monoisotopic peak at 2501.14 *m*/*z* assigned to the mass structure (n) in Figure 7.9. This mass structure formed by a fragmentation reaction of a 3-arm star PSt polymer with the mass structure (d) in Figure 7.7.

7.5 Conclusions

The heat treatment of the PSt-Br and PSt-carboxylate using a copper complex in the absence of monomer produced 3-and 4-arm polystyrene polymers formed by cross-termination reactions. These cross-termination reactions mostly occur by the combination between propagating and intermediate radicals, to yield 3-arm star polymers. Under the conditions used in this work, it appears that a substantial amount of cross-termination

reactions also occur by the combination between two intermediate radicals, to afford a 4-arm polystyrene star polymer.

All 3-and 4-arm polystyrene star polymers were separated using MNPs with high efficiency. To the best of our knowledge, this is the first time that all 3- and 4-arm star polymers (formed by cross-termination reactions), magnetically separated from all other terminated polymer chains that are formed by termination reactions other than those produced by cross-termination reactions.

The extraction process using MNPs made it easy to obtain structural information of all 3- and 4-arm polystyrene polymers produced during the heat treatment reaction of the PSt-Br and PSt-carboxylate in the absence of monomer. All the 3- and 4-arm star polymers were characterized by ^{1}H-NMR and ^{13}C-NMR and MALDI-ToF-MS.

This work is significant since it showed that a cross-termination reaction of the intermediate radical could occur in the RAFT process. It also shows that the extraction process using MNPs could be used to obtain more information about the RAFT mechanism.

7.6 References

1. Chiefari, J.; Chong, Y. K.; Ercole, F.; Krstina, J.; Jeffery, J.; Le, T. P. T.; Mayadunne, R. T. A.; Meijs, G. F.; Moad, C. L.; Moad, G.; Rizzardo, E.; Thang, S. H. *Macromolecules* **1998,** 31, 5559-5565.
2. Moad, G.; Chiefari, J.; Chong, Y. K.; Krstina, J.; Mayadunne, R. T. A.; Postma, A.; Rizzardo, E.; Thang, S. H. *Polym. Int.* **2000,** 49, 993-1001.
3. Calitz, F. M.; Tonge, M. P.; Sanderson, R. D. *Macromolecules* **2003,** 36, 5-8.
4. Barner-Kowollik, C.; Quinn, J. F.; Morsley, D. R.; Davis, T. P. *J. Polym. Sci., Part A.: Polym. Chem.* **2001,** 39, 1353-1365.
5. Barner-Kowollik, C.; Quinn, J. F.; Nguyen, T. L. U.; Heuts, J. P. A.; Davis, T. P. *Macromolecules* **2001,** 34, 7849-7857.
6. de Brouwer, H.; Schellekens, M. A. J.; Klumperman, B.; Monteiro, M. J.; German, A. L. *J. Polym. Sci., Part A.: Polym. Chem.* **2000,** 38, 3596-3602.
7. Monteiro, M. J.; de Brouwer, H. *Macromolecules* **2001,** 34, 349-352.
8. Kwak, Y.; Goto, A.; Komatsu, K.; Sugiura, Y.; Fukuda, T. *Macromolecules* **2004,** 37, 4434-4440.
9. Kwak, Y.; Goto, A.; Tsujii, Y.; Murata, Y.; Komatsu, K.; Fukuda, T. *Macromolecules* **2002,** 35, 3026-3029.
10. Calitz, F. M.; McLeary, J. B.; Mckenzie, J. M.; Tonge, M. P.; Klumperman, B.; Sanderson, R. D. *Macromolecules* **2003,** 36, 9687-9690.
11. Buback, M.; Vana, P. *Macromol. Rapid Commun.* **2006,** 27, 1299-1305.
12. Buback, M.; Janssen, O.; Oswald, R.; Schmatz, S.; Vana, P. *Macromol. Symp.* **2007,** 248, 158-167.
13. Chong, Y. K.; Krstina, J.; Le, T. P. T.; Moad, G.; Postma, A.; Rizzardo, E.; Thang, S. H. *Macromolecules* **2003,** 36, 2256-2272.
14. Chiefari, J.; Mayadunne, R. T. A.; Moad, C. L.; Moad, G.; Rizzardo, E.; Postma, A.; Skidmore, M. A.; Thang, S. H. *Macromolecules* **2003,** 36, 2273-2283.
15. Coote, M. L.; Radom, L. *J. Am. Chem. Soc.* **2003,** 125, 1490-1491.
16. Vana, P.; Quinn, J. F.; Davis, T. P.; Barner-Kowollik, C. *Aust. J. Chem.* **2002,** 55, 425-431.

17. Kwak, Y.; Goto, A.; Fukuda, T. *Macromolecules* **2004,** 37, 1219-1225.

18. Van Geet, A. L. *Anal.Chem.* **1968,** 40, 2227-2229.

19. Ladavie#re, C.; Lacroix-Desmazes, P.; Delolme, F. *Macromolecules* **2009,** 42, 70-84.

20. Räder, H. J.; Schrepp, W. *Acta Polym.* **1998,** 49, 272-293.

21. Destarac, M.; Brochon, C.; Catala, J.-M.; Wilczewska, A.; Zard, S. Z. *Macromol. Chem. Phys.* **2002,** 203, 2281-2289.

22. Catherine, L.; Patrick, L.-D.; Frederic, D. *Macromolecules* **2009,** 42, 70-84.

23. Michael J, P.; Manuela, O.; Roderic, P. Q.; Alyison, M. L.; Chrys, W. Supporting information in *Anal.Chem.* **2008,** 80, 355-362.

Chapter 8:
Synthesis and separation of polymers grafted to the surface of magnetic nanoparticles

Abstract: Reversible Addition-Fragmentation Chain Transfer (RAFT) agents attached to the surface of magnetic nanoparticles (MNPs) via the Z group have been used as mediating agents for the synthesis of polymers grafted to the surface of MNPs. The polymers grafted to the surface of MNPs were separated from the remainder of dissolved polymer by applying an external magnetic field. The amounts of the polymers grafted to the surface of MNPs greatly increased as the number of RAFT agents attached to the surface of MNPs decreased. It reached 65% by weight and 50% by number of chains, when ethyl acetate was used as solvent. Separated polymers grafted onto the surface of MNPs showed high polydispersity index (PDI) and contained RAFT functionality. The kinetics of RAFT-mediated polymerization reactions of styrene (St) using a RAFT agent attached to the surface of MNPs by the Z group was also investigated. The molecular weight of the grafted polymer increased linearly with conversion, and the reaction rate was pseudo-first-order.

8.1 Introduction

Polymer nanocomposites are of great interest in both industrial and scientific applications due the fascinating electrical, optical and magnetic properties of such polymer particles on a nanoscale.[1,2] The control of polymer chain length (layer thickness) and interfacial interaction between the polymer matrix and nanoparticles are especially important as they determine the properties of these polymer nanocomposites. It is therefore of great advantage to be able to attach RAFT agents onto the surface of particles and to see if they can be used for the synthesis of well defined polymers with controlled chain length and livingness. The attachment of RAFT agents to the surface of particles is also an excellent method for the separation of all dead chains from living chains formed in RAFT-mediated polymerization reactions using RAFT agents attached to the surface of particles.

Immobilization of RAFT agents on solid supports can be performed using the R group approach and the Z group approach, both of which have advantages and disadvantages.[3,4] In the R group approach, the RAFT agent attaches to the surface of particles/substrates via the leaving (R) group. In this case densely grafted polymer on the surface of particles can be obtained.[5-7] The limitation of this approach is that chain termination reactions that involve at least one R group attached to the surface of the solid particle cannot be prevented. These reactions produce dead chains attached to the surface of the particles. Thus in the separation of the R group grafted polymer, not all dead chains are isolated from the living chains. In the Z group approach, however, the RAFT agent attaches via the living (Z) group, and thus the RAFT process in this case involves the reaction of linear chains with the functional RAFT agent attached to particle surfaces, resulting in a better defined grafted living polymer, but limited grafting surface density.[8-10] The Z group approach thus is unique in the application of the RAFT polymerization on solid particles, specifically onto the surface of MNPs. This is because all living polymer chains grafted onto the surface of MNPs can essentially be separated from dead chains by applying an external magnetic field.

In this study, a RAFT agent attached to the surface of MNPs via its Z group using benzyl-(4-carboxyldithiobenzoate) RAFT agent (Z-carboxylate RAFT agent) was used for the synthesis of polymer grafted to the surface of MNPs. The strategy used in this study for generation of polymer grafted to the surface of MNPs is described in Scheme 8.1. It shows RAFT agent attached to the surface of MNPs via its Z group that is added to free radical polymerization reactions. The resulting polymer grafted to the surface of MNPs is attached to the surface of MNPs by its living Z group, as depicted in Scheme 8.1b. This polymer is termed as "living chains", as it contains RAFT functionality (dithioester groups), and is capable of further chain growth. Scheme 8.1c shows the application of a strong external magnetic field to separate living chains from the remainder of a polymer solution (free polymer) formed in this RAFT-mediated polymerization reaction.

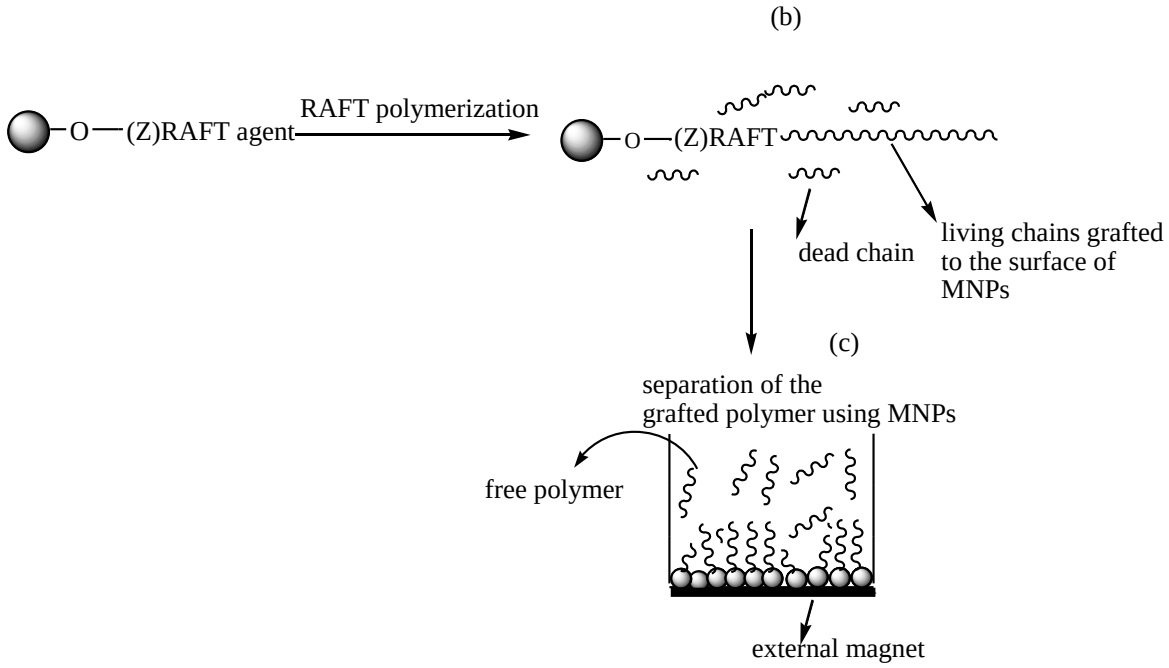

Scheme 8.1: Grafting of a polymer to the surface of MNPs via RAFT-mediated polymerization reaction using a RAFT agent attached to the surface of MNPs by its Z group, and subsequent separation of the grafted polymer using MNPs.

8.2 Objectives

The objectives of this part of the study were the following:

1. To investigate the effect of MNPs on RAFT-mediated polymerization reactions.

2. To investigate RAFT-mediated polymerization reactions on the surface of MNPs for synthesis of grafted polymer, whereby the RAFT agent is attached to the surface of MNPs via its Z group. This separates all free polymers from polymers grafted to the surface of MNPs by applying an external magnetic field.

3. To investigate the effect of surface density of a RAFT agent attached to the surface of MNPs on PDI and amounts of polymer grafted to the surface of MNPs.

4. To investigate effect of solvent on the amounts of the grafted polymer to the surface of MNPs.

5. To investigate the kinetics of RAFT-mediated polymerization reactions using a RAFT agent attached to the surface of MNPs by comparison with that of RAFT-mediated polymerization reactions using a free RAFT agent.

8.3 Experimental

8.3.1 Materials

The following materials were used as received: hydrochloric acid (32 wt%; Merck), dichloromethane (DCM) (99%; Saarchem) and ethyl acetate (99%; Saarchem).

Styrene (St) monomer (99%; Aldrich) was purified by washing with KOH (0.03 M) and then distilled under reduced pressure prior to use. 2,2'-Azobis(isobutyronitrile) (AIBN) (98%; Aldrich) was recrystallized twice from methanol and dried prior to use. Tetrahydrofuran (THF) (99%; Saarchem) was distilled under reduced pressure prior to use in the polymerization reactions.

8.3.2 Synthesis and stabilization of MNPs

MNPs were synthesized and stabilized using the methods described in Sections 4.3.2 – 4.3.3, respectively.

8.3.3 Synthesis of RAFT agent attached to the surface of MNPs by its Z group

The Z-carboxylate RAFT agent was attached to the surface of MNPs by its Z group using an isothermal adsorption process (see Section 4.3.4), and using a ligand exchange process (see Section 4.3.5).

8.3.4 Synthesis of benzyl dithiobenzoate RAFT agent

Benzyl dithiobenzoate RAFT agent (will be termed as blank RAFT agent in this study) was synthesized using the procedure described in Section 3.4.3.

8.3.5 RAFT-mediated polymerization reaction of St using a Z-carboxylate RAFT agent attached to the surface of MNPs

All RAFT-mediated polymerization reaction conditions of St are tabulated in Table 8.1. In a typical polymerization, the Z-carboxylate RAFT agent attached to the surface of MNPs (520 μmol/1 g magnetite), St (16.40 g; 155 mmol), THF (60 mL) and AIBN (0.015 g; 6×10^{-2} mmol) were placed to a 150 mL 3-neck round-bottom flask. The flask was purged with N_2 for 15 min to remove the oxygen, and then placed in an oil bath preheated to 70 °C. The reaction mixture was stirred at this temperature for 6 h. The polymerization reaction was quenched by placing the flask in ice water. A dispersion of MNPs was obtained. A strong external magnetic field (provided by an NdFeB magnet, with a magnetic field intensity of 4.5×10^5 A/m) was applied to the dispersion of MNPs. This attracted all of the MNPs and any chains grafted to the surface of MNPs, thus separating the MNPs from a remainder of solution polymer (the non-grafted solution that contains the free polymer). The MNP dispersion was then mixed at room temperature (by stirring at ca. 300 – 400 rpm) with a 32% HCl solution (20 mL for 4.0 g of MNPs) until the MNPs completely dissolved (which took less than 5 minutes), as indicated by the disappearance of the black colour of the MNPs. The organic phase (containing the oleic acid and the grafted polymer) was separated from the aqueous phase, and the aqueous phase extracted with DCM (15 mL × 2). The solvent was evaporated to afford the PSt

polymer. In the case of MNPs remaining in the non-grafted solution, this solution was also washed and extracted as above. The final grafted and non-grafted polymers were characterized using Size Exclusion Chromatography (SEC).

Table 8.1: Formulation and reaction conditions used for St RAFT polymerizations using Z-carboxylate RAFT agents attached to the surface of MNPs.[a]

Run	[St]/ [RAFT]	Conversion (C%)	RAFT/ MNPs (μmol/g)	Time (h)	$\overline{M}_n$, SEC (g)[d]	$\overline{M}_n$, SEC (f)[e]	PDI (g)[d]	PDI (f)[e]	W (%)
1[b]	450	8	520	8	15900	9890	2.10	1.53	5
2[b]	450	3	96	2	6000	2250	1.35	1.60	12
3[b]	900	4.5	96	6	15890	9900	1.40	1.66	45
4[c]	900	5	96	6.5	19000	12000	1.45	1.70	55

[a]Polymerization conditions: 70 °C; $[RAFT]_0$:$[AIBN]_0$ = 1:0.1. Runs (1 – 2): The Z group RAFT agent was attached to the surface of MNPs by the isothermal adsorption process. Runs (3 – 4): The Z group RAFT agent was attached to the surface of MNPs by the ligand exchange process. [b]THF solvent (60 mL) was used in the polymerization reactions. [c]Ethyl acetate solvent (20 mL) was used in the polymerization reaction. [d,e] Number average molecular weights and polydispersity indexes (PDIs) of the grafted (g) and free (f) polystyrene (PSt) polymers, respectively, as determined by SEC using PSt standards. W%: weight amounts of the grafted polymer to the surface of MNPs.

8.3.6 RAFT-mediated polymerization reactions of St using a blank RAFT agent

St polymerization reactions using the blank RAFT agent with MNPs and that using the blank RAFT agent with no MNPs are used in this study to investigate the effect of MNPs on RAFT-mediated polymerization reactions. The two polymerization reaction conditions are identical except that one contains 4.5 g of freshly stabilized MNPs. In a typical polymerization the blank RAFT agent (0.11 g; 0.45 mmol), St (25 g; 240 mmol), AIBN (0.01 g; 0.06 mmol), and THF (60 mL) were placed in a 150 mL 3-neck round-bottom flask. The flask was purged with N_2 for 15 min to remove the oxygen, and then placed in an oil bath preheated to 70 °C. The reaction mixture was stirred at this temperature for 6 h. Samples of the reaction product were taken at different intervals, left in a fume hood for 3 days to dry, weighted, and then characterized using SEC. Samples that contain MNPs were treated as described in Section 8.3.5.

8.4 Characterization of PSt polymers

8.4.1 Determination of the molecular weights and molecular weight distributions

The molecular weight (*M*) and molecular weight distributions (MWDs) of the grafted and free PSt polymers synthesized were determined using SEC. Polymer samples were dissolved in stabilized THF (HPLC grade) at a concentration of 5 mg/mL, and filtered through a 0.45 μm nylon filter prior to injection to the SEC columns. The SEC apparatus comprised a Waters 1515 isocratic HPLC pump, Waters 717 plus autosampler, Waters 24141 refractive index detector, two pLgel 5 μm Mixed-C (300 × 7.5 mm) columns, and one pLgel 5 μm guard column (50 × 7.5mm). The samples were eluted using THF (HPLC grade) at 30 °C, using a flow rate of 1 mL/min. The instrument was calibrated using nine Polymer Laboratories Easyvial PSt standards with narrow molecular weight distributions in the range 580 – 9 × 10^5g mol^{-1} (Polymer Laboratories).

The living distribution of each polymer sample was determined by comparing of UV absorbance at 320 nm (dominated by the absorption of the RAFT group plus a small fraction by the aromatic group of the St repeat unit) and the differential refractive index (DRI) SEC traces of the polymer sample. All UV absorbances were corrected in the same way as that described in Section 5.6.1. These UV corrections will be used for all comparisons here. It should be noted that the term UV absorbance will be used for simplicity to indicate the corrected UV absorbance at 320 nm (unless otherwise stated).

8.5 Results and discussion

The main focus of this study is to use RAFT agents attached to the surface of MNPs by Z groups for the synthesis of living polymer chains grafted to the surface of MNPs, and thus, to separate all dead chains from grafted living chains by applying an external magnetic field. However, prior to this, the effect of MNPs on RAFT-mediated polymerization reactions was first investigated. Two St polymerization reactions using the blank RAFT agent, one of which contained MNPs, while the other one contained no MNPs, were used in this study and compared (reaction conditions are given in Section 8.3.6). It is to be noted that the blank RAFT agent contains no specific attachment force

to the surface of MNPs (considering that the C=S component maybe not a strong attachment force to the surface of MNPs). For this reason, it was used to investigate the effect of MNPs in RAFT-mediated polymerization reactions.

8.5.1 Effect of MNPs in RAFT-mediated polymerization reactions

Figures 8.1a and b show the DRI signal SEC traces of PSt polymers prepared by RAFT-mediated polymerization reactions of St using the blank RAFT agent with MNPs and that using the blank RAFT agent with no MNPs, respectively.

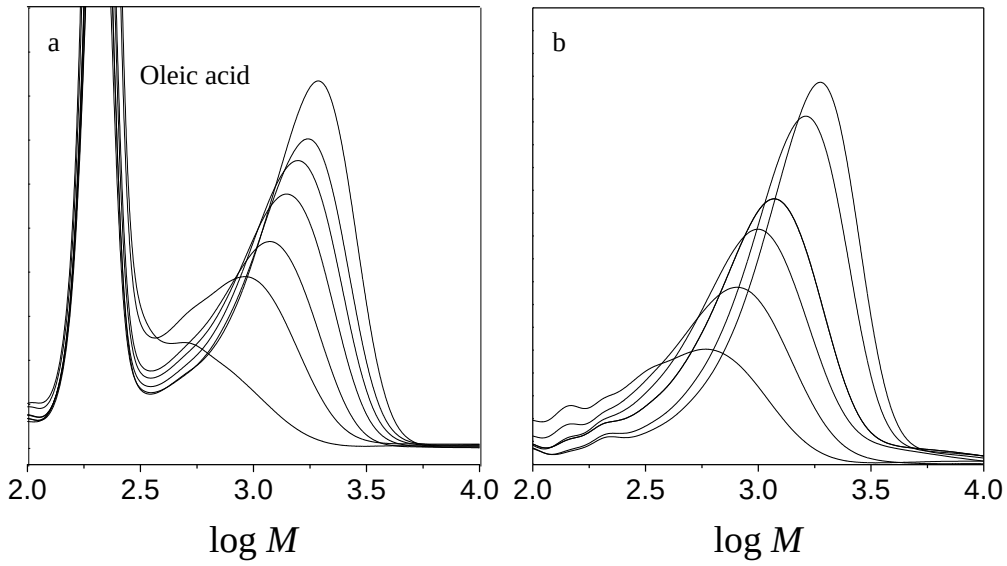

Figure 8.1: DRI signal SEC traces of PSt polymers prepared by RAFT-mediated polymerization reactions of St using the blank RAFT agent and AIBN initiator: (a) with MNPs, and (b) with no MNPs.

This result indicates that the number average molecular weight ($\overline{M}_n$) evolutions increase with monomer conversion.

Figure 8.2 shows the PDIs and $\overline{M}_n$ evolutions with monomer conversion of PSt polymer of the blank RAFT agents with MNPs (filled rectangles and circles, respectively) and that of PSt polymer of the blank RAFT with no MNPs (empty rectangles and circles, respectively). It was found that the $\overline{M}_n$ of these polymers increase with monomer

conversion, and that the PDIs remain low throughout the polymerization reactions. This indicates that these St polymerization reactions proceeded under well controlled polymerization reactions. This result also shows that there is no large difference between these polymers with respect to $\overline{M}_n$ and PDIs, and thus, the presence of the MNPs does not significantly affect the RAFT process.

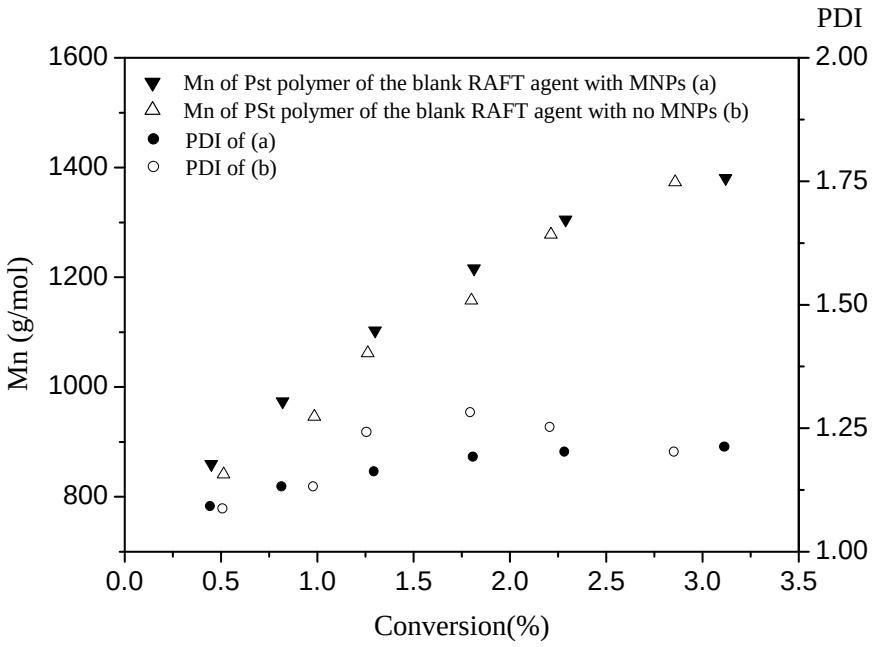

Figure 8.2: The $\overline{M}_n$ evolutions and PDIs of PSt polymer prepared by RAFT-mediated polymerization reaction of St using the blank RAFT agent with MNPs and that of PSt polymer prepared by RAFT-mediated polymerization reaction of St using the blank RAFT agent with no MNPs. Reaction conditions: ([St]:[RAFT]:[AIBN] = (550:1:0.1), 70 °C).

Figure 8.3 shows the pseudo-first order plots of the St polymerization reactions mediated using the blank RAFT agent with MNPs (filled circles) and that of St polymerization reaction mediated by the blank RAFT agent with no MNPs (empty circles). It clearly indicates that these St polymerization reaction rates are identical and that the MNPs have no observable effect on RAFT-mediated polymerization reaction rates.

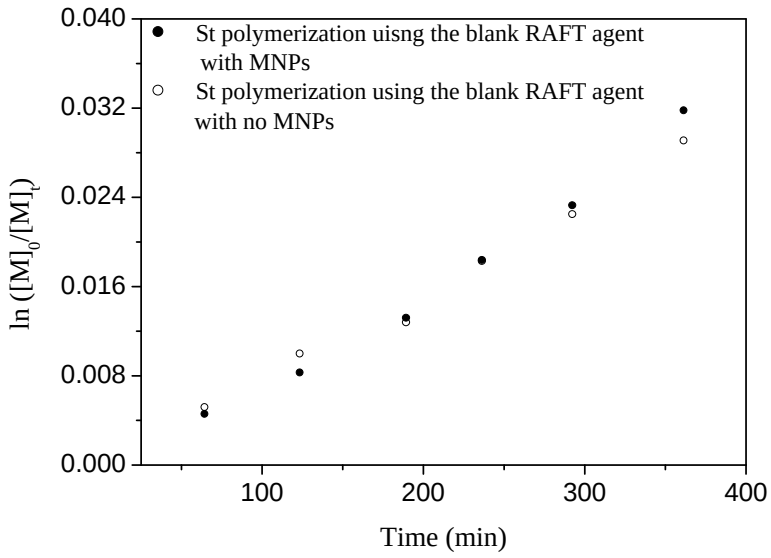

Figure 8.3: Pseudo-first order kinetic curves of RAFT-mediated polymerization reactions of St using the blank RAFT agent with MNPs and that of RAFT-mediated polymerization reaction of St using the blank RAFT agent with no MNPs. Reaction conditions: ([St]:[RAFT]:[AIBN] = (550:1:0.1), 70 °C).

8.5.2 RAFT-mediated polymerization reactions using high surface density Z-carboxylate RAFT agent attached to the surface of MNPs using the isothermal adsorption process

Figure 8.4 shows the DRI signal and corrected UV absorbance SEC traces of the grafted and free PSt polymers prepared by a RAFT-mediated polymerization reaction of St using the Z-carboxylate RAFT agent attached to the surface of MNPs, AIBN initiator, and THF solvent (see run1, Table 8.1). The Z-carboxylate RAFT agent was attached to the surface of MNPs at a concentration of 2.7 RAFT agent/ nm^2 (860 RAFT molecules/ magnetic nanoparticles or 520 μmol/ g of magnetite) using the isothermal adsorption process. The DRI signal and UV absorbance comparison Figures 8.4a – c show that there are distinct differences between the grafted and free polymers with respect to the *M*, MWD, and UV absorbance. The PDI and *M* of the grafted polymer were the highest (2.1, $\overline{M}_n$ = 15900), while the free polymer has much lower PDI and *M* (1.5, $\overline{M}_n$ = 9890). This was not expected, since in RAFT-mediated polymerization reactions using a Z group RAFT agent attached to surface of particles, there should be two competing reactions, namely,

conventional free radical polymerization reactions in the interstitial solution, and graft RAFT polymerization on the surface of the particles. The polymeric chains attached to the surface of the particle should remain in a dormant form, while all growing radicals propagate in the interstitial solution. Therefore, it is expected that the *M* of the free polymer to be much higher than that of the grafted polymer, since this polymer contains all dead chains formed by conventional free radical polymerization reactions. This was not observed in this study.

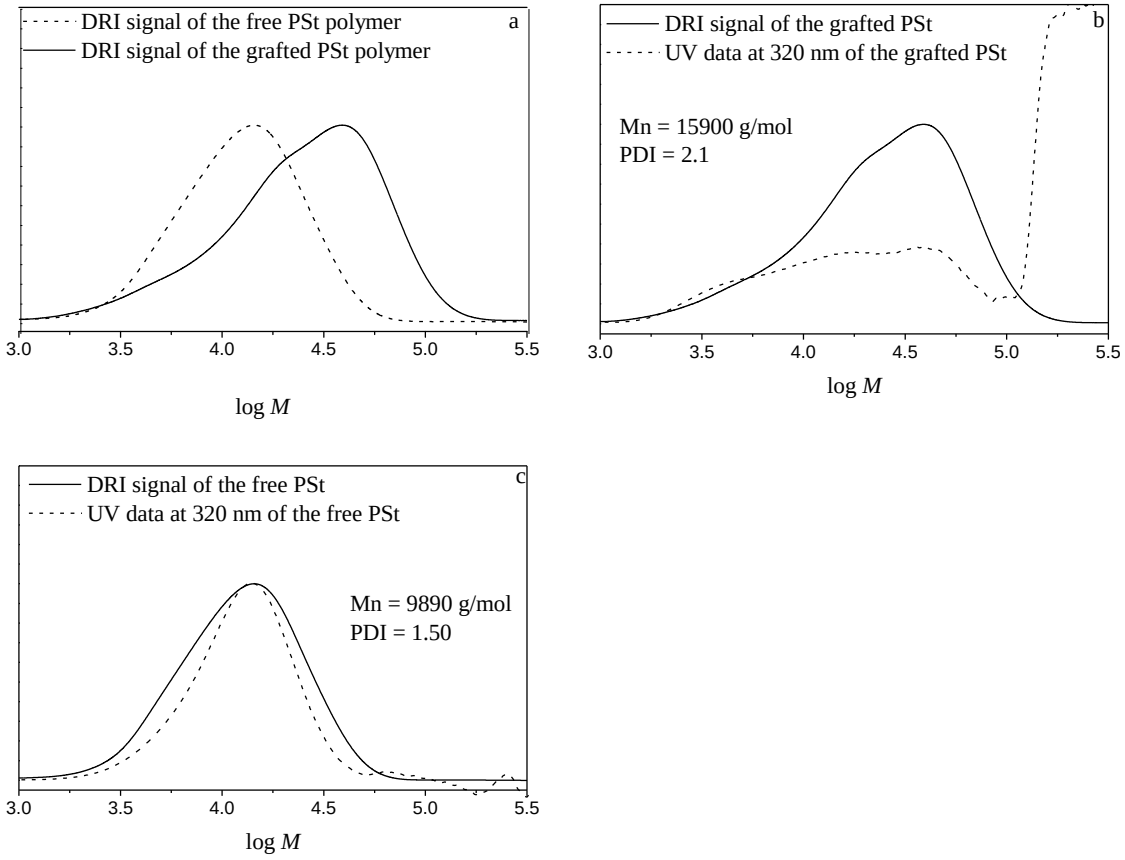

Figure 8.4: DRI signal and UV absorbance SEC traces of the grafted and free PSt polymers prepared by a RAFT-mediated polymerization reaction using AIBN and the Z-carboxylate RAFT attached to the surface of MNPs in THF solvent: (a) comparison of grafted and free polymers, (b) the grafted polymer, and (c) the free polymer. (The RAFT agent was attached to the surface of MNPs by its Z group using the isothermal adsorption process at a concentration of 2.7 RAFT agent/ nm^2).

The free polymer contains a large fraction of RAFT agents with a significant UV absorbance and dead chains with weak UV absorbance, as observed in Figure 8.4c. The large amount of RAFT agents found in the free polymer is probably because of the detachment of a large number of RAFT agents from the surface of MNPs to solution during this RAFT-mediated polymerization reaction. This is consistent with gravimetric analysis, which showed that the amount of the grafted polymer to the surface of MNPs was 5% by weight and 3% by number. This indicates that the free polymer contains the majority of RAFT polymer chains with RAFT functionality and significant UV absorbance, as was observed in Figure 8.4c.

Figure 8.4b shows that there is large deviation between UV absorbance and DRI signal of the grafted polymer. This is not expected, since the grafted polymer should contain living chains with RAFT functionality. Therefore, this suggests that the grafted polymer contains by-products with a minimal UV absorbance, as observed in Figure 8.4b. A possibly by-product could be cross-terminated polymer products, as confirmed using MALDI-ToF-MS (see Appendix A.27). This product is expected to lose UV absorbance at 320 nm, as was observed in this study, and supported by other studies.[11]

The high PDI of the grafted polymer could be due to different MNPs having different MWD. This might happen when the number of RAFT agents attached to the surface of MNPs is different from one particle to another. If different MNPs have different numbers of RAFT agents and if chain entanglement (crowding) near the surface of MNPs is high, and thus resulting in different termination rates near different particle surfaces, then grafted polymer chains on different MNPs will grow at different rates. This will result in different MNPs having different MWD, as was observed in this study. The PDI of dead chains formed in RAFT-mediated polymerization reactions is naturally high.[12] This is because dead chains are forming throughout the polymerization reaction due to termination history, yielding dead chains with different chain lengths, and thus high PDI.

The higher M of the grafted polymer than that of the free polymer is clearly suggesting faster polymerization rate near the surface of MNPs than that in the interstitial solution

phase. This might happen when the number of attached RAFT agents to the surface of MNPs is less than the number of detached RAFT agents from the surface of MNPs to solution. Therefore the detached RAFT agents can effectively slow the propagation of all growing radicals in the interstitial solution phase, and thus, the *M* of free polymer will be much lower than otherwise expected. The polymerization reaction rates of some RAFT-mediated polymerization reactions are very dependent on the concentration of the RAFT agent; and it was found that the higher the concentration of the RAFT agent the slower is the polymerization rate.[13] Thus, if the concentration of the RAFT agent (or chains) on the surface of MNPs is much higher than in solution. This means for a given number of propagating events per particle, these radicals need to be shared among a lot of chains, so the chain expects to grow only a little on average. When rate retardation adds to the effect of the propagating radicals on the surface of MNPs, it is then expected that the chains will be shorter on MNPs. However, this was not observed in this study.

Generally, in RAFT-mediated polymerization reactions, using free RAFT agents or RAFT agents attached to the surface of particles, the propagation reactions should not be significantly affected by the attachment of the RAFT agent to the surface of particles. However, the concentration of the growing polymeric radicals ($[P^{\bullet}]$) is expected to be much higher near the surface of the particles than in interstitial solution. If polymer chains are crowded near the surface of the particles, then the average termination rate coefficient ($<k_t>$) becomes low because diffusion becomes difficult in that region. This will therefore lead to a high concentration of $P^{\bullet}$ near the surface of the particles, and thus, will yield a higher polymerization rate ((R_p), ($R_p = k_p[P^{\bullet}][M]$)) near the surface of the particles, than in solution. Therefore, the polymer grafted to the surface of the particles will grow in a faster rate than that of the free polymer in solution, which was observed in this study.

Consumption and replacement of monomer near the surface of particles in RAFT-mediated polymerization reactions using RAFT agents attached to the surface of particles is also expected to be fast. This can happen when polymer chains are again crowded or

entangled near the surface of particles. Thus, relatively speaking, there will be more polymer chains produced per unit time near the surface of particles, at higher monomer conversion. This could occur when effective monomer concentration ($[M]_{effective}$) near the surface of particles is high because of chain entanglement (chain environment creating a preferable phase partioninig). In that case, the ratio of $[M]_{effective}$ /$[RAFT]_{effective}$ will be high, and if the ratios of $[M]_{effective}/[M]_{overall}$ is higher than the ratio of $[RAFT]_{surface}/[RAFT]_{overall}$, then chains produced there will be longer than otherwise predicted. However the mean reason for the higher *M* of the grafted polymer is purely that of viscosity and steric hindrance near the particle surfaces (the particles are sterically stabilized by polymer). Thus the diffusion rate of polymeric radicals to and from the RAFT agents attached to the surface of MNPs will indeed be limited, allowing longer growth times and higher *M* of grafted polymer.

The expected RAFT-mediated polymerization reactions on the surface of MNPs

Scheme 8.2 shows the expected polymerization reactions that might take place during RAFT-mediated polymerization on the surface of MNPs, whereby the RAFT agent is attached to the surface of MNPs by its Z group. An important fate of the radicals generated from the initiator decomposition (Scheme 8.2a) is for them to react (directly or after adding at least one monomer unit) with the RAFT agent on the surface of MNPs to produce an initiating radical ($R^{\bullet}$) (**b**). This radical can then propagate with monomer near the surface of MNPs to yield an R-ended polymeric radical (**c**). The R-ended polymeric radical in general might undergo different reaction pathways. It might transfer to solution, or otherwise remains near the surface of MNPs. In the very early stages of the polymerization, when the RAFT agent is still attached to the surface of MNPs, most of the radical reactions are expected to occur near the surface of MNPs. This might lead to higher radical concentrations near the surface of MNPs than that in solution. As polymerization proceeds, the amount of attached RAFT chains becomes less than that in solution. This is because of detachment of a large number of the RAFT agents from the surface of MNPs that become free in solution, as discussed earlier. Thus the number of RAFT agent attached to the surface of MNPs will become less than that in solution. This

will lead to an increase in the polymerization rate near the surface of MNPs than in solution.

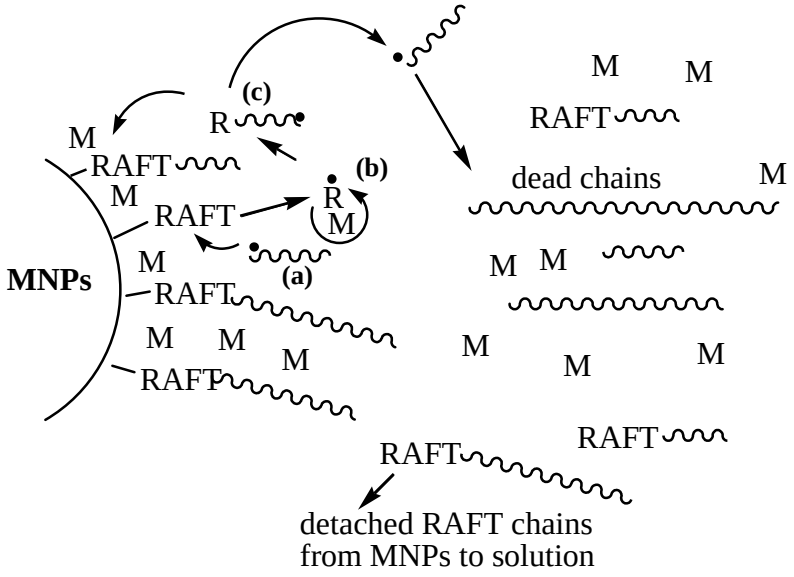

Scheme 8.2: RAFT-mediated polymerization reactions on the surface of MNPs using a RAFT agent attached to the surface of MNPs.

8.5.3 RAFT-mediated polymerization reactions using low surface density Z-carboxylate RAFT agent attached to the surface of MNPs using the isothermal adsorption process

RAFT-mediated polymerization reactions of St at variable reaction conditions, such as the surface density of RAFT agents attached to the surface of MNPs and monomer conversion, were investigated to better understand the effect of these reaction variables on *M*, PDI, and the amounts of polymer grafted to the surface of MNPs with respect to the free polymer in solution. For RAFT-mediated polymerization reaction of St using a RAFT agent attached to the surface of MNPs at a surface density of 0.05 RAFT agent/ nm^2 (90 RAFT molecules/ particle, or 96 μmol/ g of magnetite) using the isothermal adsorption process, the reaction conditions are given in Table 8.1 (run 2). Figure 8.5 shows the DRI signal and UV absorbance SEC traces of the grafted and free PSt polymers of this polymerization reaction. The DRI signal and UV absorbance comparison Figures 8.5a – c indicate that the grafted and free polymers are different with respect to

M, MWD, and UV absorbance. The grafted polymer has the lowest PDI (1.35, $\overline{M}_n$ = 6000), while the free polymer has higher PDI (1.59, $\overline{M}_n$ = 4000).

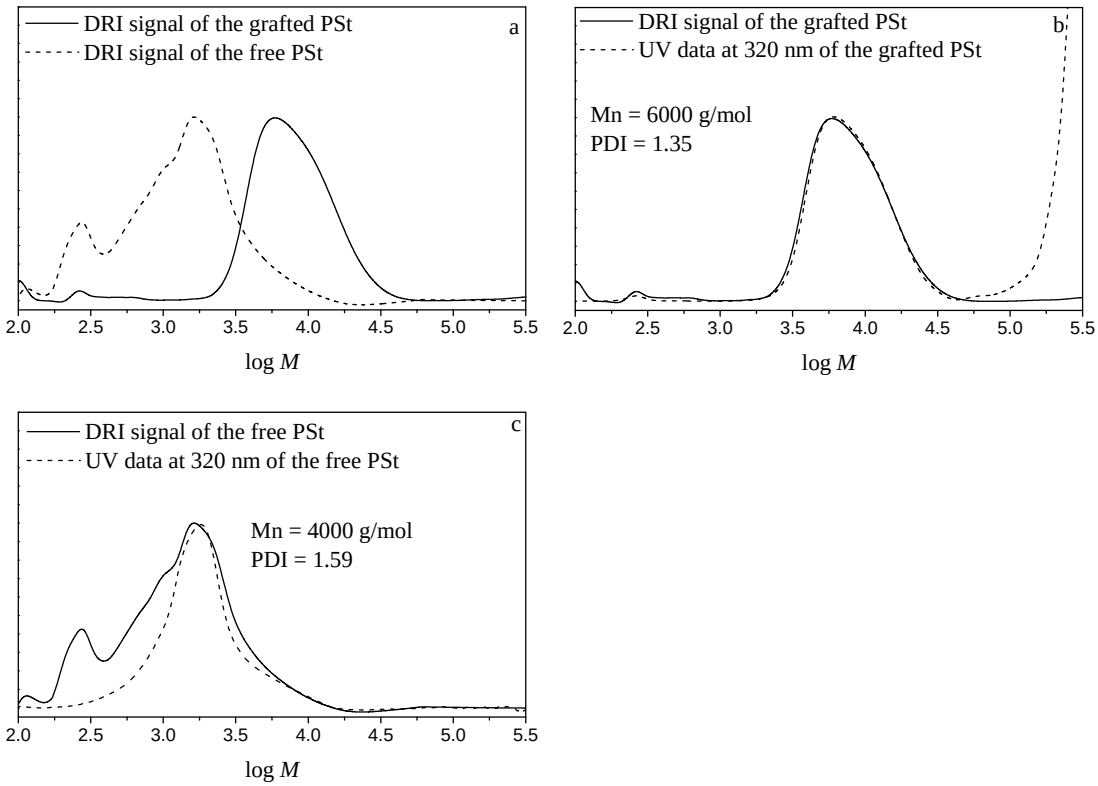

Figure 8.5: DRI signal and UV absorbance SEC traces of the grafted and free PSt polymers prepared by RAFT-mediated polymerization reactions of St using AIBN and the Z-carboxylate RAFT agent attached to the surface of MNPs in THF solvent: (a) comparison of grafted and free polymers, (b) the grafted polymer, and (c) the free polymer. (The RAFT agent was attached to the surface of MNPs using the isothermal adsorption process at a concentration of 0.05 RAFT agent/ nm^2).

The grafted polymer contains living chains with RAFT functionality and a minimal deviation between UV absorbance and DRI signal, as observed in Figure 8.5b. This indicates that a low surface density of RAFT agent attached to the surface of MNPs effectively reduced side reactions occurring during RAFT-mediated polymerization reactions. These side reactions produced by-products attached to the surface of MNPs with weak UV absorbance, as was observed in the previous case in Figure 8.4b. The free polymer contains a large fraction of dead chains with weak UV absorbance, and a significant fraction of living chains with significant UV absorbance, as observed in

Figure 8.5c. This is consistent with the previous results (Section 8.5.2) which showed that the free polymer contains a large fraction of living chains.

The grafted polymer showed a lower PDI than the free polymer and that of the grafted polymer when a high surface density of RAFT agent attached to the surface of MNPs was used (see Figure 8.4b). This clearly indicates that the number of RAFT agents attached to the surface of MNPs and monomer conversion have a great impact on PDI of the grafted polymer. It might simply be the case that the surface of MNPs was not overcrowded with polymer chains, and so detachment was not forced by crowding of the surface and cross-termination as in the previous case (Section 8.5.2). This will result in polymers grafted to the surfaces of different MNPs having similar MWDs. The free polymer contains dead chains and thus the PDI value of this polymer is normally high.

The amount of the grafted polymer was 18% by number. This indicates that the low surface density of RAFT agent attached to the surface of MNPs effectively increased the number of living chains grafted to the surface of MNPs. This shows that the number of grafted living chains with respect to free polymer chains is 6 times greater than the total number of grafted living chains when a high surface density of RAFT agent attached to the surface of MNPs was used. However, it should be noted that the surface coverage in this experiment is 0.009 RAFT agent/nm^2, which is less than that when a high concentration of RAFT agent per MNP was used (0.081 RAFT agent/nm^2).

8.5.4 RAFT-mediated polymerization reaction using a Z-carboxylate RAFT agent attached to the surface of MNPs at low surface density using a ligand exchange process

In order to improve the amount of the grafted polymer to the surface of MNPs, a RAFT-mediated polymerization reaction using a Z-carboxylate RAFT agent attached to the surface of MNPs at a low surface density using a ligand exchange process was investigated. For a RAFT-mediated polymerization reaction of St using the Z-carboxylate RAFT agent attached to the surface of MNPs using the ligand exchange process, the reaction conditions are given in Table 8.1 (run 3). The RAFT agent was attached to the surface of MNPs at 0.05 RAFT agent/ nm^2 (90 RAFT molecule/ particle, or 96 μmol/ g

of magnetite) using the ligand exchange process. For this polymerization reaction, the DRI signal and UV absorbance of the grafted and free polymers are given in Figure 8.6. The DRI signal comparison in Figure 8.6a shows that the grafted polymer features a monomodal MWD, while the free polymer features a bimodal MWD. The grafted polymer has the lowest PDI (1.40, $\overline{M}_n$ =15900), while the free polymer has much higher PDI (1.66, $\overline{M}_n$ = 9900).

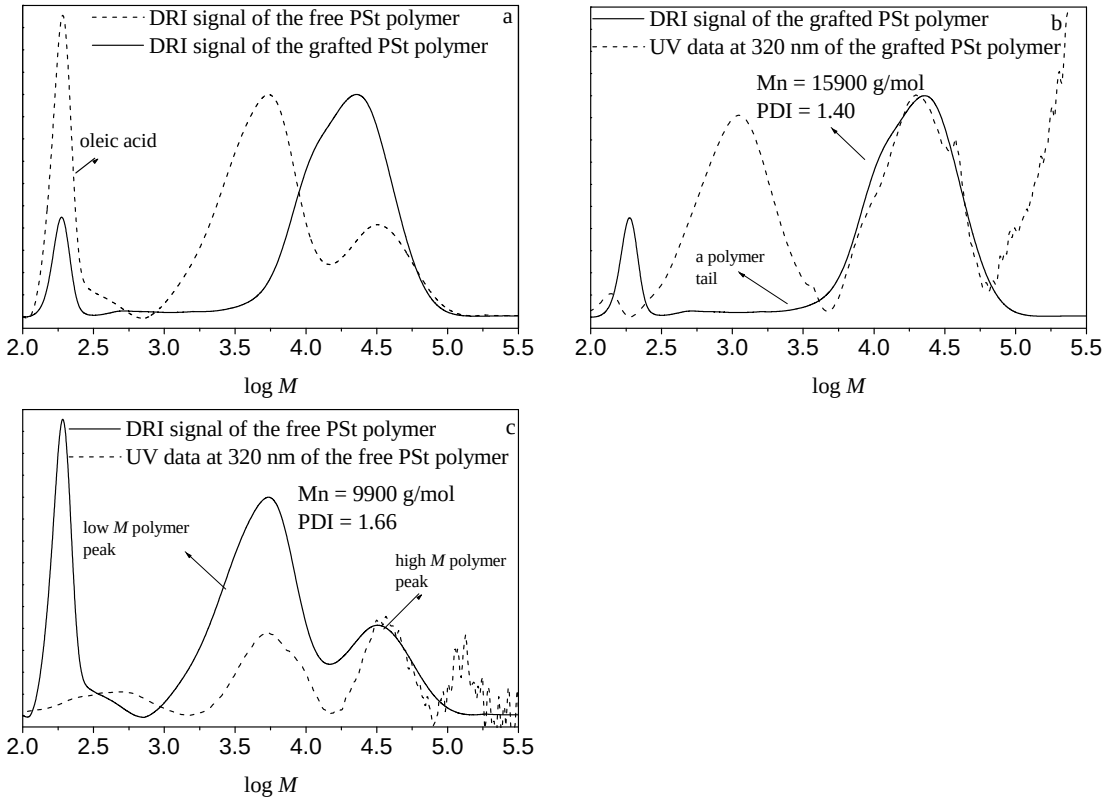

Figure 8.6: DRI signal and UV absorbance SEC traces of the grafted and free PSt polymers prepared by RAFT-mediated polymerization reactions of St using AIBN and the Z-carboxylate RAFT agent attached to the surface of MNPs in THF solvent: (a) comparison of grafted and free polymers, (b) the grafted polymer, and (c) the free polymer. (The RAFT agent was attached to the surface of MNPs using the ligand exchange process at a concentration of 0.05 RAFT agent/ nm^2).

The observation of free polymer exhibiting a bimodal MWD strongly suggests the separation of a mixture of two different polymers with different MWDs during SEC

analysis of this polymer: the low log *M* polymer peak originates from the polymerization taking place in the interstitial solution phase (low polymerization rate), while the high log *M* polymer peak possibly originates from recently detached living chains from the surface of MNPs (high polymerization rate) to solution. It is to be noted that the signal noise for the UV absorbance of the high *M* polymer peak is low. This might indicate that the UV absorbance is much weaker or smaller than the DRI signal of the high *M* polymer peak meaning that this polymer might be a distribution of dead chains at this point that these dead chains are no longer attached to the surface of MNPs. This is consistent with the DRI signal and UV absorbance comparison in Figure 8.6c, which shows that the high log *M* polymer peak contains almost only living chains with UV absorbance, while the low log *M* polymer peak contains a large fraction of dead chains with weak UV absorbance, and a significant fraction of living chains with UV absorbance. The low and high *M* polymers feature two different MWDs, thus, the free polymer exhibits a bimodal MWD, as was observed in this study.

The grafted polymer contains living chains with a small deviation between the UV absorbance and DRI signal, as observed in Figure 8.6b. It also contains a long low *M* polymer tail with strong UV absorbance. This UV absorbance peak is not suggesting that it is due to normal chains. This is because normal chains would exhibit stronger DRI signal than that observed in Figure 8.6b. The polymer tail may however suggest that the grafted polymer contains a very small fraction of living chains that the chain growth of these chains being stopped, or otherwise these chains were growing at slower polymerization rate than other living chains in this system.

The amount of grafted PSt polymer was 40% by weight and 32% by number. This indicates that the ligand exchange process enhanced the stability of the RAFT agent attached to the surface of MNPs during the RAFT-mediated polymerization reaction, and thus, the grafting efficiency of the grafted polymer to the surface of MNPs was improved, as observed in this study.

This is probably because the exchange process allows only the carboxylate group of the RAFT agent to be attached to the surface of MNPs. This is indicated by the shift in the FT-IR band of the carbonyl group of the Z-carboxylate RAFT agent attached to the surface of MNPs, as observed in Figure 4.2, with respect to that band of the carbonyl group of the free Z-carboxylate RAFT agent. On the other hand, the carboxylate and dithio groups of the Z-carboxylate RAFT agent in the isothermal adsorption process, both attach to the surface of MNPs, as indicated by shifts in FT-IR bands of both carbonyl and dithio groups of this RAFT agent attached to the surface of MNPs, with respect to those of the free RAFT agent (see Figure 4.1), resulting in different bond strengths. Therefore, the amount of the grafted PSt polymer on the MNPs, was less when the RAFT agent attached to the surface of MNPs via the isothermal adsorption process.

8.5.5 Effect of solvent on the amount of the grafted polymer to the surface of MNPs

In this part of the study, the amount of the solvent, which was used in RAFT-mediated polymerization reactions of St using the Z-carboxylate RAFT agent attached to the surface of MNPs, was reduced compared to the previously investigated studies. The reason for this was to reduce the ratio between the surface area of the MNPs and the interstitial solution phase, and thus, to improve the amount of the grafted polymer to the surface of MNPs. Ethyl acetate solvent was used in this polymerization reaction.

For the St polymerization reaction using the Z-carboxylate RAFT agent attached to the surface of MNPs, the polymerization reaction conditions are given in Table 8.1 (run 4). The RAFT agent was attached to the surface of MNPs at 0.05 RAFT agent/ nm^2 (90 RAFT molecules/ particle, or 96 μmol/ g of magnetite) using the ligand exchange process. Figure 8.7 shows the SEC DRI signal and UV absorbance of the grafted and free PSt polymers prepared using this polymerization reaction. The grafted polymer PDI was the lowest PDI (1.47, $\overline{M}_n$ = 19100), while the free polymer has much higher PDI (1.70, $\overline{M}_n$ = 10500).

The grafted polymer contains living chains with RAFT functionality and minimal deviation between UV absorbance and DRI signal, as observed in Figure 8.7b. The free polymer contains however a large fraction of dead chains with a lack of RAFT functionality and a weak UV absorbance, and a small fraction of living chains with RAFT functionality and strong UV absorbance, as observed in Figure 8.7c.

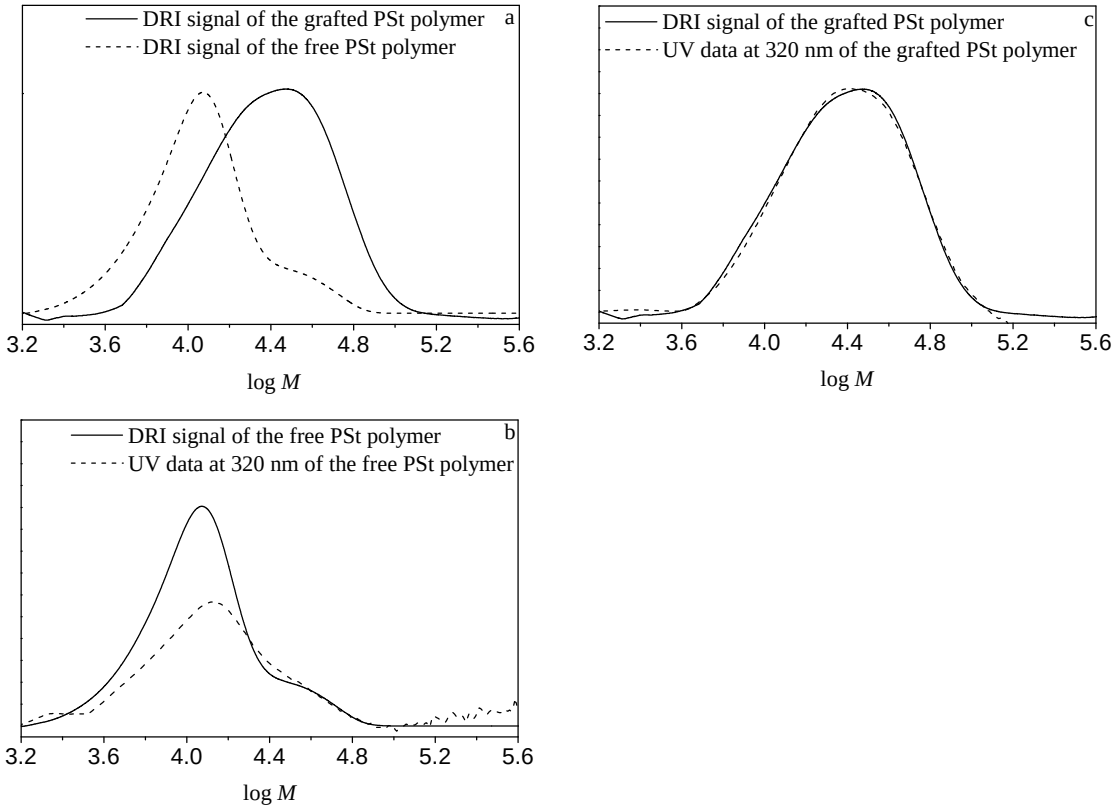

Figure 8.7: DRI signal and UV absorbance SEC traces of the grafted and free PSt polymers prepared by RAFT-mediated polymerization reactions of St using AIBN and the Z-carboxylate RAFT agent attached to the surface of MNPs in ethyl acetate solvent: (a) comparison of grafted and free polymers, (b) the grafted polymer, and (c) the free polymer. (The RAFT agent was attached to the surface of MNPs using the ligand exchange process at a concentration of 0.05 RAFT agent/ nm^2).

The amount of the grafted polymer to the surface of MNPs was 65% by weight and 50% by number. This indicates that a reduced amount of solvent increased the number of attached chains to the surfaces of the MNPs. The amount of the grafted polymer to the surface of MNPs is 13 % higher than that when the solvent THF used in the RAFT-

mediated polymerization reaction of St using Z-carboxylate RAFT agent attached to the surface of MNPs.

8.5.6 Kinetics of RAFT-mediated polymerization reaction of St using the Z-carboxylate RAFT agent attached to the surface of MNPs by its Z group

The kinetics of RAFT-mediated polymerization reaction of St on the surface of MNPs using the Z-carboxylate RAFT agent attached to the surface of MNPs was investigated to better understand the relationship between $\overline{M}_n$ of the polymer with monomer conversion. For St polymerization reactions using the Z-carboxylate RAFT agent attached to the surface of MNPs, reaction conditions are given in Table 8.1 (same as run 3). The kinetics of a RAFT-mediated polymerization reaction of St using free Z-carboxylate RAFT agent (no MNPs were used in this polymerization reaction) was also investigated for comparison. The reaction conditions of this polymerization reaction ([St]: [RAFT]: [AIBN], and solvent) are identical to those given in Table 8.1 (run 3).

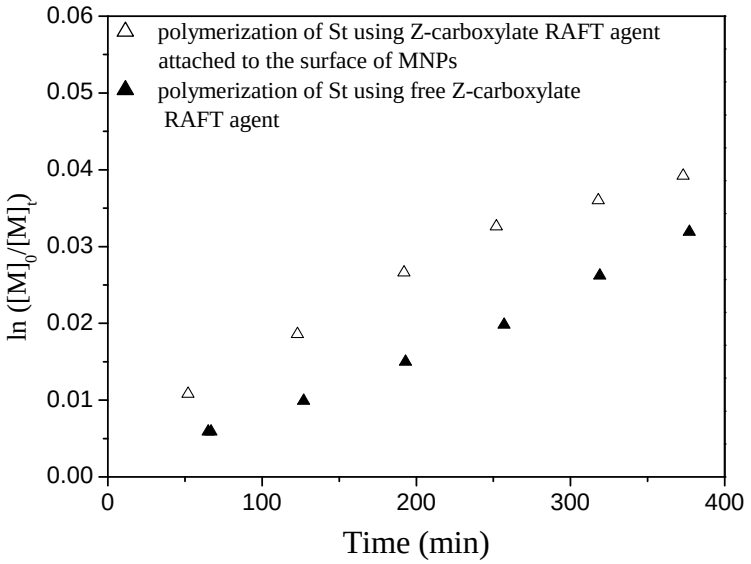

Figure 8.8: Pseudo-first-order kinetic plots of RAFT-mediated polymerization reactions of St using the Z-carboxylate RAFT agent attached to the surface of MNPs (empty rectangles) and that using the free Z-carboxylate RAFT agent (filled rectangles). Reaction conditions: ([St]: [RAFT]: [AIBN] = 900: 1: 0.1, 70 °C).

The dependence of the $\overline{M}_n$ and PDIs on monomer conversion of St polymerization using the Z-carboxylate RAFT agent attached to the surface of MNPs and that using free Z-carboxylate RAFT agent are shown in Figure 8.9, which are indicted by filled rectangles and circles, and empty rectangles and circles, respectively.

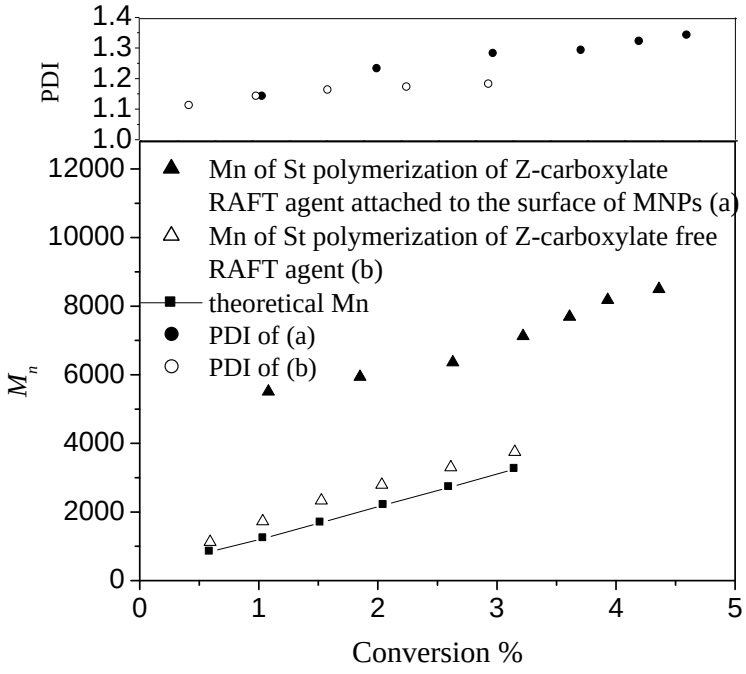

Figure 8.9: Dependence of the molecular weight and polydispersity indexes of RAFT-mediated polymerization reaction of St (a) using the Z-carboxylate RAFT agent attached to the surface of MNPs (filled rectangles and circles, respectively), and (b) using the free Z-carboxylate RAFT agent (empty rectangles and circles, respectively). Reaction conditions: ([St]: [RAFT]: [AIBN] = 900: 1: 0.1, 70 °C).

It was found that the $\overline{M}_n$ of the PSt polymers increase with monomer conversion. This indicates that these polymerization reactions proceeded under living conditions. It was also found that $\overline{M}_n$ evolutions of the PSt polymer of the Z-carboxylate RAFT agent attached to the surface of MNPs were higher than those of PSt polymer of the free Z-carboxylate RAFT agent. When comparing the experimental $\overline{M}_n$ of the polymer prepared

by the RAFT-mediated polymerization reaction using free Z-carboxylate RAFT, with theoretical values of $\overline{M}_n$ calculated via equation (2.1), a good agreement can be found in the case of St polymerization using the Z-carboxylate free RAFT agent (see Figure 8.9), indicating a very well controlled polymerization. Inspection of Figure 8.9 (see filled rectangles), however, shows that in the case of St polymerization using the Z-carboxylate RAFT agent attached to the surface of MNPs, the experimentally found values of $\overline{M}_n$ are significantly higher than the theoretical ones. Although the error of the theoretical $\overline{M}_n$ values could be considered relatively high, as the overall RAFT agent concentration $[RAFT]_0$ was calculated using UV calibration curves (see Section 4.4.4), this significant deviation may be indicative of the molecular weight control in the case of PSt polymer of the Z-carboxylate RAFT agent attached to the surface of MNPs being less effective.

The PDIs of the PSt polymer of the free Z-carboxylate RAFT agent scattered around 1.20, while those of PSt polymers of the Z-carboxylate RAFT agent attached to the surface of MNPs effectively increased with monomer conversion and reached 1.34, as observed in Figure 8.9. This is again proposed that the radicals move slower in solution in a viscous polymer medium than in a solvent medium and this limits the RAFT addition step to being majorly to be diffusion controlled at the surface of MNPs, so causing longer radical life near the surface of MNPs and thus longer molecular weights.

8.6 Conclusions

(1) MNPs have no observable effect on the tested RAFT-mediated polymerization reactions. Kinetics of RAFT-mediated polymerization reactions mediated using a RAFT agent with MNPs and that mediated with a RAFT agent with no MNPs were identical.

(2) RAFT agents attached by the Z group to the surface of MNPs at a high surface density using the isothermal adsorption process was used for synthesis of polymer grafted to the surface of MNPs. Polymer grafted to the surface of MNPs was successfully separated from the remainder of solution polymer (which contained free polymer) by

applying an external magnetic field. Grafted polymer showed a high PDI, and contained living chains with RAFT functionality and a large fraction of by-product with a low RAFT functionality. The amount of the grafted polymer was 5% by weight and 3% by number of chains.

(3) A RAFT agent attached by the Z group to the surface of MNPs at a low surface density using the isothermal adsorption process was successfully used for the synthesis of polymer grafted to the surface of MNPs. The grafted polymer contained living chains with RAFT functionality, and showed lower PDI than that of the grafted polymer when high surface density RAFT agent attached to the surface of MNPs was used. The amount of the grafted polymer reached 18% by number of chains.

(4) MNPs were successfully used to separate all polymer grafted to the surface of MNPs from free polymer formed in RAFT-mediated polymerization reactions using a Z group RAFT agent attached to the surface of MNPs using the ligand exchange process. The grafted polymer showed a high PDI, exhibited a monomodal MWD, and contained living chains with RAFT functionality. The amount of the grafted polymer reached 40% by weight and 32% by number.

(5) Reducing the amount of solvent in a RAFT-mediated polymerization reaction using a RAFT agent attached by the Z group to the surface of MNPs increased the amount of the grafted polymer to the surface of MNPs, which reached 65% by weight and 50% by number.

(6) The kinetics of a RAFT-mediated polymerization reaction of styrene using a RAFT agent attached by its Z group to the surface of MNPs was investigated. The results indicated that the polymerization reaction mediated using a RAFT agent attached by its Z group to the surface of MNPs had a faster polymerization rate than that mediated using a free Z group RAFT agent. The molecular weight values of the grafted polymers increased with conversion and were significantly higher than theoretical values.

8.7 References

1. Alivisatos, A. P. *Science* **1996,** 271, 933-937.
2. Ash, B. J.; Seigel, R. W.; Schadler, L. S. *Macromolecules* **2004,** 37, 1358-1369.
3. Perrier, S.; Takolpuckdee, P. *J. Polym. Sci. Part A: Polym. Chem.* **2005,** 34, 5347-5393.
4. Favier, A.; Charreyre, M. T. *Macromolecular Rapid Commun.* **2006,** 27, 653-692.
5. Tsujii, Y.; Ejaz, M.; Sato, K.; Goto, A.; Fukuda, T. *Macromolecules* **2001,** 34, 8872-8878.
6. Li, C., Z; Han, J.; Ryu, C. Y.; Benicewicz, B. C. *Macromolecules* **2006,** 39, 3175-3183.
7. Li, C. Z.; Benicewicz, B. C. *Macromolecules* **2005,** 38, 5929-5936.
8. Stenzel, M. H.; Davis, T. P. *J. Polym. Sci. Part A: Polym. Chem.* **2002,** 40, 4498-4512.
9. Hao, X. J.; Nilsson, C.; Jesberger, M.; Stenzel, M. H.; Malmstrom, E.; Davis, T. P.; Ostmark, E.; Barner-Kowollik, C. *J. Polym. Sci. Part A: Polym. Chem.* **2004,** 42, 5877-5890.
10. Dureault, A.; Taton, D.; Destarac, M.; Leising, F.; Gnanou, Y. *Macromolecules* **2004,** 37, 5513-5519.
11. Geelen, P.; Klumperman, B. *Macromolecules* **2007,** 40, 3914-3920.
12. Nguyen, D. H.; Wood, M. R.; Zhao, Y.; Perrier, S.; Vana, P. *Macromolecules* **2008,** 41, 7071-7078.
13. Perrier, S.; Barner-Kowollik, C.; Quinn, J. F.; Vana, P.; Davis, T. P. *Macromolecules* **2002,** 35, 8300-8306.

Chapter 9: Conclusions and recommendations

9.1 Introduction

In this study a separation process using magnetite nanoparticles (MNPs) for the separation of all dead chains from living chains formed in Reversible Addition-Fragmentation Chain Transfer (RAFT) and Nitroxide-Mediated Polymerization (NMP) processes, was investigated.

The separation process using MNPs was also used to determine the existence of by-products occurring during RAFT-mediated polymerization reactions (e.g. secondary particle formation in miniemulsion and cross-terminated products in RAFT-mediated polymerization reactions). Use of this process for separation of by-products formed in RAFT/ATRP model free radical reaction in the absence of monomer was also investigated.

MNPs were also used to separate initiator derived chains formed in RAFT-mediated polymerization reactions.

RAFT-mediated polymerization reactions on the surface of MNPs using RAFT agents attached to the surface of MNPs (through the Z group of the RAFT agents) was used for the synthesis of polymers grafted to the surface of MNPs. Separation of all polymers grafted to the surface of MNPs from solution containing free polymer (formed in the aforementioned RAFT-mediated polymerization reactions) by applying an external magnetic field were also investigated in this study.

9.2 Conclusions

With respect to the original objectives of this study, as stated in Section 1.2, the following conclusions can be made:

(1) A separation (extraction) process using MNPs was determined and successfully used for purification of products of RAFT and NMP polymerization reactions.

- MNPs were successfully used to separate living chains from dead chains formed in the RAFT process using Z-functional RAFT agents with very high efficiency. Separated living chains were efficiently recovered from MNPs and showed apparently 100% RAFT functionality, a lower PDI than the polymer that was not modified using MNPs (as-prepared polymer), and no detectable dead chains. Chains extension of living chains showed no deviation from 100% extension efficiency, whereas the remaining chains showed poor extension efficiency.

- MNPs were successfully used to separate living chains from dead chains formed in NMP process using X-functional NMP initiators. Separated living chains were effectively recovered after the separation process using MNPs. All separated living chains mainly exhibited a monomodal molecular weight distribution, contained NMP functionality, and had lower PDI than the as-prepared polymer. The separated living chains showed good living behaviour with high extension efficiency. The remaining polymer chains after the extraction process showed a broad PDI, a bimodal molecular weight distribution, and poor chain extension efficiency.

(2) MNPs selectively separated functional living polymer chains that contained a strong attachment force to the surface of MNPs, while non-functional polymer chains had no effect in the extraction process using MNPs.

- Z-functional living chains were successfully attached to the surface of MNPs and used to separate all dead chains (formed in RAFT-mediated polymerization reaction using Z-functional RAFT agent prior the attachment) and non-functional standard polymer chains (these were obtained as Gel Permanent Chromatography standards, and were mixed with RAFT polymer prior the attachment). Separated living chains showed low PDI, 100% RAFT functionality, and contained no detectable fraction of dead and non-functional chains. The remaining polymer after the separation process showed a high PDI, less RAFT functionality, and contained a large fraction of non-functional chains.

(3) MNPs were used to determine the existence of secondary particle formation by separation of living chains from dead chains formed in RAFT-mediated miniemulsion polymerization reaction using a Z-functional RAFT agent. Separated living chains

showed high RAFT functionality, broad PDI, and contained no measurable fraction of uncontrolled high molecular weight polymer formed as a result of secondary particle formation. A chain extension test of the separated living polymer chains showed that this polymer exhibited good living behaviour, with no deviation from 100% chain extension efficiency. The remaining polymer after the extraction process showed low RAFT functionality, broad PDI, and it contained a fraction of uncontrolled high molecular weight polymer. This polymer exhibited poor living behaviour and minimal chain extension efficiency.

(4) Z-functional living chains and by-products attached to the surface of MNPs were separated from dead chains formed in RAFT-mediated polymerization reaction using a high free radical concentration prior to the attachment. Separated polymer chains contained a large fraction of living chains with UV absorbance at 320 nm (RAFT functionality) and a significant fraction of extractable by-product with a weak UV absorbance at 320 nm. These chains contained however no measurable fraction of dead chains, as those were formed by combination and disproportionation reactions. The separated polymer chains had a lower PDI than the as-prepared polymer and remaining polymer after the extraction process. The remaining polymer after the extraction process and as-prepared polymer contained dead chains formed by combination and disproportionation reactions with a large deviation between the SEC UV absorbance at 320 nm and the corresponding DRI signal, and lacked RAFT functionality.

(5) MNPs were used to separate initiator derived chains formed in RAFT-mediated polymerization reactions of styrene and that of methyl methacrylate. Separated initiator derived chains in the styrene polymerization reaction showed a high PDI, contained large fraction of dead chains and a small fraction of living chains. The remaining polystyrene polymer after the extraction process contained a large fraction of living chains with a strong UV absorbance and a significant fraction of R group derived dead chains with a weak UV absorbance, and showed a lower PDI than the as-prepared polystyrene polymer.

Separated initiator derived chains in the methyl methacrylate polymerization reaction showed lower PDI than as-prepared polymethyl methacrylate polymer, and contained a

large fraction of a low molecular weight component. The separated initiator derived chains contained a large fraction of dead chains and a small fraction of living chains. The remaining polymer after the extraction process showed a broader PDI than the as-prepared polymethyl methacrylate polymer and contained living chains with RAFT functionality, and dead chains with a weak UV absorbance that lacked RAFT functionality.

(6) MNPs were successfully used to separate by-products (cross-terminated products) formed in a RAFT/ATRP model free radical reaction in the absence of monomer. Separated RAFT polymer chains were successfully recovered from MNPs and contained 3- and 4-arm star polymers with a weak UV absorbance and a high PDI. The production of 3- and 4-arm star polymers by the cross-termination reactions was evidenced using Nuclear Magnetic Resonance (NMR) and Matrix Assisted Laser Desorption Ionization-Time-of-Flight -Mass Spectroscopy (MALDI-ToF-MS). This work has shown that cross-termination of intermediate radicals formed in RAFT-mediated polymerization reactions could occur.

(7) MNPs have no observable effect on RAFT-mediated polymerization reactions. The apparent kinetics of a RAFT-mediated polymerization reaction of styrene using blank RAFT agent with MNPs, and that of a RAFT-mediated polymerization reaction of styrene using a blank RAFT agent with no MNPs were similar. There were no large differences between the polystyrene polymers prepared by RAFT-mediated polymerization reactions using blank RAFT agents with MNPs and that with no MNPs with respect to the molecular weight and PDIs.

(8) RAFT agents attached by their Z groups to the surface of MNPs were used for synthesis of grafted polymers to the surface of MNPs. Polymers grafted to the surface of MNPs were successfully separated from solutions containing free polymers by applying an external magnetic field. The amounts of grafted polymer to the surface of MNPs increased as the number of RAFT agents attached to the surface of MNPs decreased, and it reached 50% by number when the ratios of the solvent ethyl acetate/MNPs decreased. All polymers grafted to the surface of MNPs had minimal by-products when a small

number of RAFT agents attached to the surface of MNPs used. These polymers showed higher molecular weights than the free polymer that remained after the separation process. The PDIs of the polymers grafted increased as the number of RAFT agents attached to the surface of MNPs increased. The free polymers contained dead chains with weak UV absorbances at 320 nm, lack RAFT functionality, and showed higher PDIs than the polymers grafted to the surface of MNPs when a small number of RAFT agents attached to the surface of MNPs are used.

(9) Kinetics of a RAFT-mediated polymerization reaction on the surface of MNPs using a Z-functional RAFT agent attached by its Z group to the surface of MNPs and that of a RAFT-mediated polymerization reaction using free Z-functional RAFT agent were investigated for comparison. The observable polymerization rate of the RAFT-mediated polymerization reaction of styrene using the Z-functional RAFT agent attached to the surface of MNPs was faster than the RAFT-mediated polymerization reaction of styrene using the free Z-functional RAFT agent.

9.3 Recommendations

Pure controlled/living polymer standards still remain unavailable products. In this study the main research goal for synthesis of ultra pure polymer products of RAFT and NMP processes were demonstrated only on a small scale.

RAFT-mediated (solution/bulk and dispersion) polymerization reactions are very useful for the synthesis of numerous of polymeric materials. Challenges regarding the exact mechanism, involved reactions, inhibition/retardation, and by-products, are not fully understood yet, and thus require further advanced research. The study investigated and demonstrated the applications of the extraction process to determine the existence and to separate by-products formed in the RAFT process. Further investigation is however still required in order to obtain more information about the RAFT process. Separation and thereby quantification of by-products formed during the RAFT-mediated polymerization reaction in the presence of different reaction conditions (initiator concentration, type of RAFT agent (dithioester vs. trithiocarbonate RAFT agents), and concentration of RAFT

agent) would be useful investigations. The impact of by-products on the mechanism of RAFT polymerization reaction, and thus on the properties of the prepared polymers should be also investigated.

Following the goals achieved in this study, the authors would recommend aspects that require further investigations:

- Since the RAFT and NMP processes are highly compatible with different functional monomers and the extraction process produces high quality ultra pure polymer products, it is recommended, as for an industrial interest, to imply this process for production of large quantities of high quality commercial polymer standards to be used for chromatography techniques, and other applications which require pure polymers.

- To use the same methodology for the synthesis of pure star, comb-like, block, and multi block polymers.

- RAFT-mediated polymerization reactions are sensitive to reaction variables such as types of the RAFT agents (e.g. dithioester vs. trithiocarbonate RAFT agents) and mediating Z groups (e.g. Z = phenyl group), and concentrations of the RAFT agents. It would be useful to investigate the mechanistic behaviour of RAFT-mediated polymerization reactions using functional RAFT agents in the presence of these reaction variables. Separation and quantification of by-Products formed during these polymerization reactions and the impact of these on the reaction mechanism and polymer properties should be investigated. This would be highly significant in order to achieve optimum RAFT-mediated polymerization reaction conditions where undesired by-products could be minimized and reaction mechanisms could be better understood. It would also lead into possible ways where one can predict products and concentrations of various products formed during RAFT-mediated polymerization reactions. As a result, the industrial applications of the RAFT process would be increased.

- Secondary particle formation is not a desired process in RAFT-mediated miniemulsion and emulsion polymerization reactions. This is because it produces uncontrolled high molecular weight polymers that contain no RAFT groups. The

formation of uncontrolled high molecular weight polymers in miniemulsion and maybe emulsion systems is sensitive to different reaction conditions: monomers, initiators (water soluble vs. oil soluble initiators), surfactants, RAFT agents, and impurities. It would be recommended to investigate the growth of secondary particle formation during RAFT-mediated polymerization reactions using functional RAFT agents over the abovementioned reaction conditions. Separation of RAFT chains from dead chains, and thus quantification of secondary particle formation should be also investigated. This has not been able to be done in ordinary emulsion/miniemulsion systems, and has a strong mechanistic implication for these systems using RAFT process. This investigation would lead to optimum reaction conditions where the extent of the growth of these particles could be prevented, or otherwise minimized.

- To introduce a novel methodology for making perfect nanoemulsion systems for biomedical applications. This is to employ RAFT-mediated emulsion polymerization reactions using RAFT agents attached to the surface of MNPs for making nanoemulsion polymer products.

Appendix A:
Analytical data

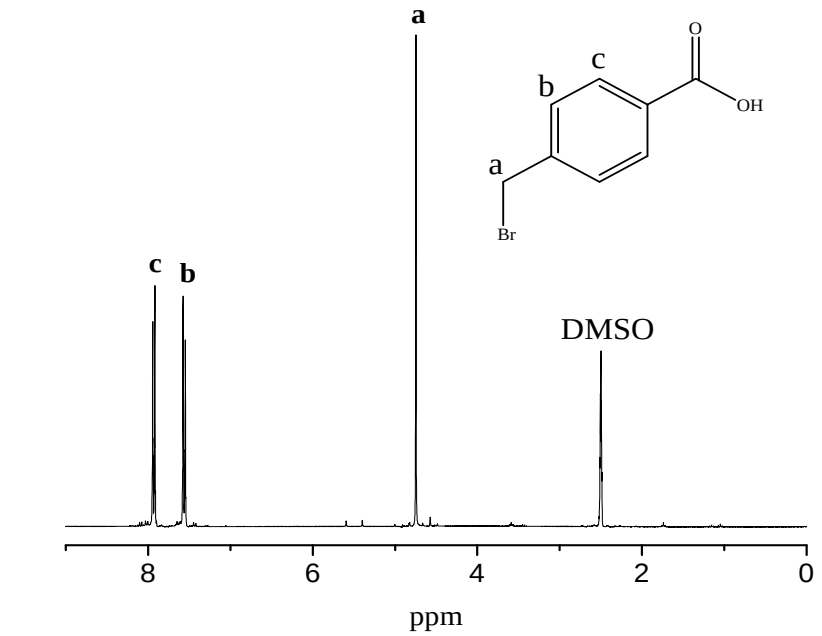

Figure A.1: ^{1}H-NMR spectrum of 4-bromomethyl benzoic acid.

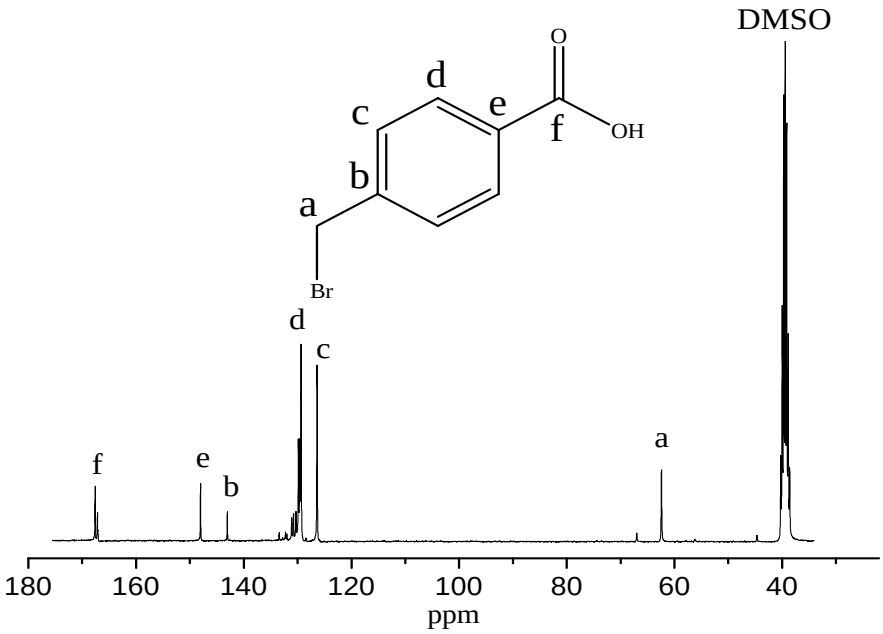

Figure A.2: ^{13}C-NMR spectrum of 4-bromomethyl benzoic acid.

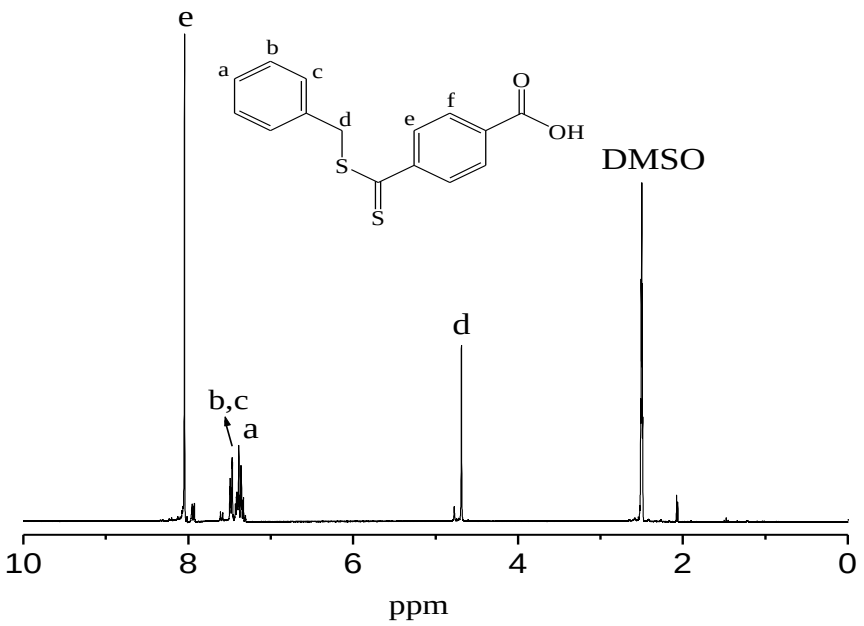

Figure A.3: ^{1}H-NMR spectrum of benzyl-(4-carboxydithiobenzoate).

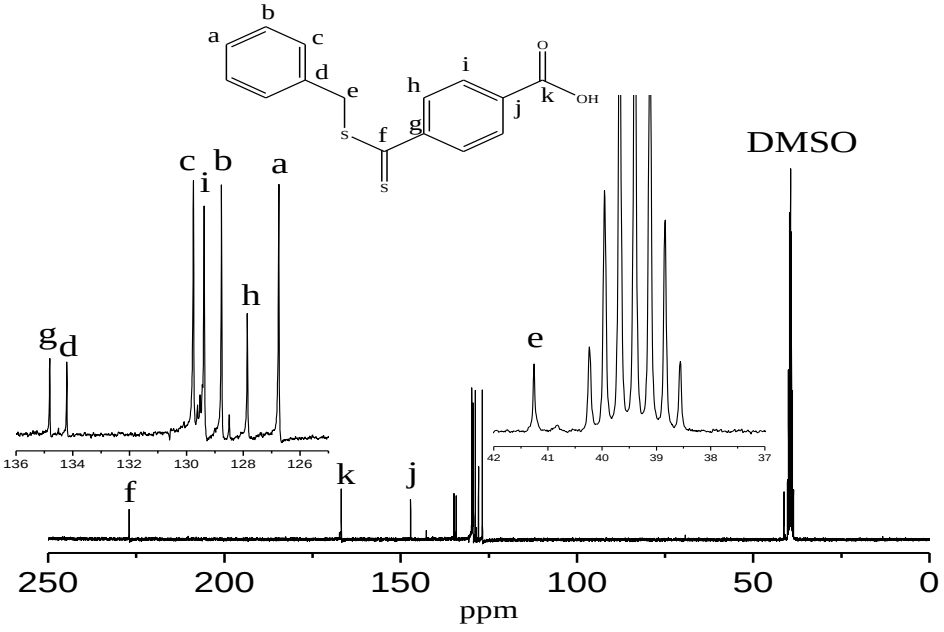

Figure A.4: ^{13}C-NMR spectrum of benzyl-(4-carboxydithiobenzoate).

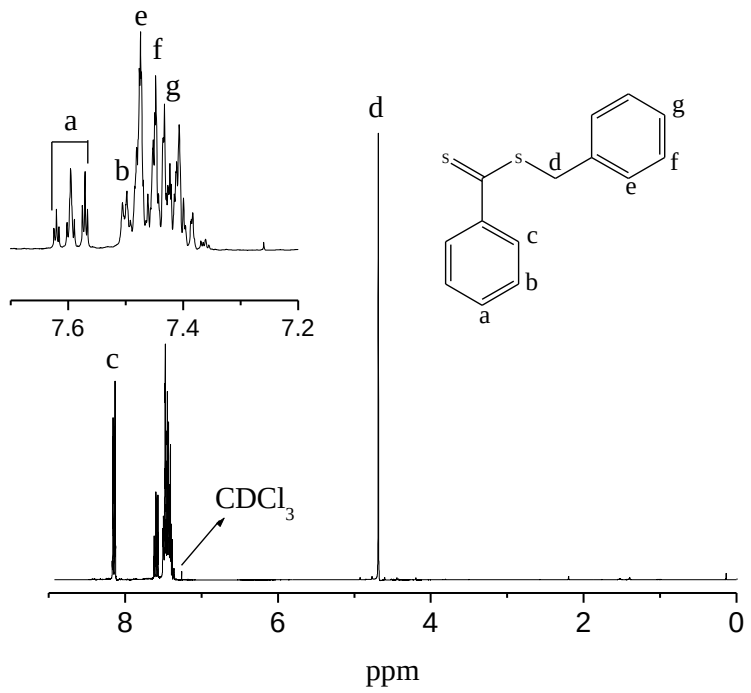

Figure A.5: ^{1}H-NMR spectrum of benzyl dithiobenzoate.

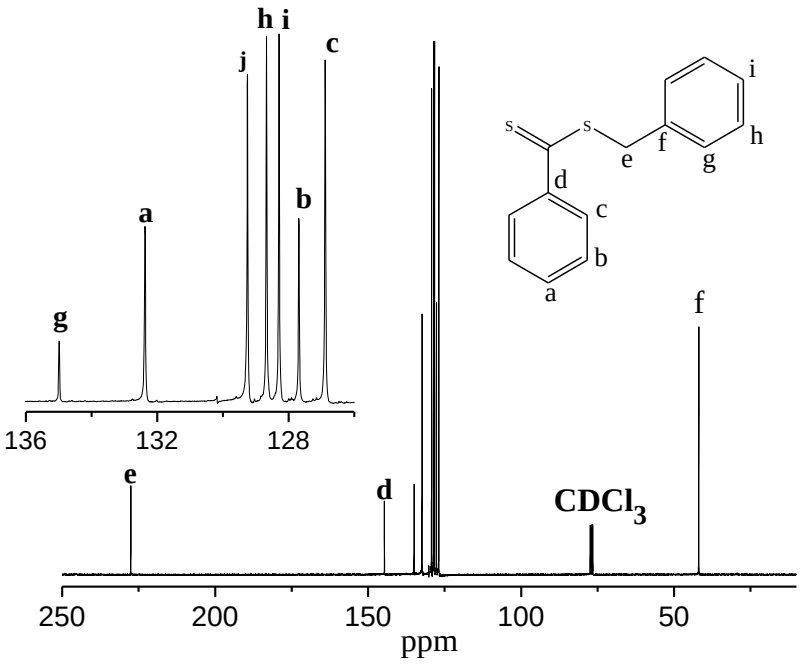

Figure A.6: ^{13}C-NMR spectrum of benzyl dithiobenzoate.

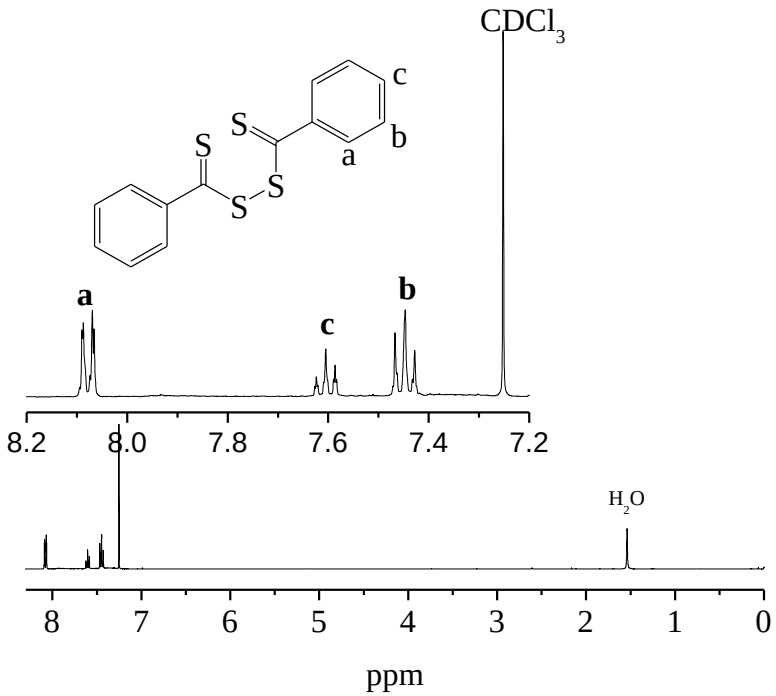

Figure A.7: ^{1}H-NMR spectrum of bis(thiocarbonyl)disulphide.

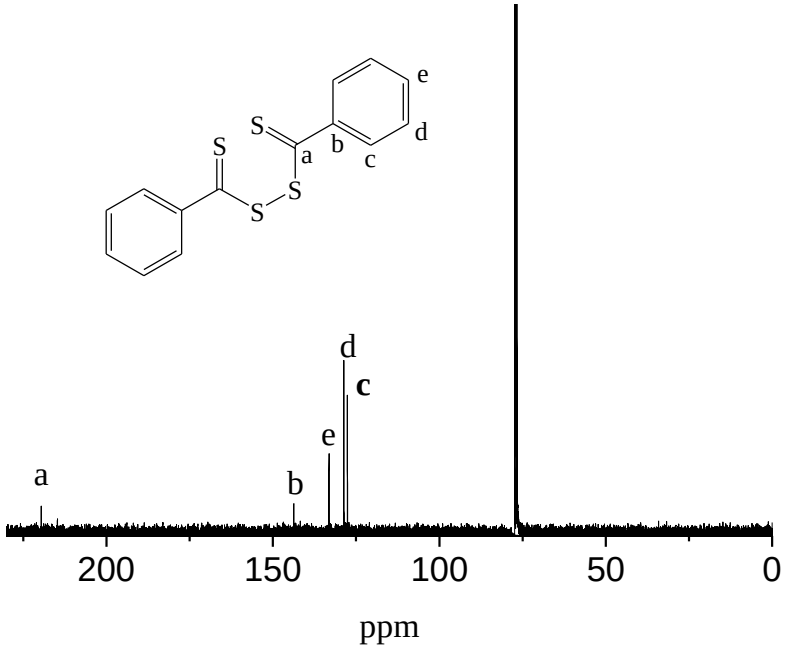

Figure A.8: ^{13}C-NMR spectrum of bis(thiocarbonyl)disulphide.

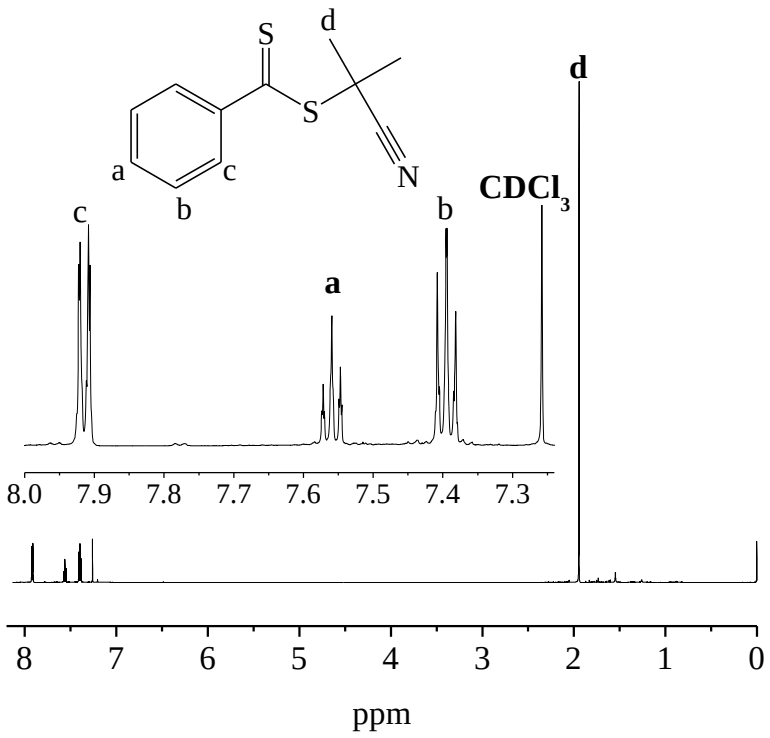

Figure A.9: ^{1}H-NMR spectrum of 2-cyanoprop-2-yl dithiobenzoate.

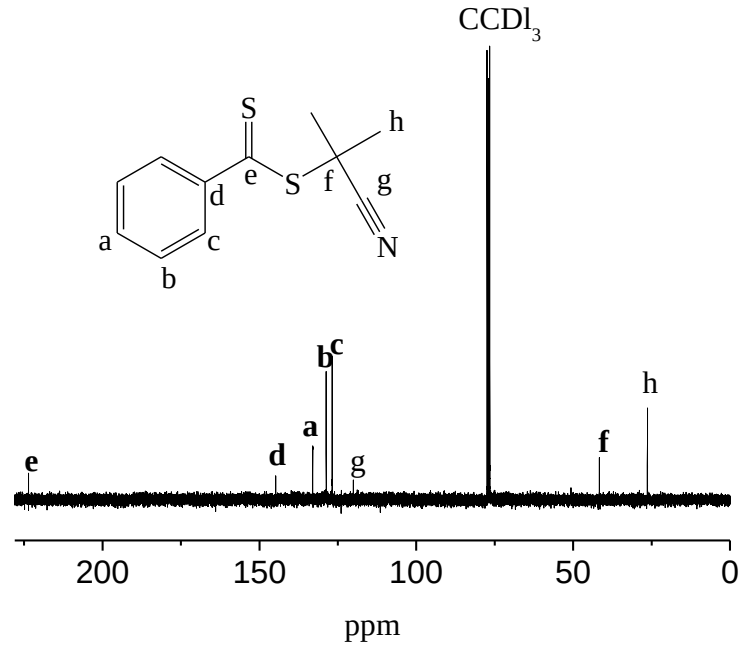

Figure A.10: ^{13}C-NMR spectrum of 2-cyanoprop-2-yl dithiobenzoate.

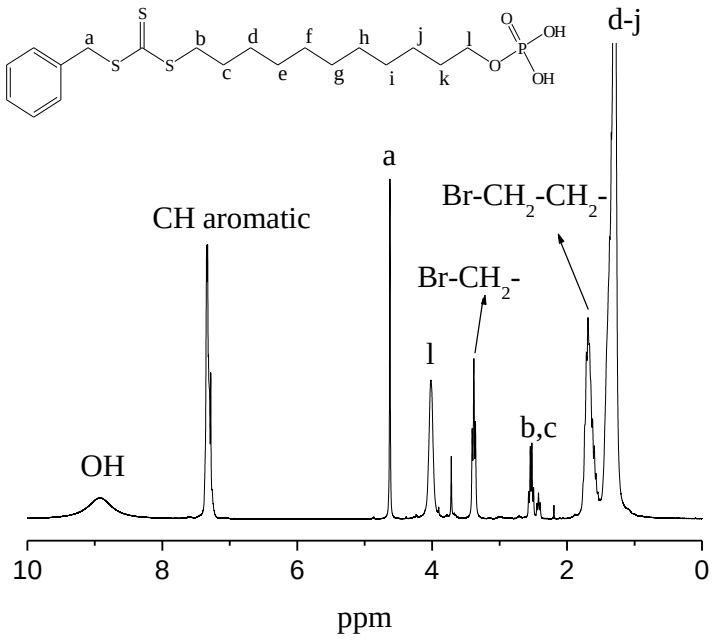

Figure A.11: ^{1}H-NMR spectrum of S-benzyl-S′-(11-phosphonoxy-undecyl) trithiocarbonate.

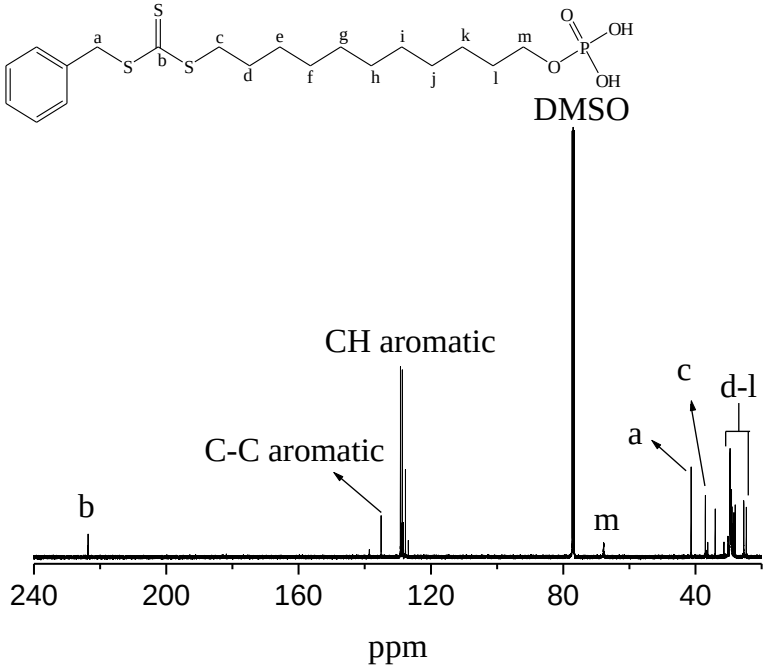

Figure A.12: ^{13}C-NMR spectrum of S-benzyl-S′-(11-phosphonoxy-undecyl) trithiocarbonate.

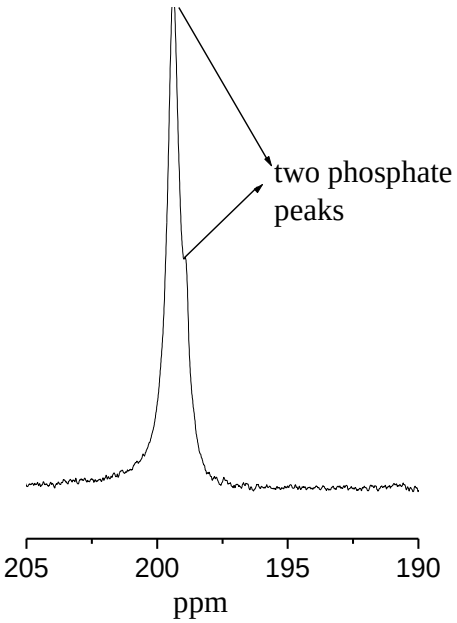

Figure A.13: ^{13}P-NMR spectrum of S-benzyl-S′-(11-phosphonoxy-undecyl) trithiocarbonate.

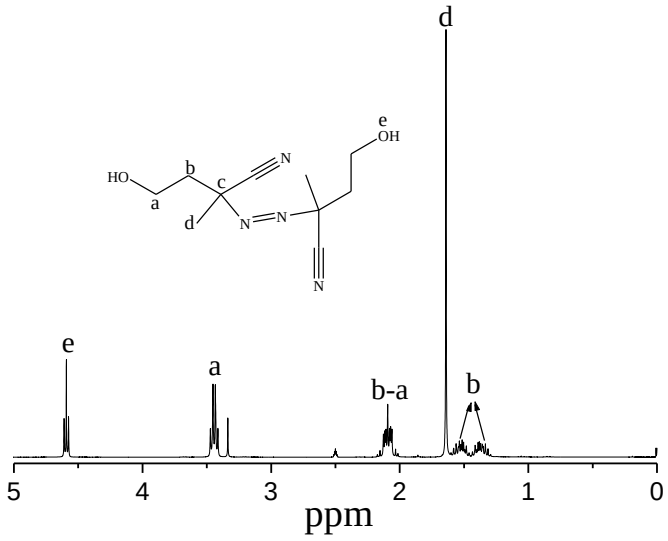

Figure A.14: ^{1}H-NMR spectrum of 4,4′-azobis(4-cyanopentanol) (the hydroxyl free radical initiator).

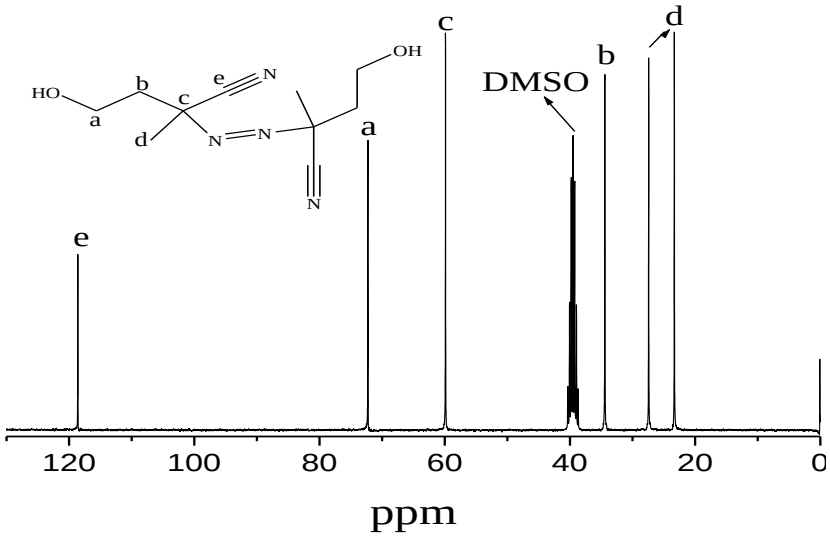

Figure A.15: ^{13}C-NMR spectrum of 4,4′-azobis(4-cyanopentanol) (the hydroxyl free radical initiator).

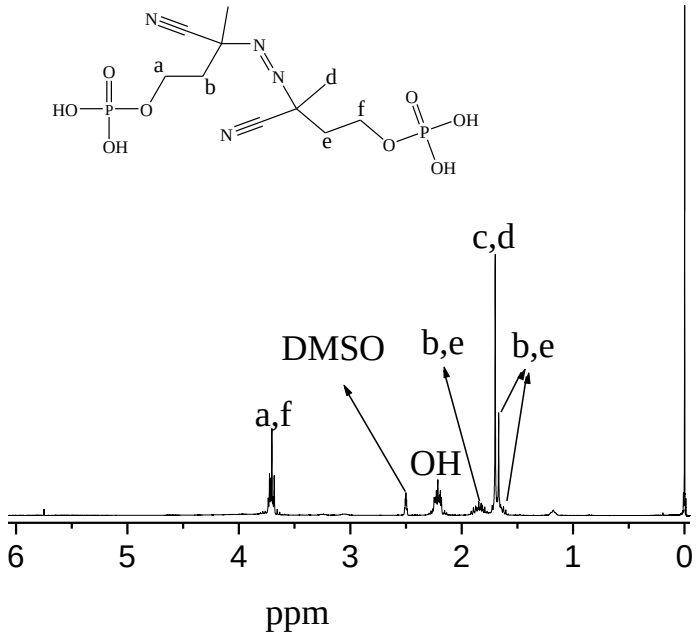

Figure A.16: ^{1}H-NMR spectrum of (E)-diazene-1,2-diylbis-3-cyanobuatne-3,1-diyl bis(dihydrogen phosphate) (the phosphate free radical initiator).

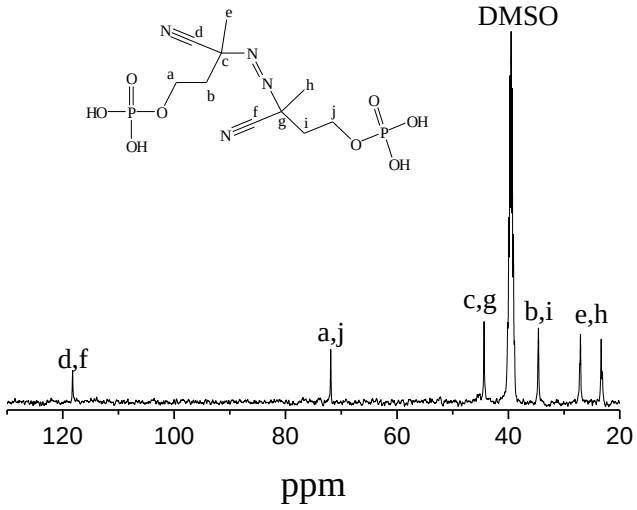

Figure A.17: ^{13}C-NMR spectrum of (E)-diazene-1,2-diylbis-3-cyanobuatne-3,1-diyl bis(dihydrogen phosphate) (the phosphate free radical initiator).

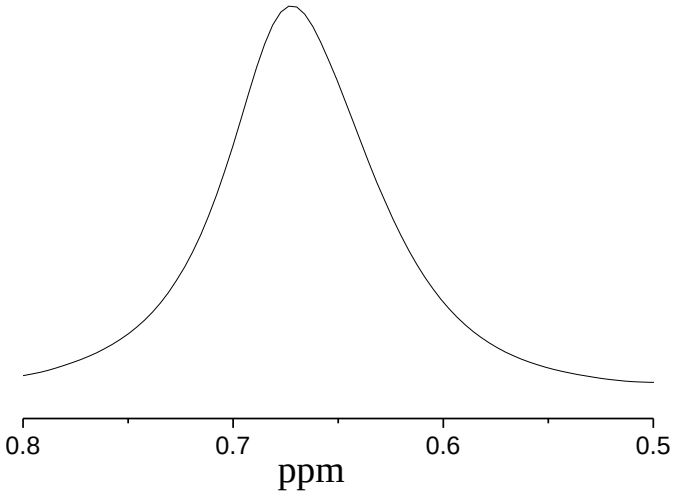

Figure A.18: ^{13}P-NMR spectrum of (E)-diazene-1,2-diylbis-3-cyanobuatne-3,1-diyl bis(dihydrogen phosphate) (the phosphate free radical initiator).

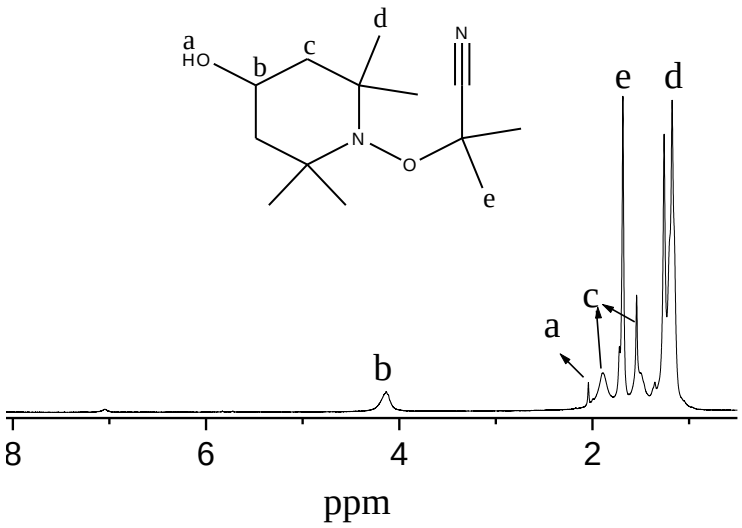

Figure A.19: ^{1}H-NMR spectrum of 1-(1-cyano-1-methylethoxy)-2,2,6,6-tetramethylpiperidine-4-yl-hydroxyl.

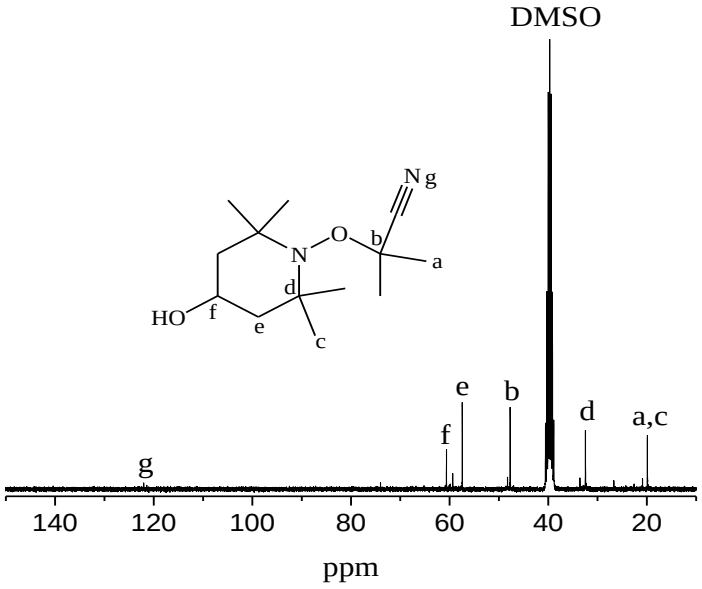

Figure A.20: ^{13}C-NMR spectrum of 1-(1-cyano-1-methylethoxy)-2,2,6,6-tetramethylpiperidine-4-yl-hydroxyl.

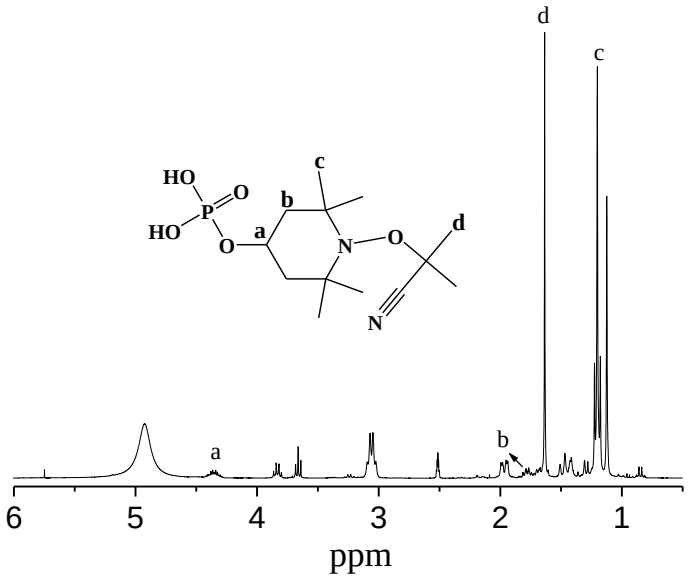

Figure A.21: ^{1}H-NMR spectrum of 1-(1-cyano-1-methylethoxy)-2,2,6,6-tetramethylpiperidine-4-yl-dihydrogen phosphate (phosphate NMP initiator).

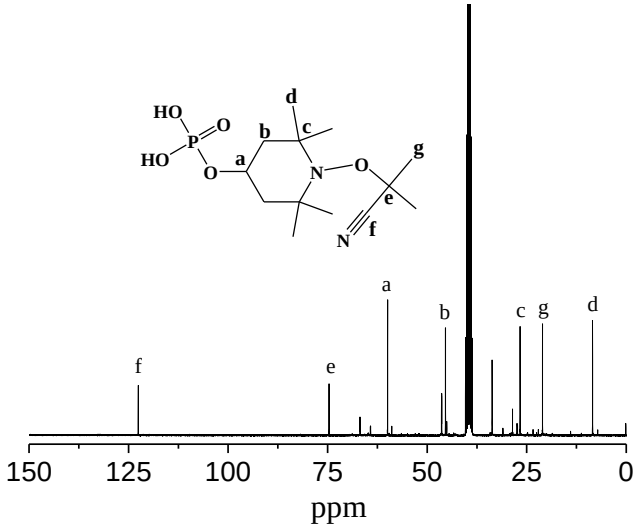

Figure A.22: ^{13}C-NMR spectrum of 1-(1-cyano-1-methylethoxy)-2,2,6,6-tetramethylpiperidine-4-yl-dihydrogen phosphate (phosphate NMP initiator).

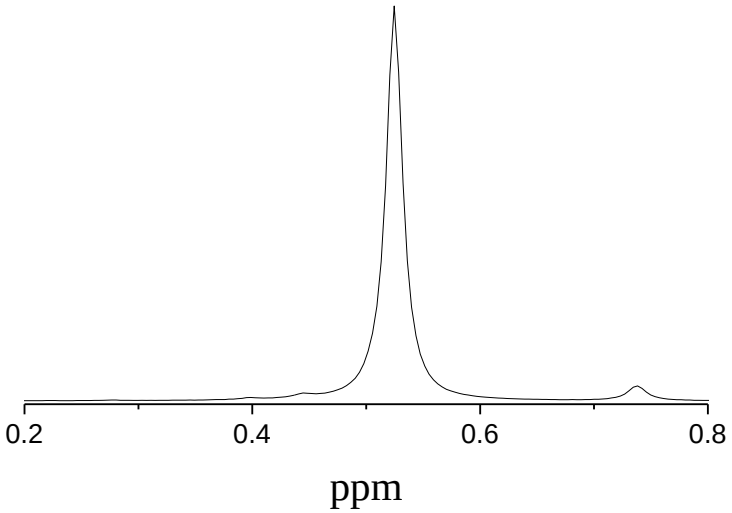

Figure A.23: ^{13}P-NMR spectrum of 1-(1-cyano-1-methylethoxy)-2,2,6,6-tetramethylpiperidine-4-yl-dihydrogen phosphate (phosphate NMP initiator).

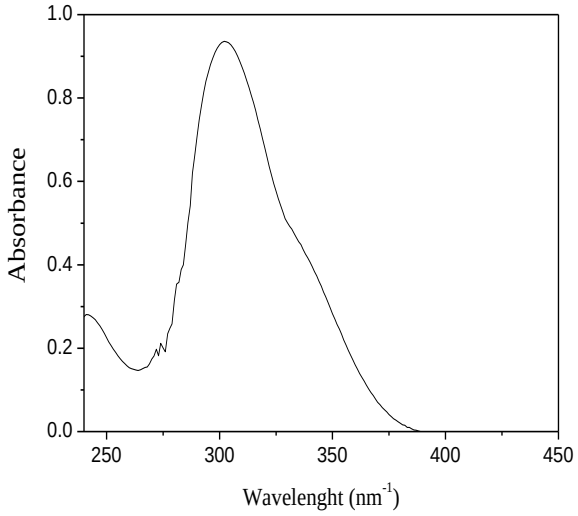

Figure A.24: UV absorbance of the phosphate free radical initiator (PFR) in dichloromethane: λ = 302 ($\pi \rightarrow \pi^*$), [PFR] = 0.014 g/L.

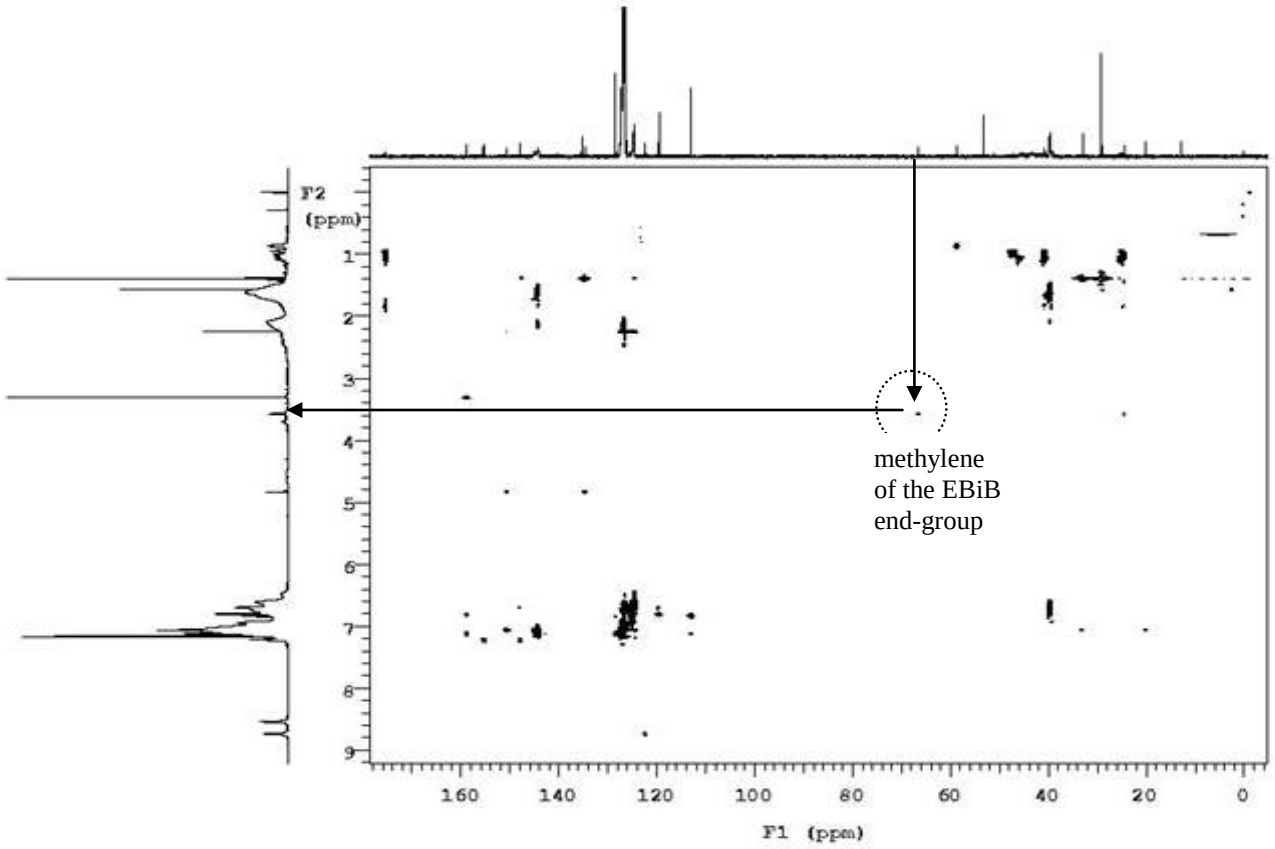

Figure A.25: $^{1}H/^{13}C$-Heteronulear Multiple-Bond Correlation (HMBC) NMR spectrum of the extracted PSt polymer (obtained after the heat treatment and extraction).

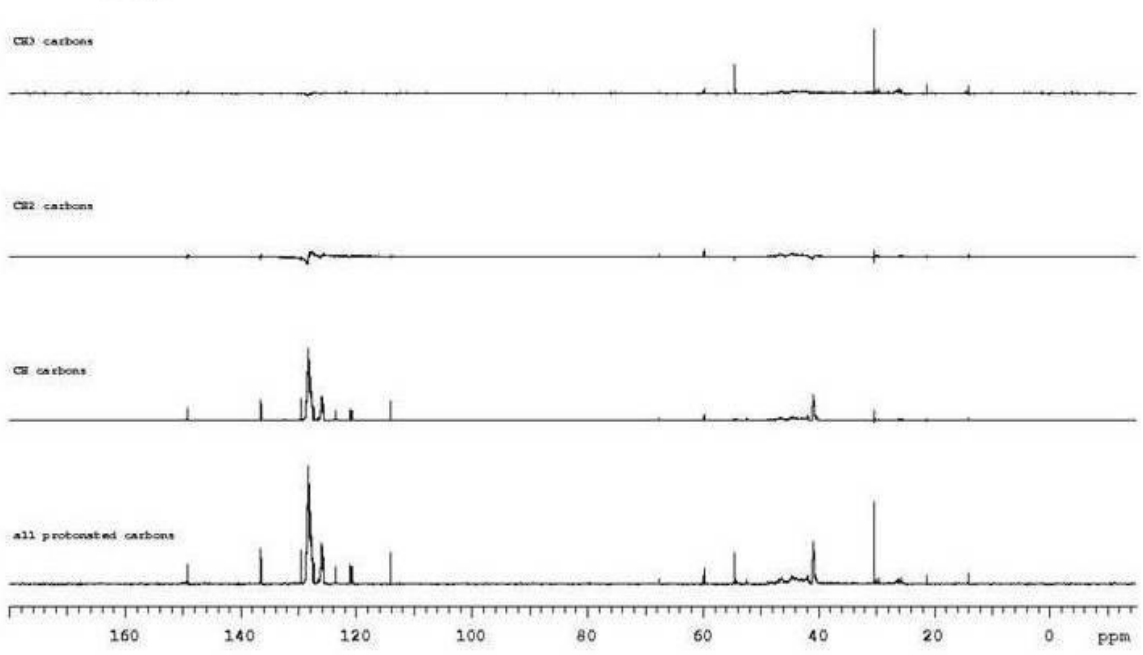

Figure A.26: ^{13}C-Distorsionless Enhancement by Polarization effect (DEPT) NMR spectrum of the extracted PSt polymer (obtained after the heat treatment and extraction).

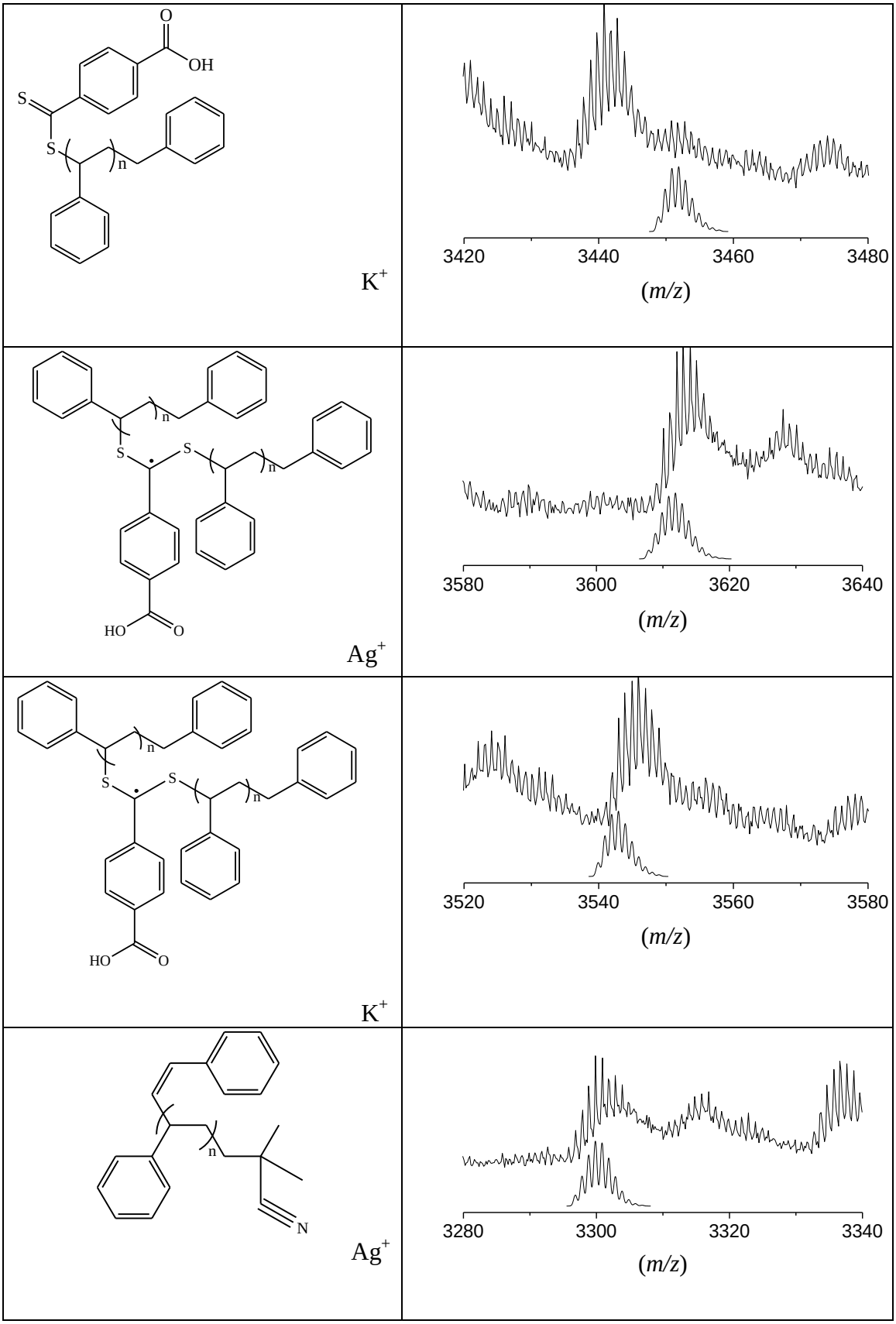
O
OH
S
S
n
K+
3420
3440
3460
3480
(m/z)
n
S
S
n
HO
O
Ag+
3580
3600
3620
3640
(m/z)
n
S
S
n
HO
O
K+
3520
3540
3560
3580
(m/z)
n
N
Ag+
3280
3300
3320
3340
(m/z)

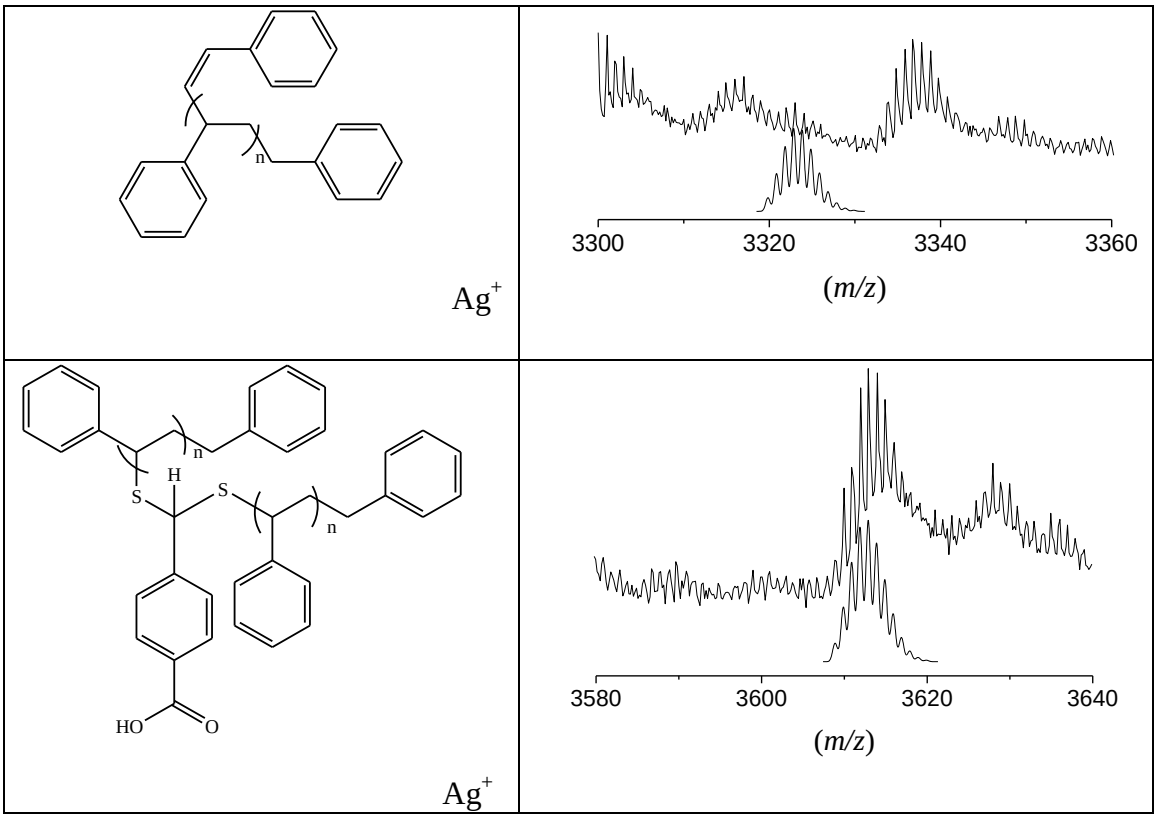

Figure A.27: PSt chain populations of the PSt polymer grafted to the surface of MNPs: as detected by MALDI-ToF-MS using the reflectron mode (above spectra) with AgTFA salt/MM matrix, as theoretically calculated spectra (below spectra) and the corresponding mass structures of each chain population (left hand side column).